Abstract Book

9th MSAT

The 9th International Conference on Materials Science and Technology

December 14th–15th, 2016

Swissôtel Le Concorde, Bangkok, Thailand

Organizers

Supporter

Platinum Sponsor

Gold Sponsor

Bronze Sponsor

Exhibitiors

www.mtec.or.th/msat-9

Download on the App Store

MSAT-9 App iOS

ANDROID APP ON Google play

MSAT-9 App Android

Disclaimer

This book contains the abstracts of the papers presented at The 9th International Conference on Materials Science and Technology (MSAT-9). They reflect the authors' opinions and are published as received after revision by the authors.

The committee assumes no responsibility for the accuracy, completeness or usefulness of the disclosed information.

Unauthorized use might infringe on privately owned patents or publication rights. Please contact the individual author(s) for permission to reprint or make use of information from their papers.

Organizers

National Metal and Materials Technology Center
National Science and Technology Development Agency
Ministry of Science and Technology

Co-organizers
Materials Research Society
Thai Society of Dental Biomaterials
Thai Corrosion of Metals and Materials Association
Thai Tribology Association

Platinum Sponsor
IRPC Public Co., Ltd.

Gold Sponsor
Thai Parkerizing Co., Ltd.

Bronze Sponsor
SCG Chemicals Co., Ltd.

Supporter
Thailand Convention and Exhibition Bureau

Contents

Preface

Dear Colleagues,

On behalf of the Organizing Committee, I would like to welcome you all to the 9th International Conference on Materials Science and Technology (MSAT-9) held from December 14th to 15th, 2016 in Bangkok, Thailand.

MSAT is recognized as one of the major series of conference in materials science and technology. The bi-annual conference strives to be a premier international multidisciplinary conference providing an arena for all stakeholders from academics, researchers and industrial leaders to share their latest research findings, to discuss novel applications and to identify the challenges that lie at the frontier of materials science.

In conjunction with MSAT-9, two special events to be run along are the 3rd meeting of Thai Society of Dental Biomaterials and the MRS-Thailand Annual Meeting.

To support of sustainable and green environment in Thailand, we are going to transform the MSAT towards paperless conference. There are all information needed for the MSAT-9 will be available for participants via the MSAT-9 mobile application and the conference website.

Regarding the conference activities, we are proud to have 4 plenary and 19 invited lectures given by distinguished researchers in the field of materials technology around the world. They include 126 oral research presentations and 112 poster presentations covering recent progress and R&D activities ranging from fundamental research to applied research in the fields of materials science and technology.

We are also delighted to announce the number of participants to MSAT-9 to be over 500 persons from Canada, India, Indonesia, Iran, Italy, Japan, Russian Federation, Malaysia, Philippines, United State of America, Singapore, South Korea, Taiwan and Thailand.

Lastly, I would like to thank all the sponsors of the MSAT-9, without whom it would be difficult to organize a successful international conference. Their contributions are greatly appreciated.

Yours sincerely,

Julathep Kajornchaiyakul
Chair of MSAT-9

Committees

Chair

Dr. Julathep Kajornchaiyakul	National Metal and Materials Technology Center

Vice-chairs

Dr. Aree Thanaboonsombut	National Metal and Materials Technology Center
Dr. Kritsada Prapakorn	National Metal and Materials Technology Center
Ms. Siriwan Tantawechkit	National Metal and Materials Technology Center

International Technical Committee

Asst. Prof. Jeremy John Mercuri	Clemson University
Assoc. Prof. Georgia Papavasiliou	Illinois Institute of Technology

Scientific Committee

Dr. Worasit Kanjanakijkasem	Burapha University
Dr. Dumnoensun Pruksakorn, M.D.	Chiang Mai University
Asst. Prof. Kedsarin Pimraksa	Chiang Mai University
Dr. Robert Molloy	Chiang Mai University
Asst. Prof. Sorada Kanokpanont	Chiang Mai University
Assoc. Prof. Thapanee Sarakonsri	Chiang Mai University
Asst. Prof. Boonrat Lohwongwatana	Chulalongkorn University
Asst. Prof. Dujreutai Pongkao Kashima	Chulalongkorn University
Asst. Prof. Mantana Opaprakasit	Chulalongkorn University
Dr. Natthaphon Raengthon	Chulalongkorn University
Assoc. Prof. Nisanart Triphol	Chulalongkorn University
Asst. Prof. Pornapa Sujaridworakun	Chulalongkorn University
Assoc. Prof. Rojana Pornprasertsuk	Chulalongkorn University
Asst. Prof. Sirithan Jiemsirilers	Chulalongkorn University
Assoc. Prof. Songphol Kanjanachuchai	Chulalongkorn University
Assoc. Prof. Supatra Jinawath	Chulalongkorn University

Asst. Prof. Thanakorn Wasanapiarnpong	Chulalongkorn University
Dr. Lada Punsukumtana	Department of Science Service
Dr. Parinya Boonmalert	Kasem Bundit University
Asst. Prof. Duangrudee Chaysuwan	Kasetsart University
Asst. Prof. Nonglak Meethong	Khon Kaen University
Assoc. Prof. Thapanee Sarakonsri	Khon Kaen University
Asst. Prof. Chonlada Ritvirulh	King Mongkut's Institute of Technology Ladkrabang
Asst. Prof. Suparat Rukchonlatee	King Mongkut's Institute of Technology Ladkrabang
Asst. Prof. Thanasan Intarakumthornchai	King Mongkut's University of Technology North Bangkok
Asst. Prof. Anak Khantachawana	King Mongkut's University of Technology Thonburi
Prof. Navadol Laosiripojana	King Mongkut's University of Technology Thonburi
Prof. Banchong Mahaisavariya, M.D.	Mahidol University
Asst. Prof. Krisda Suchiva	Mahidol University
Asst. Prof. Norased Nasongkla	Mahidol University
Dr. Phornphop Naiyanetr	Mahidol University
Assoc. Prof. Pranee Phinyocheep	Mahidol University
Asst. Prof. Somsak Dangtip	Mahidol University
Asst. Prof. Toemsak Srikhirin	Mahidol University
Prof. Suwabun Chirachanchai	Petroleum and Petrochemical College, Chulalongkorn University
Asst. Prof. Poonsub Threepopnatkul	Silpakorn University
Assoc. Prof. Pakorn Opaprakasit	Sirindhorn International Institute of Technology, Thammasat University
Prof. Santi Maensiri	Suranaree University of Technology

Asst. Prof. Sirirat Tubsungnoen Rattanachan	Suranaree University of Technology
Dr. Pinai Mungsantisuk	Thai Marine Protection Co., Ltd.
Dr. Siriporn Larpkiattaworn	Thailand Institute of Scientific and Technological Research
Asst. Prof. Benya Cherdhirunkorn	Thammasat University
Assoc. Prof. Cattaleeya Pattamaprom	Thammasat University
Asst. Prof. Weerachai Singhatanadgit, D.D.S	Thammasat University
Assoc. Prof. Kulachate Pianthong	Ubon Ratchathani University
Dr. Wannee Chinsirikul	National Nanotechnology Center
Dr. Pavadee Aungkavattana	National Nanotechnology Center
Dr. Asira Fuongfuchat	National Metal and Materials Technology Center
Dr. Chakkrist Phongphisutthinan	National Metal and Materials Technology Center
Dr. Darunee Aussawasathien	National Metal and Materials Technology Center
Dr. Doungporn Sirikittikul	National Metal and Materials Technology Center
Dr. Duangduen Atong	National Metal and Materials Technology Center
Dr. Ekkarut Viyanit	National Metal and Materials Technology Center
Dr. Kannaporn Pooput	National Metal and Materials Technology Center
Dr. Nirut Naksuk	National Metal and Materials Technology Center
Dr. Nongnuch Poolsawad	National Metal and Materials Technology Center
Dr. Noramon Intaranont	National Metal and Materials Technology Center
Dr. Nudjarin Ramungul	National Metal and Materials Technology Center
Dr. Panadda Sheppard	National Metal and Materials Technology Center
Dr. Panjawat Kongsuwan	National Metal and Materials Technology Center
Dr. Pasaree Laokijcharoen	National Metal and Materials Technology Center
Dr. Samunya Sanguanpak	National Metal and Materials Technology Center
Dr. Sinthu Chanthapan	National Metal and Materials Technology Center
Dr. Sirikarn Wisetsuwannaphum	National Metal and Materials Technology Center
Dr. Sitthisuntorn Supothina	National Metal and Materials Technology Center
Dr. Somboon Otarawanna	National Metal and Materials Technology Center

Dr. Somboon Sahasithiwat	National Metal and Materials Technology Center
Dr. Sorachon Yoriya	National Metal and Materials Technology Center
Dr. Sumittra Charojrochkul	National Metal and Materials Technology Center
Dr. Supamas Danwittayakul	National Metal and Materials Technology Center
Dr. Surapich Loykulnant	National Metal and Materials Technology Center
Dr. Sutee Olarnrithinun	National Metal and Materials Technology Center
Dr. Thanasat Sooksimuang	National Metal and Materials Technology Center
Dr. Thanya Phraewphiphat	National Metal and Materials Technology Center
Dr. Wanida Janvikul	National Metal and Materials Technology Center
Dr. Witchuda Daud	National Metal and Materials Technology Center
Dr. Yatika Somrang	National Metal and Materials Technology Center

TECHNICAL PROGRAM

Day I	December 14th, 2016									
08:00-09:00	Registration (Foyer Area, 2nd Floor) and Poster Setup (Foyer Area, 2nd & 3rdFloor)									
09:00-09:15	Opening Ceremony (Le Concorde Ballroom, 2nd Floor)									
09:15-10:00	**Plenary Lecture 1:** "Bringing it All Back Home" How Waste-to-Biobased Products is Good for Energy, the Environment, Water, and Society **by *Prof. Seth Snyder***									
10:00-10:45	**Plenary Lecture 2:** Geopolymerization as Cold-consolidation Techniques for Hazardous and Non-hazardous Wastes **by *Prof. Cristina Leonelli***									
10:45-11:00	Break									
Room	**Salon A**	**Salon B**	**Jamjuree**	**Krisana**	**Sakthong**	**Shanghai**	**Rachavadee**	**Patumchard**	**Uboncharad**	**Satabud**
Floor	2nd Floor	2nd Floor	2nd Floor	2nd Floor	2nd Floor	2nd Floor	2nd Floor	3rd Floor	3rd Floor	3rd Floor
Session	**TSDB 1**	**MRS 1**		**Ceramics 1** (Ceramics and Composite Materials)	**Materials for Energy 1**	**Polymers 1**	**Materials Technology for Environment 1**	**Metals, Alloys & Intermetallic Compounds 1** (Metal Forming)	**Surface Engineering and Heat Treatment 1**	**Design & Manufacturing and Computational Science & Engineering 1**
Session Chair	Asst.Prof. Dujreutai P. Kashima	Dr.Worawarong Rakreungdet		Dr. Apirat Theerapapvisetpong	Dr. Worawarit Kobsiriphat	Dr. Asira Fuongfuchat	Dr. Samerkhae Jongthammanurak	Dr. Sasawat Mahabunphachai	Witthawat Wongpisan	Dr. Somboon Otarawanna
11:00-11:15	The 3rd Meeting of Thai Society of Dental Biomaterials	11:00-12:30 The 1st Annual Meeting of MRS-Thailand "Innovative Materials for Industry 4.0 (Private Section)"		CER-I-01 Machinable Glass-Ceramics as a Dental Material ***Asst.Prof. Duangrudee Chaysuwan***	ENR-O-01 Graphene-$AgVO_3$ Composite for Supercapacitor Applications ***Jiaqian Qin***	POL-I-01 Polymer Research in Thailand: Past, Present and Future ***Asst.Prof. Krisda Suchiva***	ENV-I-06 Investigation of Ag- GO-TiO_2 Cocatalyst Composites for Photocatalysis Application ***Dr. Chanchana Thanachayanont***	MET-O-01 Utilization of Binding Ice Flakes with Pulp-Fibers as Fillings on Tube Forming ***Takahiro Ohashi***	SUR-O-01 Effects of Heat Treatment on Microstructure and Properties of Thermal Sprayed Ni-based alloy Coatings ***Phuangphaga Daram***	DMC-I-01 Meta-Heuristics for Engineering Optimisation ***Prof. Sujin Bureerat***
11:15-11:30					ENR-O-02 Characterization of Polyaniline/Carbon Nanotube/Pineapple-Polyester Fabric Composites as Supercapacitor Electrodes ***Felicidad Christina Ramirez***			MET-O-02 Bending Limit Curves in Sheet Metal Bending Evaluation ***Sansot Panich***	SUR-O-02 Tribological of Thermal Sprayed Coating under Slurry Erosion ***Chalermchai Sukhonkhet***	
11:30-11:45				CER-O-01 Synthesizing of Glass Ceramics-Composite for Opal Imitation by Direct Sintering Method ***Saweat Intarasiri***	ENR-O-03 Piña (*Ananas comosus*) and Water Hyacinth (*Eichhornia crassipes*) Polyester Blended Textiles with Polypyrrole as Supercapacitor Electrode Materials ***David Joseph Alzate***	POL-O-01 The Effect of Calcium Carbonate on Crystallization Behavior and Morphology of Poly(3-hydroxybutyrate-*co*-3-valerate) ***Sitthi Duangphet***	ENV-O-06 Using ZnO Nanorods Coated Porous Ceramic Monolith to remove Arsenic from Groundwater ***Kannika Khwamsawata***	MET-O-03 Effect of Fold−Forging Techniques on Mechanical Properties of Medium Carbon Steel for Sword Making Process ***Kotchaporn Paveebunvipak***	SUR-O-03 Flame Spray Coating for Erosion Protection on Water Wall Pipe in Bio-mass Fired Powder Plant Boiler ***Vasin Lertvijitpun***	DMC-O-01 Corrosion Prediction Using ANN for Offshore Pipeline in the Gulf of Thailand ***Passaworn Silakorn***
11:45-12:00				CER-O-02 Destructive & Non-destructive Behavior of Nickel Oxide Doped Bioactive Glass & Glass-ceramic ***Vikash Kumar Vyas***	ENR-O-04 Graphene Passivation of Aluminum Current Collector for Supercapacitor Electrode ***Jedsada Manyam***	POL-O-02 Low Haze and Antifog Performance of 2-layer Poly(lactic acid) Based Films ***Pitcha Liewchirakorn***			SUR-O-04 Thermal Sprayed Technique for Preparing HEA-Reinforced Oxide Matrix Composite ***Hathaipat Koiprasert***	DMC-O-02 C^1 –triangular Finite Elements on a Curvilinear Boundary Domain ***Wassamon Phusakulkajorn***
12:00-13:00	**Lunch (Sarocha Room, 3rd**		**Lunch (4th Avenue Room, 4th Floor)**							

Session	TSDB 2	MRS 2	Biomedical Materials and Devices 1	Ceramics 2 (Ceramic Materials for Energy and Environmental Application)	Materials for Energy 2	Polymers 2	Materials Technology for Environment 2	TTA 1	Surface Engineering and Heat Treatment 2	Design & Manufacturing and Computational Science & Engineering 2
Session Chair	Dr.Sani Boonyagul	Assoc.Prof. Pakorn Opaprakasit	Dr. Robert Molloy	Dr. Anucha Wannagon & Dr. Samunya Sanguanpak	Dr. Sumittra Charojrochkul	Assoc.Prof. Cattaleeya Pattamaprom	Dr. Yot Boontongkong	Dr. Sasawat Mahabunphachai	Dr. Tongjai Chookajorn	Dr. Pratarn Wongsarivej
13:00-13:15	The 3rd Meeting of Thai Society of Dental Biomaterials		BIO-I-01 Development of Joint Prosthesis ***Yoshio Nakashima***	CER-I-02 Current Researches on TiO_2-based Nanocomposites and Applications ***Assoc.Prof. Wisanu Pecharapa***	ENR-I-01 Development of Metal-supported Solid Oxide Fuel Cell (MS-SOFC) and Thin-film Solid Oxide Fuel Cell in KAIST ***Prof. Joongmyeon Bae***	POL-I-02 Hierarchic Structures and Propeties of Natural Rubber ***Assoc.Prof. Seiichi Kawahara***	ENV-I-02 Modified Soil Compositions for Removals of Acetaminophen ***Assoc.Prof. Thammarat Koottatep***	Thai Tribology Association Forum Title "Tribology in Aerospace Parts Manufacturing"	SUR-O-05 Effect of Impingement Angle on Erosion Resistance of HVOF Sprayed WC-10Co-4Cr Coating on CA6NM Steel ***Anurag Hamilton***	DMC-I-02 The Role of Advanced Numerical Simulation in Vehicle Safety Research and Development ***Assoc.Prof. Julaluk Carmai***
13:15-13:30									SUR-O-06 Sintered Metal Microstructure Influenced by Deep Rolling and Carburizing Processes ***Sai-Yan Primee***	
13:30-13:45		The 1st Annual Meeting of MRS-Thailand "Innovative Materials for Industry 4.0 (Academic Section)"	BIO-O-03 The Study of ABO-Rh Blood Typing on Reusable Polymeric Chip by Surface Plasmon Resonance Technique ***Chanwit Kataphiniharn***	CER-O-03 Effective Charge Separation and Photocatalytic Activity of Copper Ions -Modified Cerium Dioxide Nanoparticles ***Duangdao Channei***	ENR-O-05 Pre-Immobilization of Anaerobic Mixed Culture on Electrode of the Upflow Bio-Filter Circuit Microbial Fuel Cell ***Chinnatad Sinprasertchok***	POL-O-03 Effect of Poly(hexamethylene succinamide) on Crystallization of Poly(L-lactic acid) ***Panadda Yueagyen***	ENV-I-03 Practical Method for Bentonite Recovery from Foundry Sand Dust ***Asst.Prof. Pichaya Rachdawong***		SUR-O-10 Structural Characterization of Reactive DC Magnetron Co-Sputtered Nanocrystalline CrAlN Thin Film ***Amonrat Khambun***	DMC-O-03 Finite Element Analysis of the Impact Test of Alloy Wheels ***Somboon Otarawanna***
13:45-14:00			BIO-O-04 Preparation and Characterization of Artificial Nerve Guidance Conduits Based on Polycaprolactone/ Polyaniline/ Collagen Type 1 Composite Nanofibers Using Rat Sciatic Nerve Injury Model ***Christina Binag***	CER-O-04 Photocatalytic Degradation Study of Titania Sol-gel Coated on Commercial Unglazed Ceramics Tiles ***Pat Sooksaen***	ENR-O-06 Studies on CeP_2O_7-ZrP_2O_7 Solid Solutions: Electrolytes for Intermediate Temperature Proton-Conducting Ceramic-Electrolyte Fuel Cells (IT-PCFC) ***Aman Bhardwaj***	POL-O-04 Effect of Poly (D-lactic acid)-*co*-Polyethylene glycol on Crystallization of Poly (L-lactic acid) ***Ploywee Kaewlamyai***			SUR-O-11 Hardfacing of 3.5% Chromium Cast Steel by Flux Cored Wire Arc Welding Process ***Teerachod Treeparee***	DMC-O-04 The Pretensioning Value and the Mode of Failure on the Friction High Quality Bolt Connections ***Anis Rosyidah***
14:00-14:15				CER-O-05 Development of Infrared Reflective Black Pigment ***Pattana Rakkwamsuk***	ENR-O-07 Experimental Investigation of Electrospray Coating Technique for Electrode Fabrication in PEMFCs ***Natthika Chingthamai***	POL-O-05 Morphology and Properties of Polyoxymethylene/Polypropylene/Microcrystalline Cellulose Composites ***Nipawan Yasumlee***	ENV-O-03 Preparation, Characterization, and Photocatalytic Properties of rGO-TiO_2-Rubber Composite Sheets for Dye Decomposition in Wastewater ***Worapol Tejangkura***	*Asst. Prof. Numpon Mahayotsanun* 14:00-15:00 Thai Tribology Association Panel Discussion: "How to Integrate Existing Technology to Develop Aerospace Products"	SUR-O-12 Study on Friction Characteristics of Nano Filler for Friction Material ***Ratchanon Chamnipan*** CANCELLED	DMC-O-05 Design and Construction of a Restoring Force Measuring Apparatus for Assessment of Internal Stress Within Kiln-dried Lumber ***Sataporn Jantawee***
14:15-14:30					ENR-O-08 BaO-Al_2O_3-SiO_2-B_2O_3 Glass-Ceramic SOFCs Sealant: Effect of ZnO Additive ***Jiratchaya Ayawanna***	POL-O-06 Poly(lactic acid)-Polybutylene Succinate-Activated Carbon Composite Foams ***Kittimasak Ketkul***	ENV-O-04 Fabrication Study of Hydrophobic Polyurethane Sponge for Oil-Spills Cleanup ***Peeranut Prakulpawong***		SUR-O-13 Surface Modified Sterling Silver using Nitrogen Ion Implantation Technique ***Benya Cherdhirunkorn***	DMC-O-06 Formability Characterization of Advanced High Strength Steel Sheet by using Fukui Stretch-Drawing and Square Cup Drawing Tests ***Sansot Panich***
14:30-16:00	**Break & Poster Session I**									

Session		MRS 3	Biomedical Materials and Devices 2	Ceramics 3 (Electroceramics)	Materials for Energy 3	Polymers 3	Materials Technology for Environment 3	TTA 2		Design & Manufacturing and Computational Science & Engineering 3
Session Chair			Dr. Boriphat Methachan & Dr. Pacharapan Sonthithai	Dr. Natthaphon Raengthon	Dr. Pimpa Limthongkul	Asst.Prof. Somsak Dangtip	Dr. Noramon Intaranont			Dr. Somboon Otarawanna
16:00-16:15			BIO-O-05 Biological Responses of Porcine Chondrocytes and Human Bone Marrow Mesenchymal Stem Cells on Porous PCL/PHBV Blended Scaffolds ***Pakkanun Kaewkong***	CER-I-03 Exploration of Electronic Properties in "Materials Beyond Graphene": Transition Metal Dichalcogenides ***Asst.Prof. Worawat Meevasana***	ENR-O-09 Investigation of Electronic Conductivity of Co-Doped $LiFePO_4$ Material for Lithium Ion Batteries by Impedance Spectroscopy Technique ***Phongsit Krabao***	POL-O-08 Numerical Simulations of Geometric Extrudate Swelling in Polymer Melt Extrusion Using Arbitrary Lagrangian Eulerian (ALE) Based Finite Element Method on Free Surface ***Mongkol Kaewbumrung***	ENV-I-04 Experience in Sustainable Development through Textile Material Developing for the Community Enterprises (OTOPs) in Thailand ***Pilan Dhammongkol***	Thai Tribology Association Annual Meeting (Closed Session)		DMC-O-08 Effect of Feed-flow Rate on Solid-liquid Hydrocyclone based on Novel Separation Efficiency Equation ***Pichai Soison***
16:15-16:30			BIO-O-06 In Vitro Study of Biological Response by Human Gingival Fibroblast on Silk Fibroin/Alpha Tricalcium Phosphate Composite Scaffolds : A Preliminary Study ***Woradej Pichaiaukrit***		ENR-O-10 Synthesis, Structure, and Ionic Conductivity of Lithium-Strontium Aluminum/Gallium-Tantalum-Oxides with Perovskite Structure ***Thanya Phraewphiphat***	POL-O-09 Preparation of TO_2/WO_3 Composite Nanofiber by Electrospinning ***Patthamapa Chakornpradit***				DMC-O-09 Development of Regression Model of $Stk_{50}Eu$ for Hydrocyclone ***Pakpoom Supachart***
16:30-16:45		The 1st Meeting of MRS-Thailand Annual Meeting (Closed Session)	BIO-O-07 Novel Biodegradable Copolymers of Glycerol Sebacate and Amino Acid for Cartilage Tissue Regeneration ***Piyarat Sungkhaphan***	CER-O-06 Actuators Based on Bidomain Ferroelectric Crystals: Fabrication and Application ***Ilya Kubasov***	ENR-O-11 Multi-walled Carbon Nanotubes (MWCNTs) on a Metal Substrate with Quantum Dots in Photovoltaics ***Udorn Junthorn***	POL-O-10 Silane Modified-WO_3 for Improving Photochromic Properties of PC/WO_3 Composite Films ***Tanes Sangpraserdsuk***	ENV-O-05 A Feasibility Study of using Biofilter Media made from Biomass Ash for Nitrogen Compound Removal in Aquaculture ***Tahmina Sultana***			DMC-O-10 Development and Characterizations of a Projection Stereolithography ***Thossaporn Kaewwichit***
16:45-17:00			BIO-O-08 Studies on Effect of CuO on Mechanical Properties and in vitro Performance in 13–93 Bioactive Glass Scaffolds ***Akher Ali***	CER-O-07 Effects of Aluminium Concentrations and Consolidation Techniques on Composition, Microstructure and Dielectric Properties of Strontium Titanate ***Jednupong Palomas***	ENR-O-13 Synthesis of Novel Ternary Semiconductor-Silver Bismuth Telluride for Solar Cell Application ***Patamaporn Termsaithong***	POL-O-11 Effect of Silicon Carbide on Thermal and Mechanical Properties of Polypropylene Composites ***Watthanaphon Cheewawuttipong*** CANCELLED	ENV-O-02 On the Application of Electrocoagulation/Flotation (ECF) Technique for Cationic Dye Removal using Aluminium Electrode and Sodium Dodecyl Sulfate (SDS) ***Galuh Yuliani***			DMC-O-11 Effect of Post-curing Temperature and Mechanical Surface Treatment on Shear-bond Strength of Asbestos-free Brake Pad ***Danuwat Pupan***
17:00-17:15			BIO-O-09 Surface-modified PLGA Particles that Protect Against Myocardial Cell Death ***Amaraporn Wongrakpanich***	CER-O-08 Effects of Ball Milling on the Properties of $(Ba_{1-x}Ca_x)(Ti_{0.92}Sn_{0.08})O_3$ Lead-Free Ceramics ***Onchuda Wattanapradit***	ENR-O-14 Silica and Activated Carbon Nanocomposite from Rice Husks for Lithium Ion Batteries ***Yutthanakon Kanaphan***	POL-O-12 Enhancement of Dielectric β-phase PVDF Piezoelectric Composite by Base Modified Surface Activated Carbon Nanofiller ***Saiwan Nawalertpanya***	ENV-O-07 Adsorptive and Acid Properties of Zeolite; Effects of Synthesize Methods ***Galuh Yuliani***			DMC-O-07 Effect of an Anisotropic Hyperelastic Model on Blood Flow Pattern in a Small vessel with Stenosis ***Mongkol Kaewbumrung***
17:15-17:30						POL-O-15 Medicated Pressure Sensitive Adhesive Patches from STR-5L Block Rubber: Effect of Preparing Process ***Rungtiwa Waiprib***	ENV-O-08 Removal of Arsenic from Groundwater using Nano-Metal Oxide Adsorbents ***Phitchaya Muensri***			
17:30-18:00	**Poster Session II**									
18:00-20:00	**Banquet (4th Avenue Room, 4th Floor)**									

Day II	December 15th, 2016							
08:00-09:00	**Registration (Foyer Area, 2nd Floor)**							
Room	**Le Concorde Room (2nd Floor)**							
09:00-09:45	**Plenary Lecture 3:** 2D Materials: Technology, Standards and Science **by *Prof. Antonio Castro Neto***							
09:45-10:30	**Plenary Lecture 4:** Advanced Electron Microscopy and Spectroscopy for Materials Research and Development **by *Prof. Supapan Seraphin***							
10:30-10:45	**Break**							
Room		**Jamjuree**	**Krisana**	**Sakthong**	**Rachavadee**	**Patumchard**	**Uboncharad**	**Satabud**
Floor		**2nd Floor**	**2nd Floor**	**2nd Floor**	**2nd Floor**	**3rd Floor**	**3rd Floor**	**3rd Floor**
Session		**Biomedical Materials and Devices 3**	**Ceramics 4** (Geopolymers)	**Materials for Energy 4**	**Materials Technology for Environment 4**	**Metals, Alloys & Intermetallic Compounds 2** (Powder Metallurgy I)	**TCMA**	**Advanced Materials Testing and Characterization 1**
Session Chair		Dr. Jintamai Suwanprateeb & Dr.Katanchalee Mai-ngam	Prof. Cristina Leonelli	Dr. Yatika Somrang	Narueporn Vaneesorn	Dr. Dhritti Tanprayoon	Dr. Namurata Sathirachinda Palsson	Dr. Chanchana Thanachayanont
10:45-11:00		BIO-O-11 Comparison of the Release of Aloe Vera Extracts from Poly(vinyl alcohol) Electrospun Fibers and Hydrogel Films for Wound Healing Applications ***Sutasinee Sirima***	CER-I-05 Geopolymer from Industrial Wastes and its Applications ***Asst.Prof. Sirithan Jiemsirilers***	ENR-O-15 Zeolite Supported Bimetallic Catalyst System: The Effect of Metal Loading For Catalytic Pyrolysis of Jatropha Residue ***Vituruch Goodwin***	ENV-I-05 Quality Drying of Lumber: From Laboratory to Industry ***Asst.Prof. Nirundorn Matan***	MET-O-05 Sintered Dual-phase Steels with Different Alloy Compositions ***Monnapas Morakotjinda***	Thai Corrosion of Metal and Materials Association Forum	ADV-I-01 Electron Microscopy Investigation of Nanocomposites Between Metal/alloy and N-rGO for Renewable Energy Applications ***Assoc.Prof. Thapanee Sarakonsri***
11:00-11:15		BIO-O-13 Fluoride Recharge Ability of Resin-based Pit and Fissure Sealant with Synthesized Mesoporous Silica Filler ***Atikom Surintanasarn***		ENR-O-16 Two States Combustion Burner Using Used Engine Oil as Fuel ***Taveesin Lekpradit***		MET-O-06 Widmanstätten Ferrite in Fast-Cooled Ultralow Carbon Fe-Cr-Mo Steel ***Ruangdaj Tongsri***		
11:15-11:30		BIO-O-14 Factors Influencing the Deposition of Biomimetic Calcium Phosphate on 3D Printed Hydroxyapatite Substrate ***Faungchat Thammarakcharoen***	CER-O-15 Improvement of Compressive Strength and Thermal Shock Resistance of Fly Ash-Based Geopolymer Composites ***Patthamaporn Timakul***	ENR-O-17 Copper Doped Zinc Oxide: A Promising Material for Biogas Desulfurization ***Kannasoot Kanokkanchana***	ENV-O-09 Dowel Bearing Strength of Rubberwood ***Raphaela Hellmayr***	MET-O-07 Interaction between Recrystallization and Phase Transformation during Hot Squeezing of Sintered Dual-phase Fe-Cr-Mo-C Steels ***Bhanu Vetayanugul***		ADV-I-02 Structure-property Relationship of Polymeric Materials Studied by Electron Tomography ***Prof. Hiroshi Jinnai***
11:30-11:45			CER-O-16 Synthesis and Properties of Geopolymers from Two Different Power Plants Bottom Ash in Thailand **Anucha Wannagon**	ENR-O-18 Porous Carbon-doped TiO_2 on TiC Nanostructures for Co-catalyst Free Photocatalytic Hydrogen Production under Visible Light ***Jiaqian Qin***	ENV-O-10 Assessment of Hydrophilic Biochar Effect on Sandy Soil Water Retention ***Ramida Rattanakam***	MET-O-08 Dynamic Recrystallization and Cr_2O_3 Pinning Effect during Hot Squeezing of Sintered Ultralow Carbon Fe-Cr-Mo Steels ***Amornsak Rengsomboon***		
11:45-12:00					ENV-O-11 Preparation of Activated Carbon from Sugarcane Bagasse Waste for the Adsorption Equilibrium and Kinetics of Basic Dye ***Tawan Chaiwon***			ADV-O-01 Investigation of Stripe Emitter Area (Ae) on the design on Heterojunction Bipolar Transistor Silicon-Germanium (SiGe-HBT) ***Tossin Alamsyah***
12:00-12:15								ADV-O-03 Fe K-edge and Ti K-edge XAS Study of Blue Sapphires ***Nirawat Thammajak***
12:15-13:00	**Lunch (4th Avenue Room, 4th Floor)**							

Room	Krisana	Rachavadee	Patumchard	Ubonchard
Floor	2nd Floor	2nd Floor	3rd Floor	3rd Floor
Session	**Ceramics 5** (Novel Synthesis and Solid State Materials)	**Materials Technology for Environment 5**	**Metals, Alloys & Intermetallic Compounds 3** (Non-ferrous: Sintering and Casting)	**Corrosion**
Session Chair	Dr. Sorachon Yoriya	Dr. Noramon Intaranont	Dr. Chakkrist Phongphisutthinan	Dr. Pitichon Klomjit
13:00-13:15	CER-I-04 Engineering Hybrid Nanocapsules for Multifunctional Applications in Bioimaging ***Prof. John Wang***	ENV-I-01 Design of Metal Oxide Nanostructured Materials for Enhanced Photocatalytic Energy & Environmental Sustainability ***Assoc.Prof. Ho Ghim Wei***	MET-O-09 Understanding the Microstructural Features in High-Pressure Die Castings by Analogy with Granular Materials and Suspensions ***Somboon Otarawanna***	COR-O-01 Characteristics of Internal Oxide Scale of T91 Superheater Tube after 1000h Exposure to Steam Temperature at 605°C ***Suraya Nadzir***
13:15-13:30			MET-O-10 The Effect of Bottom Ash Additions on the Properties of Sintered Bronze-Graphite Composites ***Usanee Pantulap***	COR-O-03 The Role of Al-Mn Intermetallics on the Corrosion of AZ31 Magnesium Alloy ***Somi Doja***
13:30-13:45	CER-O-09 Photocatalytic Comparative Study of TiO_2, ZnO, Ag-G-ZnO and Ag-G-TiO_2 Nanocomposite Films: Biomaterial Applications ***Phuri Kalnaowakul***	ENV-O-12 Effect of Cell Wall Constituents On Internal Stress Generation During Drying of Lumber Prepared From Rubber Tree Trunks ***Jaipet Tomad***	MET-O-11 Properties of Sintered Bronze-Graphite Containing Natural Anhydrite ***Chiraporn Auechalitanukul***	COR-O-04 Corrosion Behavior of Al-Zn-In Sacrificial Anode Alloys Produced by Conventional Casting and Semi-Solid Metal Casting Processes ***Chanika Puridetvorakul***
13:45-14:00	CER-O-10 Development of Water Assisted Solid State Reaction for the Ceramic Materials ***Kenji Toda***	ENV-O-13 Improvement of Compressive Strength of Soil by Using Jute Fiber Waste ***Md. Bayezid Islam***	MET-O-12 Mechanical Properties of As-Exposed Al-SiCp Composite Fabricated by Powder Injection Moulding ***Tapany Patcharawit***	COR-O-05 Development of Pitting Corrosion Monitoring Method by Saline Solution Droplet under Wet-Dry Cycles ***Wongpat Banthukul***
14:00-14:15	CER-O-11 Effect of Particle Size Distribution on the Sinterability of Cerium (IV) Oxide using Spark Plasma Sintering ***Anil Prasad***	**Break**	MET-O-13 Effect of Aluminum Addition on $Al_xCoFeMnNiZn$ Multi-Component Production ***Amnart Suksamran***	COR-O-06 Failure Analysis of Protection Tube of a Temperature Element in a Sulfiding Environment ***Siriwan Ouampan***
14:15-14:30	CER-O-21 Optimum Partial Replacement of Cement by Nanosilica, Microsilica and Rice Husk Ash for Mass Production of Concrete ***Winai Ouypornprasert***		MET-O-14 Effect of Si Content on Mechanical Properties of Ti-Si-N Ternary Alloys Prepared by Spark Plasma Sintering ***Patcharawat Khemglad***	COR-O-07 Effect of Cr Content on the Passivation Layer Properties of Tinplate Steel ***Kosit Wongpinkaew***
14:30-14:45	**Break**		**Break**	

Session	Ceramics 6 (Glass, Film and Coating)		Metals, Alloys & Intermetallic Compounds 4 (Powder Metallurgy II)	Metals, Alloys & Intermetallic Compounds 5 (Welding, Soldering, and Evaluation)
Session Chair	Prof. John Wang		Bhanu Vetayanugul	Dr. Sinthu Chanthapan
14:45-15:00	CER-O-17 Synthesis of Silicon-Carbon Films by High-Frequency Deposition ***Alexander Temirov***		MET-O-15 Role of SiC in Sintered Fe-Mo-Si-C Steels ***Thanyaporn Yotkaew***	MET-O-22 Improvement of Semi-Solid State Joining of SSM Aluminum Alloys ***Patsapon Binrohim***
15:00-15:15	CER-O-18 Effects of Buffer Layer Growth Temperature on Micro-structures in the Cubic GaN Films Grown on GaAs (001) Substrates by MOVPE ***Pornsiri Wanarattikan***	Technical Meeting on Environmental Issues (Closed Session)	MET-O-16 Effect of SiC Particle Size on Sintered Fe-Mo-Si-C Steels ***Pongsak Wila***	MET-O-23 Fastenerless-Riveting Utilizing Friction Stir Forming for Dissimilar Materials Joining ***Takahiro Ohashi***
15:15:15:30	CER-O-19 Thermal Diffusivity of a Waterproof Glaze Layer of Clay Roof Tile Investigated by Mirage Effect ***Tanawut Rittidach***		MET-O-17 Retained Austenite in Sintered Bainitic Fe-Mo-Si-C Steels ***Dhritti Tanprayoon***	MET-O-24 Quantitative Evaluation of Hot Cracking Susceptibility of MGS6 GZ-60 Hardfacing Weld Metal Based on High Temperature Ductility Curve ***Rittichai Phaoniam***
15:30-15:45	CER-O-20 The Effect of Zirconium Oxide on Properties and Crystallization of Soda-lime Silicate Glass ***Ekarat Meechoowas***		MET-O-18 Modification of Microstructure and Tensile Property of Sintered Fe-Cr-Mo-C Steel by Nickel Addition ***Nattaya Tosangthum***	MET-O-25 Phase Equilibria and Thermodynamic Properties of the Ag-Bi-Cu-Sn Pb-free solder calculated by CALPHAD Approach ***Wojciech Gierlotka***
15:45-16:00	CER-O-14 Development of Metakaolin Based Geopolymers for Bone Graft Application ***Sarochapat Sutikulsombat***		MET-O-19 Combination Effects of Nickel and Graphite on Sintered Fe-Mo + SiC Alloy ***Rungtip Krataitong***	MET-O-26 The Investigation of Attenuation in AISI 316 Stainless Steel Weld for Ultrasonic Testing ***Mai Noipitak***
16:00-16:15			MET-O-20 Wear Properties of Sintered Fe-Mo-Si-C Steels with Spheroidal Graphite Iron/Compacted Graphite Iron-like Microstructures ***Kittikhun Ruangchai***	MET-O-27 Effect of Cooling Rate on the Microstructural and Mechanical Properties of Sn-0.3Ag-0.7Cu-0.05Ni Solder Alloy ***Kogaew Inkong***
16:15-16:30			MET-O-21 Characterization of Sintered Fe-Mo + SiC + H-BN Alloy ***Ussadawut Patakham***	MET-O-28 The Thermal-Aging Effect on the Microstructure Evolution and Shear Strength of the Sn-Rich Au-Sn Soldering between AlTiC and Si Substrate in Microelectronics ***Panaaek Athichalinthorn***

LIST OF ORAL & POSTER PRESENTATIONS

PLENARY LECTURES

PL-01 **"Bringing It All Back Home" How Waste-to-Biobased Products is Good for Energy, the Environment, Water, and Society**
Seth Snyder
Argonne National Laboratory, United State of America

PL-02 **Geopolymerization as Cold-consolidation Techniques for Hazardous and Non-hazardous Wastes**
Cristina Leonelli
University of Modena and Reggio Emilia, Italy

PL-03 **2D Materials: Technology, Standards and Science**
Antonio Castro Neto
National University of Singapore, Singapore

PL-04 **Advanced Electron Microscopy and Spectroscopy for Materials Research and Development**
Supapan Seraphin
University of Arizona, United State of America

ADVANCED MATERIALS TESTING AND CHARACTERIZATION

INVITED LECTURES

ADV-I-01 **Electron Microscopy Investigation of Nanocomposites between Metal/alloy and N-rGO for Renewable Energy Applications**
Thapanee Sarakonsri
Chiang Mai University, Thailand

ADV-I-02 **Structure-property Relationship of Polymeric Materials Studied by Electron Tomography**
Hiroshi Jinnai
Tohoku University, Japan

ORAL PRESENTATIONS

ADV-O-01 **Investigation of Stripe Emitter Area (AE) on the Design on Heterojunction Bipolar Transistor Silicon-Germanium (SiGe-HBT)**
Tossin Alamsyah
Politeknik Negeri Jakarta, Indonesia

ADV-O-03 **Fe *K*-edge and Ti *K*-edge XAS Study of Blue Sapphires**
Nirawat Thammajak
Synchrotron Light Research Institute (Public Organization), Thailand

POSTER PRESENTATIONS

ADV-P-01 **X-Ray Diffraction Analysis of ZnO Particles Prepared by Microwave Plasma**
Parinya Chakartnarodom
Kasetsart University, Thailand

ADV-P-02 **Characterization of Improved White Sapphire with Lithium-Glass**
Natthaphol Chomsaeng
Burapha University (Chanthaburi Campus), Thailand

ADV-P-03 **Influence of Scanning Parameters on X-Ray Diffraction Peaks of Copper**
Parinya Chakartnarodom
Kasetsart University, Thailand

ADV-P-04 **Temperature Effect on Synthesis of Carbon Nanotubes by Catalytic Chemical Vapor Deposition**
Visittapong Yordsri
National Metal and Materials Technology Center, Thailand

ADV-P-05 **Application of Soft X-Ray Emission Spectrometer on Microstructure Investigation of High Temperature Stainless Steel**
Viyaporn Krongtong
National Metal and Materials Technology Center, Thailand

ADV-P-06 **Rapid Analysis of Residual Styrene Monomer and Oligomer in Polystyrene Using Fragmentless Ionization Mass Spectrometry**
Takahisa Tsugoshi
National Institute of Advanced Industrial Science and Technology (AIST) , Japan

BIOMEDICAL MATERIALS AND DEVICES

INVITED LECTURE

BIO-I-01 **Development of Joint Prosthesis**
Yoshio Nakashima
Teijin Nakashima Medical Co., Ltd., Japan

ORAL PRESENTATIONS

BIO-O-03 **The Study of ABO-Rh blood Typing on Reusable Polymeric Chip by Surface Plasmon Resonance Technique**
Chanwit Kataphiniharn
King Mongkut's University of Technology North Bangkok, Thailand

BIO-O-04 **Preparation and Characterization of Artificial Nerve Guidance Conduits Based on Polycaprolactone/Polyaniline/Collagen Type 1 Composite Nanofibers Using Rat Sciatic Nerve Injury Model**
Christina Binag
University of Santo Tomas, Philippines

BIO-O-05 **Biological Responses of Porcine Chondrocytes and Human Bone Marrow Mesenchymal Stem Cells on Porous PCL/PHBV Blended Scaffolds**
Pakkanun Kaewkong
National Metal and Materials Technology Center, Thailand

BIO-O-06 **In Vitro Study of Biological Response by Human Gingival Fibroblast on Silk Fibroin/Alpha Tricalcium Phosphate Composite Scaffolds : A Preliminary Study**
Woradej Pichaiaukrit
Rangsit University, Thailand

BIO-O-07 **Novel Biodegradable Copolymers of Glycerol Sebacate and Amino Acid for Cartilage Tissue Regeneration**
Piyarat Sungkhaphan
National Metal and Materials Technology Center, Thailand

BIO-O-08 **Studies on Effect of CuO on Mechanical Properties and In vitro Performance in 13–93 Bioactive Glass Scaffolds**
Akher Ali
Indian Institute of Technology (B.H.U.), India

BIO-O-09 **Surface-modified PLGA Particles that Protect Against Myocardial Cell Death**
Amaraporn Wongrakpanich
Mahidol University, Thailand

BIO-O-11 **Comparison of the Release of Aloe Vera Extracts from Poly(vinyl alcohol) Electrospun Fibers and Hydrogel Films for Wound Healing Applications**
Sutasinee Sirima
King Mongkut's University of Technology Thonburi, Thailand

BIO-O-13 **Fluoride Recharge Ability of Resin-based Pit and Fissure Sealant with Synthesized Mesoporous Silica Filler**
Atikom Surintanasarn
Chulalongkorn University, Thailand

BIO-O-14 **Factors Influencing the Deposition of Biomimetic Calcium Phosphate on 3D Printed Hydroxyapatite Substrate**
Faungchat Thammarakcharoen
National Metal and Materials Technology Center, Thailand

POSTER PRESENTATIONS

BIO-P-01 **Improving Mechanical Properties of Biphasic Calcium Phosphate Bone Cement by Chitosan Fiber Reinforcement**
Nuan La-Ong Srakaew
Rajamangala University of Technology Isan, Thailand

BIO-P-02 ***In vivo* of Sericin-Polyurethane Nanofiber Mats for Wound Healing in Rat**
Pornpen Siridamrong
Chulalongkorn University, Thailand

BIO-P-03 ***In Vitro* Evaluation of Zein as Matrix Forming Agent in Extended Released Tablets Containing Theophylline**
Noppadol Chongcherdsak
Siam University, Thailand

BIO-P-04 **Preparation and Characterization of Hydroxyapatite Powder from Cockle Shells**
Tiwasawat Sirisoam
Chiang Mai University, Thailand

BIO-P-05 **Crystallization, Mechanical Properties and *In vitro* Bioactivity Assessment of (45S5-HA) Biocomposite**
Sunil Prasad
Indian Institute of Technology (B.H.U.), India

BIO-P-06 **Mechanical Property and Morphology of Porous Fluorcanasite Glass-Ceramics Doped with Bioglass**
Autcharaporn Srion
National Metal and Materials Technology Center, Thailand

BIO-P-07 CANCELLED **Double-walled PLA-PLGA Particles, a Particulate Delivery System for Cancer Vaccines**
Amaraporn Wongrakpanich
Mahidol University, Thailand

BIO-P-10 **Shear Bond Strength of Resin Cement between Mica Glass-Ceramic and Human Dentin**
Thapanee Srichumpong
Kasetsart University, Thailand

CERAMICS

INVITED LECTURES

CER-I-01 **Machinable Glass-Ceramics as a Dental Material**
Duangrudee Chaysuwan
Kasetsart University, Thailand

CER-I-02 **Current Researches on TiO_2-based Nanocomposites and Applications**
Wisanu Pecharapa
King Mongkut's Institute of Technology Ladkrabang, Thailand

CER-I-03 **Exploration of Electronic Properties in "Materials Beyond Graphene": Transition Metal Dichalcogenides**
Worawat Meevasana
Suranaree University of Technology, Thailand

CER-I-04 **Engineering Hybrid Nanocapsules for Multifunctional Applications in Bioimaging**
John Wang
National University of Singapore, Singapore

CER-I-05 **Geopolymer from Industrial Wastes and its Applications**
Sirithan Jiemsirilers
Chulalongkorn University, Thailand

ORAL PRESENTATIONS

CER-O-01 **Synthesizing of Glass-Ceramics Composites for Opal Imitation by Direct Sintering Method**
Saweat Intarasiri
Chiang Mai University, Thailand

CER-O-02 **Destructive & Non-destructive Behavior of Nickel Oxide Doped Bioactive Glass & Glass-ceramic**
Vikash Vyas
Indian Institute of Technology (B.H.U.), India

CER-O-03 **Effective Charge Separation and Photocatalytic Activity of Copper Ions -Modified Cerium Dioxide Nanoparticles**
Duangdao Channei
Naresuan University, Thailand

CER-O-04 **Photocatalytic Degradation Study of Titania Sol-gel Coated on Commercial Unglazed Ceramic Tiles**
Pat Sooksaen
Silpakorn University, Thailand

CER-O-05 **Development of Infrared Reflective Black Pigment**
Pattana Rakkwamsuk
King Mongkut's University of Technology Thonburi, Thailand

CER-O-06 **Actuators Based on Bidomain Ferroelectric Crystals: Fabrication and Application**
Ilya Kubasov
National University of Science and Technology (MISIS), Russian Federation

CER-O-07 **Effects of Aluminium Concentrations and Consolidation Techniques on Composition, Microstructure and Dielectric Properties of Strontium Titanate**
Jednupong Palomas
Kasetsart University, Thailand

CER-O-08 **Effects of Ball Milling on the Properties of $(Ba_{1-x}Ca_x)(Ti_{0.92}Sn_{0.08})O_3$ Lead-Free Ceramics**
Onchuda Wattanapradit
Prince of Songkla University, Thailand

CER-O-09 **Photocatalytic Comparative Study of TiO_2, ZnO, Ag-G-ZnO and Ag-G-TiO_2 Nanocomposite Films: Biomaterial Applications**
Phuri Kalnaowakun
Kasetsart University, Thailand

CER-O-10 **Development of Water Assisted Solid State Reaction for the Ceramic Materials**
Kenji Toda
Niigata University, Japan

CER-O-11 **Effect of Particle Size Distribution on the Sinterability of Cerium (IV) Oxide using Spark Plasma Sintering**
Anil Prasad
University of British Columbia, Canada

CER-O-14 **Development of Metakaolin Based Geopolymers for Bone Graft Application**
Sarochapat Sutikulsombat
Kasetsart University, Thailand

CER-O-15 **Improvement of Compressive Strength and Thermal Shock Resistance of Fly Ash-Based Geopolymer Composites**
Patthamaporn Timakul
National Metal and Materials Technology Center, Thailand

CER-O-16 **Synthesis and Properties of Geopolymers from Two Different Power Plants Bottom Ash in Thailand**
Anucha Wannagon
National Metal and Materials Technology Center, Thailand

CER-O-17 **Synthesis of Silicon-Carbon Films by High-Frequency Deposition**
Alexander Temirov
National University of Science and Technology (MISIS), Russian Federation

CER-O-18 **Effects of Buffer Layer Growth Temperature on Micro-structures in the cubic GaN Films Grown on GaAs (001) Substrates by MOVPE**
Pornsiri Wanarattikan
Huachiew Chalermprakiet University, Thailand

CER-O-19 **Thermal Diffusivity of a Waterproof Glaze Layer of Clay Roof Tile Investigated by Mirage Effect**
Tanawut Rittidach
Kasetsart University, Thailand

CER-O-20 **The Effect of Zirconium Oxide on Properties and Crystallization of Soda-lime Silicate Glass**
Ekarat Meechoowas
Department of Science Service, Thailand

CER-O-21 **Optimum Partial Replacement of Cement by Nanosilica, Microsilica and Rice Husk Ash for Mass Production of Concrete**
Winai Ouypornprasert
Rangsit University, Thailand

POSTER PRESENTATIONS

CER-P-01 **Characterization and Properties of Cordierite – Mullite Refractories from Raw Materials and Narathiwat Clay (in Thailand)**
Nattawut Ariyajinno
Chiang Mai University, Thailand

CER-P-02 **The Studies on The Mechanical and Thermal Properties of Geopolymer Mortar**
Pongsak Jittabut
Nakhon Ratchasima Rajabhat University, Thailand

CER-P-03 **Slip Degassing to Improve the Properties of Slip Cast and Reaction Bonded Si_3N_4**
Kritkaew Somton
National Metal and Materials Technology Center, Thailand

CER-P-04 **Influence of Temperature and Alkaline Activation for Synthesis Zeolite A from Natural Kaolin**
Pimpreeya Thungngern
King Mongkut's Institute of Technology Ladkrabang, Thailand

CER-P-05 **Effect of M-Type Hexaferrite on Mechanical and Magnetic Properties of Hydroxyapatite Ceramics**
Rewadee Wongmaneerung
Maejo University, Thailand

CER-P-06 **Surface Modification of TiO_2 with the Sonochemical Method**
Eakkasit Thasirisap
King Mongkut's Institute of Technology Ladkrabang, Thailand

CER-P-07 **Structure, Magnetic Property and Energy Band Gap of Fe-doped NiO Nanoparticles Prepared by co-Precipitation Method**
Buppachat Toboonsung
Nakhon Ratchasima Rajabhat University, Thailand

CER-P-08 **Synthesis of Nanocrystalline Cobalt Ferrite by the Sonochemical Method in Highly Basic Aqueous Solution**
Patchara Pasupong
King Mongkut's Institute of Technology Ladkrabang, Thailand

CER-P-09 **Fabrication of Low Cost Membrane from Anodic Aluminum Oxide (AAO)**
Peerawith Sumtong
King Mongkut's Institute of Technology Ladkrabang, Thailand

CER-P-11 **Effects of Aluminum Concentrations on Microstructure and Compressive Strength of Porous Concrete**
Napamas Jaroonvechatam
Kasetsart University, Thailand

CER-P-12 **Chemical Composition-Microstructure-Dielectric Constant Relations of Mg-doped Calcium Titanate Synthesized by Solid State Reaction Technique**
Nicha Sato
Kasetsart University, Thailand

CER-P-13 **Effect of Solids Loadings, Sintering Temperatures and Sintering Periods on Microstructure of Hydroxyapatite**
Jednupong Palomas
Kasetsart University, Thailand

CER-P-15 **Effects of Calcination Temperatures and Material Contents on Chemical Compositions of The Cement Powders Synthesized by Solution Combustion Technique**
Suphitsara Yingyuen
Kasetsart University, Thailand

CER-P-16 **Heavy Metal Immobilization of Fly Ash-based Geopolymers**
Ronnachai Pliansakul
Chulalongkorn University, Thailand

CER-P-17 **Synthesis and Characterization of Cerium- and Lanthanum -containing Bioactive Glass**
Md Ershad
Indian Institute of Technology (B.H.U.), India

CER-P-18 **Influence of Graphene Oxide on the Enhanced Photocatalytic Activity of Cerium Dioxide-Graphene Oxide Composites**
Duangdao Channei
Naresuan University, Thailand

CER-P-19 **Effect of Calcium Carbonate on Compressive Strength and Physical Properties of Alkali-activated Lightweight Concrete**
Watcharapong Wongkeo
Nakhon Ratchasima Rajabhat University, Thailand

CER-P-20 **Synthesis and Photocatalytic Activity of Visible-Light Responsive BiOBr/GO Composites**
Tuangphorn Prasitthikun
Chulalongkorn University, Thailand

CER-P-21 **Effect of Polymethylmethacrylate Content on Microstructure and Properties of Barium Orthotitanate Porous Ceramic**
Pratthana Chithit
Maejo University, Thailand

CER-P-23 **Use of Waste Glass as a Reinforce Material in Calcined-kaolin Based Geopolymer**
Siriwan Chokkha
Suranaree University of Technology, Thailand

CER-P-24 **Investigation of Physical, Mechanical and Thermal Properties of Building Wall Materials**
Jiraphorn Mahawan
Naresuan University, Thailand

CER-P-25 **Synthesis and Characterization of Zn^{+2} Doped Cobalt Ferrite Nanoparticles and 45S5 Bio-glass Composite for Application in Hyperthermia Treatment**
Aman Bhardwaj
Indian Institute of Technology (B.H.U.), India

CER-P-26 **Influence of Portland Cement on Physical, Mechanical and Thermal Properties of Cellular Lightweight Concrete**
Surirat Ketchaona
Naresuan University, Thailand

CER-P-27 **Structure and Ferroelectric Properties of $KNbO_3$ added $Bi_{0.5}Na_{0.5}TiO_3$ Ceramics**
Nuttapon Pisitpipathsin
Rajamangala University of Technology Isan, Thailand

CER-P-28 **The Effect of Calciumorthophosphate on Photocatalytic Activity of Titanium Dioxide Photocataly Beads**
Pakpassagun Somwong
Chulalongkorn University, Thailand

CER-P-30 **Effects of Air Exposure Time and Annealing Temperature on Superhydrophobic Surface of Titanium Dioxide Films**
S.Tipawan Khlayboonme
King Mongkut's Institute of Technology Ladkrabang, Thailand

CER-P-32 **Synthesis of Carbon and Zeolite Na-A Composites Powder from Rice Husk Charcoal as Raw Material for Slip Casting Process**
Thanakorn Tepamat
Chulalongkorn University, Thailand

CER-P-33 **Using of Basalt Fiber as Reinforcing Materials in Fiber-Cement Flat Sheet**
Apirat Theerapapvisetpong
Chulalongkorn University, Thailand

CER-P-34 **Effect of Silica Base Catalyst on Transformation of Methanol to Hydrocarbon**
Supranee Lao-Ubol
Thailand Institute of Scientific and Technological Research, Thailand

CORROSION

ORAL PRESENTATIONS

COR-O-01 **Characteristics of Internal Oxide Scale of T91 Superheater Tube after 1000h Exposure to Steam Temperature at 605°C**
Suraya Nadzir
TNB Research Sdn Bhd, Malaysia

COR-O-03 **The Role of Al-Mn Intermetallics On the Corrosion of AZ31 Magnesium Alloy**
Somi Doja
University of British Columbia, Canada

COR-O-04 **Corrosion Behavior of Al-Zn-In Sacrificial Anode Alloys Produced by Conventional Casting and Semi-Solid Metal Casting Processes**
Chanika Puridetvorakul
King Mongkut's University of Technology Thonburi, Thailand

COR-O-05 **Development of Pitting Corrosion Monitoring Method by Saline Solution Droplet under Wet-Dry Cycles**
Wongpat Banthukul
Kasetsart University, Thailand

COR-O-06 **Failure Analysis of Protection Tube of a Temperature Element in a Sulfiding Environment**
Siriwan Ouampan
National Metal and Materials Technology Center, Thailand

COR-O-07 **Effect of Cr Content on the Passivation Layer Properties of Tinplate Steel**
Kosit Wongpinkaew
National Metal and Materials Technology Center, Thailand

DESIGN & MANUFACTURING AND COMPUTATIONAL SCIENCE & ENGINEERING

INVITED LECTURES

DMC-I-01 **Meta-Heuristics for Engineering Optimisation**
Sujin Bureerat
Khon Kaen University, Thailand

DMC-I-02 **The Role of Advanced Numerical Simulation in Vehicle Safety Research and Development**
Julaluk Carmai
King Mongkut's University of Technology North Bangkok, Thailand

ORAL PRESENTATIONS

DMC-O-01 **Corrosion Prediction Using ANN for Offshore Pipeline in the Gulf of Thailand**
Passaworn Silakorn
PTT Exploration and Production PLC, Thailand

DMC-O-02 **C^1 –triangular Finite Elements on a Curvilinear Boundary Domain**
Wassamon Phusakulkajorn
National Metal and Materials Technology Center, Thailand

DMC-O-03 **Finite Element Analysis of the Impact Test of Alloy Wheels**
Somboon Otarawanna
National Metal and Materials Technology Center, Thailand

DMC-O-04 **The Pretensioning Value and the Mode of Failure on the Friction High Quality Bolt Connections**
Anis Rosyidah
Politeknik Negeri Jakarta, Indonesia

DMC-O-05 **Design and Construction of a Restoring Force Measuring Apparatus for Assessment of Internal Stress Within Kiln-dried Lumber**
Sataporn Jantawee
Walailak University, Thailand

DMC-O-06 **Formability Characterization of Advanced High Strength Steel Sheet by using Fukui Stretch-Drawing and Square Cup Drawing Tests**
Sansot Panich
King Mongkut's University of Technology North Bangkok, Thailand

DMC-O-07 **Effect of an Anisotropic Hyperelastic Model on Blood Flow Pattern in a Small Vessel with Stenosis**
Mongkol Kaewbumrung
Pathumthani University, Thailand

DMC-O-08 **Effect of Feed-flow Rate on Solid-liquid Hydrocyclone based on Novel Separation Efficiency Equation**
Pichai Soison
National Nanotechnology Center, Thailand

DMC-O-09 **Development of Regression Model of $Stk_{50}Eu$ for Hydrocyclone**
Pakpoom Supachart
King Mongkut's University of Technology Thonburi, Thailand

DMC-O-10 **Development and Characterizations of a Projection Stereolithography**
Thossaporn Kaewwichit
King Mongkut's University of Technology North Bangkok, Thailand

DMC-O-11 **Effect of Post-curing Temperature and Mechanical Surface Treatment on Shear-bond Strength of Asbestos-free Brake Pad**
Danuwat Pupan
Mahidol University, Thailand

POSTER PRESENTATIONS

DMC-P-01 **Computer-Aided Optimization for Multi-Pass Cold Drawing of Cobalt-Chromium Alloy Seamless Micro Tube**
Dongearn Kim
Korea Institute of Industrial Technology (KITECH), South Korea

DMC-P-02 **The Structural and Electronic Properties of FePc, CoPc and CuPc Monomer Structure: First Principles Study**
Witoon Nuleg
King Mongkut's Institute of Technology Ladkrabang, Thailand

MATERIALS FOR ENERGY

INVITED LECTURE

ENR-I-01 **Development of Metal-supported Solid Oxide Fuel Cell (MS-SOFC) and Thin-film Solid Oxide Fuel Cell in KAIST**
Joongmyeon Bae
Korea Advance Institute of Science and Technology (KAIST), South Korea

ORAL PRESENTATIONS

ENR-O-01 **Graphene-$AgVO_3$ Composite for Supercapacitor Applications**
Jiaqian Qin
Chulalongkorn University, Thailand

ENR-O-02 **Characterization of Polyaniline/Carbon Nanotube/Pineapple-Polyester Fabric Composites as Supercapacitor Electrodes**
Felicidad Christina Ramirez
University of Santo Tomas, Philippines

ENR-O-03 **Piña (*Ananas comosus*) and Water Hyacinth (*Eichhornia crassipes*) Polyester Blended Textiles with Polypyrrole as Supercapacitor Electrode Materials**
David Joseph Alzate
University of Santo Tomas, Philippines

ENR-O-04 **Graphene Passivation of Aluminum Current Collector for Supercapacitor Electrode**
Jedsada Manyam
National Nanotechnology Center, Thailand

ENR-O-05 **Pre-Immobilization of Anaerobic Mixed Culture on Electrode of the Upflow Bio-Filter Circuit Microbial Fuel Cell**
Chinnatad Sinprasertchok
National Metal and Materials Technology Center, Thailand

ENR-O-06 **Studies on CeP_2O_7-ZrP_2O_7 Solid Solutions: Electrolytes for Intermediate Temperature Proton-Conducting Ceramic-Electrolyte Fuel Cells (IT-PCFC)**
Aman Bhardwaj
Indian Institute of Technology (B.H.U.), India

ENR-O-07 **Experimental Investigation of Electrospray Coating Technique for Electrode Fabrication in PEMFCs**
Natthika Chingthamai
King Mongkut's University of Technology Thonburi, Thailand

ENR-O-08 **BaO-Al_2O_3-SiO_2-B_2O_3 Glass-Ceramic SOFCs Sealant: Effect of ZnO Additive**
Jiratchaya Ayawanna
Suranaree University of Technology, Thailand

ENR-O-09 **Investigation of Electronic Conductivity of Co-Doped $LiFePO_4$ Material for Lithium Ion Batteries by Impedance Spectroscopy Technique**
Phongsit Krabao
Khon Kaen University, Thailand

ENR-O-10 **Synthesis, Structure, and Ionic Conductivity of Lithium-Strontium Aluminum/Gallium-Tantalum-Oxides with Perovskite Structure**
Thanya Phraewphiphat
National Metal and Materials Technology Center, Thailand

ENR-O-11 **Multi-walled Carbon Nanotubes (MWCNTs) on a Metal Substrate with Quantum Dots in Photovoltaics**
Udorn Junthorn
Kochi University of Technology, Japan

ENR-O-13 **Synthesis of Novel Ternary Semiconductor-Silver Bismuth Telluride for Solar Cell Application**
Patamaporn Termsaithong
Kasetsart University, Thailand

ENR-O-14 **Silica and Activated Carbon Nanocomposite from Rice Husks for Lithium Ion Batteries**
Yutthanakon Kanaphan
Khon Kaen University, Thailand

ENR-O-15 **Zeolite Supported Bimetallic Catalyst System: The Effect of Metal Loading for Catalytic Pyrolysis of Jatropha Residue**
Vituruch Goodwin
National Metal and Materials Technology Center, Thailand

ENR-O-16 **Two Stage Combustion Burner Using Used Engine Oil as Fuel**
Taveesin Lekpradit
Ubon Ratchathani University, Thailand

ENR-O-17 **Copper Doped Zinc Oxide: A Promising Material for Biogas Desulfurization**
Kannasoot Kanokkanchana
Mahidol University, Thailand

ENR-O-18 **Porous Carbon-doped TiO_2 on TiC Nanostructures for Co-catalyst Free Photocatalytic Hydrogen Production under Visible Light**
Jiaqian Qin
Chulalongkorn University, Thailand

POSTER PRESENTATIONS

ENR-P-01 **The Study of Carbon Nanotubes as Conductive Additive of $Ca_3Co_4O_9$ Anode for Lithium-ion Battery**
Natkrita Prasoetsopha
Rajamangala University of Technology Isan, Thailand

ENR-P-02 **Microwave-Assisted Preparation of Sodium Silicate Used Rice Husk Ash as Precursor and Applications for Biodiesel Catalyst**
Jaturon Kumchompoo
Maejo University, Thailand

ENR-P-03 **Pelletization of Iron Oxide Based Sorbents for Hydrogen Sulfide Removal**
Pathompong Janetaisong
National Metal and Materials Technology Center, Thailand

ENR-P-04 **Multifunctional Magnetic Nanoparticle for Microaglal Biodiesel Production**
Kyubock Lee
Chungnam National University, South Korea

ENR-P-05 **One-pot Synthesis of $LiFePO_4$ Nano-particles Entrapped in Mesoporous Melamine-Formaldehyde Matrix as the Promising Cathode Materials for the Next Generation Lithium Ion Batteries**
Kantawich Jittmonkong
Kasetsart University, Thailand

ENR-P-06 **Large Area Fabrication of Stress-induced Lift-off Silicon Foil using Epoxy**
Hyo Sik Chang
Chungnam National University, South Korea

ENR-P-07 **Influence of Bi_2O_3 on Crystalline Phase Content and Thermal Properties of Åkermanite and Diopside based Glass-ceramic Sealant for SOFCs**
Pornchanok Lawita
Chulalongkorn University, Thailand

ENR-P-08 **The Study of Crystallization of Polyfluorene and Fullerene Derivatives in Semiconducting Layer of Organic Solar Cells**
Wantana Koetniyom
King Mongkut's Institute of Technology Ladkrabang, Thailand

ENR-P-09 **Effect of Clays on Pyrolysis of Jatropha Cake**
Yatika Somrang
National Metal and Materials Technology Center, Thailand

ENR-P-10 **The Effect of Calcium-based Salt on Hydrothermal Carbonization of Corncob**
Promporn Reangchim
King Mongkut's Institute of Technology Ladkrabang, Thailand

ENR-P-11 **Process Optimization and Characterization of YSZ Thin Film Electrolyte on Anode Substrate Prepared by Electrophoretic Deposition Technique**
Malinee Meepho
Chulalongkorn University, Thailand

ENR-P-12 **r-GO/MWCNTs Nanocomposite Film as Electrode Material for Supercapacitor**
Suttinart Noothongkaew
Ubon Ratchathani University, Thailand

ENR-P-13 **Characterisation of NiO-YSZ Porous Anode-Supported for Solid Oxide Fuel Cells Fabricated by Powder Injection Moulding**
Nutthita Chuankrerkkul
Metallurgy and Materials Science Research Institute, Thailand

ENR-P-14 **Synthesis of Calcium Titanate by Hydrothermal Method and Modification for Biodiesel Catalyst**
Ratchadaporn Puntharod
Maejo University, Thailand

ENR-P-15 **Multiwalled Carbon Nanotubes/Cobalt Hydroxide on Polyester Woven Philippine Indigenous Fibers for Supercapacitor Electrode Materials**
Stephanie Chua
University of Santo Tomas, Philippines

ENR-P-17 CANCELLED **Investigating the Impact of Double-anodization on the Performance of Titania Nanotubes in Dye-sensitized Solar Cells**
Buagun Samran
Nakhon Phanom University, Thailand

MATERIALS TECHNOLOGY FOR ENVIRONMENT

INVITED LECTURES

ENV-I-01 **Design of Metal Oxide Nanostructured Materials for Enhanced Photocatalytic Energy & Environmental Sustainability**
Ghim Wei Ho
National University of Singapore, Singapore

ENV-I-02 **Modified Soil Compositions for Removals of Acetaminophen**
Thammarat Koottatep
Asian Institute of Technology (AIT), Thailand

ENV-I-03 **Practical Method for Bentonite Recovery from Foundry Sand Dust**
Pichaya Rachdawong
Chulalongkorn University, Thailand

ENV-I-04 **Experience in Sustainable Development through Textile Material Developing for the Community Enterprises (OTOPs) in Thailand**
Pilan Dhammongkol
Thanapaisal R.O.P., Thailand

ENV-I-05 **Quality Drying of Lumber: From Laboratory to Industry**
Nirundorn Matan
Walailak University, Thailand

ENV-I-06 **Investigation of Ag- GO- TiO_2 Cocatalyst Composites for Photocatalysis Application**
Chanchana Thanachayanont
National Metal and Materials Technology Center, Thailand

ORAL PRESENTATIONS

ENV-O-02 **On the Application of Electrocoagulation/Flotation (ECF) Technique for Cationic Dye Removal using Aluminium Electrode and *Sodium Dodecyl Sulfate (SDS)***
Galuh Yuliani
Universitas Pendidikan Indonesia, Indonesia

ENV-O-03 **Preparation, Characterization, and Photocatalytic Properties of rGO-TiO_2-Rubber Composite Sheets for Dye Decomposition in Wastewater**
Worapol Tejangkura
King Mongkut's Institute of Technology Ladkrabang, Thailand

ENV-O-04 **Fabrication Study of Hydrophobic Polyurethane Sponge for Oil-Spills Cleanup**
Peeranut Prakulpawong
Mahidol University, Thailand

ENV-O-05 **A Feasibility Study of Using Biofilter Media Made from Biomass Ash for Nitrogen Compound Removal in Aquaculture**
Tahmina Sultana
Kasetsart University, Thailand

ENV-O-06 **Using ZnO Nanorods Coated Porous Ceramic Monolith to Remove Arsenic from Groundwater**
Kannika Khwamsawat
Kasetsart University, Thailand

ENV-O-07 **Adsorptive and Acid Properties of Zeolite; Effects of Synthesize Methods**
Galuh Yuliani
Universitas Pendidikan Indonesia, Indonesia

ENV-O-08 **Removal of Arsenic from Groundwater using Nano- Metal Oxide Adsorbents**
Phitchaya Muensri
National Metal and Materials Technology Center, Thailand

ENV-O-09 **Dowel Bearing Strength of Rubberwood**
Raphaela Hellmayr
Walailak University, Thailand

ENV-O-10 **Assessment of Hydrophilic Biochar Effect on Sandy Soil Water Retention**
Ramida Rattanakam
Kasetsart University, Thailand

ENV-O-11 **Preparation of Activated Carbon from Sugarcane Bagasse Waste for the Adsorption Equilibrium and Kinetics of Basic Dye**
Tawan Chaiwon
Valaya Alongkorn Rajabhat University, Thailand

ENV-O-12 **Effect of Cell Wall Constituents On Internal Stress Generation During Drying of Lumber Prepared from Rubber Tree Trunks**
Jaipet Tomad
Walailak University, Thailand

ENV-O-13 **Improvement of Compressive Strength of Soil by Using Jute Fiber Waste**
Md Bayezid Islam
Asian Institute of Technology (AIT), Thailand

POSTER PRESENTATIONS

ENV-P-01 **The Mechanical Properties of Waste Bakelite Aggregate Concrete**
Nopagon Usahanunth
Ramkamhaeng University, Thailand

ENV-P-02 **Performance Photocatalytic Degradation of Methomyl onto Composite Graphene Oxide/Bismuth Vanadate (GO/$BiVO_4$) Nanoparticle**
Pusit Pookmanee
Maejo University, Thailand

ENV-P-03 **The Photocatalytic Degradation of Methylene Blue using Bismuth Vanadate ($Bi_2VO_{5.5}$) Powder**
Jitreephan Phanmalee
Maejo University, Thailand

ENV-P-04 **Structure and Factors Affecting Mechanical Properties of Bamboo**
Suthon Srivaro
Walailak University, Thailand

ENV-P-05 CANCELLED **W-doped TiO_2 Thin Films Synthesis by Microwave-assisted Sol-gel and Dip Coating Technique on Glass with Highly Antibacterial under Fluorescent Light**
Weerachai Sangchay
Songkhla Rajabhat University, Thailand

ENV-P-06 **Exploitation of Ag_3PO_4 Impregnated Alginate Beads for The Photocatalytic Degradation of Dye Solution under Sunlight Irradiation**
Katnanipa Wanchai
Phranakhon Si Ayutthaya Rajabhat University, Thailand

ENV-P-07 **Photocatalytic Enhancement of Solar Water Disinfection using ZnO Nanorods Coated Cellulose Paper**
Supachai Songngam
National Metal and Materials Technology Center, Thailand

ENV-P-10 **Development of Epoxy Composites Reinforcement with Oil Palm Empty Fruit Bunch Fibers for Improvement in Mechanical and Thermal Properties for Bumper Beam in Automobile**
Jirachaya Boonyarit
Kasetsart Agricultural and Agro-Industrial Product Improvement Institute, Thailand

ENV-P-13 **The Effect of Carboxymathyl Celloulose fronm Various Agriculture Wastes on the Viscosity and Physical Properties of Low Concentration Solution of Surfactant**
Thritima Sritapunya
King Mongkut's University of Technology North Bangkok, Thailand

ENV-P-14 **Determination and Molecular Study of Tannin in Coffee Pulp**
Waleepan Rakitikul
Chiang Rai Rajabhat University, Thailand

ENV-P-15 **Synthesis of Carbon Nanoparticles from Used Mobil Oil and Benzene via Solution Plasma Process**
Napatsawan Saengarunthong
King Mongkut's Institute of Technology Ladkrabang, Thailand

ENV-P-16 **Efficiency of Acoustic Noise Reduction Multilayer Wall from Activated Carbon and Rice Straw**
Phiphop Narakaew
Lampang Rajabhat University, Thailand

ENV-P-17 **Porous Carbon Material Prepared from Cassava Tuber Char using Chemical Activation Assisted Sonochemical Process**
Kamonwan Aup-Ngoen
King Mongkut's University of Technology Thonburi, Thailand

ENV-P-18 CANCELLED **Utilization of Rice Straw and Coconut Coir in the Fabrication of Lightweight Precast Concretes**
Pat Sooksaen
Silpakorn University, Thailand

ENV-P-19 **Effect of Firing Conditions on Properties of Porous Hollow Cylindrical Zeolite NaA-Clay Substrates for TiO_2 Coating and Their Photodegradation of Lignin**
Nithiwach Nawaukkaratharnant
Chulalongkorn University, Thailand

ENV-P-20 **Adsorption of Reactive Dye (Blue 222) in Solution onto Chitosan-Rice Husk Ash Composite Beads Cross-Linked with Glutaraldehyde**
Ratana Sananmuang
Naresuan University, Thailand

ENV-P-21 **Removal of Reactive Dye Red 195, Blue 222 and Yellow 145 in Solution with Polyaniline-Chitosan Membrane using Batch Reactor**
Ratana Sananmuang
Naresuan University, Thailand

METALS, ALLOYS & INTERMETALLIC COMPOUNDS

ORAL PRESENTATIONS

MET-O-01 **Utilization of Binding Ice Flakes with Pulp-Fibers as Fillings on Tube Forming**
Takahiro Ohashi
Kokushikan University, Japan

MET-O-02 **Bending Limit Curves in Sheet Metal Bending Evaluation**
Sansot Panich
King Mongkut's University of Technology North Bangkok, Thailand

MET-O-03 **Effect of Fold−Forging Techniques on Mechanical Properties of Medium Carbon Steel for Sword Making Process**
Kotchaporn Paveebunvipak
King Mongkut's University of Technology Thonburi, Thailand

MET-O-05 **Sintered Dual-phase Steels with Different Alloy Compositions**
Monnapas Morakotjinda
National Metal and Materials Technology Center, Thailand

MET-O-06 **Widmanstätten Ferrite in Fast-Cooled Ultralow Carbon Fe-Cr-Mo Steel**
Ruangdaj Tongsri
National Metal and Materials Technology Center, Thailand

MET-O-07 **Interaction between Recrystallization and Phase Transformation during Hot Squeezing of Sintered Dual-phase Fe-Cr-Mo-C Steels**
Bhanu Vetayanugul
National Metal and Materials Technology Center, Thailand

MET-O-08 **Dynamic Recrystallization and Cr_2O_3 Pinning Effect during Hot Squeezing of Sintered Ultralow Carbon Fe-Cr-Mo Steels**
Amornsak Rengsomboon
National Metal and Materials Technology Center, Thailand

MET-O-09 **Understanding the Microstructural Features in High-Pressure Die Castings by Analogy with Granular Materials and Suspensions**
Somboon Otarawanna
National Metal and Materials Technology Center, Thailand

MET-O-10 **The Effect of Bottom Ash Additions on the Properties of Sintered Bronze-Graphite Composites**
Usanee Pantulap
Thailand Center of Excellence for Glass, Thailand

MET-O-11 **Properties of Sintered Bronze-Graphite Containing Natural Anhydrite**
Chiraporn Auechalitanukul
King Mongkut's University of Technology Thonburi, Thailand

MET-O-12 **Mechanical Properties of As-Exposed Al-SiCp Composite Fabricated by Powder Injection Moulding**
Tapany Patcharawit
Suranaree University of Technology, Thailand

MET-O-13 **Effect of Aluminum Addition on $Al_xCoFeMnNiZn$ Multi-Component Production**
Amnart Suksamran
National Science and Technology Development Agency, Thailand

MET-O-14 **Effect of Si Content on Mechanical Properties of Ti-Si-N Ternary Alloys Prepared by Spark Plasma Sintering**
Patcharawat Khemglad
King Mongkut's University of Technology Thonburi, Thailand

MET-O-15 **Role of SiC in Sintered Fe-Mo-Si-C Steels**
Thanyaporn Yotkaew
National Metal and Materials Technology Center, Thailand

MET-O-16 **Effect of SiC Particle Size on Sintered Fe-Mo-Si-C Steels**
Pongsak Wila
National Metal and Materials Technology Center, Thailand

MET-O-17 **Retained Austenite in Sintered Bainitic Fe-Mo-Si-C Steels**
Dhritti Tanprayoon
National Metal and Materials Technology Center, Thailand

MET-O-18 **Modification of Microstructure and Tensile Property of Sintered Fe-Cr-Mo-C Steel by Nickel Addition**
Nattaya Tosangthum
National Metal and Materials Technology Center, Thailand

MET-O-19 **Combination Effects of Nickel and Graphite on Sintered Fe-Mo + SiC Alloy**
Rungtip Krataitong
National Metal and Materials Technology Center, Thailand

MET-O-20 **Wear Properties of Sintered Fe-Mo-Si-C Steels with Spheroidal Graphite Iron/Compacted Graphite Iron-like Microstructures**
Kittikhun Ruangchai
National Metal and Materials Technology Center, Thailand

MET-O-21 **Characterization of Sintered Fe-Mo + SiC + H-BN Alloy**
Ussadawut Patakham
National Metal and Materials Technology Center, Thailand

MET-O-22 **Improvement of Semi-Solid State Joining of SSM Aluminum Alloys**
Patsapon Binrohim
Prince of Songkla University, Thailand

MET-O-23 **Fastenerless-Riveting Utilizing Friction Stir Forming for Dissimilar Materials Joining**
Takahiro Ohashi
Kokushikan University, Japan

MET-O-24 **Quantitative Evaluation of Hot Cracking Susceptibility of MGS6 GZ-60 Hardfacing Weld Metal Based on High Temperature Ductility Curve**
Rittichai Phaoniam
Rajamangala University of Technology Krungthep, Thailand

MET-O-25 **Phase Equilibria and Thermodynamic Properties of the Ag-Bi-Cu-Sn Pb-free Solder Calculated by CALPHAD Approach**
Wojciech Gierlotka
National Dong Hwa University, Taiwan

MET-O-26 **The Investigation of Attenuation in AISI 316 Stainless Steel Weld for Ultrasonic Testing**
Boonhlua Khwansri
King Mongkut's University of Technology Thonburi, Thailand

MET-O-27 **Effect of Cooling Rate on the Microstructural and Mechanical Properties of Sn-0.3Ag-0.7Cu-0.05Ni Solder Alloy**
Kogaew Inkong
Prince of Songkla University, Thailand

MET-O-28 **The Thermal-Aging Effect on the Microstructure Evolution and Shear Strength of the Sn-Rich Au-Sn Soldering between AlTiC and Si Substrate in Microelectronics**
Panaaek Athichalinthorn
Kasetsart University, Thailand

POSTER PRESENTATIONS

MET-P-01 **Improvement of Structural, Morphological and Mechanical Properties of CrN_x Sputtered Thin Films by Vacuum Annealing Process**
Intira Nualkham
King Mongkut's Institute of Technology Ladkrabang, Thailand

MET-P-02 **Effects of Processing Parameters on Microstructure and Properties of ADC12 Aluminium-Silicon Alloys Produced by Die Casting**
Kasem Charoenrut
Chiang Mai University, Thailand

MET-P-03 **Effect of Compaction Pressure and Sintering Time on the Properties of Cu-10Sn Bronze**
Narut Nakrod
King Mongkut's University of Technology Thonburi, Thailand

MET-P-04 **Properties of Sintered Bronze-Graphite Containing Calcium Sulfate Derived from Waste Plaster Molds**
Chiraporn Auechalitanukul
King Mongkut's University of Technology Thonburi, Thailand

MET-P-05 **Investigation of Burst Rupture Disc**
Warunee Borwornkiatkaew
National Metal and Materials Technology Center, Thailand

MET-P-07 **Sheet Metal Formability Characterization**
Nopparat Seemuang
King Mongkut's University of Technology North Bangkok, Thailand

MET-P-08 **Study of Microstructure and Corrosion Resistance of Zinc Electrodeposits Before and After Black Chromating**
Kanokwan Saengkiettiyut
Chulalongkorn University, Thailand

MET-P-09 **Factors Affecting on the Corrosion Resistance of Electroless Ni-Zn-P Coated Steel**
Pranee Rattanawaleedirojn
Chulalongkorn University, Thailand

MET-P-10 CANCELLED **Extension of Creep Lifetime of Iron-Nickel-Base Superalloy at High Temperature by Adjusting Ti/C Ratio**
Chien-Lin Lai
China Steel Corporation, Taiwan

MET-P-11 **Residual and Tensile Stress Measurement in Carbon Steel by Magnetic Barkhausen Noise Technique**
Mai Noipitak
King Mongkut's University of Technology Thonburi, Thailand

POLYMERS

INVITED LECTURES

POL-I-01 **Polymer Research in Thailand: Past, Present and Future**
Krisda Suchiva
Mahidol University, Thailand

POL-I-02 **Hierarchic Structures and Propeties of Natural Rubber**
Seiichi Kawahara
Nagaoka University of Technology, Japan

ORAL PRESENTATIONS

POL-O-01 **Effect of Calcium Carbonate on Crystallization Behavior and Morphology of Poly(3-hydroxybutyrate-*co*-3-valerate)**
Sitthi Duangphet
Mae Fah Luang University, Thailand

POL-O-02 **Low Haze and Antifog Performance of 2-layer Poly(lactic acid) Based Films**
Pitcha Liewchirakorn
Chulalongkorn University, Thailand

POL-O-03 **Effect of Poly(hexamethylene succinamide) on Crystallization of Poly(L-lactic acid)**
Panadda Yueagyen
Kasetsart University, Thailand

POL-O-04 **Effect of Poly (D-lactic acid)-*co*-Polyethylene glycol on Crystallization of Poly (L-lactic acid)**
Ploywawee Kaewlamyai
Kasetsart University, Thailand

POL-O-05 **Morphology and Properties of Polyoxymethylene/Polypropylene/Microcrystalline Cellulose Composites**
Nipawan Yasumlee
Silpakorn University, Thailand

POL-O-06 **Poly(lactic acid)-Polybutylene Succinate-Activated Carbon Composite Foams**
Kittimasak Ketkul
Silpakorn University, Thailand

POL-O-08 **Numerical Simulations of Geometric Extrudate Swelling in Polymer Melt Extrusion Using Arbitrary Lagrangian Eulerian (ALE) Based Finite Element Method on Free Surface**
Mongkol Kaewbumrung
Pathumthani University, Thailand

POL-O-09 **Preparation of TO_2/WO_3 Composite Nanofiber by Electrospinning**
Patthamapa Chakornpradit
King Mongkut's University of Technology Thonburi, Thailand

POL-O-10 **Silane Modified-WO_3 for Improving Photochromic Properties of PC/WO_3 Composite**
Tanes Sangpraserdsuk
King Mongkut's University of Technology Thonburi, Thailand

POL-O-11 **Effect of Silicon Carbide on Thermal and Mechanical Properties of Polypropylene Composites**
Watthanaphon Cheewawuttipong
Rajamangala University of Technology Srivijaya, Thailand

POL-O-12 **Enhancement of Dielectric β-phase PVDF Piezoelectric Composite by Base Modified Surface Activated Carbon Nanofiller**
Saiwan Nawalertpanya
King Mongkut's University of Technology Thonburi, Thailand

POL-O-15 **Medicated Pressure Sensitive Adhesive Patches from STR-5L Block Rubber: Effect of Preparation Process**
Rungtiwa Waiprib
Prince of Songkla University, Thailand

POSTER PRESENTATIONS

POL-P-01 **Effect of Preparation Techniques of Pineapple Leaf Fiber/PHBV Composites on Final Properties**
Pongsathorn Chaleerat
King Mongkut's University of Technology North Bangkok, Thailand

POL-P-02 **Effect of Octenyl Succinate Starch on Properties of Thermoplastic Tapioca Starch Blend**
Manisara Phiriyawirut
King Mongkut's University of Technology Thonburi, Thailand

POL-P-03 **The Smart Blending for Multilayer Structure of PLA/EVOH**
Wanlop Harnnarongchai
King Mongkut's University of Technology North Bangkok, Thailand

POL-P-04 **Effect of Synthesized Ag Nanoparticles with the Different Amounts of Polyvinylpyrrolidone on the Antibacterial Properties of Ag-Natural Rubber Hybrid Sheets**
Warot Prasanseang
King Mongkut's Institute of Technology Ladkrabang, Thailand

POL-P-05 **Mechanical and Thermal Properties of PS-g-NR Blended with Natural Rubber: Effect of Grafting Percentage of PS in PS-g-NR**
Tarakol Hongkeab
Kasetsart University, Thailand

POL-P-08 **Charged Iridium(III) Complexes with Varied Side Chain Length in OLEDs**
Natsiri Wongsang
Ubon Ratchathani University, Thailand

POL-P-09 CANCELLED **Strength Properties Improvement for Preparation Wood Plastic Composite by Polyester Resin and Rice Straw**
Panot Kosenter
Thai Nichi Institute of Technology, Thailand

POL-P-11 **Gelatin Films and Its Pregelatinized Starch Blends: Effect of Plasticizers**
Suchipha Wannaphatchaiyong
Prince of Songkla University, Thailand

POL-P-12 **Self-reinforced Composites from Pineapple Leaf Fibers**
Supachok Tanpichai
King Mongkut's University of Technology Thonburi, Thailand

POL-P-13 **Physical and Mechanical Properties of Wood Plastic Composites from Teak Wood Sawdust and High Density Polyethylene (HDPE)**
Duangkhae Bootkul
Srinakharinwirot University, Thailand

POL-P-14 **Degradation of Silica-reinforced Natural Rubber by UV Radiation and Humidity in Soil**
Manuchet Reowdecha
Kasetsart University, Thailand

POL-P-15 **Degradation Test of Natural Rubber/Chitosan Composite**
Chalermchat Sukthaworn
Kasetsart University, Thailand

POL-P-16 **Mechanical, Thermal and Hydrolytic Degradation of Stereocomplexed PLL/PDL–PEG–PDL Blends**
Aphinan Saengsrichan
Chiang Mai University, Thailand

POL-P-17 **Study and Development of Irradiation-based Processing System for Natural Rubber Vulcanization**
Kittiya Kosaentor
Chiang Mai University, Thailand

POL-P-18 **Mechanical and Thermal Properties of PLA Melt Blended with High Molecular Weight PEG Modified with Peroxide and Organo-Clay**
Teerani Chuawittayawut
Silpakorn University, Thailand

POL-P-19 **Investigation of Radical Polymerization Of Furfuryl Methacrylate Using ESR**
Kyoungho Kim
Pusan National University, South Korea

POL-P-20 **Photo-oxidative Degradation Polyethylene Containing Titanium Dioxide and Poly(ethylene oxide)**
Tawat Soitong
Maejo University, Thailand

POL-P-21 **Influence of Molecular Weight on the Non-isothermal Melt Crystallization of Biodegradable Poly(D-lactide)**
Wanich Limwanich
Rajamangala University of Technology Lanna, Thailand

POL-P-22 **Toughening of Poly(buthylene succinate) with Epoxidized Natural Rubber: Mechanical, Thermal and Morphological Properties**
Sudsiri Hemsri
Silpakorn University, Thailand

POL-P-24 **Fabrication and Characterization Mixed Matrix Membrane of Polysulfone/polyimide–Carbon Nanotubes**
Tawat Soitong
Maejo University, Thailand

POL-P-25 **Study of Polymer type on Microstructure of Polymer Nanofiber by Electrospinning Technique**
Pojanart Rattanavoraviset
Maejo University, Thailand

POL-P-27 **Effect of Loofah Fiber on Mechanical Properties of Epoxy Resin**
Apaipan Rattanapan
King Mongkut's University of Technology North Bangkok, Thailand

POL-P-29 **Influence of Pyrolytic Carbon Black Prepared from Waste Tires on Mechanical Properties of Natural Rubber Vulcanizates**
Sarawut Prasertsri
Ubon Ratchathani University, Thailand

POL-P-30 **Study on Latex-state ^{13}C-NMR Spectroscopy**
Yusuke Iizuka
Nagaoka University of Technology, Japan

SURFACE ENGINEERING AND HEAT TREATMENT

ORAL PRESENTATIONS

SUR-O-01 **Effects of Heat Treatment on Microstructure and Properties of Thermal Sprayed Ni-based alloy Coatings**
Phuangphaga Daram
Chiang Mai University, Thailand

SUR-O-02 **Tribological of Thermal Sprayed Coating under Slurry Erosion**
Chalermchai Sukhonkhet
National Metal and Materials Technology Center, Thailand

SUR-O-03 **Flame Spray Coating for High Temperature Erosion Protection on Water Wall Pipe in Bio-mass Fired Power Plant Boiler**
Vasin Lertvijitpun
King Mongkut's University of Technology North Bangkok, Thailand

SUR-O-04 **Thermal Sprayed Technique for Preparing HEA-Reinforced Oxide Matrix Composite**
Hathaipat Koiprasert
National Metal and Materials Technology Center, Thailand

SUR-O-05 **Effect of Impingement Angle on Erosion Resistance of HVOF Sprayed WC-10Co-4Cr Coating on CA6NM Steel**
Anurag Hamilton
Malaviya National Institute of Technology Jaipur, India

SUR-O-06 **Sintered Metal Microstructure Influenced by Deep Rolling and Carburizing Processes**
Sai-Yan Primee
King Mongkut's University of Technology North Bangkok, Thailand

SUR-O-10 **Structural Characterization of Reactive DC Magnetron Co-Sputtered Nanocrystalline CrAlN Thin Film**
Nirun Witit-Anun
Burapha University, Thailand

SUR-O-11 **Hardfacing of 3.5% Chromium Cast Steel by Flux Cored Wire Arc Welding Process**
Teerachod Treeparee
Prince of Songkla University, Thailand

SUR-O-12 **Study on Friction Characteristics of Nano Filler for Friction Material**
Ratchanon Chamnipan
King Mongkut's University of Technology Thonburi, Thailand

SUR-O-13 **Surface Modified Sterling Silver using Nitrogen Ion Implantation Technique**
Benya Cherdhirunkorn
Thammasat University, Thailand

Plenary Lectures

PL-01

"Bringing It All Back Home" How Waste-to-Biobased Products is Good for Energy, the Environment, Water, and Society

Seth W. Snyder, Ph.D.
Argonne National Laboratory
Northwestern University
University of Chicago
seth@anl.gov +1-630-252-7939

Around the world societies want better access to affordable energy and water while protecting the environment. Health and happiness are dependent on finding the answer. Biomass and waste materials offer the opportunity to provide value-added materials and energy and clean the environment without competing for food. Using renewable resources such as biomass and waste materials requires deeper insight than using fossil resources such as coal, oil, and natural gas. Renewable resources primarily use solar and have the potential to reduce greenhouse gas emissions. Renewable resources are more distributed and less dense than fossil resources so biorefineries must be designed at smaller scales than oil refineries. About half of the weight of renewable resources is oxygen. To manage the oxygen content requires either addition of hydrogen or loss of carbon as carbon dioxide. Adding hydrogen requires energy and losing carbon decreases yield so compromises must be made. Fossil resources have very little oxygen.

"Bringing it all back home" is a way to build a strong economy while protecting the environment. You avoid depletion of resources by starting with renewable resources and then reusing them. This includes energy, water, and materials. This approach to sustainability could benefit the U.S., Thailand, and many other countries. When fully implemented it could reduce conflict for resources.

We will discuss the types of energy needed for society, how renewable resources could provide that energy, new technologies for converting feedstocks and recovering the purified products, the costs for producing energy and materials from renewable resources, and policy and regulations that impact production. Separations and product recovery can account for more than half of the costs for using renewable resources. We will discuss state-of-the-art technologies the use electricity to recover valuable renewable products. We will discuss advanced methods to enhance anaerobic digestion to convert waste materials to renewable natural gas. We will discuss effectively utilize nutrients to protect cropland and produce bioenergy. Finally we will describe how these new technologies improve water quality to ensure a safe water supply and a clean environment.

Together the work will show a path to a healthy life using renewable materials and energy.

PL-02

Geopolymerization as Cold-consolidation Techniques for Hazardous and Non-hazardous Wastes

Cristina Leonelli[a,*], Elie Kamseu[b], Isabella Lancellotti[a], Luisa Barbieri[a]
[a]*Dipartimento di Ingegneria "Enzo Ferrari", Universita' degli Studi di Modena e Reggio Emilia, 41125 Modena, Italy*
[b] *Local Material Promotion Authority (MIPROMALO), Yaoundé, Cameroon*
*cristina.leonelli@unimore.it

Keywords: Geopolymers, cold-setting, inertization, leachability.

Many interesting studies on the utilization of wastes produced in different human activities (urban, agricultural and industrial) have been carried out with the goals to reduce, to recycle, to reuse or to recovery: the R4 strategy. Many of these waste contains high amount of silicoaluminates, making them suitable for alkali activation to become one of the most promising binders for the future. Other type of wastes, even if hazardous, such as incinerator fly ash, electric arc furnace dust, lead smelting slag, etc. can be easily added to the use geopolymer matrix for the immobilization of either cations or anoions or both. With the term “geopolymers” it is commonly defined an inorganic 3D polymer obtained by the alkali activation of aluminosilicate (SiO2 and Al2O3 >80 wt%)powders. These materials are generally X-ray amorphous gels in which the silicate and aluminate units, generated during the first step of alkali activation, occur in a highly connected three dimensional tetrahedral framework after the polycondensation process. So finally, they can be considered solids where the cations remain mainly associated with aluminate moieties to compensate, similarly to zeolites, the negative charge arising from the tetrahedral aluminium, Al+3. It has been proved that also anions can be entrapped in these aluminosilicate matrices, ofter described as nanozeolites. The leachability tests have been used to confirm the inertization whil e FT-IR and NMR describe the complex microstructures of th consolidated materials.
The presentation will provide a fundamental contribute for: i) a better knowledge of chemical–physical–mechanical performances of the investigated geopolymers; ii) the development of new products ready to be introduced into the market because produced with a low cost existing technology.

PL-03

2D Materials: Technology, Standards and Science

Antonio H. Castro Neto
Director of Centre for Advanced 2D Materials and Graphene Research Centre
National University of Singapore
phycastr@nus.edu.sg

Over the last five years the physics of two-dimensional (2D) materials and heterostructures based on such crystals has been developing extremely fast. From one hand, with new 2D materials, more and more truly 2D physics started to appear (Kosterlitz-Thouless (KT) behaviour, 2D excitons, commensurate-incommensurate transition, etc). From another - we see the appearance of novel heterostructure devices - tunnelling transistors, resonant tunnelling diodes, light emitting diodes, etc. Composed from individual 2D crystals, such devices utilise the unique properties of those crystals to create functionalities which were not accessible to us in other heterostructures. In this talk I will review the properties of novel 2D crystals and how those properties are used in new heterostructure devices.

PL-04

Advanced Electron Microscopy and Spectroscopy for Materials Research and Development

Supapan Seraphin
Department of Materials Science and Engineering,
University of Arizona, Tucson, AZ85721, U.S.A.
National Metals and Materials Technology Center (MTEC), and National Nanotechnology (NANOTEC), National Science and Technology Development Agency (NSTDA),
Pathumthani, 12120, Thailand
seraphin@email.arizona.edu, supapan.seraphin@nstda.or.th

Keywords: electron microscopy, electron spectroscopy

Electron microscopy/spectroscopy is one of the most critical tools enabling many advancements in science and technology. "Seeing is believing" is literary a fundamental basis for scientists to find evidence to explain how nature works. A quest to "know and look" further and further into more details of the nanoworld is a motivation to develop better resolution transmission electron microscopes. Insight into the atomic world in the level of pico-meter reveals an un-imaginable nature of materials and their functionalities. In 1931, Ernst Ruska, a German physicist and Max Knoll, an engineer, were the first to successfully build a transmission electron microscope (TEM). It was not until 1986 that Ernst Ruska received a Noble Prize in Physics for his work in electron optics. Nonetheless, it was recognition to an inventor of an important scientific tool.

The resolution of TEMs is limited primarily by two factors: the wavelength of the incident electron and the spherical aberration (C_s) of the objective lens, which is a property of the lens itself. For over 50 years, major effort to improve TEM image resolution was put over using shorter and shorter wavelength (higher and higher accelerating voltage). There was a TEM in Osaka, Japan, that can go as high as 3 million eV. Not until the last twenty years when the drive to improve the resolution was seriously shifted to improve the other factor: reducing spherical aberration of the electromagnetic lens. Currently, resolution of 0.05 nanometer (5 pico-meter) is achievable. This presentation will review and discuss the development of C_s corrected TEM and it applications.

Advanced Materials Testing and Characterization

ADV-I -01

Electron Microscopy Investigation of Nanocomposites between Metal/alloy and N-rGO for Renewable Energy Applications

Thapanee Sarakonsri[a,*], Reungruthai Sirirak[a], Viratchara Laokawee[a], Thanapat Autthawong[a], Naruephon Mahamai[a], Bralee Chayasombat[b] and Chanchana Thanachayanont[b]

[a]Renewable Energy Laboratory, Department of Chemistry, Chiang Mai University,Chiang Mai, 50200, Thailand

[b]National Metal and Materials Technology Center, 114 Thailand Science Park, Paholyothin Rd., Klong 1, KlongLuang, Pathumthani, Thailand

*E-mail address:thapanee.s@elearning.cmu.ac.th

Keywords: Electron Microscopy; Nanocomposites; Fuel cells; Catalysts; Anode; Lithium-ion Battery.

Metal/alloy nanocomposites with nitrogen doped reduced graphene oxide (N-rGO) has been studied and reported as efficient catalysts for fuel cells and as high energy density anode for next generation lithium-ion battery. To confirm the microstructure and morphology of the prepared nanocomposites, electron microscopy techniques, x-ray diffraction are the main tools. Platinum based catalysts has long been known as the most effective catalysts for many applications. In this research, Pt alloys, Pd alloys, and non-platinum alloys nanoparticles on N-rGO catalysts were prepared by methods including $NaBH_4$ reduction, microwave assisted, and polyol process. N-rGO was prepared using the well-known modified Hummer method followed by heat treatment under N_2 gas atmosphere and finally heat treated with nitrogen source. Raman spectroscopy, and x-ray photoelectron spectroscopy results confirmed the formation of multisheet graphene and nitrogen functional group on graphene surface. For lithium-ion battery application, silicon germanium and tin nanoparticles were composited with N-rGO with difference ratios. Nanoparticles of metals or alloys were observed highly distributed on N-rGO.

ADV-I-02

Structure-property Relationship of Polymeric Materials Studied by Electron Tomography

Hiroshi Jinnai[a,*]
[a] *Institute of Multidisciplinary Research for Advanced Materials (IMRAM), Tohoku University, 2-1-1, Katahira, Aoba-ku, Sendai, 980-8577, Japan*
*E-mail address: hjinnai@tagen.tohoku.ac.jp

Keywords: Transmission electron microscopy / Transmission electron microtomography / Rubber nano-composite / Finite element analysis

A variety of polymeric materials from daily commodities to high-tech-products are used in our daily life. Rubber nano-composites are one of the representative polymeric products. They are often composed of one or two nano-fillers, i.e., carbon black (CB) and silica (Si) nano-particles. The three-dimensional (3D) morphology of particulate fillers embedded in a rubbery matrix (hereafter called a rubber nano-composite) was examined by transmission electron microtomography (TEMT).

Although the CB and Si nano-particles were difficult to distinguish by conventional transmission electron microscopy (TEM), they appeared different in TEMT: the CB and Si nano-particles appeared, respectively, to be hollow and solid particles in the cross-sectional images of the TEMT 3D reconstruction. Thus, TEMT itself provided a unique particle-discriminative function [1]. The nano-particles were found to form aggregates in the matrix. It is intriguing that each aggregate was made of only one species; not a single aggregate contained both the CB and Si nano-particles [1]. The 3D images of the rubber nano-composite can be further used together with a computer simulation method, the finite element analysis, to estimate the mechanical property of the material [2, 3].

ADV-O-01

Investigation of Stripe Emitter Area (A_E) on the design on Heterojunction Bipolar Transistor Silicon-Germanium (SiGe-HBT)

Tossin Alamsyah [1], Danang Wijayanto[1], E. Shintadewi Julian[2],
[1]Jurusan Teknik Elektro Politeknik Negeri Jakarta
e-mail :alamsyah_pnj@yahoo.co.id
[2]Jurusan Teknik Elektro Fakultas Teknologi Industri
Universitas Trisakti Indonesia

Keywords—***SiGe, HBT, Stripe Emitter Area (A_E)***

Abstract— **This paper presents simulation of SiGe HBTs to investigate the effect of stripe emitter (A_E) to its cutoff frequency *ft* and maximum frequency of oscillation *fmax* using Bipole3 device simulation tool. The SiGe HBTs under study have the same vertical doping and Ge profile, but have different emitter stripe areas A_E, i.e. 0.25 μm × 2 μm, 0.25 μm × 10 μm and 0.12 μm × 10 μm.**

The device vertical profiles are as follows: 10 nm emitter width, 30 nm base width, and about 350 nm collector width. The peak emitter doping concentration is 10^{20} cm-3 at the emitter contact. The peak base doping concentration is 10^{19} cm^{-3} at the emitter side of the base and the collector has selective implanted collector (SIC) with 5×10^{17} cm^{-3} doping concentration at the base side of the collector to 2×10^{18} cm^{-3} at the buried layer side of the collector. The results show that SiGe HBTs with same emitter stripe width yield nearly the same value of *ft* and *fmax*, but the peak values of *ft* and *fmax* for device with longer emitter stripe are located at higher collector current *IC*. For SiGe HBT with same emitter stripe length, device with smaller emitter stripe width yields higher *ft* and *fmax*.

ADV-O-03

Fe *K*-edge and Ti *K*-edge XAS Study of Blue Sapphires

Nirawat Thammajak[a,*], **Rachanon Klondon**[a]
[a]*SLRI-GeM Consortium, Synchrotron Light Research Institute, 111 University Avenue, T. Suaranaree, A. Muang, Nakhon Ratchasima 30000 Thailand.*
*E-mail address: n.thammajak@gmail.com

Keywords: X-ray Absorption Spectroscopy, Synchrotron, Blue Sapphire, Linear Combination Fit

X-ray Absorption Spectroscopy (XAS) is a powerful technique for studying local structure in materials using an energy-tuneable source of x-rays from a synchrotron. The absorption of x-rays by an atom can provide a meaningful spectrum which qualitatively and quantitatively related to its chemical compositions, forms, and bonding structure. XAS is therefore sensitive to the oxidation state, coordination geometry, and the distances, coordination number and species of the atoms immediately surrounding the selected element. Hence, the technique is capable to provide an effective analysis of trace elements and dilute compositions, which commonly affect the color of gemstones. Oxidation state, electronic structure, and local atomic structures of trace Fe and Ti cations in various blue sapphire samples were investigated by fluorescent-mode XAS. In blue sapphire, Fe and Ti are key elements that cause the blue colour. All the samples showed Fe absorption edge at 7124 eV, corresponding to Fe^{3+} state; and Ti at 4984 eV, corresponding to Ti^{4+}. The measured XAS spectra were also used to analyze a weight fraction of TiO_2 phases, anatase and rutile TiO_2, found in blue sapphire samples by a Linear Combination Fit (LCF). This result provided a remarkable potential in using XAS as an indicative technique for heat treated blue sapphires.

ADV-P-01

X-Ray Diffraction Analysis of ZnO Particles Prepared by Microwave Plasma

Parinya Chakartnarodom[a], Nuntaporn Kongkajun[b,*]
[a]*Department of Materials Engineering, Faculty of Engineering, Kasetsart University, Chatuchak, Bangkok, 10900, Thailand*
[b]*Materials Science Program, Department of Physics, Faculty of Science and Technology, Thammasat University, Klong Luang, Prathumthani, 12121, Thailand*
* n-kongkj@tu.ac.th

Keywords: ZnO, X-Ray Diffraction, Scherrer's equation, Microwave Plasma

The aim of this work is to use x-ray diffraction (XRD) technique to analyze ZnO particles prepared by the reaction between the zinc vapor and oxygen within microwave plasma. The microwave plasma was created by the interaction between the 1200-W 2.45-GHz microwave, the conductive material, and the argon-oxygen gas mixture. Due to the high effective temperature of the plasma, it was thermodynamically and kinetically possible to generate zinc vapor from the solid zinc and then reacted with the oxygen in the gas mixture to form ZnO particles.

The synthesis of ZnO in the microwave plasma has been done for 10 to 15 minutes. The XRD results show that the synthesized ZnO samples have wurtzite structure. Moreover, by using the breadth of XRD peaks, Scherrer's equation, and Williamson–Hall plots, the increasing of synthesis time from 10 to 15 minutes affects the crystallite size but does not affect the magnitude of strain in ZnO crystals.

ADV-P-02

Characterization of Improved White Sapphire with Lithium-Glass

Natthaphol Chomsaeng[a,*], Ameena Srisuriya[a], Ekarat Meechowas[b]
[a] *Jewelry Materials Research and Development Center, Faculty of Gems, Burapha University, Chanthaburi Campus, Thamai, Chanthaburi, 22170 Thailand*
[b] *Department of Science Service, Ministry of Science and Technology of Thailand, Ratchathewi, Bangkok, 10400, Thailand*
*natthapholc@gmail.com

Keywords: White sapphire, Lithium glass, Heat treatment

Sapphire is main raw material for jewelry production. In present, the demand for improved sapphire has gained a lot of attention in jewelry maker due to inexpensive stone. In this work, fractured white sapphire was improved by filling lithium-glass. The sapphire was soaked in concentrate hydrofluoric acid for 5-10 days. Subsequently, sapphires were heat treated with lithium glass in oxidation ambient at 1100 °C for 1-5 hrs. Rough sapphire, etched sapphire and treated sapphire were investigated the physical properties by refractive index (RI), specific gravity (SG), optical microscope (OM), scanning electron microscope (SEM) and UV-Vis NIR spectrophotometer. The experiment result shown that RI and SG of glass (1.52 and 1.30) were lower than that of sapphire (1.77 and 3.89). RI and SG of treated sapphire were slightly decreased from 3.89-4.15 to 3.26-3.69 because lithium glass penetrated into cracks of sapphire. The result of absorbance spectrum in the range 250-800 nm found that peak of Fe^{3+} at 330-350 nm, 388 and 450 nm which was trace elements. These peaks were found in all of condition of samples. SEM image revealed that lithium-glass can be filled in fissure of white sapphire.

ADV-P-03

Influence of Scanning Parameters on X-Ray Diffraction Peaks of Copper

Parinya Chakartnarodom[a], **Nuntaporn Kongkajun**[b,*]
[a]*Department of Materials Engineering, Faculty of Engineering, Kasetsart University, Chatuchak, Bangkok, 10900, Thailand*
[b]*Materials Science Program, Department of Physics, Faculty of Science and Technology, Thammasat University, Klong Luang, Prathumthani, 12121, Thailand*
* n-kongkj@tu.ac.th

Keywords: X-Ray Diffraction, FWHM, Integrated Intensity, Statistical Analysis

The aim of this work is to study the influence of scanning parameters of x-ray diffractometer on the integrated intensity and full-width at half maximum (FWHM) of the x-ray peaks of copper powder on the x-ray diffraction (XRD) patterns by using statistical analysis methods. XRD analysis was done on copper powder by using step scan mode, 0.03^{o} 2θ step size, and preset time 0.1-3.5 s. Integrated intensity of a XRD peak was the area under x-ray peak which was calculated by the numerical method. FWHM was measured from the width of a x-ray peak at half-maximum intensity. The statistical analysis methods including linear regression and statistical hypothesis test were used to analyze the correlation between the preset time and the error on integrated intensity calculation, or the magnitude of FWHM of a peak on the XRD pattern. The results from statistical analysis show that the increasing of preset time from 0.1 s to 3.5 s does not affect the magnitude of FWHM of a x-ray peak, but it reduces the relative error in integrated intensity calculation. Moreover, using the preset time greater than 1 s will minimize the relative error in integrated intensity calculation of a XRD peak.

ADV-P-04

Temperature Effect on Synthesis of Carbon Nanotubes by Catalytic Chemical Vapor Deposition

Thanattha Chobsilp[a], Chaisak Issro[a], Visittapong Yordsri[b], Worawut Muangrat[c,*]
[a]*Department of Physics, Faculty of Science, Burapha University, Chonburi, 20131, Thailand*
[b]*National Metal and Materials Technology Center, Pathumthani, 12120, Thailand*
[c]*Navamindradhiraj University, Bangkok, 10300, Thailand*
*E-mail address corresponding author: worawut@nmu.ac.th

Keywords: Carbon nanotubes, catalytic chemical vapor deposition, acetylene, ferrocene.

Carbon nanotubes (CNTs) were synthesized by catalytic chemical vapor deposition (CCVD) at temperatures ranging from 800 to 900°C with acetylene (C_2H_2) gas and ferrocene acting as carbon source and catalyst precursors, respectively. Ferrocene was taken in the quartz boat and placed inside the first heating furnace, then was vaporized at 200°C and carried by argon (Ar) gas with a flow rate of 500 sccm to the second heating furnace after the temperature reached to synthesis temperature. C_2H_2 gas was flowed with a flow rate of 30 sccm for 10 min. Finally, the second heating furnace was cooled to room temperature under Ar ambient. To remove iron nanoparticles, synthesized CNTs were immersed in 37% of hydrochloric (HCl) acid for 6 h, then washed with distilled water until the pH reached to 7, finally dried in an oven furnace at 100°C for 60 min. The purified CNTs were characterized by field emission electron microscopy (FESEM), transmission electron microscopy (TEM) and Raman spectroscopy. The results exhibited that the synthesis temperature could affect the degree of purity, graphitization and diameter of CNTs.

ADV-P-05

Application of Soft X-Ray Emission Spectrometer on Microstructure Investigation of High Temperature Stainless Steel

Viyaporn Krongtong[a]*, Bralee Chayasombat[a], Chanchana Thanachayanont[a]
[a]*National Metal and Materials Technology Center, National Science and Technology Development Agency, Khlong Luang, Pathum Thani, 12120, Thailand*
*viyapork@mtec.or.th

Keywords: Soft X-Ray Emission Spectrometer, Stainless Steel, Electron Probe Microanalysis, Wavelength Dispersive Spectrometer

Stainless steel Type 321 is stabilized austenitic stainless steel similar to Type 304 with additional titanium (Ti) content at low ratio comparing to the carbon and the nitrogen contents. The low titanium addition increases strengthening phases such as titanium nitride (TiN) or titanium carbide (TiC) in the matrix of the stainless steel. These phases prevent and reduce precipitation of carbon and other elements at grain boundary during service because titanium increases stabilization of carbide. If carbide precipitations such as chromium carbide occur at the grain boundaries, they reduce corrosion resistance and creep resistance at elevated temperature. These affect the applications in petrochemical industries, heavy duty automotive exhaust systems, firewalls, boiler tube of recovery gas in separated hydrocarbon systems, jet aircraft and oil refinery components. However, the developed strengthening phases are too small and has a very low concentration to be analyzed by commercial scanning electron microscope (SEM) and energy dispersive spectrometer (EDS). It is necessary to be analyzed by high performance apparatus and advanced techniques. The soft X-ray emission spectrometry technique (SXES) consists of an ultra-high resolution x-ray spectrometer. By combining the varied line spacing (VLS) diffraction grating together with a high sensitive X-ray CCD camera, the SXES has the energy resolution at 0.3 eV. This high energy resolution allows a more detailed characterization such as chemical state analysis.

In this study, the characteristics of strengthening phases were analyzed using FE-SEM, EDS and SXES attached to the FE-SEM. The strengthening phase was found to have a core-shell structure. Titanium spectra were found in both the core and the shell but with different emission energy levels and significantly different spectral structures. This suggests different chemical states of the titanium in the strengthening phase. Spectral mapping from SXES allows mapping of the different chemical states of titanium. The microstructure and its chemical states will be analyzed in detail. This information is useful for more understanding of the microstructure of the strengthening phase in stainless steel.

ADV-P-06

Rapid Analysis of Residual Styrene Monomer and Oligomer in Polystyrene Using Fragmentless Ionization Mass Spectrometry

Takahisa Tsugoshi[a,*], Yuji Mishima[b]
[a]*National Institute of Advanced Industrial Science and Technology (AIST), Tsukuba, Ibaraki, 305-8563, Japan*
[b]*Kobe Material Testing Laboratory Co., Ltd., Tokyo, 110-0015, Japan*
*tsugoshi.takahisa@aist.go.jp

Keywords: Polymer, Fragmentless ionization, Mass spectrometry, Rapid analysis

Polystyrene (PS) is used widely as general-purpose plastic that is mostly reused by recycling. The PS contains styrene monomer and oligomer as impurities, which are formed during a heat-treatment process within a manufacturing process. Generally and usually the impurities are determined with Gas Chromatography, however it takes about 30 min.
Ion attachment ionization mass spectrometry that is one of fragmentless ionization mass spectrometry offers rapid analysis of those impurities. In the mass spectrum, one peak indicates one chemical species because no fragmentation exists during the ionization, so that it does NOT require any separation technique. The separation is realized in the mass spectrum. In this study, this technique has been applied for rapid analysis of the impurities in the polystyrene.
Samples were heated until about 240 °C in 100 Pa chamber. The impurities were thermally extracted to gaseous phase and detected as (quasi-)molecular ions and then no pyrolysis existed during the heating because the heated temperature was still below the pyrolysis temperature of the polymer. Same samples were heated until about 270 °C as 2nd heating scan and then no more evolved gas species were detected. It means that the thermal extraction as 1st heating was almost perfect.
Some examples for usual polystyrene products will be presented.

Biomedical Materials and Devices

BIO-I-01

Development of Joint Prosthesis

Yoshio Nakashima
Teijin Nakashima Medical Co., Ltd., Japan
E-mail: y.nakashima@teijin-nakashima.co.jp

The number of cases of bipolar hip arthroplasty and total hip arthroplasty exceeded 120,000 cases in Japan last year. The total of approximately 200,000 patients had joint replacement surgeries for one year including the number of 80,000 cases for total knee arthroplasty. Considering the increase in elderly population, the further increase in the number of artificial joint replacements is expected.

On the other hand, Japanese manufactures have approximately 20 % share in the market of artificial joint replacement and fall behind the Western manufacturers. As a Japanese manufacturer, we have promoted a variety of researches and developments in order to change the current situation. For example, we have engaged in the improvements in design suitable for the Japanese bony shape and lifestyle, the development for the material which aims to offer greater longevity of joint prosthesis, the surface treatment technique which increases biocompatibility with bones and metals, and the technology which adds the anti-infection function.

This presentation will provide mainly the current situation of the market and technology development for joint prosthesis in Japan.

BIO-O-03

The study of ABO-Rh blood typing on reusable polymeric chip by surface plasmon resonance technique

Chanwit Kataphiniharn[a], Chinnawut Pipatpanukul [b,c], Toemsak Srikhirin [b,c] , Thidarat Wangkam [a,*]

[a] *Department of Industrial Physics and Medical Instrumentation, Faculty of Applied Science, King Mongkut's University Technology North Bangkok, Bangkok,10800, Thailand*

[b]*Materials Science and Engineering Program, Mahidol University, Bangkok, 10400, Thailand*

[c] *Center of Intelligent Materials and Systems, Nanotec Center of Excellence at Mahidol University, Bangkok,10400, Thailand*

*E-mail address thidarat.w@sci.kmutnb.ac.th

Keywords: Spin coating, Surface plasmon resonance, contact angle, Red blood cell

The point of care (POC) blood typing have been developed for naked eye detection by functionalized poly(methyl methacrylate) (PMMA) strip. However, the behavior of antibody immobilization on these surfaces are not distinctly understood. SPR technique was used to determine the antibody against red blood cell (RBC) antigen immobilized on gold (Au) sensor chip. The experiment was carried out by making a thin-film layer of PMMA on the gold surface SPR sensor chip with spin coating technique. The thickness of PMMA layers were controlled by spin coating speed to optimize the suitable condition for surface modification. After that, those surfaces were grafted by 3-glycidoxylpropyl trimethoxysilane (GPTMS) and Dextran for the study of the detection of RBC and surface regeneration. The contact angle measurement and SPR to monitor the change of thin film properties before and after treating by UV-ozone. Initially, spin casting speed was varied in the range of 200-3500 rpm and the contact angle results were shown in the range of 71-76 degree. Then the PMMA film were treatment by UV-ozone 250 mWatt at different the exposure time (0-20 min). The results were shown that there were significantly decrease of the angles because the hydroxyl groups were creating on PMMA surface after UV treatment. The optimization condition analyzing by the contact angle and SPR signal were 3000 rpm for spin speed and 5 min for UV treatment. Finally, antibody-A, B and D were immobilized on the optimized GPTMS-PMMA/Au and Dextran-PMMA/Au surface for studying RBC detection. The results were revealed that antibodies preformed homogeneously on GPTMS-PMMA/Au surface rather then Dextran-PMMA/Au surface. However, both surface functionalization can be applied to detect RBC and ABO-Rh blood grouping by crossing immobilized antibody array. The concept of Dextran and GPTMS grafted on PMMA chip can be accommodated for reusable SPR chip.

BIO-O-04

Preparation and Characterization of Artificial Nerve Guidance Conduits Based on Polycaprolactone/Polyaniline/Collagen Type 1 Composite Nanofibers Using Rat Sciatic Nerve Injury Model

Lizah B. Dorao[a] , Rowen T. Yolo[b] and Christina A. Binag[a,c,d]*
[a]Graduate School, [b]Faculty of Medicine and Surgery,
[c]Chemistry Department, College of Science,
[d]Research Center for the Natural and Applied Sciences
University of Santo Tomas, Manila 1015, Philippines
*cabinag@yahoo.com

Keywords: artificial nerve guidance conduit, polycaprolactone, polyaniline, collagen type 1

Peripheral nerve injuries (PNIs) are very common in clinical practice, and may cause life-long disability in patients. The current gold standard in the treatment of PNIs with long nerve gaps is autologous nerve grafting, which, although is effective in supporting nerve regeneration, unfortunately has associated drawbacks such as donor site morbidity, limited availability of donor nerves, and mismatch between donor and recipient nerves; such drawbacks are overcome by the use of artificial nerve guidance conduits (NGCs), which have become an attractive alternative to autografts. However, to date, although a wide variety of materials have been used as NGCs by many research groups, no single material has yet been proven to yield results that are at least comparable to those of autografts. In this study, polycaprolactone/polyaniline/collagen (PCL/PANi/Col) type I polymeric composite was prepared by solvent casting for use as artificial NGC that could potentially be comparable to autografts. These materials were evaluated for their nerve regenerating capacity in a rat sciatic nerve injury model by assessment of motor function recovery via motor sciatic function index (SFI) scoring over an observation period of 2-3 months, and were subjected to histological studies at the end of the study period. Rats with a 1-cm nerve gap bridged by the test material, PCL/PANi/Col composite was compared with rats with 1-cm nerve gap repaired using nerve autograft as the positive control group and with rats with 1-cm nerve gap without intervention as negative control. This composite material was demonstrated by four-point probe conductivity testing to have a conductivity ranging from 1.575×10^{-7} Scm^{-1} to 2.090×10^{-6} Scm^{-1}, and thermograms of the composites showed thermal stability that is maintained up to 400°C. Scanning electron micrographs of the composites showed interconnected nanorod structures, with diameters ranging from 27 nm to 110 nm. Nerve functional recovery assessment by motor sciatic function index scoring revealed that motor function recovery in rats treated with the PCL/PANi/Col composite nanofiber-based NGCs was better than that observed in rats that did not receive any intervention, and was slightly better than that for rats treated with autograft. Nerve morphological study by histopathological analysis revealed that transected nerves bridged using this composite material remained viable and did not exhibit untowardly reaction to the scaffold, demonstrating its biocompatibility. The scaffold material was demonstrated by light microscopy to be partially resorbed after 12 weeks *in vivo*,

demonstrating its biodegradability. These data suggest the potential applicability of the PCL/PANi/Col composite nanofibers as artificial NGCs.

Acknowledgement. One of the authors, LBD would like to thank the Science Education Institute of the Department of Science and Technology (SEI-DOST) of the Philippines for her scholarship grant.

BIO-O-05

Biological Responses of Porcine Chondrocytes and Human Bone Marrow Mesenchymal Stem Cells on Porous PCL/PHBV Blended Scaffolds

Pakkanun Kaewkong, Pacharapan Sonthithai, Wasana Kosorn, Tareerat Lertwimol, Wanida Janvikul*
National Metal and Materials Technology Center, Pathumthani 12120, Thailand
*E-mail address: wanidaj@mtec.or.th

Keywords: PCL/PHBV scaffolds, Salt particles, Chondrocytes, Mesenchymal stem cells.

Cartilage tissue engineering is a promising technology to repair damaged articular cartilage and knee arthritis. It involves the use of a scaffold to support growth of cultured cells that are subsequently to secrete extracellular matrix molecules essential for restoration of damaged tissue. In this study, two different porous biodegradable PCL/PHBV (50/50 wt%) blended scaffolds were fabricated by an in-house built fused deposition modeling (FDM) machine to have a dimension of 6.0 x 6.0 x 2.5 mm^3 (length x width x height) and a channel size (size of primary pores) ranging between 250-300 μm. Secondary pores on the polymeric filaments of the scaffold were generated when 50 wt% NaCl particles were primarily mixed with the blend prior to the fabrication and then leached out by 1 M NaOH at 50°C for 60 min. The surface morphology and hydrophilicity of the scaffolds prepared with and without NaCl were determined by SEM and water contact angle measurement, respectively. It was noted that the PCL/PHBV scaffold with primary and secondary pores possessed a rougher and more hydrophilic surface. The chondrogenicity of porcine chondrocytes cultured on individual PCL/PHBV blended scaffolds for 28 days was assessed by real-time RT-PCR and a confocal laser scanning microscope. Upregulation of cartilage-specific genes, i.e., type II collagen and aggrecan, and round shaped cells were observed when the cells were cultured on the PCL/PHBV blended scaffold prepared with the salt particles. When human bone marrow mesenchymal stem cells (hMSCs) were cultivated on the PCL/PHBV scaffold with primary and secondary pores in chondrogenic differentiation culture for 21 days, a drastic expression of both cartilage-specific genes and a notable accumulation of cartilage-specific extracellular matrix (ECM) protein, i.e., type II collagen, were vividly observed. In summary, the PCL/PHBV blended scaffold with primary and secondary pores had exhibited its great potential use as a cell culture construct in cartilage tissue engineering as it promoted the functionality of porcine chondrocytes and the chondrogenic differentiation of hMSCs.

BIO-O-06

In Vitro Study of Biological Response by Human Gingival Fibroblast on Silk Fibroin/Alpha Tricalcium Phosphate Composite Scaffolds: A Preliminary Study

Woradej Pichaiaukrit[a,*], Wiriya Juwattanasamran[a], Sorada Kanokpanont[b]
[a]*Faculty of Dental Medicine, Rangsit University, Phahonyothin Road, Lak-hok, Patumtanee, 12000 Thailand*
[b]*Assistant Professor, Department of Chemical Engineering, Faculty of Engineering, Chulalongkorn University,254 Phayathai Road, Pathumwan, Bangkok, 10330 Thailand*
*woradej059@gmail.com

Keywords: SILK FIBROIN, ALPHA TRICALCIUM PHOSPHATE, 3D SCAFFOLD, HUMAN GINGIVAL FIBROBLAST

Silk fibroin is a natural biodegradable polymer that has been demonstrated for use as scaffolds for bone tissue engineering. To improve the osteoconductivity and the osteoinductivity of silk fibroin scaffolds, ceramics were added. α-TCP is the expected ceramic that useful for scaffolds for bone tissue engineering either alone or blended with silk fibroin. From the previous study, we evaluated the mechanical properties of three-dimensional porous silk fibroin/alpha tricalcium phosphate scaffolds and concluded that the scaffolds containing 8% (w/w) α-TCP exhibited the highest compressive modulus. The objective of this study was to evaluate the biological properties of three-dimensional porous silk fibroin/alpha tricalcium phosphate scaffolds. The scaffolds were constructed using a solvent casting and salt leaching technique. The hybrid strain of degummed Thai silk fibroin, Nangnoi Srisaket 1 x Mor, was dissolved in hexafluoroisopropanol at 16% (w/v). Alpha tricalcium phosphate (α-TCP) was incorporated to produce 4, 8, 12, and 16 wt% solution. Sucrose (particle size 250-450 μm; sucrose/silk fibroin = 8.5/1 w/w) was used as a porogen. Human gingival fibroblasts (passage 5) were cultured in these scaffolds. After 72 h, the biocompatibility of seeded scaffolds was evaluated under the inverted phase contrast microscopy. Cell proliferation was determined by DNA assays and scanning electron microscopy. The images from inverted phase contrast microscopy revealed the human gingival fibroblasts can be attached at the surface of scaffolds in all groups. The results from the DNA assays showed that the number of human gingival fibroblasts was increased as the culture period was prolonged but was not as the increasing of α-TCP. At 120 h, the scaffolds containing 8% (w/w) α-TCP exhibited the highest cell number ($3.75 \pm 0.66 \times 10^4$ cells). The scanning electron microscope images at 24, 72, and 120 h after cell culturing presented human gingival fibroblasts can be expanded well and exhibited the normal morphology. The results suggested that the scaffolds containing 8% (w/w) α-TCP may be a potential candidate for bone tissue engineering applications.

BIO-O-07

Novel Biodegradable Copolymers of Glycerol Sebacate and Amino Acid for Cartilage Tissue Regeneration

Piyarat Sungkhaphan[a], Tharinee Theerathanagorn[a], Jeerawan Klangjorhor [b,c], Wanida Janvikul[a,*]

[a]*National Metal and Materials Technology Center, Pathumthani 12120, Thailand*
[b]*Department of Orthopedics, Faculty of Medicine, Orthopedic Laboratory and Research Netting Center (OLARN Center)*
[c]*Thailand Excellence Center for Tissue Engineering and Stem Cells, Department of Biochemistry, Faculty of Medicine, Chiang Mai University, Chiang Mai 50200*
*E-mail address: wanidaj@mtec.or.th

Keywords: Glycerol sebacate, Amino acid, Copolymer scaffolds, Articular chondrocytes.

The aim of this study was to develop novel biodegradable scaffolds from copolymers of glycerol sebacate and amino acid (PGS-*co*-amino acid). The precopolymers were first synthesized via stepwise condensation polymerization under nitrogen atmosphere at 130°C for 24 h, using two different types of amino acids, i.e., glutamic acid and serine, yielding PGS-*co*-glu and PGS-*co*-ser precopolymers, respectively. The average molecular weights and chemical structures of synthesized precopolymers were determined by GPC and ^{13}C NMR, respectively. The weight (M_w) and number (M_n) average molecular weights of PGS-*co*-glu precopolymer were found to be about 8000 and 2700 g/mol, respectively, whereas those of PGS-*co*-ser precopolymer were around 10300 and 3500 g/mol, respectively. Each synthesized precopolymer was homogenously mixed with NaCl particles at a 10 precolymer/90 NaCl weight ratio, cast in molds, and heated at 140°C for 16 h. Porous PGS-*co*-glu and PGS-*co*-ser scaffolds were ultimately obtained after a NaCl-leaching process. The highly interconnected porous structures of both copolymer scaffolds were revealed by SEM. To enhance surface hydrophilicity of the scaffolds, the materials were subjected to a low oxygen plasma treatment. The results of a water contact angle measurement demonstrated that a water droplet on PGS-*co*-ser surface turned to a flat puddle faster than that on PGS-*co*-glu surface. The surface wettability of both scaffolds was considerably increased after plasma treatment. The swelling ability of these two scaffolds was also comparatively determined. In the biological assessment, human articular chondrocytes were cultured on the untreated and plasma-treated PGS-*co*-ser and PGS-*co*-glu scaffolds for given days. Cell viability was assessed by Alamar blue assay at days 1, 7, and 21. No significant difference in numbers of live cells was found between the cells cultured on PGS-co-ser and PGS-co-glu scaffolds. The cartilaginous matrix production by human chondrocytes was determined on day 21 of culture. The greatest contents of GAGs, collagen and HA were detected in the cells cultivated on the plasma-treated PGS-*co*-ser scaffold ($p<0.01$). This suggested that the incorporation of amino acid, i.e., serine, into the scaffold in the form of amino acid copolymer in conjunction with the use of plasma treatment greatly facilitated the human chondrocyte functions. Thus, this novel amino acid copolymer scaffold appeared to be a promising scaffold for cartilage tissue regeneration.

BIO-O-08

Studies on effect of CuO on mechanical properties and in vitro performance in 13–93 bioactive glass scaffolds

Akher Ali[a*], Vikash Kumar Vyas[a], Sunil Prasad[a], Md Ershad[a], S.P.Singh[a*], Ram Pyare[a*]

[a]Indian Institute of Technology(BHU), Varanasi, Uttar Pradesh, 221005, INDIA

Keywords: Bioglass, glass ceramics, scaffold, MTT assay

13-93 bioactive glass with the general formula (54.6-X) SiO2 $6Na_2O$ 7.9 K_2O 7.7MgO 22CaO $1.74P_2O_5$ (all are in mole %) where X= 1, 2 and 3 mole % CuO, were prepared by traditional melt-quenching route. Polymer foam with interconnected pores has been used on later stage to prepare porous (Porosity>50 %) bioactive scaffolds. CuO addition in the glass was aiming mainly in the purpose of a comparative study on cytotoxicity, cell proliferation and antibacterial ability with the base glass scaffold. Additionally Increasing trend of CuO has found to increase the fracture strength of the glass and compressive strength as well. Mechanical properties have been measured and the observed values were found similar to the values of cancellous bone reported. The invitro bioactivity of the scaffold has been observed by FTIR, SEM and XRD after immersing the samples in SBF for various time periods. The colorimetric MTT (Methylthiazol Tetrazolium) assay was used for study of cell cytotoxicity, cell proliferation and viability for the glasses. The results indicate that CuO incorporated 13-93 scaffold could be applied to bone repair and regeneration.

BIO-O-09

Surface-modified PLGA Particles that protect against Myocardial Cell Death

Amaraporn Wongrakpanich[a,b,#], Angie S. Morris[a], Sean M. Geary[a], Mei-ling A. Joiner[c] and Aliasger K. Salem [a*]

[a]*Pharmaceutics and Translational Therapeutics, College of Pharmacy, University of Iowa, IA, 52246, USA*

[b]*Department of Pharmacy, Faculty of Pharmacy, Mahidol University, Bangkok, 10400, Thailand*

*Corresponding author: aliasger-salem@uiowa.edu

#Presenting author: amaraporn.won@mahidol.ac.th

Keywords: PLGA, CaMKII, sub-cellular targetting

Myocardial infarction (MI) or a heart attack in coronary heart disease is a leading cause of death. One of the causes of myocardial cell death during ischemic/reperfusion injury in MI patients is an excess of calcium (Ca^{2+}) influx into mitochondria during mitochondrial re-energization. This overload of Ca^{2+} triggers the opening of the mitochondrial permeability transition pore (mPTP) and increased levels of reactive oxygen species (ROS), which eventually induces programmed cell death. The Ca^{2+} and calmodulin-dependent protein kinase II (CaMKII) enzyme is activated during the ischemic/reperfusion stage and is responsible for mitochondrial Ca^{2+} influx. Sub-micron particles composed of polylactic-co-glycolic acid (PLGA), loaded with a CaMKII inhibitor peptide, and coated with a mitochondria targeting moiety, triphenylphosphonium cation (TPP), can enter, accumulate and release the peptide inside cardiomyocytes mitochondria to inhibit CaMKII activity, thus reducing myocardial cell death.

CaMKII inhibitor peptide-loaded particles or "CIP" were made using two types of polymer: Poly lactic-co-glycolic acid (PLGA) and PLGA-NH_2. A double emulsion-solvent diffusion method using 1% polyvinyl alcohol as a surfactant and ethyl acetate as a solvent was used to manufacture the particles. These particles had diameters < 200 nm and were negatively charged. To formulate mitochondria-targeting particles or "TPP-CIP", particles were functionalized with TPP using carbodiimide crosslinker chemistry. The conjugation was confirmed using zeta potential measurement and an assay measuring fluorescamine reactivity. To develop an in vitro system for testing the potency of the particles, a differentiated rat cardiomyocyte (H9c2) cell line was used. Isoprenaline (ISO) was introduced to cells to activate CaMKII in mitochondria. Using flow cytometry, fluorescence labeled TPP-CIP were assessed to be taken up into mitochondria and successfully reduced intracellular reactive oxygen species induced by ISO. When differentiated H9c2 cells were treated with TPP-CIP prior exposed them to ISO, they maintained mitochondrial membrane potential.

This study reports on the development of a new submicron sized particulate drug delivery system carrying a CaMKII inhibitor peptide designed to protect cells against mitochondrial injury. The cellular uptake and mitochondrial targeting ability was achieved through the surface conjugation of PLGA-based carriers with a mitochondrial targeting molecule, TPP. TPP-CIP protected cardiomyocyte-like cells from ISO-induced ROS production and decreased mitochondrial membrane potential. TPP-CIP have the potential to be used in protection against ischemia/reperfusion injury in patients susceptible to heart attacks.

BIO-O-11

Comparison of the Release of Aloe Vera Extracts from Poly(vinyl alcohol) Electrospun Fibers and Hydrogel Films for Wound Healing Applications.

Sutasinee Sirima[*], Manisara Phiriyawirut [a], Khomson Suttisintong [b]
[a] Department of Tool and Materials Engineering, Faculty of Engineering, King Mongkut's University of Technology Thonburi, Bangkok, 10140, Thailand
[b]National Nanotechnology Center, Thailand Science Park, Pathum Thani 12120, Thailand
*E-mail address : **sutasinee.sirima@hotmail.com**

Keywords: Electrospun fibers, Hydrogel film, Aloe vera extract, Poly(vinyl alcohol)

Aloe vera extracts, consisting of active compounds that decrease pain and inflammation and stimulate skin growth and repair, are selected as a drug model in this work. Polyvinyl alcohol (PVA) was used as base material. Release profiles of aloe vera extracts from PVA electrospun fibers were compared to those from PVA hydrogel films prepared by freezing/thawing method. This method provided a physical crosslinked polymer. The concentration of PVA solution used for electrospinning and hydrogel preparation was 10% wt with different contents of aloe vera extracts (0, 30, 50, 70 and 90% w/w). The properties of electrospun fibers and hydrogel films were evaluated in terms of morphology, chemical structure, swelling behavior and release profiles. The morphological properties of electrospun fibers and hydrogel film were observed by SEM. Electrospun fibers were smoothly round, high surface area, and non-woven (Fig 1a), while hydrogel film possessed rough surface and was covered with porous (Fig 1b). Fourier transform infrared spectroscopic measurement exhibited the existence of relevant functional groups of both PVA and aloe vera extracts. The results showed relevant functional groups of aloe vera extracts in both electrospun fibers and hydrogel film. The release of aloe vera extracts from both electrospun fibers and hydrogel film was evaluated in phosphate buffer of pH 5.5 at 25 ^{o}C and was monitored by UV–vis spectroscopy. It was revealed that as the content of aloe vera increased, the amount of aloe vera extracts released from electrospun fibers decreased. This result contrasts with the release of aloe vera from hydrogel film which increased when the content of aloe vera increased. It was also noticed that the amount of aloe vera extracts released from electrospun fibers was more than that from hydrogel films at 600 minutes. The results also showed that the releasing rate of aloe vera from electrospun fibers was faster than that from hydrogel films. This is probably because electrospun fibers had much higher surface area than that of hydrogel film thus, the release was faster.

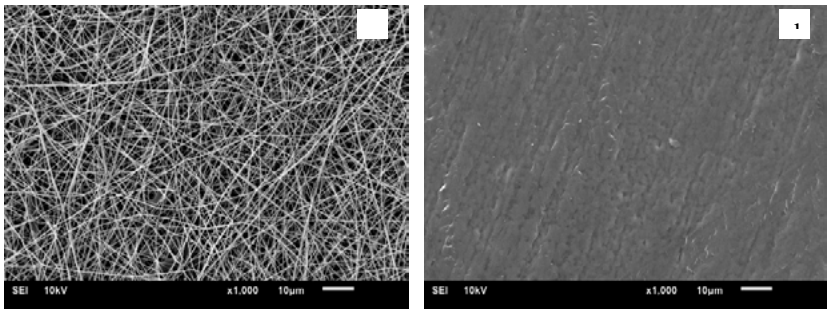

Figure.1 SEM images of (a) electrospun fibers and (b) hydrogel films at 30 w/w of aloe vera in PVA.

BIO-O-13

Fluoride Recharge Ability of Resin-based Pit and Fissure Sealant with Synthesized Mesoporous Silica Filler

Atikom Surintanasarn[a], Krisana Siralertmukul[b], Niyom Thamronganansku[a,*]
[a]*Department of Prosthodontics, Faculty of Dentistry, Chulalongkorn University, 34 Henri-Dunant Rd., Pathumwan, Bangkok 10330, Thailand*
[b]*Metallurgy and Materials Science Research Institute, Chulalongkorn University, Soi Chulalongkorn 12, Phayathai Rd., Pathumwan, Bangkok 10330, Thailand*
*Niyom.t@chula.ac.th

Keywords: Fluoride recharge, Mesoporous silica, Pit and fissure sealant

Pit and fissure sealant could be described as a material applied to pit and fissure of caries-susceptible teeth which is the most frequently attacked area by dental caries. Resin-based sealant has been generally used because of high retention rate but secondary caries could form at the margin of material. Glass-ionomer sealant has also been introduced because of fluoride release and recharge properties which could reduce prevalence of secondary caries but retention rate is still questionable. The addition of fluoride in resin-based sealant which has short-term fluoride release and does not have fluoride recharge ability seems to be unproductive. The aim of this study was to examine the effects of synthesized mesoporous silica, calcium carbonate, and fluoro-alumino silicate glass as active filler in resin-based pit and fissure sealant on fluoride release and recharge abilities. Mesoporous silica was synthesized from tetraethyl orthosilicate (TEOS) using sol-gel method. Resin-based sealant was incorporated with 5% w/w of filler (<45 μm): synthesized mesoporous silica (S), calcium carbonate (C), and fluoro-alumino silicate glass (F). Resin-based sealant without filler added was the control. Ten disc-shaped specimens of each group were prepared in plastic mold (diameter of 10 mm and depth of 1 mm). The filler was added and mixed for 60 seconds in an amber plastic chamber to prevent visible light that could affect the polymerization process of light-curing material. An LED light curing unit was used for light activation. Specimens of each group were separately stored in 3 mL of deionized water in plastic container at 37°C. Then, the fluoride concentration of the solution was measured every 3 days (from day 3 to day 27) using a fluoride selective electrode. The solution left in plastic container was discarded after each measurement. To determine the fluoride recharge ability of the specimens, each specimen was separately soaked in 2 mL of 1.23% acidulated phosphate fluoride (APF) gel for 4 minutes at day 9 and day 18 after taking fluoride measurements. Specimen was then rinsed and cleaned with deionized water and then stored in 3 mL of fresh deionized water in new plastic container. Fluoride release before recharge was only found in F (0.1024±0.0077 ppm) at day 3 and then gradually decreased to baseline by day 9. After both recharges, the highest fluoride release was found in S (0.0804±0.0095 ppm after first recharge and 0.0601±0.0092 after second recharge), followed by F (0.0386±0.0024 ppm after first recharge and 0.0313±0.0027 ppm after second recharge), and then decreased to baseline. Fluoride recharge was not found in C and control. This result suggested that resin-based pit and fissure sealant containing synthesized mesoporous silica filler has fluoride recharge ability which might prevent secondary caries at material-enamel interface.

BIO-O-14

Factors Influencing the Deposition of Biomimetic Calcium Phosphate on 3D Printed Hydroxyapatite Substrate

Faungchat Thammarakcharoen[a] and Jintamai Suwanprateeb[a]*

[a]*National Metal and Materials Technology Center (MTEC),*
114 Paholyothin Road, Klong 1, Klongluang, Pathumthani 12120 Thailand

*jintamai@mtec.or.th (corresponding author)

Keywords: Bone substitutes, Calcium phosphates, Hydroxyapatite, Biomimetic.

It was shown that biomimetic technique which mimics the biological process in nature could be applied to co-deposit calcium phosphate layer and active ingredients to alter the storage and releasing profile compared to typical direct absorption technique. However, this technique was mainly limited to the production of coating on metallic substrate. Recently, three dimensionally printed hydroxyapatite (HA) was developed for using as novel bone graft. It was contemplated that this biomimetic co-deposition could also be adapted to 3D printed hydroxyapatite substrate. This biomimetic process was done by immersing in accelerated calcium phosphate solution containing calcium and phosphate ions at the concentration of 3.87 mM and 2.32 mM, respectively to produce the deposition of calcium phosphate on such substrate. To investigate the factors influencing biomimetic calcium phosphate deposition on HA substrate, soaking times (2, 4 and 6 hrs) and solution temperatures (23, 37 and 50 °C) in refreshed and non-refreshed solutions were studied. The results showed that the deposition content of calcium phosphate increased with increasing soaking times at each temperatures regardless of solution refreshment. Using refreshed solution resulted in greater content of coating than using non-refreshed solution. At the soaking time of 4 and 6 hrs, it was found that increasing solution temperatures in non-refreshed solution exhibited a decrease in calcium phosphate deposition content whereas the increase in calcium phosphate content was observed when using refreshed solution. The newly deposited calcium phosphate crystals were observed to grow on the HA substrate crystals and octacalcium phosphate and HA were found to be the main phases. These results indicated that soaking temperature, soaking time and ionic strength of the solutions were important factors for calcium phosphate crystals depositing on HA using biomimetic process.

BIO-P-01

Improving Mechanical Properties of Biphasic Calcium Phosphate Bone Cement by Chitosan Fiber Reinforcement

Nuan La-ong Srakaew[a,b]*, Sanong Suksaweang[c], Sirirat Tubsungnoen Rattanachan[b]

[a]*Department of Materials Engineering, Faculty of Engineering and Architecture, Rajamangala University of Technology Isan, Muang District, Nakhon Ratchasima, 30000, Thailand*

[b]*School of Ceramic Engineering, Institute of Engineering, Suranaree University of Technology, Muang District, Nakhon Ratchasima, 30000, Thailand*

[c]*School of Pathology & Laboratory Medicine, Institute of Medicine, Suranaree University of Technology, Muang District, Nakhon Ratchasima, 30000, Thailand*

*E-mail address: n_srakaew@hotmail.com

Keywords: Chitosan fiber, Biphasic calcium phosphate, Bone cement

Calcium phosphate cement (CPC) is used as a self-setting material for dental, craniofacial and bone repairs. However, CPC exhibits poor mechanical properties and low biodegradable rate so that it is limited in use to non-load bearing defects. Biphasic calcium phosphate cement (BCPC) composed of β-tricalcium phosphate (β-TCP) and hydroxyapatite (HA) has been extensively investigated because of their good biodegradation rate, bioactivity and osteoconductivity. To improve the mechanical properties of BCPC, fiber reinforcement is a useful and frequently used method. In this work, 0 - 2 % (w/w) chitosan fibers were incorporated in BCPC, containing 0 – 20 % (w/w) β-TCP and 80 - 100 % (w/w) HA, to improve the mechanical properties of the bone cement. The effect of chitosan fiber addition on the properties of BCPC such as setting time, compressive strength, injectability, pH, phase composition and *in vitro* degradation were studied and compared with apatite-based cement.

BIO-P-02

In vivo of Sericin-Polyurethane Nanofiber Mats for Wound Healing in Rat

Pornpen Siridamrong[a*], Piyaporn Kampeerapappun[b], Chaweewan Poonthananiwatkul[c], Ghit laungsapapun[c]

[a]Engineering Department, Thailand Institute of Scientific and Technological Research, Khlong Luang, Pathum Thani, 12120, Thailand
[b]Division of Textile Chemical Engineering, Faculty of Textile Industries, Rajamangala University of Technology Krungthep, Nanglingee Road, Sathorn, Bangkok, 10120, Thailand
[c]Material Properties Analysis and Development Center, Thailand Institute of Scientific and Technological Research, Khlong Luang, Pathum Thani, 12120, Thailand
*E-mail address: pornpen295@gmail.com

Keywords: Electrospinning: Sericin: Wound healing: Rat

The objective of this study was to investigate sericin-polyurethane nanofiber cover (SUC) for wound dressing materials in a rat skin. Sericin-polyurethane blended nanofibers were fabricated by using electrospinning. The composition of 3% w/v polyurethane in ethanol and 19% w/v sericin were blended and electrospun at 15 kV, 20 cm from tip to collector with a feed rate of 6.2 ml/h. The mats, approximately 1.5 mm thick, were sterile by gamma irradiation with a radiation dose of 15 kGy. The samples for *in vitro* and *in vivo* testing were separated into three groups; sham, polyurethane nanofiber cover (UC), and SUC. *In vitro* cultured L929 cell lines were investigated with inverted microscope. It was found that cells migrated to SUC. For *in vivo* tests, the remaining wound in rats was measured on day 3, 7, 14, and 21 after incision. Compared to the original size of wound samples, the size of the wound remained 24% for SUC, 33% for sham, and 34% for UC at day 7. It can be concluded that sericin is non-toxic to cells and can promote wound healing process in rats.

BIO-P-03

In Vitro Evaluation of Zein as Matrix Forming Agent in Extended Released Tablets Containing Theophylline

Noppadol Chongcherdsak[a], Nawinda Chinatangkul[a,d], Chutima Limmatvapirat[b], Sontaya Limmatvapirat[c,d],*

[a]*Faculty of Pharmacy, Siam University, Phasi Charoen, Bangkok, 10160, Thailand*
[b]*Department of Pharmaceutical Chemistry, Faculty of Pharmacy, Silpakorn University, Meuang, Nakhon Pathom, 73000, Thailand*
[c]*Department of Pharmaceutical Technology, Faculty of Pharmacy, Silpakorn University, Meuang, Nakhon Pathom, 73000, Thailand*
[d]*Pharmaceutical Biopolymer Group (PBiG), Faculty of Pharmacy, Silpakorn University, Meuang, Nakhon Pathom, 73000, Thailand*
*Limmatvapirat_S@su.ac.th

Keywords: THEOPHYLLINE, KINETICS, ZEIN, MATRIX TABLET

Zein, a natural polymer derived from corn, has been widely used as a film coating material for controlling the release of drug. However, the role as matrix forming agent in tablets, especially extended release dosage forms, was not clearly studied. In this study, zein was aimed to be applied in matrix tablets containing theophylline as a model drug in order to reduce drug toxicity and improve oral bioavailability providing effective asthma treatment. The impact of zein on tableting properties was investigated. The matrix tablets with different amounts of zein were prepared by direct compression method. The zein based matrix tablets were then comparatively evaluated for their properties, including weight variation, thickness, diameter, hardness, friability, disintegration and drug release profile. The kinetics of drug release from matrix tablets in 0.1 N HCl and phosphate buffer pH 6.8 medium were also analyzed by using various mathematical models. The average weight and hardness were well-controlled in the specified range of 300±10 mg and 60±10 N, respectively demonstrating the compressibility property. As increasing the amount of zein, the friability was decreased from 1.34% to 0.58% due to the effect of binding property of zein leading to the formation of cohesive matrix tablets. The disintegration and drug release was also extended. When 30%w/w or more of zein was used, the prepared tablets did not disintegrate, and drug release was sustained over a period of 8 h resulting from the gel barrier form of zein after contacting with media. The kinetics of drug release in both media were best fitted with Higuchi's model, revealing that the diffusion process was the main mechanism of drug release from the zein based matrix tablet. These results suggested that zein had a good potential to be used as a matrix forming agent for extended-release dosage forms.

BIO-P-04

Preparation and Characterization of Hydroxyapatite Powder from Cockle shells

Tiwasawat Sirisoam[a*], Cherdsak Saelee[a], Sakdiphon Thiansem[b], Sittiporn Punyanitya[c]

[a] *Department of Physics and Materials Science, Faculty of Science, Chiang Mai University, Chiang Mai, 50200, Thailand*
[b] *Department of Industrial Chemistry, Faculty of Science, Chiang Mai University, Chiang Mai 50200, Thailand*
[c] *Biomedical Materials and Ceramic Industrial Research Unit, Chiang Mai, 50200, Thailand*

Corresponding author: t.sirisoam@gmail.com

Keywords: bioceramic, hydroxyapatite, biomaterial, cockle shells

Hydroxyapatite (HA) is one of the most popular materials used for bone repair. Many methods have been developed to produce synthetic HA such as solid-state synthesis, co precipitation or sol-gel method. Cockle shell contains plenty of $CaCO_3$ which can be used as raw material for HA synthesis. In our study, we reported a method to prepare HA from cockle shells. Before using the cockle shells, we measure the heavy metal level using atomic absorption spectroscopy (AAS) to ensure they are safe for use in human. Mercury, arsenic, lead and cadmium levels are < 0.25, 0.75, 0.31 and 0.14 ppm, respectively, which are in the acceptable range according to ASTM F1581-99. To synthesize HA, the cockle powder was calcined at 900^{o}C, yielding CaO with 95% purity. Then, CaO was co-precipitated with PO_4^{3-} in $NH_4H_2PO_4$ solution at Ca/P ratio of 1.67 to synthesize the HA powder. The optimized coprecipitation time to obtain HA was 8 hr. Structural characterization of the synthesized material was done by X-ray diffractometer, X-ray fluorescence and fourier transform infrared spectroscopy. Lattice parameter of the synthesized HA was matched with JCPDS NO: 09-0432 (hexagonal HA). The obtained HA powder had light blue color with an average particle size of 16 micrometer and a density of 3.167 g/cm^3.

BIO-P-05

Crystallization, mechanical properties and in vitro bioactivity assessment of (45S5-HA) biocomposite

Sunil Prasad*, Vikas Kumar Vyas, Md. Ershad, Akher Ali and Ram Pyare

Department of Ceramic Engineering, Indian Institute of Technology (BHU), Varanasi U.P.-221005, India

*sunilmnnit25@gmail.com

Keywords: Bioglass, Hydroxyapatite (HA), Biocomposites, SBF.

Abstract:

Bioglass® (45S5) was prepared by conventional melting process. Hydroxyapatite (HA) was prepared by sol-gel method. The bioglass (45S5) and hydroxyapatite ($Ca_{10}(PO_4)_6(OH)_2$) samples were mixed in a particular proportion to prepare composite by using hydraulic pressing. Based on thermogravimetric and differential thermal analysis, the composite were sintered with a suitable heat treatment process at 1000-1050°C. The in-vitro bioactivity of samples was determined in simulated body fluid for 1, 3, 7, 14, 21 and 30 days. The bioactivity was examined in vitro with respect to the ability of hydroxyapatite layer formation on the surface of samples when they were immersed in simulated body fluid (SBF). DTA/TGA, XRD, FTIR, SEM and mechanical studies were conducted for different characteristic measurement of biocomposites. The result shows the enhancement in bioactivity and mechanical properties of (45S5-HA) biocomposites for clinical implantation.

BIO-P-06

Mechanical Property and Morphology of Porous Fluorcanasite Glass-Ceramics Doped with Bioglass

Autcharaporn Srion[a,*], Katanchalee Nampuksa[a], Naruporn Monmaturapoj[a]

[a]*National Metal and Materials Technology Center (MTEC), Klong Luang, Pathumthani, 12120, Thailand*

*autchars@mtec.or.th

Keywords: Fluorcanasite, Bioglass, Scaffold, Glass ceramic, Biomedical

Fluorcanasite ($Ca_5Na_4K_2Si_{12}O_{30}F_4$) is the chain silicate glass-ceramic which obtained bulk nucleate and have good mechanical properties. Several fluorcanasite-based glass compositions have been reported in which attained an excellent bioactive and biocompatibility, potentially used in hard-tissue augmentation. Previously, our research group have fabricated porous fluorcanasite-based glass-ceramics by using a polymeric sponge technique. The influence of the heat treatment temperature (750, 800, 850 and 900ºC) on the phase formation, morphology and mechanical strength of the porous fluorcanasite glass-ceramic were investigated and reported. The results from that study showed that the porous fluorcanasite glass ceramic obtained the weak porous structure. Therefore, in this study, we aimed to improve the mechanical properties of the porous fluorcanasite glass-ceramic by doping bioglass which is the well-known bioactive and excellent mechanical properties as an additive in this system. Later on, the influence of bioglass additive (5%wt) on phase formation and morphology of the samples after heat treatment at 750, 800, 850 and 900ºC were investigated by using the X-ray diffractometer (XRD) and the scanning electron microscopy (SEM), respectively, as well as the compressive strength of the specimens also measured. The XRD results show canasite/canasite-A (ICDD No. 13-0553 and ICDD No. 45-1398) and fluorapatite (ICDD No.15-0876) were the dominant phase present with the minor phases of xonotlite (ICDD No. 23-0125) and cristobalite (ICDD No. 39-1425) in every porous glass-ceramic samples (with and without bioglass). The higher the heat treatment temperatures performed, the more the peaks of xonotlite were observed particularly in the sample after heat treatment at 900ºC. Meanwhile, SEM images presented the interconnected pore structures which having an average macropore size around 600 µm. At the same time, SEM images also showed the microstructure of needle-like crystals in the samples heat treated at 750°C, 800°C and 850°C which became the lath-like crystals after heat treatment at 900°C in the porous samples without bioglass. A similar microstructure of needle-like crystals also observed in sample with bioglass but these crystals were started to become the lath-like shape after heat treatment at 850°C rather than at 900°C. It seems that the greater the heat treatment temperatures, the coarser the crystals could be noticed. This could be implied that the addition of bioglass has less affected on the phase formation of the porous fluorcanasite-based glass-ceramics. In addition, the mechanical strength of the sample with bioglass seems slightly higher (~0.9 MPa) than that of samples without bioglass (~0.3 MPa). So that, it possibly conclude that the addition of bioglass could slightly improve the mechanical strength of the porous fluorcanasite-based glass-ceramics.

BIO-P-07

Double-walled PLA-PLGA particles, a particulate delivery system for cancer vaccines

Jarinya Supapattranon [a,#], Pichaporn Rodlamul [a,#] and Amaraporn Wongrakpanich[a,*]

[a]*Department of Pharmacy, Faculty of Pharmacy, Mahidol University, Bangkok, 10400, Thailand*

*Corresponding author: amaraporn.won@mahidol.ac.th
#Co-first authors

Keywords: PLGA, PLA, double-walled particles

Cancer vaccines are new emerging systems which can either be used as a prophylactic tool to prevent future cancer development or as a therapeutic approach to boost the immune system against an existent cancer. In recent years, a biodegradable and biocompatible polymer called poly lactic-co-glycolic acid (PLGA) has been widely used in cancer vaccine formulations. Although PLGA particles can deliver both antigen and adjuvant to the dendritic cells at the controlled manner, PLGA particles often give burst release which caused by a fast degradation profile. Thus, adding poly lactic acid (PLA), which degrades slower than PLGA, as particle shell can retain the antigen and/or adjuvant inside the particles, resulted in a more sustained release manner.

These double-walled particles composed of PLGA core and PLA shell were made using a double emulsion solvent evaporation method with 1% polyvinyl alcohol as a surfactant and dichloromethane as a solvent. The particles were collected using differential centrifugation and were lyophilized. These particles had diameters approximately equal to 1 μm with narrow size distribution and were negatively charged. According to the scanning electron micrograph, the particles were sphere with smooth surface. Since various antigens and adjuvants are protein/peptide, bovine serum albumin (BSA) was used as a model drug in this study. PLGA particles that prepared with the same method mentioned above were used as a control group. The in vitro release studies showed that BSA-loaded double-walled particles gave no BSA release in the beginning and slowly release BSA into the solution after 30 days. In contrast, BSA-loaded PLGA particles released its cargo in the first 4 hours.

In summary, double-walled PLA-PLGA particles can retain BSA inside their PLGA core. The particles released BSA after PLA shell degraded. Along with the traditional PLGA particles, this double-walled PLA-PLGA particles offer a versatile antigen-adjuvant release profile that could be tailored to generate a robust immune responses in cancer immunotherapy.

BIO-P-10

Shear Bond Strength of Resin Cement between Mica Glass-Ceramic and Human Dentin

Thapanee Srichumpong[a], Kallaya Suputtamongkol[b], Noparat Thongpun[b], Sukanda Angkulpipat[a], Sahadsaya Prasertwong[a] and Duangrudee Chaysuwan[a,*]

[a] *Department of Materials Engineering, Faculty of Engineering, Kasetsart University, 50 Ngam Wong Wan Rd, Chatuchak, Bangkok, 10900, Thailand*

[b] *Department of Prosthodontic, Faculty of Dentistry, Mahidol University, 6 Yothi Rd, Rajthawee, Bangkok, 10400, Thailand*

[a,*]E-mail address: fengddc@ku.ac.th, [b]E-mail address: kallaya.sup@mahidol.ac.th

Keywords: Mica glass-ceramics, Machinable glass-ceramics, Resin cement, Shear bond strength

The purpose of the research was to evaluate the shear bond strength of resin cement, for instance, Rely X™ Ultimate, Rely X™ U200 and Panavia F2.0 applied between mica glass-ceramic and human dentin. The mica glass-ceramic is a restorative dental material consisting of a glass system SiO_2-Al_2O_3-MgO-MgF_2-$SrCO_3$-$CaCO_3$-CaF_2 and P_2O_5 by melting at 1420°C for 1 h, pouring into a carbon mold and annealing 580°C for 1 h 30 min. The cylindrical specimen was cooled down in a furnace to room temperature to be a glass rod. Then, the heat treatment of the glass was processed for the nucleation and the crystallization. The glass rod was heated to the optimum nucleating temperature of 643°C for 3 h and to the crystallization temperature at 892°C for 3 h, respectively in order to transform into a glass-ceramic rod. Molar teeth specimens were cut, mounted with epoxy resin cold mounting and well-polished their surfaces. For mica glass ceramics, twelve disk specimens (n = 12) with 5 mm diameter and 5 mm thickness were prepared. The mica glass-ceramic surfaces were polished, ultrasonic cleaned and etched with a 9.6% hydrofluoric acid etching gel for 15s, rinsed with water and finally dried. At the contact area between the human dentin and the glass-ceramics, a 5 kg weight was loaded for 5 min while the dental curing light was using around this area to obtain cured specimens. All specimens were stored in distilled water at 37°C for 24 h. For shear bond strength test by a universal testing machine, a shear force was applied to each specimen at a cross-head speed of 1 mm/min until failures. The resin cement bond between the dentin and the glass-ceramic interfaces was examined by a stereo microscope and a scanning electron microscope. The mean shear bond strength of three different resin cement groups were reported as follows: Rely X™ Ultimate (11.51±3.04 MPa), Rely X™ U200 (4.57±1.40 MPa) and Panavia F2.0 (14.57±4.87 MPa).

Ceramics

CER-I-01

Machinable Glass-Ceramics as a Dental Material

Duangrudee Chaysuwan*
Department of Materials Engineering, Faculty of Engineering, Kasetsart University, Bangkok, 10900 Thailand
E-mail: *fengddc@ku.ac.th

Keywords: Mica-based glass-ceramics, Machinable glass-ceramics, All ceramic restorations, Translucency parameters, ISO 6872:2015(E)

The aim of this research was to develop a mica-based glass-ceramic for restorative dental materials according to Dentistry-Ceramic materials ISO 6872: 2015. The glass system of SiO_2-Al_2O_3-MgO-MgF_2-$SrCO_3$-$CaCO_3$-CaF_2 and P_2O_5 was prepared with 4.0 mol% fluorapatite called GCF4.0. The glass compositions were melted in 1 h. at 1450°C. with heating rate of 10°C/min and then the molten glass was quenched into the water to become glass frits. The obtained frits were crushed by a high-speed milling in alumina bowl, then sieved for <45 μm frits. Consequently, the pigments (metal oxides) were added into the glass frit and then homogenously milled. It was remelted and poured into the carbon mould at high temperature approximately 1450 °C, after that kept to annealing temperature 580°C (T_m-50°C) and cooled to room temperature to obtain a glass rod. Then, the heat treatment of the GCF4.0 glass was processed to the nucleation and crystallization, respectively, to transform to a glass-ceramic. The GCF4.0 glass-ceramic presented biaxial flexural strength (210 MPa), fracture toughness (2.04 MPa•√m) and chemical solubility (~380 μg•cm^{-2}) values, which were suitable to use as single-unit anterior or posterior prostheses for dental restorations according to ISO 6872:2015. However, the heat treatment time affected to crystal sizes and spatial distribution; the longer heat treatment time, the smaller crystals. However, the translucency parameters (TP) of the resultant glass-ceramics were affected by short heat treatment time for better translucency. The values of the properties were comparable to those of human enamel and suitable for some restorative dental applications.

CER-I-02

Current Researches on TiO_2-based Nanocomposites and Applications

Wisanu Pecharapa
College of Nanotechnology, King Mongkut's Institute of Technology Ladkrabang, Ladkrabang, Bangkok 10520, Thailand
E-mail: kpewisan@gmail.com

Keywords: TiO_2, nanocomposite

Abstract

Current researches on TiO_2-based nanocomposite materials are introduced. Low-dimensional TiO_2 structures were successfully synthesized by hydrothermal method starting from natural mineral and their composites were utilized as a potential material in practical optical applications. Nanocomposite films of electrospun N-doped TiO_2 nanofibers and TiO_2 nanoparticles Degussa (P25) were utilized as working electrode of typical dye-sensitized solar cells (DSSCs). The energy conversion efficiency (η) of the device tended to increase with increasing calcined temperature of the fibers with specific nanofiber loading content, indicating the significant enhancement in the device performance by the incorporation of the nanofibers. TiO_2/V_2O_5 nanocomposites were synthesized by sonochemical and hydrothermal process and then mixed with conventional mechanical milling process. As-prepared composites was utilized as energy storage material. The significant variation of charge storage properties of the composites under ultraviolet irradiation were achieved by varying V_2O_5 content in the composite. Next, synthesis of photosensitive Ag-doped SiO_2/TiO_2 hybrid composite films using for fabrication of the photo patterning by photo mask lithography technique is represented. The optical properties in the visible region of the photosensitive hybrid film were enhanced by the incorporation of Ag nanoparticles into the hybrid films. The fabrication of optical element utilizing as-prepared thin films was carried out by photo masking technique. Finally, TiO_2-based/PMMA/R6G composite thin films were prepared and employed as an effective light scattering layer in light-guided plate and optical concentrator applications.

CER-I-03

Exploration of Electronic Properties in "Materials Beyond Graphene": Transition Metal Dichalcogenides

Worawat Meevasana
School of Physics, Suranaree University of Technology, Nakhon Ratchasima, 30000, Thailand
e-mail: worawat@g.sut.ac.th

Keywords: transition metal dichalcogenide, MoS_2, WSe_2, $PdTe_2$, angle-resolved photoemission spectroscopy, electronic structure

Transition-metal dichalcogenides (TMD), or so called "materials beyond graphene", have gained much attention due to their properties which have higher potential for certain usages in optoelectronics, valleytronics, and spintronics. Among them, monolayer MoS_2 is one of the most-studied dichalcogenides. The transition from indirect (bulk) to direct band gap (monolayer) and controllable valley polarization are reported in atomically thin MoS_2. From our recent study, by using angle-resolved photoemission spectroscopy, we find that a quasi-freestanding MoS2 monolayer can be created on the surface of bulk MoS_2 by evaporating and subsequently intercalating potassium in the interlayer gap. This surface also exhibits strong spin-orbit coupling as expected in monolayer. And, more recently, we have experimentally observed a new type of spin character in bulk WSe_2. Furthermore, we also observed a pronounced effect of the so called "negative electronic compressibility" in WSe_2 where the chemical potential counterintuitively becomes lower upon increasing electron density; this allows more charge to be stored in this atomically-thin material, prompting application of high-density energy storage. If time allows, I will briefly discuss about our study of the topological quantum states in TMD and some basic concept in topological quantum computing.

CER-I-04

Engineering Hybrid Nanocapsules for Multifunctional Applications in Bioimaging

John Wang
Department of Materials Science and Engineering, National University of Singapore

For targeted bioimaging and theranostic applications, we have successfully developed a class of PEOlated polymeric micelle/silica as multifunctional nanocapsules for targeted bioimaging and controlled delivery. Bioimaging contrast agents, such as fluorescent conjugated polymers, CdSe/CdS/ZnS quantum dots (QDs), MnO_2 and Fe_3O_4 nanocrystals have been successfully encapsulated into poly(ethylene oxide) (PEO)-based polymeric micelle/silica dual layers via interfacial templating condensation. The encapsulation follows a green and straightforward microemulsion mechanism that directly proceeds in a near neutral pH aqueous environment. No detriment effects to the optical and magnetic properties of fluorescent conjugated polymers, QDs, MnO_2, and Fe_3O_4 nanocrystals are observed during encapsulation. The core-shell nanocapsules thus generated possess a polymeric micelle framework with a single QD/Fe_3O_4 nanocrystal encapsulated in the hydrophobic micellar core, an ultrathin (<5 nm in thickness) yet robust silica shell confined to the micellar core/corona interface and free PEO chains dangling on the surface. The free PEO chains effectively prevent nonspecific adsorption of biomolecules to the nanoparticles. Double shielding of polymeric micelle/silica shell remarkably improves the fluorescence resistance of conjugated polymers and QDs to strong acids and highly salted buffers. In vitro testing using MDA-MB-231 breast cancer cells demonstrates that these organic/inorganic dual layer-protected nanocapsules conjugated with folate show noncytotoxicity, bright fluorescence cellular imaging with high target specificity and improved performance in controlled delivery. In this talk, the latest development for the multifunctional nanocapsules is presented. The processing parameters involved in developing the multifunctional nanocapsules and their performance in bioimaging, both for T1 and T2, and theranostic applications are presented and discussed.

CER-I-05

Geopolymer from Industrial Wastes and its Applications

S. Jiemsirilers[*a] , A. Anchaleerat[a], A. Saikrasoon[a], S. Onutai[a,c], R. Pliansakul[a], T. Kobayashi[c], P. Laorattanakul[b], and P. Thavorniti[b],

[a]*Research Unit of Advanced Ceramics, Department of Materials Science, Faculty of Science, Chulalongkorn University, Thailand*

[b]*National Metal and Materials Technology Center, Thailand*

[c]*Department of Materials Science and Technology, Nagaoka University of Technology, 1603-1 Kamitomioka, Nagaoka, Niigata 940-2188, Japan*

*E-mail: Sirithan.j@chula.ac.th

Keywords: geopolymer, heavy metal adsorption, porous geopolymer

Geopolymer is known as environmentally friendly and sustainable material. It can be synthesized with low energy consumption process at room temperature or slightly above. Geopolymers can be prepared from any materials composed of silica (SiO_2) and alumina (Al_2O_3). Wide range of materials is presently used for geopolymerization. Besides the natural aluminosilicate materials such as clay like metakaolin and bentonite, the industrial by product and industrial wastes which included the materials rich in silica and alumina for examples; fly ash, blast furnace slag, aluminium waste, and rice husk ash. In our study, series of geopolymer have been synthesized; using local kaolins in Thailand, porous geopolymers, microwave assisted geopolymer, geoplymer for heavy metals adsorption and immobilization. Geopolymer can be prepared in bulk or porous form depends on the desire properties and applications. Proportion of H_2O and Na_2O, curing temperatures and time were varied to study their effects. The existing phases were investigated by using XRD. Compressive strength and density of the geopolymers were also examined. Geopolymerization was determined by FTIR. The main properties for example phases, mechanical strength, bonding, microstructure and thermal properties were characterized and compared.

CER-O-01

Synthesizing of Glass-Ceramics Composites for Opal Imitation by Direct Sintering Method

Duangkhae Bootkul[a], Saweat Intarasiri[b,*]
[a]*Department of General Science (Gems and Jewelry), Faculty of Science, Srinakharinwirot University, Bangkok 10110, Thailand*
[b]*Science and Technology Research Institute, Chiang Mai University, Chiang Mai 50200, Thailand*
*saweat@yahoo.com

Keywords: Glass-ceramics, Opal, Sintering, Waste

Basically, glass-ceramics composite materials are produced through controlling crystallization of base glass. These materials share the properties of both glass and ceramics. Generally, they contain an amorphous phase together with one or more crystalline phases. The purpose of the present study was to synthesize glass-ceramics materials which were opal-like appearance from soda lime glass (SLG), obtained from community discarded bottles, silica powder, titanium dioxide, and other coloring oxides. The glass bottles were grounded by ball milling and sieved to ~100 μm of particles size. The glass powders were pre-mixed with other raw materials in a mixer and poured to a stainless steel die of 35 mm inner diameter, then, the die was closed by two plungers of the same material. After manually compression, the die was brought to the pressing machine, using uniaxial isostatic cold pressing with constant pressure at 15 ton per square inch. Sintering processes were conducted at different temperature between 1000°C and 1200°C with 4 to 6 hrs holding time. Several techniques were applied for characterizing the ingots. The chemical analysis was performed by Energy Dispersive X-ray Fluorescence (ED-XRF). The mineralogical compositions were determined by X-ray diffraction (XRD) analysis. Raman spectroscopy was applied for optical characterization. The condition which made the best results for producing glass-ceramic materials for opal costume jewelry applications, in terms of color and appearance, was 60:35:2:2:1 wt.%, according to the ratio of SLG to silica powder to titanium dioxide to zinc oxide to other coloring oxides, with 1000°C and 4 hr heating. The major component of the ingots was SiO_2. CaO as a part of SLS glass was remained detectable and few percent of coloring oxides as intentionally mixed were also detected. Their specific gravity (S.G. = 2.07) was in the average value of opal and below the value of quartz (S.G. = 2.65) and their refractive index (n = 1.53) was close to the natural one. Natural opals are hydrous form of silica (SiO_2-n-H_2O) with α-cristobalite, tridymite and, in some cases, quartz in a very ordered structure (namely opal C) or disordered structure (namely opal CT) or completely amorphous (namely opal A). Opal A or precious opal is a poor Raman scatterer and it does not show any crystalline X-ray diffraction patterns. According to XRD results, our products were appeared to be in a non-crystalline form, confirming by no clear reflexed in the spectrum and the occurrence of raised background. The Raman measurement revealed that they were mostly in amorphous phase with the remaining of some other silicas, e.g. α-cristobalite, tridymite and quartz, confirming the XRD measurement. The hardness of the glass-ceramics composite (7-8 mohs scale) was higher than the natural one (5.5-6.5 mohs scale). The products were tough enough to be cut, polished and decorated to the jewelry settings. Thus, the invent technology is able to serve for the production of jewelry opal for the niche market.

CER-O-02

Destructive & Non-destructive Behavior of Nickel Oxide Doped Bioactive Glass & Glass-ceramic

Vikash Kumar Vyas [a*], A. Sampath Kumar, Sunil Prasad, Akher Ali, Manas Ranjan Majhi, Md Ershad, Niraj Singh Mehta, S. P. Singh and Ram Pyare
Department of Ceramic Engineering,
Indian Institute of Technology (Banaras Hindu University)
Varanasi -221005, India.

Keywords: Bioactive Glasses, Bioactive Glass - ceramics, Mechanical Properties, Elastic Modulus

Nickel oxide substituted bioactive glasses (45S5) have been prepared by the melting and annealing techniques. The doping of Ni^{2+} ion from 0-1.65 mol% of nickel oxide was done to replace Si^{4+} ion and yielded a non charge balanced bioactive glass. Polycrystalline bioactive glass ceramics were prepared through controlled heat treatment. The glass and glass-ceramic structure was evaluated using FTIR and XRD techniques. The crystalline phases in bioactive glass-ceramics were identified using X-ray diffraction. The destructive tests like micro hardness, compressive and flexural strengths and the non-destructive tests of elastic moduli were carried out. Both the results indicated that substitution of nickel oxide by silica in 45S5 bioactive glass and glass-ceramic enhanced its density, compressive strength, flexural strength, micro hardness and elastic properties.

CER-O-03

Effective Charge Separation and Photocatalytic Activity of Copper Ions -Modified Cerium Dioxide Nanoparticles

Duangdao Channei[a,b] Auppatham Nakaruk[c], Panatda Janneoy[d], and Sukon Phanichphant[e*]

[a]*Department of Chemistry, Faculty of Science, Naresuan University Phitsanulok 65000, Thailand*

[b]*Research Center for Academic Excellence in Petroleum, Petrochemicals and Advanced Materials, Naresuan University, Phitsanulok 65000, Thailand*

[c]*Department of Industrial Engineering, Faculty of Engineering, Naresuan University, Phitsanulok 65000, Thailand*

[d]*Department of Biochemistry, Faculty of Medical Science, Naresuan University, Phitsanulok 65000, Thailand*

[e]*Materials Science Research Center, Faculty of Science, Chiang Mai University, Chiang Mai 50200, Thailand*

*E-mail address corresponding author: sphanichphant@yahoo.com

Keywords: CeO_2, Photocatalytic activity, Cu-doped CeO_2, Charge separation

Pure CeO_2 and Cu-doped CeO_2 nanoparticles with different doping amounts of Cu in the range of 0.5-2.0 wt% were synthesized by the combination of homogeneous precipitation and impregnation methods. The samples were physically characterized in order to obtain the correlation between structure and photocatalytic properties by X-ray diffraction (XRD), transmission microscopy (TEM), UV-vis diffuse reflectance spectrophotometry (UV-vis DRS), X-ray photoelectron spectroscopy (XPS), and photoluminescence emission (PL). XRD results indicated that phase structures of pure CeO_2 and Cu-doped CeO_2 were cubic fluorite phase of CeO_2 and no other characteristic peaks related to impurities were detected. TEM images revealed that all samples were spherical in shape with the size less than 10 nm.The results from UV-vis reflectance spectra clearly indicated the shift of absorption band edge towards visible region (red shift) upon doping CeO_2 with Cu. The photocatalytic performances of the Cu-doped CeO_2 exhibited higher activity than pure CeO_2 for photocatalytic degradation of methylene blue under visible light irradiation, and the CeO_2 doped with 1.0 wt% Cu exhibited the highest photocatalytic activity. The improved photocatalytic performance is attributed to a decrease in band gap energy as well as increases the separation efficiency of photoinduced electrons and holes. As found from XPS analysis, Cu existed as Cu^{2+} ions in CeO_2. The presence of Cu^{2+} may act as electron acceptor (Cu^{2+}/Cu^{+}) and/or hole donor (Cu^{+}/Cu^{2+}) to facilitate charge carrier localization.

CER-O-04

Photocatalytic Degradation Study of Titania Sol-gel Coated on Commercial Unglazed Ceramic Tiles

Pat Sooksaen[a, b]*, Nawapan Saowaros[a], Khemphatsorn Ngamkaruhasereethorn[a], Angkoona Pringkasemchai[a]

[a] *Department of Materials Science and Engineering, Faculty of Engineering and Industrial Technology, Silpakorn University, Nakhon Pathom 73000 Thailand*

[b] *Center of Excellence for Petroleum, Petrochemicals and Advanced Materials, Chulalongkorn University, Bangkok, 10330, Thailand*

* *sooksaen_p@su.ac.th*

Keywords: Titania, Nanoparticles, Porosity, Ceramic tiles, Sol-gel

In this research photocatalytic degradation of nano-titania synthesized via sol-gel method and coated on commercial unglazed ceramic tiles was investigated. The starting precursors were titanium (IV) tetraisopropoxide ($Ti[OCH(CH_3)_2]_4$; TIP) , ethanol, hydrochloric acid and distilled water. Unglazed ceramic tiles were sintered at 900°C and 1100°C. The nano-titania sol-gels were applied on the tile surfaces using air-brush and calcined at 500°C for 3 h. The particle size of the synthesized TiO_2 varied in the range 8-20 nm. The photocatalysis of nano-titania was studied through the photodegradation of methylene blue solution under UVC irradiation using the UV-Vis Spectroscopy technique. The presence of nano-titania on unglazed ceramic tiles was confirmed by a scanning electron microscope equipped with energy dispersive X-ray spectrometer (EDS). Ceramic tiles sintered at 900°C gave higher open porosity of the surface and larger pores and hence higher nano-titania content was found within the porous surface. After the first test of photocatalytic degradation, the ceramic tiles were tested for adhesion of nanotitania by cross cut test following ASTM D3359 standard. The results showed that all unglazed ceramic tiles coated with nano-titania were able to show photodegradation of methylene blue both before and after the adhesion test in a similar manner. The reduction in UV absorption peak of MB from the UV-Vis technique was attributed to both the presence of nano-titania as a photocatalyst and porosity of the ceramic tile.

CER-O-05

Development of Infrared Reflective Black Pigment

Teerasak Tangkittimasak[a], Sirithan Jiemsirilers[b] and Pattana Rakkwamsuk[a]*
[a]*School of Energy, Environment and Materials, King Mongkut's University of Technology Thonburi, Bangkok, Thailand*
[b]*Department of Materials Science, Faculty of Science, Chulalongkorn University, Phyathai Road, Patumwan, Bangkok 10330, Thailand*
** Corresponding author E-mail: pattana.rak@kmutt.ac.th*

Keywords: Near-infrared reflective pigment, Black pigment, Cool pigment

The aim of the study was to synthesize a black pigment that reflects the near infrared radiation (NIR). The pigment can be used as reflective painting materials for buildings that help reduce heat penetration into buildings. The black pigments based on Fe_2O_3 – Cr_2O_3 – TiO_2 were mixed into 8 different compositions by varying Fe_2O_3 at 40, 50, 60 and 70 % by weight. For any given Fe_2O_3 wt%, Cr_2O_3 and TiO_2 were then added and its ratio was designed at x:y where y was 0 and 2 wt% and x was the weight percent that contributes the total. All mixed raw materials were calcined at 1150 ^oC and 1250 ^oC. This experimental preparation then produced 16 samples altogether for analysis. The NIR reflectance depended on the composition of the compound and the calcine temperature. It was found that the sample with Fe_2O_3, Cr_2O_3 and TiO_2 at 40, 58, and 2 wt%, respectively, gives maximum near infrared solar reflectance of 46.4%. Its color in the CIE color system was measured and the values of L*,a*, b* were found to be 20.95, 4.22 and 1.69, respectively. An XRD analysis was employed to investigate a microstructure of a complex inorganic pigment. It revealed that the degree of the NIR reflectance depended on the percentage of the phases of chromium titanium oxide and chromium iron oxide in the compound. The increase of NIR reflectance tended to be due to the increase of chromium titanium oxide.

CER-O-06

Actuators Based on Bidomain Ferroelectric Crystals: Fabrication and Application

Ilya Kubasov [a,*], Sergey Ksenich[a], Alexandr Temirov[a], Mikhail Malinkovich[a], Alexander Bykov[a], Dmitry Kiselev[a]

[a]National University of Science and Technology "MISiS", Moscow, 119991, GSP-1, 4, Leninsky av. (339) Russian Federation

Keywords: Bidomain crystal, Lithium niobate, Lithium tantalate, Scanning probe microscopy

Modern engineering is impossible without precision actuators that can provide predictable and accurate movements. One of the most widely used types of these devices is based on utilizing of converse piezoelectric effect. Piezoelectric actuators provide precision movements in scanning probe microscopes (SPM), laser gyroscopes, and deformable mirrors etc. Perspective devices based on piezoelectric actuators include: graphene-based and composite multiferroic laminates, moveable x-ray mirrors, optical waveguides with exact variable geometrical characteristics, MEMS and radioisotope generators.

Mostly, piezoelectric actuators are made of PZT-ceramics ($PbZr_xTi_{1-x}O_3$). However, such disadvantages of ferroelectric PZT ceramic as creep, non-linear character of deformation vs. applied voltage dependence, narrow range of operating temperatures limit the possibility to create highly precision actuators based on this material. On the other hand, piezoelectric single crystals do not possess these drawbacks, demonstrate high thermal and electrical stability and almost do not degrade but have too low piezoelectric coefficients. One of the ways to overcome this problem is to form bidomain structure in plate of ferroelectric crystal such as lithium niobate ($LiNbO_3$) or lithium tantalate ($LiTaO_3$). The bidomain plates with appropriate quality bend according to bimorph scheme when voltage is applied.

In this study we suggest a new technique to create bidomain $LiNbO_3$ and $LiTaO_3$ crystals. The method is based on annealing of a crystalline plate in non-uniform thermal field near Curie point. Main advantages of this technique are rapidity and the possibility to form bidomain structures equally successful in thick plates as in thin ones. We managed to create single crystalline bidomain actuators of large area (up to 10 cm^2) in plates of 0.5 mm thickness. The actuators demonstrated strongly linear dependence of deformation on applied voltage without hysteresis and creep. Movements up to 1000 μm were reached when the actuator was fastened as a console.

We also made an attempt to use bidomain crystals as piezoelectric positioning system of SPM and some scans were obtained.

The study was supported by the Ministry of Education and Science of the Russian Federation (Federal Targeted Programme for Research and Development in Priority Areas of Development of the Russian Scientific and Technological Complex for 2014-2020) (Project ID RFMEFI57815X0102)

CER-O-07

Effects of Aluminium Concentrations and Consolidation Techniques on Composition, Microstructure and Dielectric Properties of Strontium Titanate

Jednupong Palomas[a] and Oratai Jongprateep[a,*]
[a]*Department of Materials Engineering, Faculty of Engineering, Kasetsart University, Bangkok, 10900, Thailand*
* E-mail address: oratai.j@ku.ac.th

Keywords: Strontium titanate, Dielectric, Combustion, Doping

It has been accepted that compositions and microstructure significantly affect dielectric properties of materials. In general, chemical compositions are influenced by additive concentrations, while consolidation techniques control microstructure of the materials. This study, therefore, aimed at examining effects of aluminium concentrations and consolidation techniques on chemical compositions and microstructure of the strontium titanate. Experimental results revealed that at higher aluminium concentrations, only small quantities of TiO_2 secondary phase were present, while grain sizes generally decreased. The results also indicated that the cold isostatic pressing technique led to high sintered density. The greatest dielectric constant of 281.5 at 1 MHz obtained in this study was achieved in strontium titanate samples with 30 at% Al, pressed by cold isostatic pressing. Enhancement of dielectric constant of the samples was attributed to low secondary phase, fine grain sizes and high sintered density.

CER-O-08

Effects of Ball Milling on the Properties of $(Ba_{1-x}Ca_x)(Ti_{0.92}Sn_{0.08})O_3$ Lead-Free Ceramics

Onchuda Wattanapradit[a] and Pornsuda Bomlai[a,*]
[a]*Department of Materials Science and Technology, Faculty of Science, Prince of Songkla University, Hat Yai, Songkhla, 90110, Thailand*
*E-mail address: pornsuda.b@psu.ac.th

Keywords: Lead-free materials, Two-step sintering, Ball-milling

The $(Ba_{1-x}Ca_x)(Ti_{0.92}Sn_{0.08})O_3$ (x = 0 and 0.02) lead-free ceramics were prepared by using different ball-milling method and time (common ball milling-24 h, high energy ball milling -1 and 3 h). The two-step sintering method was used for sintered the samples. The densification, structure, dielectric and piezoelectric properties of the ceramics were investigated. The results showed that Ca addition could reduce sintering temperature effectively and enhanced densification at lower temperature when using the common ball-milling type. The XRD patterns of $(Ba_{1-x}Ca_x)TiO_3$ ceramics revealed the change in crystal symmetries from tetragonal to cubic phase with increasing Ca content from 0 to 0.02. However, the crystal structure did not change due to the effect of ball-milling method. Ca incorporation caused a decrease of the grain size and Curie temperature. Moreover, the largest grain size was found in the ceramics with 24 h-common ball-milling, whereas the smallest size was obtained for the ceramics with 1 h-high energy ball-milling. The dielectric and piezoelectric properties were also affected to Ca addition and ball-milling. High piezoelectric coefficient of d_{33} = 173 pC/N, dielectric constant $\varepsilon_r \sim 3200$ and dissipation factor $\tan\delta \sim 0.05$ were obtained for the x = 0 sample with high energy ball-milling for 1 h.

CER-O-09

Photocatalytic Comparative Study of TiO_2, ZnO, Ag-G-ZnO and Ag-G-TiO_2 Nanocomposite Films: Biomaterial Applications

Phuri Kalnaowakul[a,b,c] , Tonghathai Phairatana[d] and Aphichart Rodchanarowan[a,*]
[a]*Department of Materials Engineering, Faculty of Engineering, Kasetsart University, Chatuchak, Bangkok, 10900, Thailand*
[b]*College of Industrial Technology, King Mongkut's University and Technology North Bangkok, Bangsue, Thailand 10800*
[c]*Center of Welding Engineering and Metallurgical Inspection, Science and Technology Research Institute of King Mongkut's University and Technology North Bangkok, Bangsue, Thailand 10800*
[d] *Institute of Biomedical Engineering, Faculty of Medicine, Prince of Songkla University, Songkhla, Thailand 90110*
E-mail address: phurikalnaowakun@hotmail.com, t.phairatana@gmail.com, and fengacrw@ku.ac.th[*]

Keywords: ZnO, TiO_2, Composite materials, Photocatalytic activity.

In this study, the photocatalytic properties and morphology of TiO_2, ZnO, Ag-graphene-zinc oxide (Ag-G-ZnO) and Ag-graphene-titanium dioxide (Ag-G-TiO_2) nanocomposite were compared. The Ag-G-ZnO and Ag-G-TiO_2 nanocomposite were successfully prepared by thermal decomposition colloidal solution. These prepared composites were characterized by X-ray diffraction (XRD), scanning electron microscopy (SEM), UV-Vis spectroscopy and photocatalytic activities. The results from XRD patterns show that Ag-G-TiO_2 composites and the Ag-G-ZnO nanocomposites were in the form of fcc and hcp crystal structure, respectively. The SEM images show that at calcination of 500 °C for 3 h, the composite thin film of Ag-G-ZnO and Ag-G-TiO_2 were homogenous. In case of the photocatalytic experiments using methylene blue dye (MB) under UV irradiation, the order of the photocatalytic activities from high to low performances are Ag-G-ZnO, Ag-G-TiO_2, ZnO and TiO_2, respectively.

CER-O-10

Development of Water Assisted Solid State Reaction for the Ceramic Materials

Kenji Toda[a,*], Sun Woog Kim[a], Takuya Hasegawa[a], Mizuki Watanabe[a], Tatsuro Kaneko[a], Ayano Toda[a], Atsushi Itadani[a], Mineo Sato[a], Kazuyoshi Uematsu[a], Tadashi Ishigaki[a], Junko Koide[b], Masako Toda[b], Emiko Kawakami[b], Yoshiaki Kudo[b], Takaki Masaki[c] and Dae Ho Yoon[c]

[a]Niigata University, Niigata, 950-2181, Japan

[b]N-Luminescence Corporation, Niigata, 950-2101, Japan

[c]Sungkyunkwan University, Kyunggi-do, 400-746, Republic of Korea

*ktoda@eng.niigata-u.ac.jp

Keywords: Solid State Reaction, Soft Chemistry, Water

Most of ceramic materials are usually synthesized by a conventional solid state reaction method. Rapid progress of the solid state reaction required to fulfill two conditions of "Thermodynamics" and "Kinetics". Based on defect thermodynamics, ionic diffusion in the ionic crystal during a conventional solid state reaction is very slow at around room temperature. Therefore, the solid state reaction method requires a high temperature for increasing of the reactivity among raw material powders. The high temperature processing will probably bring irregular particle morphology of the obtained powders. Since some liquid phase reactions can occur at relatively low temperatures as compared to the conventional solid state reactions, solution process required to dry the solvent and special equipment for the separations. On the other hand, we have proposed a new simple water-assisted solid state reaction method (WASSR). This process is very simple and can synthesize the ceramic materials just by mixing of raw materials added a small amount (only 10 wt% for raw material mixture) of water. This reaction is accelerated solid state reaction by the water.

For example, YVO_4 can be synthesized at room temperature just by 3 h mixing the raw materials (Y_2O_3 and V_2O_5) with a small amount (10 wt%) of water. A stoichiometric ratio mixture of Y_2O_3 (0.2769 g) and V_2O_5 (0.2231 g) was mixed using a mortar. A small amount of de-ionized water was added to the mixture in a ratio of 10 wt% and mixed using mortar for 3 h to synthesize to a single phase. The average particle sizes were approximately under 100 nm for the sample synthesized by the WASSR method.

The reaction mechanism of WASSR method is different from the conventional solid state, solution and mechano-chemical reactions. The solubility of the Y_2O_3 and V_2O_5 raw materials in water are 0.018 g/l and 0.700 g/l, respectively. Total amount of dissolved Y_2O_3 and V_2O_5 in water is negligible low in the reaction of the WASSR method. This result suggests that the reaction is also different from a solution reaction, which occurs by the dissolution of the raw materials. In addition, the WASSR method proceeds without strong mechanical load (hand mixing). Therefore, these results indicate that the reaction mechanism of the samples prepared by the WASSR method was water assisted solid state reaction and not a mechano-chemical reaction.

We can successfully synthesize many nano-sized ceramics (BaTiO3, LiCoO2, BiVO4, CsVO3, Li3PO4) below 373 K using the WASSR method. Our proposed the WASSR method is promising for an industrial processing of practical ceramic materials.

CER-O-11

Effect of Particle Size Distribution on the Sinterability of Cerium (IV) Oxide using Spark Plasma Sintering

Anil Prasad[a,*], Linu Malakkal[b], Lukas Bichler[a] and Jerzy Szpunar[b]
[a]*School Of Engineering, University of British Columbia Okanagan, Kelowna, British Columbia, V1X 2P4, Canada*
[b]*University of Saskatchewan, Saskatoon, S7N 5A9, Saskatchewan, Canada*

Keywords: Spark Plasma Sintering C, Cerium dioxide C, Particle Size Distribution C

Spark Plasma Sintering (SPS) is a novel sintering technique, which has been used effectively for processing a wide range of materials such as ceramics, metals and composites. Cerium Dioxide (CeO_2) finds application as an electrolyte in solid oxide fuel cells owing to its excellent ionic conductivity. However, SPS processing of CeO_2 at high temperatures has been challenging due to the electric current flowing through the micro CeO_2 (particle size: 15µm) powder during consolidation resulting in undesirable phase transformations, since typical processing conditions range from 1500°C, 50 MPa and holding times of 5 min [1]. Therefore, it is crucial to investigate alternate routes to improve the sinterability of CeO_2 via SPS. Literature on experimental and theoretical studies on sintering of ceramics suggests that a modulation of particle size distribution may lead to an improvement in sinterability. Thus, in this study, the effect of only particle size distribution on SPS processing of CeO_2 was investigated. Four powder blends were prepared by mixing a nano CeO_2 (particle size: 80nm) and a micro CeO_2 (particle size: 15µm) powder, to yield: 100% n-CeO_2+ 0% m-CeO2; 100% n-CeO_2+ 0% m-CeO2; 100% n-CeO_2+ 0% m-CeO2; 0% n-CeO2 + 100% u-CeO2). The as-sintered pellets were characterized using XRD and SEM to relate the effect of particle size distribution on the densification kinetics and phase evolution during SPS processing. Though particle size distribution is not the only factor that might affect the sintering kinetics of cerium dioxide, it is important to study this route too, so as to check if it influences the densification of cerium dioxide during SPS.

CER-O-14

Development of Metakaolin Based Geopolymers for Bone Graft Application

Sarochapat Sutikulsombat[a], Alice Du Granrut[b], Chayanee Tippayasam[a], Duangrudee Chaysuwan[a,*]

[a]*Department of Materials Engineering, Faculty of Engineering, Kasetsart University, 50 Ngam Wong Wan Rd, Chatuchak, Bangkok, 10900, Thailand.*

[b]*National School of Engineering, ENSIL, Parc ester technophole, 7 rue Atlantis, Limoges, 87000, France*

[*]E-mail address : fengddc@ku.ac.th

Keywords: Biogeopolymer, Geopolymer for bone graft, Metakaolin based geopolymers

The formation of apatite layer was investigated above the surface of geopolymer samples after soaked in the stimulated body fluid (SBF) called the *in vitro* study for use as biomaterials. Normally, geopolymer consists of alkali activators and other raw materials, the ratio of alkali activators and raw materials for this research was 1:1. Alkali activators were potassium hydroxide (KOH) and potassium silicate (K_2SiO_3) with a ratio of KOH and K_2SiO_3 = 2:3. Metakaolin (MK) and calcium hydroxide ($Ca(OH)_2$) were used as raw materials by using 100 wt% MK : 20 wt% ($Ca(OH)_2$). Eggshell (E), hydroxyapatite (HA) and polylactic acid (PLA) were chosen as additivesin order to increase calcium content and to improve the biocompatability of the geopolymer. Hydroxyapatite was synthesized by the sol-gel method. Geopolymer spicemens were named as pure (No additives), E, HA and PLA. Then, geopolymers were calcined at 550 °C for 6 h to eliminate water and PLA as well as to create pores. Consequently, the specimens were commonly soaked in the SBF solution for 7, 14, 21 and 28 days at 36.5°C in an incubator. The results of geopolymers have been characterized by SEM, XRD and FTIR. The SEM micrographs presented the apatite-like layer appearing in form of spherical particles and grew progressively day after day. For XRD results, they showed the carbonate apatite, calcium carbonate, calcium silicate and geopolymer peaks. The results of the FTIR analysis strongly supported the XRD patterns that the functional groups were detected on the surface of samples such as phosphate and carbonate groups, moreover, water was also found because of moisture in the chamber. These observations raised an importance with respect to the apatite-like layer which occurred on surfaces of all geopolymers depending upon the length of soaking in SBF.

CER-O-15

Improvement of Compressive Strength and Thermal Shock Resistance of Fly Ash-Based Geopolymer Composites

Patthamaporn Timakul[a,*], Weerada Rattanaprasit[a] and Pavadee Aungkavattana[b]
[a]National Metal and Materials Technology Center (MTEC), National Science and Technology Development Agency (NSTDA), 114 Thailand Science Park, Pahonyothin Rd., Klong Luang, Pathumthani, 12120, Thailand
[b]National Nanotechnology Center(Nanotec), NSTDA, 111 Thailand Science Park, Pahonyothin Rd., Klong Luang, Pathumthani, 12120, Thailand
∗patthamt@mtec.or.th

Keywords: Geopolymer composites; Titanium dioxide; Compressive strength; Thermal shock resistance

One ton of cement production releases about one ton of CO_2 to the atmosphere, which is responsible for 7% of the total CO_2 emission. Hence, the effort of reducing greenhouse gas emission from Portland cement production has become a motivation to develop environmental friendly construction materials. Geopolymers are generally alkali-activated aluminosilicate materials which possess excellent strength and thermal properties for wide range of applications in building and construction materials. This study presented the effect of 0−5 wt% TiO_2 addition on compressive strength and thermal shock resistance of fly ash−based geopolymer composites. The composites were prepared by activating high calcium fly ash reinforced with basalt fibers and added TiO_2. The compressive strength of the composites after aging for 28 days increased to 52 MPa when 5 wt% TiO_2 was added. The retained compressive strength, when 5 wt% TiO_2 was added, after 15 thermal cycles from 800 °C to R.T. was 26 MPa, increased by 44% compared to TiO_2 free composites. Such an enhancement was ascribed to the acceleration of hydration reactions in geopolymer structures resulting more calcium silicate hydrate (C−S−H) phases, which could be detected by XRD and EDS techniques. C−S−H phases resulted in a denser matrix with increased strength.

CER-O-16

Synthesis and Properties of Geopolymers from Two Different Power Plants Bottom Ash in Thailand

Anucha Wannagon[a,*], Pattarawan Choeycharoen and Watcharee Sornlar
[a]*National Metal and Materials Technology Center, NSTDA, Thailand Science Park, Pathumthani, 12120, Thailand*
*anuchaw@mtec.or.th

Keywords: Geopolymer, Bottom ash, Property

Geopolymers synthesized from two sources of bottom ash were compared in terms of their forming ability and properties. The bottom ashes were collected from the coal-fired power plants located in Lampang and Rayong provinces. The alkaline solution used for geopolymerization include sodium silicate and 10 molar sodium hydroxide and the proportion of the bottom ash to alkaline solution was 70:30 by weight. The geopolymer synthesized from Lampang bottom ash has setting time within 1 day faster than the one from Rayong which was 2-7 days. After 28 day-curing in the air, the properties were measured and the results showed that geopolymer from Lampang bottom ash has 1.74-1.99 g/cm3 density, 10.15-17.96% water absorption and 22.05-31.04 MPa compressive strength while the geopolymer from Rayong bottom ash has 1.81-1.93 g/cm3 density, 9:36-13:25% water absorption and 11.31-26.90 MPa compressive strength. The XRF analysis showed the consistent results that the Lampang bottom ash has high amounts of Al and Ca which can be referred to the strength and setting time of the geopolymer. It has elemental weight ratio of Si/Al = 1.57, which is less than the Rayong bottom ash of Si/Al = 2.60. Therefore, the chemical composition is the main cause of the geopolymer synthesized from Lampang bottom ash featured the better properties than the Rayong bottom ash.

CER-O-17

Synthesis of Silicon-Carbon Films by High-Frequency Deposition

Alexander Temirov[a], Nikita Timushkin[a], Roman Zhukov[a], Ilya Kubasov[a], Mikhail Malinkovich[a] and Yurii Parkhomenko[a]
[a]National University of Science and Technology "MISiS", Moscow, Russia,
E-mail: temirov.alex@yandex.ru

Keywords: Silicon-Carbon, Diamond-Like Carbon, Films.

Silicon-carbon diamond-like films are a promising class of amorphous materials. Due to its unique physical properties – high hardness, low coefficient of friction, high chemical resistance and radiation resistance, they find an application in various fields of industry, mainly as protective coatings.

There are many methods of synthesis of diamond-like films. However, currently the development of new technologies is an important task.

This work presents a method of silicon-carbon films production by high-frequency deposition from the vapor mixture. This method is based on the diamond-like films synthesizing technology described by Parkhomenko et al (1). Here we managed to resolve the main drawback of this technology - the uncontrollable amount of background impurities in the resulting films.

The specimens described in this work were investigated by atomic force microscopy and ESCA. The absence of background impurities in the samples, and the presence of the ratio of sp2 and sp3 links, typical for silicon-carbon films presented Angus et all (2). The method of receiving allows creating doped silicon-carbon films with well-defined physical properties, primarily conductivity, eliminating the influence of background impurities.

The research was financially supported by the Federal Target Program "Investigation and Engineering in HighPriority Lines of Development of Science and Technology in Russia for 2014–2020" (unique project identifier RFMEFI57814X0071, contract no. 14.578.21.0071)

CER-O-18

Effects of Buffer Layer Growth Temperature on Micro-structures in the cubic GaN Films Grown on GaAs (001) Substrates by MOVPE

Pornsiri Wanarattikan[a,*], Surang Sumnavadee[b], Sakuntam Sanorpim[b] and Kentaro Onabe[c]

[a]*Department of Physical Science, Faculty of Science and Technology, Huachiew Chalermprakiet University, Samut Prakarn, 10540, Thailand*

[b]*Department of Physics, Faculty of Science, Chulalongkorn University, 10330 Bangkok, Thailand*

[c]*Department of Advanced Materials Science, The University of Tokyo, 5-1-5 Kashiwanoha, Kashiwa, Chiba 277-8561, Japan*

*Pornsiri.wa@gmail.com

Keywords: Cubic GaN, Metal organic vapor phase epitaxy, Transmission electron microscopy

Cubic GaN (c-GaN) films grown on GaAs (001) substrates by metalorganic vapor phase epitaxy (MOVPE) were investigated using transmission electron microscope (TEM) to verify effects of buffer layer growth temperature on micro-structures in the c-GaN films. Growth temperature of the GaN buffer layer was varied in a range of 550 to 600°C and the GaN film was grown at high temperature (~900°C). It is found that all the c-GaN grown films have a cubic structure as a main crystal structure. However, for higher growth temperature of buffer layer, hexagonal phase inclusions found to easily construct along the {111} facets of c-GaN associated with a formation of stacking faults (SFs) starting from the (111) step on the GaAs (001) surface.

For the growth temperature of GaN buffer layer at 550°C, the plan-view TEM micrographs of c-GaN films show high density of SFs and dislocations. At GaN/GaAs interface, the electron diffraction (ED) pattern demonstrated different type of single diffraction spots which include the high intensity of streaking. These intensity of streaks are indicated that the high density of SFs become dense into hexagonal phase single crystal. For the growth temperature of GaN buffer layer at 575°C, the wide SFs are observed that these broad lines are not expanding to the GaN surface and the dislocation are less found than the other temperature. Moreover, cross-sectional TEM micrographs and the ED pattern at GaN/GaAs interface show pyramid like structure and less intensity of the steak lines connecting the {111} reciprocal points to the (002) and (220) diffraction spots. There is no diffraction spots related to hexagonal structure. For the highest growth temperature of GaN buffer layer (600°C), there are the steaking of diffraction spots which represent hexagonal phase inclusions at the GaN/GaAs interface. It is found V-shape voids defect penetrating into the GaAs surface which were caused the thermal decomposition of As. Our results indicated that, the best quality of c-GaN films grown on GaAs (001) with cubic phase purity was achieved with the optimum growth temperature GaN buffer layer of 575°C.

CER-O-19

Thermal Diffusivity of a Waterproof Glaze Layer of Clay Roof Tile Investigated by Mirage Effect

Tanawut Rittidach, Puchong Kijamnajsuk*, Pongsakorn Tipmonta, Uthed Achathongsuk and Sutharat Chotikaprakhan
Department of Physics, Kasetsart University, Bangkok, 10900, Thailand
*puchong.k@ku.ac.th

Keywords: Clay roof tile, Nondestructive method, Mirage effect, Thermal diffusivity

Clay roof tiles have been generally used to keep the rain and the sun out of the houses or the temples in Thailand. Some clay tiles commonly have a waterproof glaze as a top layer. In the past, Thai people's houses were thatched the clay roof tile without a waterproof glaze. In this research, we study the clay roof tile with a waterproof glaze surface, which affects heat transfer to the clay roof tile. A nondestructive method or the so-called "mirage effect" is used in order to determine the thermal diffusivity of a waterproof glaze layer on clay roof tile. The top layer of sample is heated by a modulated laser pump beam. The deflection of probe beam which is mainly caused by the heat flow induced by the waterproof glaze layer is detected. Our works use mirage technique because of simple, rapid and accuracy thermal characterization for research, development and commercialization. In addition, the mirage technique can be used to analyze the frequency-dependent signals, which are measured by lock-in amplifier. The range of frequency is 0.01 Hz – 20 kHz. Thermal diffusivity of the waterproof glaze layer is determined by the theoretical model.

CER-O-20

The Effect of Zirconium Oxide on Properties and Crystallization of Soda-Lime Silicate Glass

Ekarat Meechoowas[a,1], Surisa Suriyoporn[b,2], Usanee Pantulap[a,3], Kanit Tapasa[a,4]
[a]Department of Science Service, Ratchathewi, Bangkok, 10400, Thailand
[b]Material Science, Faculty of Science, Maejo University,Chiangmai, 50290, Thailand
[1]ekarat@dss.go.th, [2]surisas@hotmail.com, [3]usanee@dss.go.th, [4]kanit@dss.go.th

Keywords: Glass-ceramics; Cullet; Modified composition; Crystallization

In this study, the properties and crystallization of re-melted soda-lime silicate glass cullet added with Al_2O_3, $CaCO_3$ and ZrO_2 were investigated in order to study the potential usage as a parent glass for glass-ceramics. Al_2O_3, $CaCO_3$ and ZrO_2 were added into the $71SiO_2$-$10Na_2O$-$6K_2O$-5CaO-4MgO-2SrO-ZrO_2-Al_2O_3 glass cullet to increase the crystallization of the glass. The glass batches (%wt) of (65-x) Cullet:$13Al_2O_3$:$22CaCO_3$:xZrO_2 (x = 0, 1, 2, 4, 6 and 8) were melted at 1500°C for 3 hours. The concentration of SiO_2 in the glasses were found 46-50 wt%. The glasses with 0, 1, 2 and 4 wt% ZrO_2 were clear and the rapid crystallization during casting was found in the glasses with 6 and 8 wt% ZrO_2. The crystallization was investigated by Differential Scanning Colorimetry technique (DSC). The results exhibited the evident of crystallization. That meant ZrO_2 acted as nucleating agent in this glass system. The crystalline in the glass with 6 and 8 wt% ZrO_2 were determined by X-ray diffraction technique (XRD) were found silica (SiO_2), wollastonite ($CaSiO_3$) potassium silicate ($K6Si_3O_9$) and zirconium oxide (ZrO_2). The thermal expansion of glasses was determined by dilatometric method. The thermal expansion curve indicated the characteristic of glass-ceramics and the effect of ZrO_2 on the thermal properties of glass. In conclusion, modifying the composition of soda-lime silicate cullet with Al_2O_3 $CaCO_3$ and ZrO_2 had potential to produce glass-ceramics.

CER-O-21

Optimum Partial Replacement of Cement by Nanosilica, Microsilica and Rice Husk Ash for Mass Production of Concrete

Winai Ouypornprasert[a,*], Narong Traitruengtatsana[b], Kong Kamollertvara[b]
[a]*Rangsit University, Muang, Pathumthani, 12000, Thailand*
[b]*Asia Group (1999) Co. Ltd., Bangmod, Bangkok, 10150, Thailand*
*owinai@yahoo.com

Keywords: Partial Replacement of Cement by Silica, Strength Activity Index, Goodness-of-Fit Tests, Mass Production of Concrete

The objective of this research project was to study the optimum partial replacement of cement by several forms of silica ash based on the concept of complete consumption of calcium hydroxide from cement hydration [1] for the mass production of concrete. Three forms of silica were considered i.e. nanosilica, silica fume and grounded RHA (**R**ice **H**usk **A**sk). Firstly cement hydration and pozzolanic reaction of calcium hydroxide and silicon dioxide as well as stoichiometry would be reviewed [2]. Based on these and the chemical compositions of cement as well as nanosilica, silica fume and grounded RHA the formulations for the complete consumption of calcium hydroxide originated from cement hydration for the pozzolanic reaction of silicon dioxide would be restated. Consequently the optimum partial replacement of cement by each form of silica could be determined. These optimum partial replacements should be considered as the thresholds for the corresponding forms of silica, since the over-replacement of cement by silica could result in significant reduction in mechanical properties of the cement product.

In this study the long-term SAI (**S**trength **A**ctivity **I**ndex) would also be proposed based on equivalent C-S-H (calcium silicate hydrate). It was concluded that C-S-H from pozzolanic reactions had the same structure as C-S-H from hydration of cement (Taylor, 1997). However the rate of hydration of C_2S (dicalcium silicate) as well as the strength development is much slower at the early age of cement paste than developed from C_3S (tricalcium silicate). Fortunately the long-term strength of C-S-H developed from C_2S is only insignificantly lower than that from C_3S, the long-term strength of C-S-H from the pozzolanic reaction could be assumed to be the average strength of C-S-H from C_3S and C_2S without significant errors. Contribution to strength by C_3AH_6 (calcium aluminate hydrate) and calcium ferrate hydrate would be transformed to equivalent C-S-H. Furthermore the contribution of C_4AF from the hydration reactions of cement and pozzolanic reactions take minor contribution to the overall strength of binder. Therefore the strength of C_3AH_6 can be assumed equal for both type of reactions. Based on the reasons mentioned above and the given values of strength for the age of 360 days, the long-term SAI can be defined. Furthermore this concept could be generalized for SAI at any age of cement hydration [3].

The main parameters considered were three forms of silica i.e. nanosilica, silica fume and grounded RHA, ages of mortars, water to binder ratios and the amount of partial replacement of cement by each form of silica within the corresponding threshold.

Chemical and physical properties of cement and all forms of silica would be tested. Several series of mortars would be cast and tested. The SAI in terms of the compressive strength of mortars would be discussed and compared with the theoretical predictions and the tested results from the other researchers.
The **accurate** optimum partial replacement of cement by each type of silica within the corresponding threshold together with the pre-specified criteria for all specifications [4] would be of utmost importance for mass production of concrete.

References

[1] Kong Kamollertvara, Winai Ouypornprasert and Narong Traitruengtatsana, Statistical Analyses of Optimum Partial Replacement of Cement by Rice Husk Ash Based on Complete Consumption of Calcium Hydroxide, in the Proceedings of the RSU International Research Conference 2016, 29 April 2016, Rangsit University, 14 pages.
[2] Taylor, H. F. W. (1997). *Cement Chemistry*, 2nd Ed., London: Thomas Telford Publishing, Thomas Telford Services, Ltd.
[3] Bouge, R. H. (1955). *Chemistry of Portland Cement*. New York: Reinhold.
[4] Kong Kamollertvara and Winai Ouypornprasert, Determination of Mean Values of Common Distributions in Civil Engineering from the Specifications for Mass Production, in the proceedings of The 7th PSU-UNS International Conference on Engineering and Technology (ICET-2015) & The 11th PSU-Engineering Conference (PEC-11) June, 19-20, 2015 at Duangjitt Resort & Spa, Patong Beach, Phuket, Thailand, p.40-43.

CER-P-01

Characterization and Properties of Cordierite – Mullite Refractories from Raw Materials and Narathiwat Clay (In Thailand)

Nattawut Ariyajinno[1,2,*] and Sakdipown Thiansem[3]
[1]*Department of Physics and Materials Science, Faculty of Science, Chiang Mai University, Chiang Mai 50200, Thailand*
[2]*Department of Ceramics Technology, Industrial Faculty of Technology, Loei Rajabhat University, Loei 42000, Thailand*
[3]*Department of Industrial Chemistry, Faculty of Science, Chiang Mai University, Chiang Mai 50200, Thailand*
* E-mail : Nattawut.ari@gmail.com,

Keywords: Mullite; Cordierite; Refractory; Narathiwat Clay

In the present study the relationship between characterization and properties of mullite-cordierite refractory were investigated. Talc, alumina oxide and kaolin (Narathiwat clay(Thailand):NRT) were mixed by varying the ratio of $MgO+Al_2O_3+SiO_2$ as NRT1 (31:66:3), NRT2 (45:54:1), NRT3 (13:86:1) and NRT4 (50:49:1). The mixture were pressed into rectangular shape by a hydraulic press under a pressure of 150 kg/cm^2 and sintered at 1300 ^oC with a heating rate of 5 ^oC/min for 1 hour of soaking time and cooled down to room temperature in a furnace chamber. Sample dimensions, density, water absorption, porosity, shrinkage, and mechanical properties were measured as a function of firing temperature. The chemical composition and loss on ignition (LOI) of the raw materials were performed using an X-ray fluorescence spectrometer(XRF). Effects on the phases formation and morphology that capable to improve mullite and cordierite in specimens were performed using an X-ray diffractometer (XRD). The results revealed that mullite was the major phase in sintered specimens and cordierite was also found which formed during expense of the other phases with talc. SEM pictures exhibited the role of talc in the grain growth of mullite and also showed the formation of pseudohexagonal cordierite which were observed by Scanning electron microscope (SEM).

CER-P-02

The Studies on the Mechanical and Thermal Properties of Geopolymer Mortar

Pongsak Jittabut[a,*]
[a]*Physics and General Science Program, Faculty of Science and Technology, Nakhon Ratchasima Rajabhat University, Nakhon Ratchasima, 30000, Thailand*
* Pongsak.ey@gmail.com

Keywords: Geopolymer mortar, fly ash, bagasse, husk ash, mechanical properties, thermal properties

This research objective is to studies the mechanical and thermal Properties of geopolymer mortar made with fly ash and bagasse ash. Rice husk ash was used to replace part of at the sand ratios of 0%, 2%, 4%, 6%, 8% and 10%, respectively. Sodium silicate (Na_2SiO_3) and sodium hydroxide (NaOH) with a concentration of 15 molar were used as ageopolymer agent. Geopolymer mortars were cured in the air at ambient temperature for 7 and 28 days. The properties analysis of the geopolymer mortar such as compressive strength, bulk density, water absorption, thermal conductivity, thermal diffusivity and thermal capacity were tested. The result indicated that geopolymer mortar at RHA10 at 28 day gave the maximum compressive strength at 84.42 kg/cm^2, water absorption at 1.16 %, bulk density at 2065.71 kg/cm^3 thermal conductivity was 1.1173 W/m.K, thermal diffusion was 6643 μm^2/s and thermal capacity at 1.6819 MJ/m^{3}K, respectively. The utilization of waste from agriculture and industry in geopolymer mortar for green building materials can be achieved which can improve mechanical propoties and themal insulation of geopolymer mortar.

CER-P-03

Slip Degassing to Improve the Properties of Slip Cast and Reaction Bonded Si_3N_4

Kritkaew Somton[a,*], Mana Rodchom[a], Thassanee Wonglom[a], Kannigar Dateraksa[a] and Ryan McCuiston[b]
[a]*National Metal and Materials Technology Center, Pathumthani 12120*
[b]*King Mongkut's University of Technology Thonburi, Bangkok 10140*
* kritkaes@mtec.or.th

Keywords: Si_3N_4, Degas, Flexural strength, Slip casting

The effect of slip degassing on the microstructure and mechanical properties of slip cast and reaction bonded Si_3N_4 was studied. The slip was prepared by aqueous ball milling of silicon (Si) powder. Hydrogen bubbles, a result of Si oxidation during milling, were degassed from the slip using a combination of vacuum and heat. The slip was then cast into a plaster mould to obtain rectangular green bodies. The Si green samples were sintered in a nitrogen atmosphere at 1500°C to convert the Si to Si_3N_4. After that the nitrided samples were polished to dimensions of 3 x 4 x 30 mm. The density, porosity, flexural strength, phase content and microstructure of the sintered samples were studied. The results showed that the degassing process increased the slip density. After casting and subsequent nitridation, it was found that the average apparent density of the samples increased from 2.89 to 2.95 g/cm^3, the porosity decreased from 52.9 to 49.5 %, and the flexural strength increased from 8.1 to 9.3 MPa, when the degassed slip was used. A microstructural examination showed that the pores in the samples were filled with whiskers, which most likely resulted from a vapor phase growth mechanism. The samples produced from the degassed slip tended to have fewer whiskers, due to the reduced pore size and volume. A comparison of the XRD patterns showed no phase differences between the samples. The appearance of Si_2N_2O, and SiC likely resulted from the reactions between O_2 and C impurities with Si_3N_4.

CER-P-04

Influence of Temperature and Alkaline Activation for Synthesis Zeolite A from Natural Kaolin

Pimpreeya Thungngern[a], Phanwatsa Amnaphiang[a], Panuruj Asawaworarit[b], Nuwong Chollacoop[c], Nawin Viriya-empikul[d] and Apiluck Eiad-ua[a,*]

[a]College of Nanotechnology, King Mongkut's Institute of Technology Ladkrabang, Ladkrabang, Bangkok, 10520 Thailand

[b]The Joint Graduate School of Energy and Environment, King Mongkut's University of Technology Thonburi, Thungkru, Bangkok,10140 Thailand

[c]National Metal and Materials Technology Center (MTEC), Paholyothin Rd, KlongNueng, KlongLuang, Pathumthani 12120, Thailand

[d]The Thailand Research Fund (TRF), Paholyothin Rd, Samsan Nai,Phyathai, Bangkok 10400, Thailand

*E-mail address: apiluck.ei@kmitl.ac.th

Keywords: Zeolite A, Kaolin, Calcination, Hydrothermal

Zeolite A from natural kaolin have been successfully synthesized via calcination and hydrothermal. However, these techniques have one drawback since, the impurities in kaolin such as muscovite and quartz in the kaolin structure, which depend on temperature and alkaline activation. This work was separated into two steps, first step was used calcination technique, and second step was used hydrothermal technique. Reaction of temperature in the first step was studied the influence of temperature from 500°C to 800°C for 3 hours. In this step, kaolin transformed to metakaolin and remain the impurities. Next, reaction of alkaline activation in second step was studied about the influence of NaOH. The concentration of NaOH in hydrothermal was varied from 1M to 4M and mixed with metakaolin at 90°C for 72 hours. X-ray diffraction (XRD) and Scanning Electron Microscope (SEM) were used for characterization. The solid products were formed to zeolite A at 1M NaOH hydrothermal with 500°C to 700°C calcination can seem euhedral structure of zeolite A.

CER-P-05

Effect of M-Type Hexaferrite on Mechanical and Magnetic Properties of Hydroxyapatite Ceramics

Rewadee Wongmaneerung[a,*]
[a]*Materials Science Program, Faculty of Science, Maejo University, Chiang Mai, 50290, Thailand*
*E-mail address: re_nok@yahoo.com

Keywords: hexaferrite magnetic, hydroxyapatite, magnetic properties, mechanic properties

The overall aim of this study is to establish the inter-relationships between key processing parameters, phase formations, microstructures, mechanical properties and magnetic properties of the novel ceramic in hydroxyapatite system for biomaterial applications. First, barium hexaferrite, strontium hexaferrite and hydroxyapatite powders were prepared. After that, all samples will be fabricated by using the mixed-oxide method via a combination between hydroxyapatite+barium hexaferrite and hydroxyapatite+strontium hexaferrite, shaping and sintering at 1100-1300 ºC for 2 h. The sintered samples were characterized phase formation, microstructure, mechanical and magnetic properties by using X-ray diffraction (XRD), scanning electron microscopy (SEM), universal testing and VSM measurements, respectively. It can be seen that the XRD patterns for all samples showed a combination between hydroxyapatite and magnetic phases. Moreover, it should be noted that the overall microstructure of composites are totally different due to densification mechanism and amount of barium hexaferrite and strontium hexaferrite. SEM micrographs pointed out a heterogeneous microstructure with different grain size distribution. Compressive and bending strength of all samples tend to increase with increasing of the amount of barium hexaferrite and strontium hexaferrite. However, the increasing of these values, it appears that there is no difference in the statistical significant. The Vicker's hardness result also shows low values. For magnetic properties, the coexistence of barium hexaferrite and strontium hexaferrite phases reveals magnetic hysteresis loops, showing the change from diamagnetic to ferromagnetic behavior.

CER-P-06

Surface Modification of TiO_2 with the Sonochemical Method

Eakkasit Thasirisap, Chaval Sriwong, Naratip Vittayakorn, Panpailin Seeharaj*
Advanced Materials Research Unit, Department of Chemistry, Faculty of Science, King Mongkut's Institute of Technology Ladkrabang, Bangkok, 10520, Thailand
*panpailin.se@kmitl.ac.th

Keywords: Titanium dioxide, Sonochemistry, Surface modification, Photocatalytic property

Titanium dioxide (TiO_2) is a widely used material for photocatalytic application due to its advantages in high chemical and thermal stability, non-toxicity and low cost. The photocatalytic property of TiO_2 has been reported to strongly depend on the surface area and the electron-hole recombination rate. Therefore, this study investigated the surface modification of TiO_2 for improving the surface activity and optical property using the sonochemical method. To modify TiO_2 surface, TiO_2 powders (anatase phase, 100-200 nm) were dispersed in 10 M sodium hydroxide (NaOH) solution with and without using surfactant, tetrabutylammonium hydroxide (TBAOH). Then the mixture was irradiated with high intensity ultrasonic wave (20 kHz, 150 W/cm^2) for 30, 60 and 90 min. The surface modified TiO_2 was characterized with various techniques including transmission electron microscopy (TEM), X-ray diffraction (XRD), Raman spectroscopy, BET analysis by N_2 adsorption, UV-visible and fluorescence spectroscopy. TEM images showed that after irradiation TiO_2 particles with high intensity ultrasonic wave for 60 min in 10 M NaOH and TBAOH solution, TiO_2 nanosheet was split from TiO_2 layer stack on the outer surface of primary TiO_2 particles. XRD patterns and Raman spectra showed that the surface modified TiO_2 was TiO_2 with anatase structure (JCPDS No.01-073-1764) and there was no significant change in the crystal structure after the ultrasonication. The specific surface area of the surface modified TiO_2 increased from 12.92 m^2/g to 93.65 m^2/g due to the formation of TiO_2 nanosheet. UV-visible spectra of the surface modified TiO_2 showed slightly shift in the onset absorption to higher wavelength compared with unmodified TiO_2 corresponding to reduction of the band gap energy (E_g) from 3.25 eV to 3.21 eV. Fluorescence spectra of the surface modified TiO_2 exhibited lower intensity indicating decreasing of the electron-hole recombination rate. These results suggest that the sonochemical method could be used for enhancing the specific surface area and the optical property of TiO_2 by inducing the formation TiO_2 nanosheet on the outer surface of TiO_2 particles.

CER-P-07

Structure, Magnetic Property and Energy Band Gap of Fe-doped NiO Nanoparticles prepared by co-Precipitation Method

Buppachat Toboonsung
Physics and General Science Program, Faculty of Science and Technology, Nakhon Ratchasima Rajabhat University, Nakhon Ratchasima 30000, Thailand,
*buppachattt@yahoo.co.th

Keywords: Fe-doped NiO, Magnetic property, Energy band gap, co-precipitation method

Fe-doped NiO nanoparticles was prepared by the co-precipitation method. The precipitation solution were used the concentration of $FeSO_4$ mixing $NiCl_2$ for 0.5 M. The precipitation process was used a magnetic stirrer of 1100 rpm, a temperature of 40 ^{O}C for 0.5 h and the dropping a NaOH of 0.5 M in the mixing solution. The precipitate product was dried at the temperature of 120 ^{O}C for 9 h and calcined in a furnace at the temperature of 400 ^{O}C for 4 h in air atmosphere. The crystal structure and a magnetic property of the product were analyzed by an x-rays diffractometer and a vibrating sample magnetometer, respectively. It was found that the optimum of coercive and magnetic moment was found at the doping Fe of 8 wt.%. Next, the temperature of 30-60 ^{O}C in the precipitation process was varied. An ultraviolet-visible spectrophotometer was used in order to characterize an optical property and an energy band gap of the product. Finally, the morphology of Fe-doped NiO nanoparticles was analyzed by scanning electron microscope.

CER-P-08

Synthesis of Nanocrystalline Cobalt Ferrite by the Sonochemical Method in Highly Basic Aqueous Solution

Patchara Pasupong [a], **Kittisak Choojun**[b] ,**Naratip Vittayakorn** [a], **Panpailin Seeharaj**[a*]

[a]*Advanced Materials Research Unit and* [b]*Catalytic Chemistry Research Unit, Department of Chemistry, Faculty of Science, King Mongkut's Institute of Technology Ladkrabang, Ladkrabang, Bangkok, 10520, Thailand*

[*]panpailin.se@kmitl.ac.th

Keywords: Cobalt ferrite, Nanocrystalline materials, Sonochemical method, Magnetic property

Cobalt ferrite ($CoFe_2O_4$) is a potential material to be used in electronic, magnetic and catalytic applications. The microstructure of $CoFe_2O_4$ manipulated by various synthesis methods plays an important role in controlling the properties of $CoFe_2O_4$. This study reported the preparation of monosized nanocrystalline $CoFe_2O_4$ in single step by the sonochemical method in highly basic aqueous solution without requiring of calcination process. To prepare nanocrystalline $CoFe_2O_4$, the mixed solution of the required molar ratio of cobalt nitrate hexahydrate ($Co(NO_3).6H_2O$) and ferric nitrate nonahydrate ($Fe(NO_3).9H_2O$) was precipitated in high concentration of sodium hydroxide solution (NaOH) under high intensity ultrasonic irradiation (20 kHz, 150 W/cm^2). The effect of NaOH concentration (5, 10, 15 and 20 M) on phase formation, microstructure and magnetic property of $CoFe_2O_4$ was investigated using X-ray diffraction (XRD), Fourier transform infrared spectroscopy (FT-IR), scanning electron microscopy (SEM), transmission electron microscopy (TEM) and vibrating sample magnetometry (VSM). XRD and FT-IR results showed that the as-prepared powders were $CoFe_2O_4$ with cubic structure (JCPDS no.22-1086). The crystallite size calculated from XRD data tended to increase with increasing the NaOH concentration by having the size range from 6-10 nm. TEM and SEM analysis showed that the nanocrystalline $CoFe_2O_4$ had monosized spherical morphology and an agglomeration of the nanocrystalline $CoFe_2O_4$ into microsized particles was observed. The nanocrystalline $CoFe_2O_4$ exhibited superparamagnetic property. The maximum saturation magnetization (M_s) was found to depend on the crystallite size and varied from 39-44 emu/g.

CER-P-09

Fabrication of Low Cost Membrane from Anodic Aluminum Oxide (AAO)

Peerawith Sumtong and Apiluck Eiad-ua*
College of Nanotechnology, King Mongkut's Institute of Technology Ladkrabang, Chalongkrung Rd., Ladkrabang, Bangkok, 10520, Thailand
*apiluck.ei@kmitl.ac.th

Keywords: nanoporous alumina membrane, two-step anodization, pore diameter, interpore distance

Nanoporous alumina membrane has been successfully fabricated from anodic aluminum oxide (AAO) substrate with aluminum low grade (Al6061) and well known for its nanoscopic structures and its applications in sensors, templates and nanoelectronics. The pore density, the pore diameter, and the interpore distance can be controlled by varying anodization process conditions. In this research the self-organized two-step anodization is carried out varying time at 24, 48 and 72 hours, respectively with 40V at the temperature 2-5ºC. The optimum conditions of AAO with two-step anodization is 40V 48 hr. Finally, AAO substrate is separated from aluminum low-grade and enlarged pore diameter with pore widening process by 5% H_3PO_4. The data from FE-SEM show that the average pore diameter and average interpore distance increase with the anodization time, and the Al6061 aluminium substrate can be used to fabricate a nanoporous AAO film with an average pore diameter and average interpore distance larger than 70 and 90 nanometers, respectively.

CER-P-11

Effects of Aluminum Concentrations on Microstructure and Compressive Strength of Porous Concrete

Oratai Jongprteep[a,*], Napamas Jaroonvechatam[a], Supicha Stienkijumpai[a], Sicha Kaewsuwan[a], and Thanawat Meesak[a]

[a]*Department of Materials Engineering, Faculty of Engineering, Kasetsart University, Bangkok, 10900, Thailand*

[*]E-mail address fengotj@ku.ac.th

Keywords: Porous Concrete, Aluminum Powder, Air Entrainment Agent, Compressive Strength

High porosity in porous concretes contributes to benefits in terms of lightweight, high water permeability, and superior insulation properties in the concretes. Nevertheless, excessive porosity can lead to diminished compressive strength. This study, therefore, aimed at fabricating porous concretes with porosity and compressive strength in the range suitable for practical applications which are 11.53 - 16.30% and 24.92 – 33.44 MPa, respectively. Since addition of aluminium powder is a well-known technique for porosity production, this study also assessed effects of aluminium addition on properties of porous concretes. Relationships among concentrations of aluminium, porosity, and compressive strength of the specimens were examined. Microstructural analysis from scanning electron microscope (SEM) images and compressive strength testing according to ASTM C109 revealed that the specimens with 0.15 wt% Al demonstrated porosity and compressive strength were in an acceptable range. Additionally, porosity production and specimen strengthening were discussed with respect to chemical compositions.

CER-P-12

Chemical Composition-Microstructure-Dielectric Constant Relations of Mg-doped Calcium Titanate Synthesized by Solid State Reaction Technique

Oratai Jongprateep[1,a], Nicha Sato[1], Jednupong Palomas [1], and Pongsakorn Jantarat [2]

[1]Department of Materials Engineering, Faculty of Engineering, Kasetsart University, Bangkok 10900 Thailand

[2]Department of Physics, Faculty of Science Kasetsart University, Bangkok 10900 Thailand

Email: [a]fengotj@ku.ac.th

Keywords: Calcium Titanate; Doping; Solid State Reaction; Dielectric Constant

It has been generally accepted that doping as well as compositional and microstructural control of dielectric materials could significantly contribute to enhancement of dielectric properties. The effects of magnesium on chemical composition and microstructure of calcium titanate synthesized by solid state reaction technique was assessed in this study. In addition, relationships among Mg doping content, compositions, microstructure, and dielectric constant were examined. Experimental results indicated that even though grain coarsening occurred in calcium titanate with 5 at% Mg, the specimen exhibited high density, in the range comparable to others. Moreover, the samples with 5 at% Mg contained only single phase of $Mg_xCa_{1-x}TiO_3$. On the contrary, MgO secondary phase was present in the samples with 10 and 20 at% Mg. Enhanced dielectric constant of 388 at 1 MHz in calcium titanate samples with 5 at% Mg was mainly attributed to their homogeneous chemical compositions.

.

CER-P-13

Effect of Solids Loadings, Sintering Temperatures and Sintering Periods on Microstructure of Hydroxyapatite

Oratai Jongprateep[a,*], Chonthicha Nueangjumnong[a], Jednupong Palomas[a]
[a]*Department of Materials Engineering, Faculty of Engineering, Kasetsart University, Bangkok, 10900, Thailand*
* E-mail address oratai.j@ku.ac.th

Keywords: Hydroxyapatite, Combustion, Microstructure, Porosity

Attributed to its biocompatibility and osteocondutivity, hydroxyapatite (HAp, $Ca_{10}(PO_4)_6(OH)_2$) has been extensively utilized as a bioactive material. As the implant material, HAp is required to be fabricated into a porous form. The present study was therefore aimed at synthesizing HAp powder by solution combustion technique and at fabricating porous HAp specimens. Calcium nitrate and ammonium dihydrogenphosphate ($NH_4H_2PO_4$), with Ca/P ratio equal to 2.3, were used as initial reagents in the HAp synthesis process. X-ray diffraction analysis confirmed that HAp was present as the primary phase, while minor secondary phases, βTCP and CaO, were also observed. To prepare porous specimens, HAp slip with solids loadings ranging from 15 to 25 vol% was cast into acrylic molds and sintered. The sintering temperatures ranged from 1350ºC to 1450ºC, and sintering periods ranged from 2 to 4 hours. Results from microstructural analysis revealed that high solids loadings, sintering temperatures and sintering periods resulted in decreasing of porosity. Porosity in the range of 33.94%, which was in an acceptable range for the application, was observed in the sample with 25 vol% solids loading, sintered at 1450ºC for 4 hours.

CER-P-15

Effects of Calcination Temperatures and Material Contents on Chemical Compositions of the Cement Powders Synthesized by Solution Combustion Technique

Oratai Jongprateep[a,*], Korapin Saiwongpanya[a] , and Suphitsara Yingyuen[a]
[a]*Department of Materials Engineering, Faculty of Engineering, Kasetsart University, Bangkok, 10900, Thailand*
[*]E-mail address fengotj@ku.ac.th

Keywords: Calcination Temperatures, Combustion Synthesis, Cement Powder

Severe detrimental effects on the environment caused by quarrying process, in the conventional production of Portland cement, has been widely concerned. Utilization of eco-friendly cement production techniques as well as usage of wastes as alternative raw materials can be potential practices to eliminate the problems. This study aims at synthesizing cement-like materials using the eco-friendly solution combustion technique, while using agricultural wastes, specifically cockleshells and rice husk ashes, as raw materials. Effects of calcination temperatures and material contents on chemical compositions of the synthesized powders were also examined. Experimental results indicated that fine particles of the major constituents in cement, including di-calcium silicate (C_2S), tri-calcium silicate (C_3S), and tri-calcium aluminate (C_3A), were successfully synthesized by the solution combustion technique and the resulting powders were calcined at temperatures ranging from 1100°C to 1300 °C. At calcination temperature of 1100 °C, moderately high intensity x-ray diffraction peaks corresponding to C_2S were present. At a higher calcination temperature of 1300°C, C_3S formation was promoted. X-ray diffraction analysis was also performed on synthesized powders with varied ratios of calcium silicate (C_2S and C_3S) to calcium aluminate (C_3A). The powder mixtures with high ratios of calcium silicate to calcium aluminate exhibited chemical compositions resembled to those of commercial type I Portland cement.

CER-P-16

Heavy Metal Immobilization of Fly Ash-based Geopolymers

Ronnachai Pliansakul [a], Sirithan Jiemsirilers [a,b,*], Pitak Laoratanakul [c] and Takaomi Kobayashi [d]

[a] *Research Unit of Advanced Ceramics, Department of Materials Science, Faculty of Science, Chulalongkorn University, Thailand*

[b] *Center of Excellence on Petrochemical and Materials Technology*

[c] *National Metal and Materials Technology Center, Thailand*

[d] *Department of Materials Science and Technology, Nagaoka University of Technology, 1603-1 Kamitomioka, Nagaoka, Niigata 940-2188, Japan*

*sirithan.j@chula.ac.th

Keywords: Geopolymer, Fly ash, Immobilization, Heavy metal salts

Geopolymer is a material from the polymerization of silica and alumina reactions under high alkali condition as activator. This research's study factors affected the heavy metal immobilization capacity of prepared fly ash-based geopolymer. The geopolymer was made of mixtures of fly ash and alkali solution at room temperature. The weight ratio of solid to liquid is 1.5 by alkali solution using sodium silicate to sodium hydroxide (10 molars) was fixed at 2.5 and then add mixed heavy metal salts at ratio 0.1, 0.2, 0.3, 0.4 and 0.5 by weight. The heavy metal salts using were Pb Cu and Cr. The as-cast geopolymer samples were cured at room temperature for 7, 14 and 28 days. Geopolymer were characterized in terms of phase analysis, chemical composition, morphology, functional group, and mechanical strength by X-ray Diffractometer (XRD), X-ray Fluorescence (XRF), Scanning Electron Microscope (SEM), Fourier Transform Infrared Spectroscope (FT-IR), Universal Testing Machine (UTM), respectively. In addition, the Toxicity Characteristics Leaching Procedure (TCLP) was used to assess the potential toxicity of the heavy metal immobilized geopolymer samples. Leaching test was performed to determine the efficiency of Pb Cu and Cr immobilization then compared to the Thai Pollution Control Department (PCD) between industrial effluent standards and surface water quality standards.

CER-P-17

Synthesis and Characterization of Cerium- and Lanthanum -containing Bioactive Glass

Md Ershad [a]*, Vikas Kr Vyas [a], Sunil Prasad [a], Akher Ali [a] and Ram Pyare [a]
*[a] *Department Ceramic Engineering, Indian Institute of Technology (BHU) Varanasi-India 221005*
Corresponding author: mdershad.rs.cer13@iitbhu.ac.in

Keywords: Bioactivity, Chemical durability, FTIR and SBF.

Synthesis and characterization of bioglass of general composition (45-X) SiO_2, 24.5 Na_2O, 24.5 CaO and 6.0 P_2O_5 (wt %) was modified by addition of X= (0.5, 1.0 and 1.5) wt % of CeO_2 and(45-Y) SiO_2, 24.5 Na_2O, 24.5 CaO and 6.0 P_2O_5 (wt %) was modified by addition of Y= (0.5 and 1.0) wt % of La_2O_3. These five samples were prepared in alumina crucible via melting route at a temperature of 1400 ±5 ºC with air as a furnace atmosphere. These glass samples were immersed in simulated body fluid (SBF) for different time period and their bioactivity were determined by Fourier transform infrared spectroscopy (FTIR) analysis. Surface morphology was studied by using Scanning electron microscope (SEM). Bioactivity, chemical durability and mechanical properties of these glasses increased with increasing concentration of CeO_2 and La_2O_3.

CER-P-18

Influence of Graphene Oxide on the Enhanced Photocatalytic Activity of Cerium Dioxide-Graphene Oxide Composites

Duangdao Channei[a,b*], Auppatham Nakaruk[c], Sukon Phanichphant[d]
[a]*Department of Chemistry, Faculty of Science, Naresuan University Phitsanulok 65000, Thailand*
[b]*Research Center for Academic Excellence in Petroleum, Petrochemicals and Advanced Materials, Naresuan University, Phitsanulok 65000, Thailand*
[c]*Department of Industrial Engineering, Faculty of Engineering, Naresuan University, Phitsanulok 65000, Thailand*
[d]*Materials Science Research Center, Faculty of Science, Chiang Mai University, Chiang Mai 50200, Thailand*
*E-mail address corresponding author: duangdaoc@nu.ac.th

Keywords: Photocatalysis; Visible light irradiation; Graphene oxide (GO); CeO_2

Graphene oxide (GO) was prepared by oxidizing purified natural flake graphite via modified Hummers method. The suspension of GO particles and cerium-based precursors were hydrothermal treated in order to prepare CeO_2-GO composites. The characterization of GO and CeO_2-GO composites were determined by using X-ray diffraction (XRD) , Brunauer-Emmett-Teller (BET) surface area, and Transmission electron microscopy (TEM). In comparison with pure CeO_2, photoluminescence spectroscopy (PL) of CeO_2-GO composite was further employed to estimate emission spectra. The results showed that the diffraction peaks of pure CeO_2 and CeO_2-GO composites can be assigned to CeO_2 phase with cubic fluorite structure, which exhibited the most active photocatalysis under visible light irradiation. However, the disappearance of the (001) diffraction peak was observable in the XRD pattern for CeO_2-GO composites. This is due to during the hydrothermal heat treatment, crystal growth of CeO_2 between the interlayer of GO destroyed the regular layer stacking of GO phase. From TEM images, the composite materials indicated the single layer GO sheets fully decorated with spherical CeO_2 particles. The photocatalytic activity measurements demonstrated that the CeO_2-GO photocatalysts revealed much higher photocatalytic activity for degradation of methylene blue (MB) under visible light irradiation. The enhancement can be attributed to the effective inhibition of the recombination of photogenerated electron-hole pairs in the CeO_2 and GO coupling system, as shown by the photoluminescence results. A high BET surface area and pore volume of CeO_2-GO composites increased the number of active photocatalytic sites per unit area, as well as enhanced the adsorbability of the organic pollutants on catalyst surface.

CER-P-19

Effect of Calcium Carbonate on Compressive Strength and Physical Properties of Alkali-activated Lightweight Concrete

Watcharapong Wongkeo[a]
[a]*Physics and General Science Program, Faculty of Science and Technology, Nakhon Ratchasima Rajabhat University, Nakhon Ratchasima 30000, Thailand*
*E-mail address: watcharapong_l@hotmail.com

Keywords: Alkali-activated, Lightweight concrete, Fly ash, Calcium carbonate.

This study presents the compressive strength and physical properties of alkali-activated lightweight concrete. Alkali-activated lightweight concrete was synthesized by fly ash and calcium carbonate. Calcium carbonate was designed to replace part of fly ash at 5 and 10 wt.%. Sodium hydroxide solutions at 5, 7.5 and 10 M and liquid to ash ratio (L/A ratio) at 0.45 were designed to produce alkali-activated lightweight concrete. Aluminium powder was used to create the bubble for lightweight concrete production. The results showed that, the compressive strength of alkali-activated lightweight concrete made with fly ash was developed with increased NaOH concentration. The maximum compressive strength at 6.0 MPa was obtained from 10M NaOH. For the alkali-activated lightweight concrete prepared with fly ash and calcium carbonate, the compressive strength of lightweight concrete was improved when containing calcium carbonated, especially at 5 and 7.5 M NaOH. The maximum compressive strength at 8.1 MPa and maximum bulk density were obtained from 5 wt.% calcium carbonated with 10M NaOH, while water absorption of this mixture was lowest. Bulk density and water absorption of alkali-activated lightweight concrete made with both fly ash and fly ash-calcium carbonated were acceptable in accordance with the specified criteria of TIS 2601. In addition, the pore structure of alkali-activated lightweight concrete was investigated by using optical micrograph.

CER-P-20

Synthesis and Photocatalytic Activity of Visible-Light Responsive BiOBr/GO Composites

Prasitthikun T.[a], Wu X. [c], Sato T.[c], Mongkolkachit C.[d] and Sujaridworakun P.[a,b,*]
[a]*Research Unit of Advanced Ceramics, Department of Materials Science, Faculty of Science, Chulalongkorn University, Bangkok, Pathumwan, 10330, Thailand*
[b] *Center of Excellence on Petrochemical and Materials Technology, Chulalongkorn University, Bangkok, Pathumwan, 10330, Thailand*
[c]*Institute of Multidisciplinary Research for Advanced Materials (IMRAM), Tohoku University, Sendai, Miyagi, 980857, Japan*
[d] *National Metal and Materials Technology Center, Pathumthani, Klong luang, 12120, Thailand*
*E-mail: pornapa.s@chula.ac.th

Keywords: BiOBr, Graphene oxide, Composites, Visible-light responsive photocatalyst

High efficiency BiOBr/GO composites photocatalyst were successfully synthesized via a facile precipitation method. The precursors were prepared by dissolving $Bi(NO_3)_3.5H_2O$ and KBr in glycerol and distilled water, respectively. Various amounts (0.1-2 wt%) of graphene oxide were added into the mixed solution precursors, and stirred at room temperature to get precipitated powder without further heat treatment. The obtained products were characterized for phase, morphology, optical properties and surface area by X-ray diffraction (XRD), transmission electron microscopy (TEM), filed-emission scanning electron microscopy (FE-SEM), UV-Vis diffuse reflection spectroscopy (DRS) and Brunauer–Emmett–Teller (BET), respectively. The morphology and structure of as-synthesized samples were composed of numerous fine plates of BiOBr dispersed on the GO sheets. The photocatalytic activities of BiOBr/GO composites were evaluated by rhodamine B degradation under visible light irradiation. As the results, the significant increase in photodegradation of BiOBr/GO composite comparing with pure BiOBr was observed. Among all samples, the composite with 1 wt% of graphene oxide showed the highest photocatalytic performance.

CER-P-21

Effect of Polymethylmethacrylate Content on Microstructure and Properties of Barium Orthotitanate Porous Ceramic

Pratthana Chithit[a,*], Supattra Wongsaenmai[a]
[a]*Program in Materials Science,Faculty of Science, Maejo University, Sansai, Chiang Mai, 50290, Thailand*
*E-mail address: Pratthana_chithit@hotmail.com

Keywords: barium orthotitanate, conventional mixed oxide method, polymethylmethacrylate

In this work, carbon dioxide adsorbent, barium orthotitanate (Ba_2TiO_4) porous ceramics were prepared with conventional mixed oxide method. The porous ceramics were fabricated employing polymethylmethacrylate (PMMA), as the pore-forming agent (PFA). Its amount ranged from 0, 2.5, 5 and 10 wt.%. Green samples were sintered at 1200-1500 ° C for 8 h where the porosity was controlled at 12~52%. Phase formation and microstructure were investigated by x-ray diffraction (XRD) and scanning electron microscopy (SEM), respectively. The porosity of the ceramics was measured using the Archimedes method. The strong tendency of increasing porosity with PMMA content and decreasing porosity with sintering temperature was observed.

CER-P-23

Use of Waste Glass as a Reinforce Material in Calcined-kaolin Based Geopolymer

Siriwan Chokkha*, Phiarphin Phetnat, Watthanaphon Chandadi, Maythawee Srisitthigul
School of Ceramic Engineering, Institute of Engineering,
Suranaree University of Technology, Nakhon Ratchasima 30000, Thailand
*E-mail address corresponding author: Siriwan@sut.ac.th

Keywords: Geopolymer, Waste material, Metakaolin, Compressive strength

Geopolymer is widely known as an environmentally-friendly construction material due to the remarkably low emission of CO_2 in its manufacturing process. It is an inorganic material technology that can be produced via two precursors including a solid component (alumino-silicate materials) and alkaline activators (an erosive or salts alkaline). In the present work, the studied program was divided into two steps. In Step 1, the molarity of NaOH was investigated. The calcined-kaolin from Lamphang city (Thailand source) was used as base alumino-silicate material. In addition, the concentrations of NaOH (5M, 10M, 15M and 20M) were utilized as alkaline activator for geopolymerization. After mixing, the geopolymer slurry was casted into a size of a 50 mm × 50 mm × 50 mm steel mold. The curing condition of all specimens was maintained at 60^{o}C for 7 days. The compressive strength of all specimens was tested. The utilization of 10M of NaOH yielded the highest compressive strength with the value of 22.01 MPa. In Step 2, 10M of NaOH was fixed and used as alkaline activator. In this case, the amount of waste glass (0%, 10%, 20%, 30%, 40% and 50% by weight) was studied on partial calcined-kaolin replacement. However, the compressive strength of all samples slightly changed with an increasing weight percentage of waste glass (0% - 20 %). The highest compressive strength of 20 wt% waste glass was 25.22 MPa. For percentage of 30 to 50, the compressive strength decreased. To support the results from compressive strength, the microstructure, and geopolymerization of all compositions were investigated using a scanning electron microscope (SEM) and a Fourier-transform infrared spectroscopy (FT-IR), respectively.

CER-P-24

Investigation of Physical, Mechanical and Thermal Properties of Building Wall Materials

Jiraphorn Mahawan, Somchai Maneewan, Atthakorn Thongtha*
Department of Physics, Faculty of Science, Naresuan University, Phitsanulok, 65000, Thailand
*E-mail address: atthakornt@nu.ac.th (A. Thongtha)

Keywords: Cellular lightweight concrete, Compressive strength, Thermal conductivity.

This research aims to study the various proportions of sand on the physical, mechanical and thermal properties of building wall materials (Cellular lightweight concrete). The research was divided into two stages, first step, the density, water absorption and compressive strength of 7.0cm x7.0cm x7.0cm sample size were studied. It was found that the optimal proportions were the sample with decreasing 5% by weight of sand (the weight of this condition is lighter than commercial lightweight concrete) and that with increasing 10% by weight of sand (this condition showed the highest value of compressive strength). At the tested time of 7, 14, 28 and 60 days, the compressive strength of samples with decreasing 5% by weight of sand was 2.49 MPa, 2.62 MPa, 2.96 MPa and 3.00 MPa and that with increasing 10% by weight of sand was 2.98 MPa, 3.05 MPa, 3.08 MPa and 3.15 MPa, respectively. The physical and mechanical properties of both lightweight concrete conditions conformed to the Thai Industrial Standard 2601-2013. Step 2, the thermal properties of improved lightweight concrete (the composition with increasing 10% by weight of sand), brick and commercial concrete were compared to test heat transfer in the testing room. It was found that the samples with increasing 10% by weight of sand showed the highest thermal time lag that was longer than that of brick and commercial concrete of around 1 hour. The increase in thermal effectiveness was applied to the cellular lightweight concrete.

CER-P-25

Synthesis and Characterization of Zn^{+2} doped Cobalt Ferrite Nanoparticles and 45S5 Bio-glass Composite for Application in Hyperthermia Treatment

Aman Bhardwaj[a,*], Lakshya Mathur[a], Sampath Kumar A[a], Himanshu Tripathi[a], B. Singh[a], D. Kumar[a], S.P. Singh[a]

[a]*Department of Ceramic Engineering, Indian Institute of Technology (Banaras Hindu University), Varanasi-221005, India*

*Corresponding author; E-mail: amanb.cer15@iitbhu.ac.in

Keywords: Zinc doped cobalt ferrite, 45S5 Bio-glass, Bio-compatibility, Cancer.

Magnetic nanoparticle-based hyperthermia treatment has appeared to be a promising salutary approach for cancer treatment. Super paramagnetic and ferrimagnetic materials such as Fe_3O_4 have been scrutinized adequately. In this present work, effect of doping of Zn^{+2} on magnetic properties of cobalt ferrite as well as biocompatibility of composites prepared using these ferrites and 45S5 bio-glass was analyzed.

Zn^{+2} doped cobalt ferrites $Co_{1-x}Zn_xFe_2O_4$ (x=0, 0.25, 0.5, and 0.75) nanoparticles were synthesized via co-precipitation method using Co, Fe, and Zn-nitrates as precursors. Effect of pH of the precursor solution on resulting particle size was also analyzed. These nanoparticles were composited in different proportion with 45S5 bio glass prepared via sol-gel route. The phase composition and microstructure were studied using X-ray diffraction (XRD) and scanning electron microscopy (SEM). The magnetic properties of pure ferrites and bio-glass composites were characterized by magnetic property measurement system (MPMS) and the appraisal of bio-compatibility was done by immersing the composite into simulated body fluid (SBF) for a predefined period prior to fourier transform infrared spectroscopy (FTIR) to obtain an IR spectrum of absorption or emission of liquid. It was observed that even after 14 days of the immersion, pH of the SBF solution remained within the permissible range for human body. The Zn^{+2} doped cobalt-ferrite bio-glass composite having high biocompatibility would be a potential material for hyperthermia treatment application.

CER-P-26

Influence of Portland Cement on Physical, Mechanical and Thermal Properties of Cellular Lightweight Concrete

Atthakorn Thongtha*, Surirat Ketchaona, Jutarud Wattana, Rattanaporn Boonyasak

Department of Physics, Faculty of Science, Naresuan University, Phitsanulok, 65000, Thailand

*E-mail address: atthakornt@nu.ac.th (A. Thongtha)

Keywords: Cellular lightweight concrete, Portland cement, Thermal conductivity.

This work focuses on the physical, mechanical and thermal properties of Cellular lightweight concrete with different proportions of Portland cement. The research was separated into two parts, first part, the density, water absorption and compressive strength of the 7.0 cm x 7.0 cm x 7.0 cm concrete sample were investigated. It was found that the optimal proportion was the sample with an increase of 15% by weight of Portland cement (this condition showed the highest value of compressive strength). At the tested time of 7, 14, 28 and 60 days, the compressive strength of samples with an increase of 15% by weight Portland cement was 3.3 MPa, 3.5 MPa, 3.3 MPa and 3.6 MPa, respectively. The physical and mechanical properties of lightweight concrete conditions conformed to the Thai Industrial Standard 2601-2013. Step 2, the thermal properties of the improved lightweight concrete, brick and commercial concrete were compared. It was found that the samples with increasing 15% by weight of cement showed the best thermal time lag that was longer than that of brick and commercial concrete of around 1 hr as well.

CER-P-27

Structure and Ferroelectric Properties of $KNbO_3$ added $Bi_{0.5}Na_{0.5}TiO_3$ Ceramics

Puripat Kantha[a], Phathaitep Raksa[b], Muangjai Unruan[b], Tawee Tunkasiri[c], Panupong Jaiban[d], Nuttapon Pisitpipathsin[b,*]

[a]*Division of Physics, Faculty of Science and Technology, Rajamangala University of Technology Thanyaburi, Pathumthani 12110, Thailand*

[b]*Department of Applied Physics, Faculty of Sciences and Liberal Arts, Rajamangala University of Technology Isan, Nakhon Ratchasima 30000, Thailand*

[c]*Department of Physics and Materials Science, Chiang Mai University, Chiang Mai 50200, Thailand*

[d]*Faculty of Science, Energy and Environment, King Mongkut's University of Technology North Bangkok, Rayong Campus, Rayong 21120, Thailand*

*nuttapon.pi@rmuti.ac.th

Keywords: lead-free piezoelectric ceramics, ferroelectric properties, BNT-KN

The fabrication of lead-free (1-x)$Bi_{0.5}Na_{0.5}TiO_3$ - x$KNbO_3$ or (1-x)BNT-xKN ceramics where x = 0.00, 0.05, 0.10, and 0.15 was carried out by the modified two-step mixed oxide method. The effects of $KNbO_3$ on structure and ferroelectric properties were systematically investigated. XRD results revealed that the (1-x)BNT-xKN ceramics with low KN content of x less than 0.05 contained ferroelectric phase with a rhombohedral symmetry while the higher KN content ceramics had mixed symmetries between rhombohedral and orthorhombic. At room temperature, the highest P_r and low E_c were obtained when the composition of x = 0.05.

CER-P-28

The Effect of Calciumorthophosphate on Photocatalytic Activity of Titanium Dioxide Photocatalyst Beads

Pakpassagun Somwong[a], Neeranut Kuanchertchoo[b], Dujreutai Pongkao Kashima[a,*]
[a]*Research Uunit of Advanced Ceramics, Department of Materials Science, Faculty of Science, Chulalongkorn University, Pathumwan, Bangkok 10330, Thailand.*
[b]*Department of Materials Technology, Faculty of Science, Ramkamhaeng University, Huamark, Bangkapi, Bangkok 10240, Thailand.*
*E-mail: dujreutai@gmail.com, muxiang_pakpassagun@yahoo.com

Keywords : Calciumorthophosphate, Titanium dioxide, Photocatalytic activity

Calciumorthophosphate compounds such as hydroxyapatite (HA), and monetite (DCPA) normally act as good adsorbents. The appropriate amount of these adsorbents can promote the photocatalytic activity of TiO_2 photocatalyst. In this work, calciumorthophosphate powders with different aspect ratio were hydrothermally synthesized using formic and acetic acid route. As-synthesized powders with various weight percentages (5, 10 and 15 wt%) were mixed with TiO_2 – P25 (Degussa), then coating on porous silica beads (Ecolite®) using calcium aluminate cement (CAC) as a binder. The strength of coating layer on Ecolite® beads was developed via hydration of CAC binder in aging step. Finally, the photocatalytic activity test of photocatalyst beads was performed by methylene blue degradation technique. Moreover, phase analysis and microstructure of coating layer on the beads were analyzed by XRD and SEM respectively.

CER-P-30

Effects of Air Exposure Time and Annealing Temperature on Superhydrophobic Surface of Titanium Dioxide Film

S.Tipawan Khlayboonme [a,*] , Warawoot Thowladda
[a]*Surface Physics and Plasma Application Laboratory, Department of Physics, Faculty of Science, King Mongkut's Institute of Technology Ladkrabang, Bangkok, 10520, Thailand*
* s.tipawan.kh@kmitl.ac.th

Keywords: Superhydrophobic surface, TiO_2 thin films, Contact angle.

Superhydrophobic surfaces of titanium dioxide films for self-cleaning applications were prepared by an automated sol-gel dip-coating apparatus. The influence of annealing temperature and air exposure time on the wettability of the film surface was investigated by a contact angle measurement. The annealing temperature of 100, 200 and 300 °C were used. The surface morphology of the films was observed by FE-SEM. Elemental distributions on the film surfaces were provided by X-ray mapping. Atomic-bonding was confirmed by FTIR. The contact angle of the as-coated film was 25°. During storage in the laboratory atmosphere for 20 days, the contact angle of the films with an annealing temperature of 20 °C increased to 140°. This film was then heat-treated at a temperature of 100 °C for 20 min, its contact angle increased to 152°. The association of contact angle among the surface morphology, elemental distribution and atomic bonding of the film surface will be discussed.

CER-P-32

Synthesis of Carbon and Zeolite Na-A Composites Powder from Rice Husk Charcoal as Raw Material for Slip Casting Process

Thanakorn Tepamat[a,*], Thanakorn Wasanapiarnpong[a,b], Pornapa Sujaridworakul[a,b], Charusporn Mongkolkachit[c]

[a] *Research Unit of Advanced Ceramics, Department of Materials Science, Faculty of Science, Chulalongkorn University, Bangkok, 10330, Thailand*

[b] *Center of Excellence on Petrochemical and Materials Technology, Bangkok, 10330, Thailand*

[c] *National Metal and Materials Technology Center, Pathumthani, 12120, Thailand*

*thanakorn.tepamat@hotmail.com

Keywords: Zeolite Na-A, Composites, Rice husk charcoal, Carbon

Activated carbon and zeolite Na-A are widely used in water treatment due to adsorption and ion exchange properties. In this research, we specifically target on the preparation of carbon and zeolite Na-A composites powder from rice husk charcoal as raw material for fabrication of activated carbon and zeolite Na-A composites filter by the slip casting process. Rice husk, a by-product of the rice milling industries, was fired in an incineration furnace around 700 ^{o}C to obtained rice husk charcoal (RHC). The rice husk charcoal as a precursor of carbon and silica sources for the synthesis of carbon and zeolite Na-A composite by hydrothermal method together with sodium aluminate was used as alumina source at a molar ratio of Si/Al as 1 in sodium hydroxide solution. Synthesis temperatures are varied as 85, 90, 95 and 100 ^{o}C. Synthesis times are 1, 2, 3, 4 and 5 hours. In this synthesis to make a comparison between nonaging and aging time for 12 hours. Composites powder were characterized phase analysis and morphology by X-ray diffraction (XRD) and scanning electron microscopy (SEM), respectively.

CER-P-33

Using of Basalt Fiber as Reinforcing Materials in Fiber-Cement Flat Sheet

Apirat Theerapapvisetpong[a,b,*], Thanakorn Wasanapiarnpong[a,b], Supatra Jinawat[a,b]

[a]*Research Unit of Advanced Ceramics, Department of Materials Science, Faculty of Science, Chulalongkorn University, Bangkok, 10330 Thailand*

[b]*Center of excellence on Petrochemical and Materials Technology, Chulalongkorn University, Bangkok, 10330 Thailand*

*apirat.t@chula.ac.th

Keywords: Basalt Fiber, Fiber Reinforce Cement, Glass, Composite

Basalt fiber has the composition similar to glass fiber but it has better mechanical characteristics and higher chemical resistance. In this work three types of basalt fiber with deferent chemical compositions were used as reinforcing element in fiber-cement flat sheet to evaluate their performances to be used as an alternative reinforcing element. A fiber-cement sample was prepared from the mixture of the basalt fiber, ordinary Portland cement and the other additives before forming by the Hatschek process. Two kinds of basalt fiber sample were received from insulation industry. Another one was derived from Chai Badan basalt rock melted with small amount of fluxing agents. This basalt fiber was prepared by melt blowing process. The results showed that the fiber-cement sample containing basalt fiber from Chai Badan basalt rock performed the highest flexural strength. Its flexural strength was higher than the minimum requirement according to the standard test method ASTM C1185 and ASTM C1186. The SEM observation showed a good bond between the Chai Badan basalt fiber and cement matrix interface zone.

CER-P-34

Effect of Silica Base Catalyst on Transformation of Methanol to Hydrocarbon

Supranee Lao-ubol[a,*], Pasinee Panith[a], Phunthinee Somwongsa[a], Siriporn Tong-on[a], Shih-Yuan Chen[b], Wasana Kongwong[a] and Siriporn Larpkiattaworn[a]

[a]Material Innovation Department, Thailand Institute of Scientific and Technological Research, Klongluang, Pathumthani, 12120, Thailand

[b]Energy Catalyst Technology Group, Research Institute of Energy Frontier, National Institute of Advanced Industrial Science and Technology, Tsukuba, Ibaraki, 305-8569, Japan

*supranee@tistr.or.th

Keywords: Methanol to Olefins, Mesoporous, Zeolite

Five different types of silica catalyst (SBA-15, PO_4-SBA-15, and three different Si/Al ratio of commercial zeolites (30 ~ 280)) was used to study the transformation of methanol to hydrocarbon (MTH). The aim of this study was to investigate the effect of pore diameter and acidity in the structure of silica catalysts on the process performances in terms of methanol conversion and hydrocarbon selectivity. The mesoporous silica catalysts were prepared by co-condensation method. The catalysts samples were characterized by GC-MS, SEM, XRD, BET, and NH_3-TPD techniques. The catalytic performance of synthesized and commercial catalysts for MTH process was evaluated using a homemade fixed bed reactor at temperature (200-300 ^oC) and pressure (0-20 bar). It was found that the liquid hydrocarbon product provided by zeolite catalysts is cyclic hydrocarbons-rich. High Si/Al zeolites with larger pore size lead to higher selectivity and yield to paraffins (C_1-C_7) and was more favorable at high pressure. In contrast to commercial zeolite catalyst, mesoporous PO_4-SBA-15 catalyst showed high selectivity for dimethyl ether while no conversion was observed for pure mesoporous SBA-15. These results indicate that both pore diameter and acidity influence the product distribution in methanol to hydrocarbon process.

Corrosion

COR-O-01

Characteristics of Internal Oxide Scale of T91 Superheater Tube after 1000h Exposure to Steam Temperature at 605°C

Suraya MN[a,*], Hariffin B[a], Astuty A[b], Roslina M[b]
[a] *TNB Research Sdn Bhd, No 1, Kawasan Institusi Penyelidikan, Kajang 43000 Selangor, Malaysia*
[b] *UTM Razak School of Engineering and Advanced Technology, UTM Kuala Lumpur, Jalan Sultan Yahya Petra, 54100 Kuala Lumpur, Malaysia*
*suraya.mnadzir@tnbr.com.my; astuty@utm.my

Keywords: Superheater tube, T91 steel, Steam Oxide Scale

Superheater tubes in Coal Fire Power Boiler are generally made of heat resistant steel such as grade T91 which has high creep resistant property. This is because superheater tubes are exposed to steam temperature around 540 to 605°C and creep property is the main life factors for these tubes. Actual operating condition for superheater tube is depending to the generation capacity and type of the boiler. Based on service experience, T91 tube that exposed to steam temperature higher than 600°C is subject to overheating damage due to excessive formation of steam oxide on internal surface. Therefore characteristic of steam oxide scale on T91 tube need to be evaluated to understand the behavior of heat transfer barrier that cause overheating failure. This paper will discuss on the characteristics of the steam oxide scale on internal surface of T91 tube after exposure to steam at temperatures of 605°C. The as-received T91 tube was subjected to steam oxidation tester with steam flowing inside the tube at temperature of 605°C. The developed steam oxide scale on the internal surface of T91 tube was examined using Scanning Electron Microscope and X-Ray Diffraction. The oxide scale was observed having two distinct layers which were identified as Cr_2O_3 (at metal-scale interface) and Fe_2O_3 (at scale-gas interface). The total intact oxide scale thickness is about 100µm. It is also observed that the oxide scale is separated by voids and cracks at some location with the gaps thickness between 30-70µm. Microstructure examination on metal of oxidized sample has showing the sign of overheating as compared metal of non-oxidized sample. The increment of oxide scale thickness together with the air gaps will generally increase the tendency of overheating damage.

COR-O-03

The Role of Al-Mn Intermetallics On the Corrosion of AZ31 Magnesium Alloy

Somi Doja[a*], Lukas Bichler[a], Simon Fan[b]

[a] *School of Engineering, University of British Columbia, Kelowna, British Columbia, V1V 1V7, Canada*
[b] *ZincNyx Energy Solutions, Vancouver, British Columbia, V6P 6T3, Canada*

*doja.somi@gmail.com

Keywords: Al-Mn intermetallics; AZ31

Magnesium alloys are widely used in automobile and aircraft industries. In thi research, the corrosion behavior of commercially available AZ31 plate in basic aqueou solution was investigated. Immersion tests used to study the bulk degradation of th alloy revealed that sites rich in Al-Mn were preferentially corroded and acted a corrosion pit initiation sites. Subsequently, SEM micrographs revealed that diffusio gradients of Al and Mn evolved on the surface and in the vicinity of the pitted site Electrochemical Impedance Spectroscopy was performed to further understand the rol of these precipitates in corrosion behavior of the plate. The Nyquist plot indicates th presence of Warburg impedance attributed to diffusion of aluminum ions. Thes aluminum ions are believed to originate from the Al-Mn intermetallics due to de alloying. Thus, Al-Mn intermetallics acted as cathodes to the anodic α-Mg substrat resulting in micro-galvanic corrosion.

COR-O-04

Corrosion Behavior of Al-Zn-In Sacrificial Anode Alloys Produced by Conventional Casting and Semi-Solid Metal Casting Processes

Chanika Puridetvorakul[a,*], Nuchthana Poolthong[a], Napachat Tareelap[a]
[a]Division of Materials Technology, School of Energy, Environment and Materials, King Mongkut's University of Technology Thonburi, Bangkok 10140, Thailand.
*chanika.p@mail.kmutt.ac.th

Keywords: Anode efficiency, Current capacity, Semi-solid metal casting

One problem in producing a sacrificial anode by conventional casting is segregation of alloying elements in casting structure during freezing. This phenomenon is the cause of non-uniform anode attacks which lead to the reduction of anode performance. The aim of this study was to compare performance of Al-5Zn-0.02In anode produced by conventional casting and semisolid casting using cooling slope technique (Rheo-casting). The performance of produced anode was measured in terms of anode potential, current capacity, consumption rate and anode efficiency in 3.5% NaCl solution for 14 days. As the microstructure of semisolid cast anode was homogeneous with fine grains and no dendritic, the surface after being attacked was uniform micro-hemispherical pits. In contrast, the conventional casting anode with dendritic and coarse grain structure was localized attack along the grain boundaries, whereas the anode matrix was remained. However, the anode efficiency of conventional cast was a bit higher than that of semisolid cast anode.

COR-O-05

Development of Pitting Corrosion Monitoring Method by Saline Solution Droplet under Wet-Dry Cycles

Wongpat Banthukul[a*], Namurata Sathirachinda Palsson[b], Ekkarut Viyanit[b], Aphichart Rodchanarowan[a]

[a]*Faculty of Engineering, Kasetsart University, Ngam Wong Wan Rd., Ladyaow, Chatuchak, Bangkok, 10900, Thailand.*

[b] *National Metal and Materials Technology Center, Paholyothin Rd., Klong 1, Klong Luang, Pathum Thani, 12120, Thailand.*

*wongpat.banthukul@gmail.com

Keywords: Pitting corrosion, Wet-dry cycle, Droplet, Stainless steel

Localized corrosion under droplet of corrosive media is one of the most common forms of corrosion for metallic structures exposed to the atmosphere and/or moisture in the air. This scenario is mainly responsible for the economic cost of materials due to corrosion and its prevention on every-day-life. In this study, pitting corrosion monitoring method under droplet of electrolyte generated by means of fluid handling device was simulated under wet-dry cyclic condition in order to examine pit initiation and propagation. Wet-dry cycle process started with a droplet of saline solution on the surface of stainless steel sample in certain volumes and sizes, the sample was then left until the saline droplet was completely dried in the temperature-humidity controlled condition, i.e. 10% and 60% relative humidity (RH) at 27°C. By the time water evaporated salt deposit presented. This considers as a completion of one wet-dry cycle. Next cycle proceeded by a droplet of deionized water on the previous same spot as the saline solution and the droplet was left until completely dried again. The cycle continued until red-brown rust can be visually noticed. The time required to finish each cycle was varied depending on temperature and humidity, electrolyte droplet morphology and concentration. After finishing the wet-dry cycles and the rust was noticed, the samples were characterized under laser optical microscope. In most cases when the samples were exposed at 60%RH, red rust start to be visually noticable after 10-15 of the wet-dry cycles. However, when the humidity is low (10%RH), rust was unnoticeable even up to 30-40 cycles. Therefore, the samples exposed at 10%RH were characterized after the first wet-dry cycle, pit and rust can be detected, however; they were observable only under the 100X. Time-lapse photography was performed to investigate pit initiation and propagation during the wet-dry cycles based on visible red rust. The study on the development of a methodology using droplet and wet-dry cycle for pitting corrosion monitoring is discussed here.

COR-O-06

Failure Analysis of Protection Tube of a Temperature Element in a Sulfiding Environment

S. Ouampan*, S. Kaewkumsai, N. Sathirachinda

Failure Analysis and Surface Technology Laboratory (FAST), National Metal and Materials Technology Center (MTEC), National Science and Technology Development Agency (NSTDA),

114 Thailand Science Park, Paholyothin Rd., Klong 1, Klong Luang, Pathumthani 12120, Thailand

E-mail: Siriwano@mtec.or.th

Keywords: Cobalt-based alloy; High temperature failure; Intergranular oxidation; Sulfidation

ABSTRACT

The degradation of cobalt-based alloy protection tube of a temperature element, used at high temperature in sulfur-dioxide atmosphere, was investigated in this work. In order to examine the cause of failure, various techniques including optical microscopy, scanning electron microscopy, energy dispersive spectroscopy, X-ray fluorescence, X-ray diffraction, metallography, and micro-hardness measurement were carried out. From the results, it was found that the severe metal loss was only observed at the outer surface, although the degraded layer was found at the inner surface and at the tip portion of the protection tube as a result of overheating in high temperature sulfur environment. The severe metal loss of the protection tube impaired sensor wire inside the temperature element and led to subsequent furnace shutdown. Growth of sulfide/oxide precipitates suggests that sulfur-dioxide reacted with alloy at high temperature leading to catastrophic sulfidation. It is recommended to inspect the temperature element periodically. The service temperature should not exceed the melting point of metal sulfides. Material selection is also discussed as an alternative means for prevention the recurrence in the future.

COR-O-07

Effect of Cr Content on the Passivation Layer Properties of Tinplate Steel

Kosit Wongpinkaew[*], **Ekkarut Viyanit, Siam Kaewkumsai, Piya Kumsuk**
National Metals and Materials technology Center, Pathum Thani, 12120, Thailand
*kositw@mtec.or.th

Keywords: Chromium content, Tinplate Steel, Passivation Layer, Corrosion Behaviors

Chromium or metallic chrome was used in new type tinplate steel. Chromium coated on the top of tin layer to form passivation layer and improve adhesion property between lacquer and steel. In this work, the properties of passive layer by different chromium contents were investigated using GDS, EPMA, Electrochemical Polarization and Electrochemical Impedance Spectroscopy. The results indicated that the Cr content higher than 10 g/cm^2 could from uniform passivation layer and changed corrosion behaviors of on the tinplate steel.

Design & Manufacturing and Computational Science & Engineering

DMC-I-01

Meta-Heuristics for Engineering Optimisation

Sujin Bureerat[a,*]
[a]*Sustainable Infrastructure Research and Development Center, Department of Mechanical Engineering, Faculty of Engineering, Khon Kaen University, Khon Kaen, Thailand, 40002*
*E-mail: sujbur@kku.ac.th

Keywords: Meta-heuristics, Optimisation, Multiobjective evolutionary algorithms, Manufacturing processes.

Meta-heuristics (MHs) are a type of optimisers relying on randomisation and population reproduction. The methods usually employ a set of design solutions traditionally called a population for searching. MHs have several attractive features that make them more popular compared to classical gradient-based optimisers. They are simple to understand, use and code. The methods are derivative-free and capable of dealing global optimisation, thus, they can be used to solve almost any kind of optimisation problems. This talk is concerned with the use of MHs for engineering optimisation. Several practical optimisation problems in the fields of mechanical engineering and manufacturing including a strip coiling process, a wire drawing process, truss optimisation, and heat sink design are introduced. Demonstration on how to solve those optimisation problems using MHs is presented and discussed.

DMC-I-02

The Role of Advanced Numerical Simulation in Vehicle Safety Research and Development

Julaluk Carmai
Automotive Safety and Assessment Engineering Research Centre,
The Sirindhorn International Thai-German Graduate School of Engineering,
King Mongkut's University of Technology North Bangkok
Julaluk.C@tggs.kmutnb.ac.th

As computer technology continues to get more advanced while the predictive quality of the calculations is growing steadily, numerical simulation has then established itself as an essential tool in the development of motor vehicles. The existing of high performance computing allows for simulations to be increasingly used in the field of vehicle safety ranging from component impact tests to whole vehicle crash tests. Virtual prototyping and testing have become generally accepted in automotive industry. Safety assessment of sub-systems or whole vehicles require a full-scaled anthropometric device or a crash test dummy which is employed to predict human responses in a vehicle crash. The crash test dummy can be modelled using multibody dynamics technique or finite element technique. However, a crash test dummy cannot provide detailed injury such as brain/lung contusion, bone fracture, liver rupture or whiplash injury. An advanced finite element human body model has then been developed to address this issue and the ethic issue of cadaveric tests. The human body model is more biofidelity than the dummy model and can provide better understanding of injury mechanisms of occupants and pedestrians in various crash scenarios.

The talk will start with introduction of the two widely used numerical modelling techniques for simulating vehicle crash scenario which are multibody dynamics and finite element method. Case studies of crash reconstruction and virtual testing for type approval will be presented. The highlight will also be on the development of advanced finite element human body model together with related research projects at the Automotive Safety and Assessment Engineering research centre, KMUTNB.

DMC-O-01

Corrosion Prediction Using ANN for Offshore Pipeline in the Gulf of Thailand

Passaworn Silakorn[a,*], **Taneth Puncreobutr**[a,*], **Asst. Prof. Thanawin Rakthanmanon**[b]
[a] *PTT Exploration and Production Public Company Limited, Bangkok, 10900, Thailand*
[b] *Kasetsart University, Bangkok, 10900, Thailand*
*passaworns@pttep.com, tanethp@pttep.com

Keywords: Artificial Neural Network; Top of Line Corrosion; Pipeline; Metal Loss Database

Top-of-Line-Corrosion (TOLC) is the main corrosion mechanism of PTTEP's pipelines in the Gulf of Thailand. Causes of TOLC can be from many relevant factors, such as temperature, flow regime, production rate, and amount of corrosive agents i.e. CO_2 content. Without cautious monitoring, the pipeline leakage can occur, which leads to significant impact to the company in terms of cost, reputation and environment issues.

From literature search, it is found that a learning based model Artificial Neural Network (ANN) can be used to predict pipeline degradation accurately. ANN is a learning computational model in the field of Artificial Intelligence (AI). ANN is a self-learning and self-development algorithm inspired by neural computing in human brain. Successful results are reported for the application of ANN on metal loss database to which linear regression cannot be achieved. Therefore, company has decided to develop ANN prediction model to predict TOLC.

In the first phase of the development of ANN modelling to predict TOLC, 3 pipelines were used for model learning and validation. It was shown that the ANN prediction model could obtain more accurate results, comparing to a conventional TOLC simulation program. In the current phase of the development, 12 more pipelines have been included. Moreover, sensitivity analysis has been performed on each model input parameter to find key parameters.

Results from the current development phase reveal that the latest version of the ANN prediction model can obtain more accurate results when compared to the previous version. In addition, it is found that when some pipelines are removed intentionally in learning process, the model can predict corrosion rates of those unseen pipelines accurately. Sensitivity analysis also indicates that topography, condensate flow rate, gas flow rate, and process temperature are the key parameters that have significant effect on TOLC corrosion rates. Successful results would lead to the application of ANN prediction model to predict TOLC metal loss for company pipelines in the Gulf of Thailand.

With accurate TOLC prediction and more confidence in TOLC characterization, company can save pipeline installation cost (from the reduction of corrosion allowance from 8 to 5 mm) by approximately 28 MTHB per year.

Based on the success of the TOLC prediction model development, it is suggested that ANN should be also applied to perform data analytical process on other process equipment, operation and/or production e.g. flowline erosion, intelligent process control and production optimization.

DMC-O-02

C^1 –triangular Finite Elements on a Curvilinear Boundary Domain

Wassamon Phusakulkajorn[a,*], Andrew L. Hazel[b], Matthias Heil[b]
[a]*CAD/CAE Laboratory, Design and Engineering Research Unit,*
National Metal and Materials Technology Center (MTEC), Pathumthani 12120, Thailand
[b]*School of Mathematics, University of Manchester, Manchester M13 9PL, UK*
*wassamon.phu@mtec.or.th

Keywords: C^1-curved triangular finite element, Bell element, Curvilinear boundary domain, Finite element method

Many engineering problems, for instance in areas of continuum mechanics including linear elasticity theory and the solution of Stokes flows, are governed by the biharmonic equation. In mathematics, the biharmonic equation is a fourth-order partial differential equation. Employing the finite element method mathematically suggests that the biharmonic solution has to be represented by a finite element that is continuously differentiable, i.e. C^1-finite element.

The objective of this work is to investigate the performance of C^1-triangular finite elements on a curvilinear boundary domain. To this end the Bell triangular finite element and the C^1-triangular finite element implemented for the forth-order partial differential equation are investigated on two kinds of boundary domains; straight and curved. The results show that, when the physical boundary is curved, a straight-line approximation is not exact and the performance of the Bell triangular element decreases in terms of both accuracy and convergence rate. In order to retain a convergence rate and accuracy of the solution of a C^1-problem on a curvilinear boundary domain, the C^1-triangular finite element is introduced. It is proved to show superiority in both convergence rate and accuracy when solving the C^1-problem on a curved boundary domain.

DMC-O-03

Finite Element Analysis of the Impact Test of Alloy Wheels

Somboon Otarawanna[a,*], Rattanasuda Naewngerndee[a], Sedthawatt Sucharitpwatskul[a], Piyamabhorn Uttamung[a], Atipong Malatip[a]
[a] *National Metal and Materials Technology Center, Pathumthani 12120, Thailand*
*Corresponding Author: E-mail address: somboono@mtec.or.th

Keywords: Alloy wheel, Impact test, Finite element, Aluminum alloy

Alloy wheels are typically made from an aluminum alloy by gravity die casting or low-pressure die casting process. They are a critical component of the automobile that has to meet requirements for driving safety. The impact test is one of the three main mechanical tests used to ensure the structural integrity of alloy wheels produced. The test represents the situation where the wheel hits a curb. In the impact test, a specified mass, the so-called striker, is dropped from a specified height onto the tire-wheel assembly. Finite element analysis (FEA) of the wheel impact test can reduce time and cost associated with the wheel design and development. Furthermore, better wheel performance can also be obtained by the use of FEA. This study aims to find suitable methods for modeling the wheel impact test by FEA. The modeling methods investigated are: 1) Dynamic simulation with tire, 2) Dynamic simulation without tire and 3) Static simulation without tire. The three modeling methods were evaluated in terms of solution accuracy and computational resources used. In order to obtain realistic mechanical properties of the wheel for inputting into the FEA software, tensile tests of the wheel material are performed. Regarding the comparison between FEA and experimental results, regions in the wheel where high stresses are predicted by FEA were compared with regions where cracking or relatively-large deformation occurs in the impact test experiment.

DMC-O-04

The Pretensioning Value and the Mode of Failure on the Friction High Quality Bolt Connections

Rosyidah, Anis[a,*] and Irawan, Okky[b]
[a]*Politeknik Negeri Jakarta, Depok, 16425, Indonesia*
[b]*Graduate Politeknik Negeri Jakarta, Depok, 16425, Indonesia*
*anis.rosyidah@gmail.com

Keywords: pretensioning, mode of failure, bolt connection, friction type.

High quality bolt connections used on the steel bridge are the mechanism of slip-critical. This mechanism relies on the clamping force of high quality bolt pretension led to friction between the surface of the tied steel plates, so the forces acting on the elements of the steel bridge held by the friction. In order to get the ratio of the pretensioning and observe the mode of failure, then the experiments in the laboratory and the simulation using software were carried out. The method used in this experiment was trial and error, so that the value of the pretensioning of high quality bolts needed to reach the maximum axial load press was retrieved. There are four types of surface coating of the tied steel; milling, grit-blast cleaning, coat of primer paint by grit-blast cleaning and coat of hot-dip galvanized given chromate treatment. The results obtained show that the ratio of the pretensioning on high quality bolt between the simulation and the experiments do not vary much, the range is 0.97. The mode of failure that occurs in the simulation tends to be more regular and quite small in comparison with the experimental results.

DMC-O-05

Design and Construction of a Restoring Force Measuring Apparatus for Assessment of Internal Stress Within Kiln-dried Lumber

Sataporn Jantawee[a,*], Satjapan Leelatanon[a], Prawate Diawanich[b], Nirundorn Matan[a]

[a] Materials Science and Engineering, School of Engineering and Resources, Walailak University, Thasala district, Nakhon Si Thammarat 80160, Thailand [b] Nakhon Si Thammarat Seaboard Industrial College, Pakpanang district, Nakhon Si Thammarat 80140, Thailand

*E-mail: sata_porn@yahoo.com

Keywords: Residual stress, Kiln-dried lumber, Stress measurement, Apparatus

A new approach of a restoring force measurement technique on "half-split" specimens has been proposed to directly assess the level of internal stress within kiln-dried lumber. The equipment consists mainly of a relatively stiff steel frame, two clamping jigs and a load cell. One jig is fixed to the steel frame and another is attached to a steel rod connected to the load cell. While being clamped to the frame, the specimen is half-split at half the thickness for a required length. The restoring force can be then measured online both in a single sawing mode at a particular half-split length and a multiple sawing mode at various half-split lengths. Screw contact area of 24 mm^2 with

An optimal applied torque on each screw of 2-3 N·m is suitable to hold the specimen to the apparatus. Cracks could be developed in the specimen if the screw contact area is too small or the applied torque is too high. The magnitude of the restoring force is proportional to length of the specimen. For the 30 mm thick specimen, the measured restoring force at a particular half-split length is constant if the remaining unsplit length of the lumber is greater than 25 mm. The measured restoring force dramatically decreases below this value. Both distance and angular deviations of cutting away from the half-split line reduce the measured restoring force value. By keeping the distance deviation away from the half-split line to within 1 mm, an error resulting in a reduction in the measured restoring force is less than 5%. The proposed restoring force measuring apparatus together with a suitable set up of the half-split specimen is proved to provide a repeatable measurement of the restoring force of the kiln-dried lumber at various half-split lengths. Interpretation of the restoring force in term of internal stress will be performed in the future work.

DMC-O-06

Formability Characterization of Advanced High Strength Steel Sheet by using Fukui Stretch-Drawing and Square Cup Drawing tests

Sansot Panich[a,*], Nopparat Seemuang[a], Taratip Chaimongkon[b]
[a]*Deparment of Production Engineering, Faculty of Engineering*
[b]*Division of Tools and Die Engineering Technology, Department of Mechanical Engineering Technology, College of Industrial Technology*
King Mongkut´s University of Technology North Bangkok, Bangsue Bangkok, 10800, Thailand.
*sansot.p@eng.kmutnb.ac.th

Keywords: Forming limit Curve, Forming Limit Stress Curve
Fukui Test, Square Cup Test

In this work, the experimental and numerical analyses of Forming Limit Curve (FLC) and Forming Limit Stress Curve (FLSC) for Advanced High Strength Steel (AHSS) sheet, grade JAC780Y, were performed. Initially, the FLC was experimentally determined by means of the Nakazima Stretch forming test. Subsequently, the strain based FLC was transformed into FLSC by using numerical calculation. Additionally, the FLSC of investigated steel was plastically calculated using the experimental FLC data. The strain based FLC was then transformed into stress triaxiality and plastic strain space through numerical calculation. Different yield criteria including Hill48, and Yld89, were applied to describe plastic flow behavior of the AHS steel and Swift hardening laws were taken into account. Hereby, influences of the constitutive yield models on the numerically-determined FLSCs were evaluated regarding to those results from the experimental data. The obtained stress based forming limits, stress triaxiality, and plastic strain were affected significantly by the yield criteria. Finally, the experimental and numerical formability analyses of Fukui stretch-drawing and square cup drawing tests were studied using FLC, FLSCs, stress triaxiality, and plastic strain curve, so-called stress triaxiality curve.The Fukui and Square cup tests were carried out and simulated. Then,the calculation of strain and stress paths were compared with the FLC, FLSCs, and stress triaxiality curve. It was observed that all stress based curves can be used very well to describe material formability of the examined steel compared to the strain based FLC. The strain based FLC was developed by Nakazima Stretch forming test based on localized necking state. The strain based FLC is not sufficient to evaluate the formability for AHS Steel since this material exhibits fracture without localized necking stage and also strain based depend on forming history and strian paths change. In the other hand,the stress based FLC and stress triaxiality curve do not depend on these issue. In this study, it can be concluded that the FLSC and stress triaxiality curve could predict failure more realistically and better than the strain based FLC. In future work, this stress triaxiality space will be examined on further geometries of real parts and will be expanded to martensite steel grades up to 1150 MPa UTS or to use other yield functions such as Yld2000.

DMC-O-07

Effect of an Anisotropic Hyperelastic Model on Blood Flow Pattern in a Small Vessel with Stenosis

Mongkol Kaewbumrung[a,*], Benchawan Wiwatanapataphee[b]
[a]*Pathumthani University, Department of Mechanical Engineering , Faculty of Engineering and Technology , Pathum Thani, 12000, Thailand*
[b]*Curtin University,Department of Mathematics and Statistics, Faculty of Science and Engineering , Bentley, Perth, Western Australia 6102*
*Mongkol.kaewbumrung@gmail.com

Keywords: Anisotropic Hyperelastic material, Visco-hyperelasticity, Stenosed artery

Over the last few decades, a number of boundary value problems have been proposed to study the blood flow in a small vessel which is assumed to be either linear or nonlinear elastic material. The results obtained from existing models and type of arterial blood vessel still remain questionable in biomechanics applications. In this paper, we study the effect of an anisotropic hyperelastic model on the blood flow pattern in a small vessel with stenosis. Three types of arterial material including Neo-Hookean, Mooney-Rivlin and Holzapfel are taken into consideration. Due to the heart pump, the pulsatile velocity and pulse pressure are assigned on the inflow and outflow boundaries, respectively. Numerical techniques based on Finite Element method and Finite Volume method are implemented respectively for the arterial wall deformation and the blood flow through the channel with varying cross section. The effect of nonlinear elasticity of the vessel is prescribed and investigated. In order to clearly precise the less numerical error with mesh independence, the High Performance Computing (HPC) is applied in this study.

DMC-O-08

Effect of Feed-flow Rate on Solid-liquid Hydrocyclone based on Novel Separation Efficiency Equation

Soison Pichai, Wongsarivej Pratarn*
National Nanotechnology Center, National Science and Technology Development Agency, 111 Thailand Science Park, Phahonyothin Road, Khlong Nueng, Khlong Luang, Pathumthani 12120, Thailand.
* pratarn@nanotec.or.th

Keyword: Hydrocyclone / Flow ratio / Concentration ratio / Separation / Efficiency

Many articles of hydrocyclone confirmed that the increasing of feed-flow rate resulted in higher separation efficiency. The purpose of this research is to investigate the separation efficiency of 100 mm solid-liquid hydrocyclone at various feed-flow rates of 2, 3, 4, 5 and 6 m^3/hr by adding 1 and 2% of soil particles. The solid concentration and particle size distribution were analyzed using drying-weighing method and Mastersizer. The experimental results showed that when feed-flow rate increased from 2 to 4 m^3/hr, the separation efficiency decreased. Conversely, when feed-flow rates increased from 4 to 6 m^3/hr, the separation efficiency increased. However, the higher feed-flow rate, the smaller cut size. The novel separation efficiency equation in form of flow ratio and concentration ratio is proposed in this paper.

DMC-O-09

Development of Regression Model of $Stk_{50}Eu$ for Hydrocyclone

Supachart Pakpoom[a,1], Rattanaphan Santita[a,2], Soison Pichai[b,3], Swasdisevi Thanit[a,4] and Wongsarivej Pratarn[b,*]

[a]*King Mongkut's University of Technology Thonburi, 126 Pracha-utid Road, Bangmod, Toongkru, Bangkok 10140, Thailand.*

[b]*National Nanotechnology Center, National Science and Technology Development Agency, 111 Thailand Science Park, Phahonyothin Road, Khlong Nueng, Khlong Luang, Pathumthani 12120, Thailand.*

[1]pakpooms243@gmail.com, [2]santita.r@dti.or.th, [3]pichai@nanotec.or.th, [4]thanit.swa@kmutt.ac.th,

*pratarn@nanotec.or.th

*Corresponding Author

Keywords: Conical length, Regression model, Stokes number, Euler number

Abstract

Hydrocyclone is a device used widely in various industries, especially the separation of solids from liquids. Operations of the hydrocyclone are found that there are many factors affecting on efficiency separation. In this research, the main objectives were studied on the conical length that affected to the separation efficiency and proposed the regression model of $Stk_{50}Eu$ of hydrocyclone. First, the research was studied on the separation efficiency using a 40 mm hydrocyclone. The effects of conical lengths of 200, 240 and 280 mm were investigated. The tested suspension was the mixed of silica and water. The silica particles have an average size of 9-10 micrometer at the solid concentration of 0.5% *w/v*. The feed flow rate of 1 m^3/hr was operated with the flow ratio of 0.1. From experimental result, it was found that the shorter conical length, the higher separation efficiency. At the condition of the cone length of 200 mm, the cylindrical length of 60 mm and the vortex finder length of 40 mm revealed the best separation efficiency up to 84.06 percent. Second, regression model of $Stk_{50}Eu$ of hydrocyclone was established. In this work, data obtained from the experiments in the first part and from the earlier researches totally of 75 were used to make the relationship between the proportion of hydrocyclone and $Stk_{50}Eu$. By the multiple linear regression method, it was found that the constants, k_1 was 3.582×10^{-5} and the regression coefficient, n_2, n_3, n_4 and n_5 were -0.7080, 0.5043, 6.3145 and 2.9900, respectively.

DMC-O-10

Development and Characterizations of a Projection Stereolithography

Pornsak Srisungsitthisunti[a] and Thossaporn Kaewwichit[b*]
[a]*Department of Production Engineering, King Mongkut's University of Technology North Bangkok, Bangkok, 10800, Thailand*
[b]*Department of Mechanical Engineering Technology, King Mongkut's University of Technology North Bangkok, Bangkok, 10800, Thailand*
*thossaporn.k@cit.kmutnb.ac.th

Keywords: Rapid prototyping, Custom-made projection stereolithography, 3D printing technology, Characterizations specification.

Abstract
Stereolithography is a manufacturing process which builds the truly high resolution 3D structures by solidifying the liquid monomer in a layer by layer fashion. There are many new 3d printing technologies which require method of characterizations to achieve desired performance. In this study, we develop a bottom-up custom-made projection stereolithography to accommodate a new 3D printing of multi-material process technique. In addition, we propose a method for characterizations different specifications of a custom-made projection stereolithography. Our 3D printer can establish the object up to 25 mm x 25mm x 15 mm of length, width and height, respectively. The vertical stepping technique strongly affected the error of the layer thickness. To reduce such error, a screw component with spring modification were included to reduce movement of the vertical step which can minimize the layer thickness error. The light source distance and the calibration factor were also importance factors to obtain the better precision of the built parts. Based on the proposed characterization method, the 3d printer was able to achieve the lateral resolution of 0.05 mm and a vertical step resolution of 0.01 mm. The average percentage error of built part were 0.83 % laterally and 1.76 % error on the layer thickness

DMC-O-11

Effect of Post-curing Temperature and Mechanical Surface Treatment on Shear-bond Strength of Asbestos-free Brake Pad

Danuwat Pupan[a], Chakrit Suvanjumrat[a], Watcharapong Chookaew[a,*]
[a]*Mechanical Engineering Department, Faculty of Engineering, Mahidol University, Nakhon Pathom, 73170, Thailand*
*watcharapong.chk@mahidol.ac.th

Keywords: Processing temperature, Surface treatment, Bonding strength, Brake pad

In general, brake pad fabrication is the combination of lining and metallic components, e.g. steel backing plate (disc brake) and aluminum brake shoe (drum brake). Shear bond strength plays a major role to provide the safety and/or driving performances. This work aimed to study the processing factors affected the bonding strength. The molding temperature couple with post-curing temperature was simultaneously analyzed in order to optimize the processing temperature. The shear bond strengths of metallic plates were continually investigated with regard to the effect of different surface treatments. The obtained results indicated that the mechanical strength was increased as the molding temperature raised in ranges of 160°C to 180°C. Conversely, the deterioration of adhesive strength was progressively presented with rising post curing temperature. In comparing different backing plate, aluminum showed the higher shear bond strength than that of steel plate. In fact, the weakened property of aluminum in nature would be easily destroyed by mechanical treatments. From the shear tested results, an increase of surface roughness was inversely changed the shear bond strength. On the other hand, the contact angle of water droplet affected directly to adhesive strength. It was suggested that an adding surface roughness usually used in industry was inappropriate criteria whist geometrical surface should be taken into account for improving the shear bond strength. Moreover, the contact angle and mechanical interlocking were recommended to use as a criteria of brake pad shear strength.

DMC-P-01

Computer-Aided Optimization for Multi-Pass Cold Drawing of Cobalt-Chromium Alloy Seamless Micro Tube

Seokkwan HONG[a], Jeongjin KANG[a], Jongdeok KIM[b], Dongearn KIM[b,*], Okrae KIM[b]

[a]Molds & Dies Technology Group, Korea Institute of Industrial Technology (KITECH), 64, Saneop-ro 7 beon-gil, Ojeong-gu, Bucheon-si, Gyeonggi-do, South Korea

[b]Molds and Dies Technology Group, Korea Institute of Industrial Technology(KITECH), 156, Gaetbeol-ro, Yeonsu-gu, Incheon, South

*kdu0517@kitech.re.kr

Keywords: Seamless tube, Multi-pass cold drawing, Cobalt-chromium alloy, Finite element analysis.

Although the cobalt-chromium alloys are widely used materials for various stents, the cold drawing of seamless micro tube is very difficult due to its high strength. In this paper FE simulations of multi-pass drawing process were conducted to obtain the cobalt-chromium alloy micro tubes which have external diameter 1.0mm and thickness 0.1mm from the seamless tubes which have initially external diameter 10.5mm and thickness 0.5mm. In order to successfully get the final tube without fracture, optimal pass schedule and design parameters of drawing die in each pass were obtained by computer-aided optimization (CAO). Fig.1 shows the distribution of the effective strain during the cold drawing process.

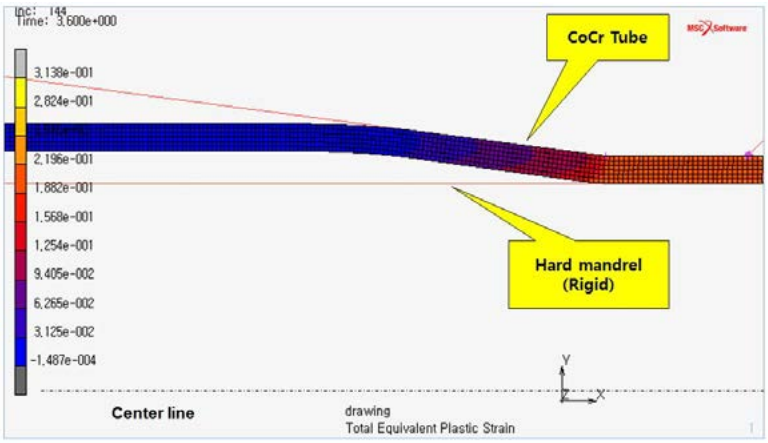

Fig.1 The cold drawing process for obtaining the micro cobalt-chromium alloy tube

DMC-P-02

The Structural and Electronic Properties of FePc, CoPc and CuPc Monomer Structure: First Principles Study

Witoon Nuleg[a, d,*], Pitiporn Thanomngam[a, b, c], Kanoknan Sarasamak Phacheerak[a, b, c]
[a]*College of Nanotechnology, King Mongkut's Institute of Technology Ladkrabang, Bangkok 10520, Thailand*
[b]*Thailand Center of Excellence in Physics (ThEP Center), CHE, 328 Si Ayutthaya Rd, Bangkok 10400, Thailand*
[c]*Nanotec-KMITL Center of Excellence on Nanoelectronic Devices, King Mongkut's Institute of Technology Ladkrabang, Chalongkrong road, Ladkrabang, Bangkok, 10520, Thailand*
[d]*Faculty of Science and Technology, Rambhai Barni Rajabhat University, Chanthaburi 22000, Thailand*
*witoon_nuleg@hotmail.com

Keywords: first principles; electronic properties; metal phthalocyanine

The structural and electronic properties of metal phthalocyanine (MPc;M=Fe, Co and Cu) is investigated by first principles calculation based on density functional theory (DFT). The generalized gradient approximation (GGA) is used to describe the exchange-correlation with the projector-augmented wave (PAW) method. The magnetic properties of the metal phthalocyanine were investigated with spin-polarized calculation. The calculated bond length and bond angles of metal phthalocyanine are correspond with other calculations and experimental data. The electronic properties of central metal atom are essential in shaping the ground state electronic structure of the metal phthalocyanine near the Fermi level. Metal phthalocyanine show interesting magnetic properties.

Materials for Energy

ENR-I -01

Development of Metal-supported Solid Oxide Fuel Cell (MS-SOFC) and Thin-film Solid Oxide Fuel Cell in KAIST

Joongmyeon Bae[1*]
[1] *Department of Mechanical Engineering, Korea Advance Institute of Science and Technology, Republic of Korea*
*E-mail: jmbae@kaist.ac.kr

Keywords: Metal-supported solid oxide fuel cell, Thin-film solid oxide fuel cell, Auxiliary power unit

Solid oxide fuel cell (SOFC) is an energy conversion device which can generate electricity from hydrogen energy. SOFC is composed of ceramic materials such as Yttria-stabilized Zirconia (YSZ), Gd-doped CeO_2 (GDC), and $La_{0.6}Sr_{0.4}Co_{0.2}Fe_{0.8}O_3$ (LSCF). However, for this reason, SOFC is brittle and has low mechanical strength. To overcome this limitation, metal-supported SOFC (MS-SOFC) has been developed recently. MS-SOFC is composed of metal substrate for higher mechanical strength. In my research group, sinter-joining method for the fabrication of MS-SOFC was developed and 15 X 15 cm^2 unit cells were successfully fabricated. Based on sinter-joining method, 3-layer short stack was also developed and tested for more than 130 hrs. Currently, auxiliary power unit (APU) system based on MS-SOFC is being developed. In addition, interconnect-coating based MS-SOFC fabrication method was recently developed in my group. This novel MS-SOFC is fabricated by only heat-treated under air atmosphere and conventional wet-chemical coating processes. It is believed that this new fabrication method can reduce manufacturing cost considerably.

SOFC is usually operated at high temperature of 600-800°C. However, operating at high temperature can cause high degradation of electrochemical performance, oxidation of interconnects, and high cost by oxidation-resistant materials. Therefore, low-temperature SOFC is attracting attentions. To operate SOFC at low temperature, thin electrolyte layer is required because of low ionic conductivity of electrolyte materials at low temperature. For this reason, thin-film coating method of sputtering is successfully applied for anode-supported SOFC with thin-film electrolyte layer in my group.

To facilitate commercialization of SOFC using the advantage of fuel flexibility, development of fuel processing technology and its commercialization efforts will be also briefly introduced.

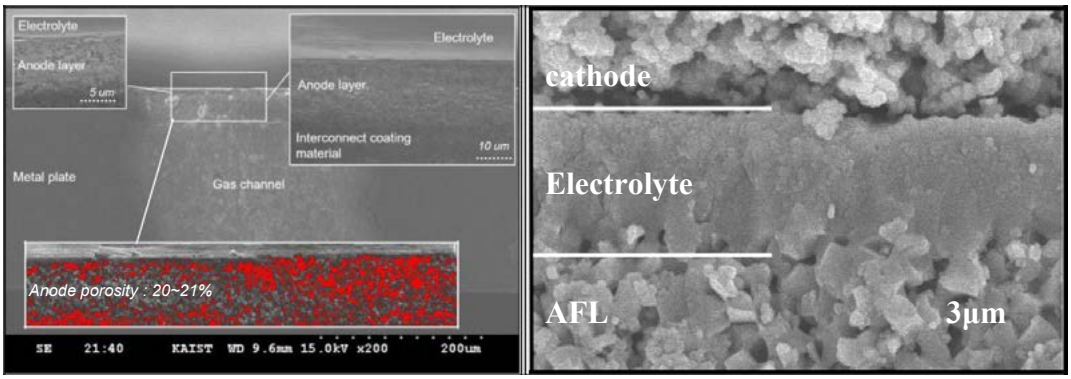

Fig. Cross-section images of MS-SOFC fabricated by interconnect-coating method and thin-film anode-supported SOFC fabricated by sputtering

ENR-O-01

Graphene-$AgVO_3$ composite for supercapacitor applications

Jiaqian Qin[a,*], **Weerapong Nuanwat**[b]

[a]*Metallurgy and Materials Science Research Institute, Chulalongkorn University, Bangkok, 10330, Thailand*

[b] *Department of Materials Science, Chulalongkorn University, Bangkok, 10330, Thailand* *E-mail address: jiaqian.q@chula.ac.th, jiaqianqin@gmail.com

Keywords: Graphene, $AgVO_3$, Supercapacitor.

In this work, the graphene-$AgVO_3$ composites were successfully synthesized by precipitation methods from graphene, $AgNO_3$, and NH_4VO_3. The electrode was prepared from polytetrafluoroethylene (PTFE), conductive carbon, and the prepared materials with weight ratio of 1:1:8. The cyclic voltammetry (CV), electrochemical impedance spectroscopy (EIS), and Galvanostatic charging-discharging (GCD)methods were performed to study the prepared electrode by an Autolab Type III. The results show that the specific capacitance of the composite electrode can be significantly improved. Furthermore, the supercapacitor device was also fabricated from two electrodes with filter paper as separator. The GCD shows that both specific capacitance and cycle stability can be enhanced with $AgVO_3$ incorporation.

ENR-O-02

Characterization of Polyaniline/Carbon Nanotube/Pineapple-Polyester Fabric Composites as Supercapacitor Electrodes

Felicidad Christina Ramirez[a,b,c*], **Sangaraju Shanmugam**[d], **Christina A. Binag**[a,b,c]

[a]*Department of Chemistry, College of Science,* [b]*Graduate School*
[c]*Advanced and Nano Materials Laboratory, Research Center for the Natural and Applied Sciences, University of Santo Tomas, Manila 1015, Philippines*

[d]*Department of Energy Systems Engineering, Daegu Gyeongbuk Institute of Science and Technology, Daegu, 711873 South Korea*

*felicidad.christina.ramirez@ust.edu.ph

Keywords: supercapacitor electrodes, conductive textiles, polyaniline

The exponential growth and fast development of mobile technology has led to an ever-increasing demand for portable energy storage devices, such as supercapacitors and batteries. Enhanced supercapacitor performance can be achieved by development of new electrode materials. Flexible supercapacitor electrodes were fabricated by combining carbon nanotubes (CNT) and polyaniline (PANi) with pineapple-polyester woven fabric (PPWF) via dipping and drying technique and *in situ* chemical polymerization, respectively. CNT/PPWF, PANi/PPWF and PANi/CNT/PPWF were then characterized using Fourier Transform Infrared Spectroscopy (FTIR), Thermal Gravimetric Analysis (TGA), Scanning Electron Microscopy (SEM), and four-point probe conductivity testing. Cyclic voltammetry (CV), Galvanostatic Charge Discharge (GCD) and Electrochemical Impedance Spectroscopy (EIS) using a three-electrode set-up were done to study the electrochemical properties. FTIR spectra indicated the presence of polyester, cellulose and PANi in the composites. The weak adsorption bands of CNT could not be observed because they coincided with polyester. TGA results showed that the composites were stable within the operating temperature range of supercapacitors (-40^{o}C-85^{o}C)[1] as all composites began to degrade above 280^{o}C. SEM micrographs show that the intertwined, web-like structure of CNT and cauliflower-shaped PANi completely cover both pineapple and polyester fibers. PANi/CNT/PPWF produced the highest conductivity (0.3877 S/cm), followed by CNT/PPWF (0.2615 S/cm), and PANi/PPWF (6.850x10^{-3} S/cm). PANi/CNT/PPWF exhibited significant areal capacitance (338.7mF/cm^2) compared to CNT/PPWF (18.8mF/cm^2) and PANi/PPWF (30.7mF/cm^2) based on CV at 5mV/s. These capacitance values are higher than those obtained from pure polyester composites, indicating that the addition of pineapple fibers is beneficial as it allows electrolyte to freely pass through the material. A similar trend was observed using GCD. Combining CNT and PANi on PPWF led to interesting properties, as CNT provided the needed conductivity and served as scaffolds for PANi growth. PANi further bridged the CNT web-like structure that led to low charge transfer resistance (12Ω based on EIS) and provided the faradaic reactions for higher capacitance values. These results are comparable with the PANi/SWCNT/cloth prepared by Wang and co-workers in 2011 wherein they obtained areal capacitance of 282mF/cm^2.[2] PANi/CNT/PPWF composites exhibited remarkable conductivity (0.3877 S/cm) and areal capacitance (338.7mF/cm^2), making them promising flexible electrodes for supercapacitors.

Acknowledgements:
This work was supported by the Philippine Council for Industry, Energy, and Emerging Technology Research and Development of the Department of Science and Technology (PCIEERD-DOST), and the Commission on Higher Education-Faculty Development Program (CHED-FDP).

References:

1 Hung, K., Masarapu, C., Ko, T., & Wei, B. (2009). Wide-temperature range operation supercapacitors from nanostructured activated carbon fabric. Journal of Power Sources, 193(2), 944-949. doi:10.1016/j.jpowsour.2009.01.083

2 Wang, K., Zhao, P., Zhou, X., Wu, H., & Wei, Z. (2011). Flexible supercapacitors based on cloth-supported electrodes of conducting polymer nanowire array/SWCNT composites. Journal of Materials Chemistry, 21(41), 16373-16378. doi:10.1039/c1jm13722k

ENR-O-03

Piña (*Ananas comosus*) and Water Hyacinth (*Eichhornia crassipes*) Polyester Blended Textiles with Polypyrrole as Supercapacitor Electrode Materials

David Joseph Alzate[1*], Felicidad Christina Ramirez[1, 3], Christina Binag[1, 2, 3]

[1]*Graduate School, Thomas Aquinas Research Center, University of Santo Tomas, Manila City, 1008, Philippines*

[2]*Research Center for the Natural and Applied Sciences, Thomas Aquinas Research Center, University of Santo Tomas, Manila City, 1008, Philippines*

[3]*Department of Chemistry, College of Science, Thomas Aquinas Research Center, University of Santo Tomas, Manila City, 1008, Philippines*

*djgalzate19@gmail.com

Keywords: Polypyrrole, Textile supercapacitors

Supercapacitors are gaining a lot of recognition due to their better power densities of up to 1kW/kg, cycling time, and charging time compared to conventional batteries. As the electrical properties of a supercapacitor are determined by the electrode material, there is increasing interest into applying these materials onto textiles for flexible and "wearable" batteries. This study aims to fabricate flexible supercapacitor electrodes by coating polypyrrole (PPy) onto locally available pineapple (*Ananas comosus*) and water hyacinth (*Eichhornia crassipes*) fibers woven with polyester. PPy was coated onto the fabrics via *in situ* polymerization using $FeCl_3$ as the oxidant. These electrodes were characterized with four-point probe conductivity technique, scanning electron microscopy (SEM), cyclic voltammetry (CV), electrochemical impedance spectroscopy (EIS), galvanostatic charge-discharge (GCD), and thermogravimetric analysis (TGA). SEM micrographs indicate globular structures of PPy on the surface of the composites. PPy-coated pineapple-polyester woven fabric (PPy/PPWF) and PPy-coated water hyacinth-polyester woven fabric (PPy/WHPWF) composites have conductivities of 0.3730S/cm, and 0.2039S/cm, respectively. Cyclic voltammograms show PPy/PPWF and PPy/WHPWF composites have areal capacitances (C_a) of 164.52mF/cm^2, and 89.16mF/cm^2, respectively at a scan rate of 5mV/s. PPy/PPWF and PPy/WHPWF composites had specific capacitances (C_s) of 132.88F/g, and 108.39F/g, respectively, at a scan rate of 5mV/s. Three electrode EIS data indicate that the composites have low impedance and good capacitive behavior. As an energy storage device charges and discharges energy, it generates heat, thus knowing the thermal stability and degradation of a composite is crucial. TGA results show that the pristine PPWF and WHPWF had three degradation steps at around 300°C, 350°C, and 422°C. While the PPy/PPWF and PPy/WHPWF composites only had two degradation steps at around 305°C and 422°C, indicating an improvement on the thermal stability due to PPy. PPy/PPWF and PPy/WHPWF composites exhibited better characteristics than pure polyester composites (C_a = 55.17mF/cm^2, C_s = 126.64F/g). These characteristics were lower than cotton fabric composites (C_s = 268F/g) by Firoz Babu and co-workers (2013). The Ca and Cs of the fabrics could be improved by (a) weaving pineapple or water hyacinth fibers with cotton, (b) use non-woven fabrics with polyester, or (c) through the inclusion of carbon nanotubes. The fabricated PPy textile composites showed promising characteristics as electrode materials for supercapacitors.

ENR-O-04

Graphene Passivation of Aluminum Current Collector for Supercapacitor Electrode

Jedsada Manyam[a,*], **Prayoon Songsiriritthigul**[b]

[a]*National Nanotechnology Center (NANOTEC), National Science and Technology Development Agency (NSTDA), Pathum Thani 12120, Thailand*

[b]*School of Physics, Institute of Science, Suranaree University of Technology, Nakhon Ratchasima 30000, Thailand*

*jedsada@nanotec.or.th

Keywords: Graphene, Aluminum, Current collector, Supercapacitor

Electrical contact resistance arising at interface between carbon electrode material and a metal current collector can limit performance or lead to deterioration in an energy storage device such as supercapacitor. Several studies have been revealed that passivation of a current collector with a thin layer of carbonaceous material could reduce the contact resistance and thus improve stability of the electrode. In this work, we present a study on deposition of a thin layer of graphene oxide (GO) or reduced graphene oxide (rGO) sheets on an aluminum current collector and investigate a role of such graphitic passivation to the internal resistance and charge-discharge performance of an electrical double layer capacitor (EDLC) electrode. It was found that a large percentage coverage of GO sheets greater than 90% could be achieved by a single dip coating a pre-etched aluminum foil in modified Hummers' GO suspension. In addition, film thickness could be controlled by repetitive dipping or alternatively by applying electrophoretic deposition. Microwave heating was utilized to produce rGO coating with different degrees of reduction. Electrochemical characteristics of the graphene coated samples and bare aluminum in 0.5 M Na_2SO_4 solution were determined using electrochemical impedance spectroscopy (EIS). Preliminary results for dip coated samples showed that graphene oxide coated aluminum exhibited a time constant peak at low frequency in a bode plot which fade away after several scans, representing charge transfer processes such as adsorption or reduction of GO and oxidation of aluminum. In contrast to GO coating, a rGO/aluminum sample was relative inert to electrochemical reaction, while it was observed that a bare aluminum possessed the greatest polarization with respect to a Ag/AgCl reference electrode and a protective oxide layer was formed. The results showed the feasibility to utilize a dip coated rGO/aluminum as a superior current collector for a supercapacitor electrode, in which further investigation on its performance and detailed analysis will be presented.

ENR-O-05

Pre-Immobilization of Anaerobic Mixed Culture on Electrode of the Upflow Bio-Filter Circuit Microbial Fuel Cell

Chinnatad Sinprasetchok[a], Nuwong Chollacoop[a], Sumittra Charojrochkul[a] and Korakot Sombatmankhong[a,*]

[a]*National Metal and Materials Technology Center, Pathumthani, 12120, Thailand*

*E-mail address: korakots@mtec.or.th

Keywords: Microbial fuel cell, Immobilization, Granular activated carbon, Anaerobic microorganism

Microbial extracellular electron transfer is a significant process in a microbial fuel cell (MFC). Owing to many potential losses in the electron transfer from microorganism to an electrode, a promotion of microbial attachment to electrode should be a productive solution to this difficulty of MFC. We also introduced here a prior colonization of microbes on electrode instead of a conventional immobilization which entirely occurred in a MFC reactor to expedite an attachment of microorganisms on the electrode surface. Coconut shell-based granular activated carbons (CGACs) used as one of the electrodes in the upflow bio-filter circuit microbial fuel cell were immersed in Lysogeny broth (LB) at pH 7 before an inoculation of anaerobic consortium from a wastewater treatment plant was performed. The immobilization was proceeded in a 125 mL Erlenmeyer flask containing 10mL of LB at 30^{o}C with a shaking speed of 100 rpm throughout an experiment. CGACs taken from a collection of flasks into which new LB was added every two days were examined a surface with scanning electron microscopy (SEM). On the 3rd day of immobilization, SEM images showed that a colonization was seen obviously in large pores on CGAC surface while there were sparse possessions on a rough and moderately rough surface with tiny pores. Smooth surface not supporting well at the beginning of immobilization was filled with plenty of bacteria when 12 days elapsed from the day of inoculation. An increment of electrostatic attraction force between bacteria and electrode was introduced in this study by applying a heat treatment on CGAC so as to accelerate the microbial attachment to the carbon surface. An increase of point of zero charge (PZC) of CGAC treated at 800 and 900^{o}C indicated that some acidic functional groups were partly removed on the CGAC surface. Because PZC value of the treated CGAC being a bit higher than the other, the number of bacteria on the treated CGAC was approximately as same as the untreated CGAC at the same day of immobilization. The surface of both CGACs densely shrouded in living cells of microbes with extracellular filaments and biofilms could be successfully established within 14 days.

ENR-O-06

Studies on CeP_2O_7-ZrP_2O_7 Solid Solutions: Electrolytes for Intermediate Temperature Proton-Conducting Ceramic-Electrolyte Fuel Cells (IT-PCFC)

Aman Bhardwaj[*,a], **Sandeep K. Gautam**[a], **Om Prakash**[a], **D. Kumar**[a], **Sun-Ju Song**[b], **Bhupendra Singh**[**, a]

[a]*Department of Ceramic Engineering, Indian Institute of Technology (Banaras Hindu University), Varanasi-221005, India*

[b]*Department of Materials Science & Engineering, Chonnam National University, Gwangju-500757, South Korea*

*Presenting author: amanb.cer15@iitbhu.ac.in, **Corresponding author: bhup.bhu@gmail.com

Keywords: Tetravalent metal pyrophosphate; CeP_2O_7-ZrP_2O_7 solid solution; Ionic conductivity; Intermediate temperature proton-conducting ceramic-electrolyte fuel cells

Acceptor doped tetravalent metal pyrophosphates (TMPs) have shown high proton conductivity in dry and humid atmosphere in intermediate temperature range (150-500 ^oC). However, the fabrication of dense electrolyte samples has been one of major challenges towards their application as electrolytes in PCFCs, they require sintering at >1200 ^oC to get fairly dense electrolyte specimen. But not only some of these TMPs, e.g., CeP_2O_7, have narrow range of thermal stability, sintering them at such a high temperature has been found to be detrimental to their proton conductivity. In order to utilize TMPs as electrolyte, therefore, it is necessary to look for new alternatives for the densification of TMP electrolytes.

It has been observed that, although CeP_2O_7 are thermally unstable at >400 ^oC, they give fairly dense specimen even on sintering at temperatures ~400 ^oC. Also, it is observed that the partial substitution of Sn^{4+} by Ce^{4+} in SnP_2O_7 improves its densification and ionic conductivity. Therefore, the partial substitution by Ce^{4+} in other TMPs can be beneficial in improving the densification and ionic conductivity behavior. On the other hand, zirconium pyrophosphates are thermally stable at temperatures >1200 ^oC, but they have significantly lower ionic conductivity as compared to the cerium pyrophosphates. The TMPs of cerium and zirconium are generally isomorphous, with both having cubic lattice and $Pa\bar{3}$ space group, and it is expected that on partially replacing Zr^{4+} by Ce^{4+}in ZrP_2O_7, Ce^{4+} would easily incorporate into ZrP_2O_7 lattice and may improve its sinterability. Although the ionic radius of Ce^{4+} ion (r=0.87 Å) is larger than that of Zr^{4+} ion (r=0.72 Å), the cerium-zirconium solid solutions are well-known, e.g. $BaCeO_3$-$BaZrO_3$ solutions with cubic perovskite-type structure. In $BaCeO_3$-$BaZrO_3$ solid solutions, it has been observed that the partial substitution by Zr improves thermodynamic stability of $BaCeO_3$ and the partial substitution by Ce improves protonic conductivity of $BaZrO_3$ and, therefore, a number of solid solutions of $BaCeO_3$-$BaZrO_3$ have been reported. Although, $BaCeO_3$-$BaZrO_3$ solid solutions are totally different crystal system from the cubic TMPs, we can expect some interesting outcomes, e.g., on the densification behavior and ionic conductivity, from CeP_2O_7-ZrP_2O_7 solid solutions. Therefore, in this work we have prepared a number of solid solutions based on CeP_2O_7-ZrP_2O_7 system by digesting oxide powders with 85% phosphoric acid. The maximum solubility limit of Ce^{4+} in ZrP_2O_7 system and that of Zr^{4+} in CeP_2O_7 system is determined and its effect on the phase composition, sinterability and microstructure, and ionic conductivity analyzed.

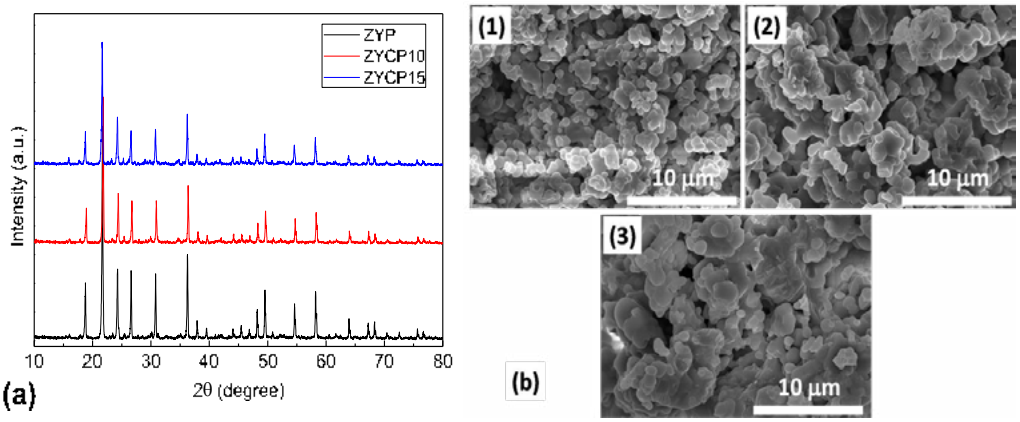

Figure 1. XRD patterns (a) and SEM images (b) of $Zr_{0.9}Y_{0.1}P_2O_7$ (ZYP), $(Zr_{0.9}Y_{0.1})_{0.9}Ce_{0.1}P_2O_7$ (ZYCP10) and $(Zr_{0.9}Y_{0.1})_{0.85}Ce_{0.15}P_2O_7$ (ZYCP15) heat-treated at 1200 °C for 12 h.

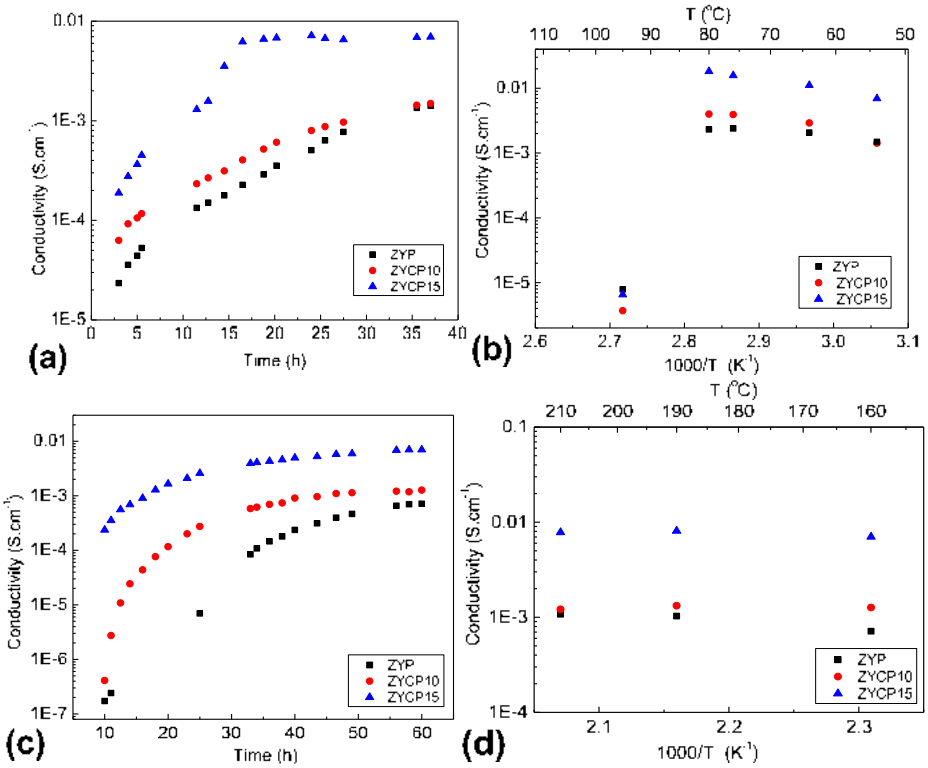

Figure 2. Variation of ionic conductivity of ZYP, ZYCP10 and ZYCP15 in wet air (pH_2O=0.12 atm) (a) with time during humidification at 54 °C; (b) with temperature after humidification; (c) with time during humidification at 160 °C; (d) with temperature after humidification at 160 °C.

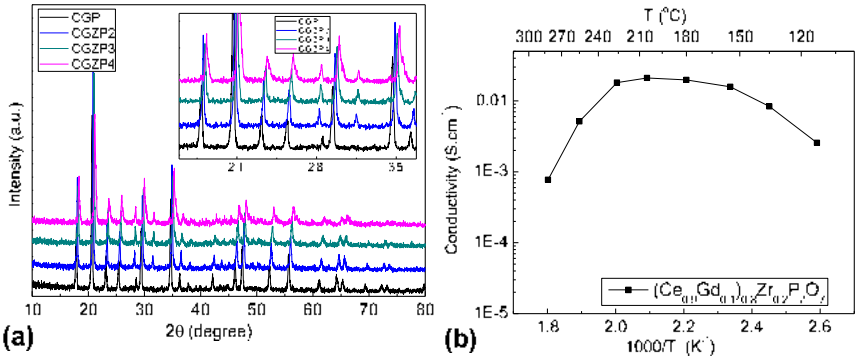

Figure 3. XRD patterns (a) and SEM images (b) Variation of ionic conductivity of $(Ce_{0.9}Gd_{0.1})_{1-x}Zr_xP_2O_7$ with temperature after humidification in wet air (pH_2O=0.12 atm) at 110 °C.

ENR-O-07

Experimental investigation of electrospray coating technique for electrode fabrication in PEMFCs

Natthika Chingthamai[a], Yossapong Laoonual[a], Korakot Sombatmankhong[b,]

[a] Department of Mechanical Engineering, Faculty of Engineering, King Mongkut's University of Technology Thonburi (KMUTT), 126 Pracha Uthit Ro Bangmod, Thung Khru, Bangkok, 10140, Thailand

[b]Electrochemical Materials and System Laboratory, National Metal and Materials Technology Center (MTEC), 114 Thailand Science Park, Phahonyothin Road, Khlor Nueng, Khlong Luang, PathumThani, 12120, Thailand

*E-mail address corresponding author: Korakots@mtec.or.th

Keywords: Electrospray coating, Microporous layer, Proton exchange membrane fi cell, Electrode fabrication

The electrospraying technique is a promising method for liquid atomization by mea of electric forces to produce uniformly distributed and dispersed particles in a range nanometers. In this research work, the electrospray conditions were developed a thoroughly investigated in order to produce a well-distributed microstructure of microporous layer (MPL) coated on a gas diffusion layer (GDL). The MPL suspensi was mainly composed of carbon black (Vulcan XC-72R) using 5%wt Nafion soluti and isopropanol as a binder and solvent respectively. Several fabrication variables the electrospray deposition were investigated including an appropriate range of appli voltage to generate a stable cone-jet mode, the working distance between the nee and the GDL substrate in the range of 1.0 - 3.0 cm and the flow rate of MPL suspensi in the range of 0.4 - 0.8 ml/hr with a fixed carbon loading 0.2 mg/cm^2. The particle s distributions and the surface morphology of the as-prepared MPL were characteriz

ENR-O-08

$BaO-Al_2O_3-SiO_2-B_2O_3$ Glass-Ceramic SOFCs Sealant: Effect of ZnO additive

Jiratchaya Ayawanna[a,*], **Nattapol Laorodphan**[b]

[a]*School of Ceramic Engineering, Institute of Engineering, Suranaree University of Technology, Muang, Nakhon Ratchasima, 30000, Thailand*

[b]*Department of Industrial Chemistry and Textile Technology, Faculty of Science, Maejo University, Sansai, Chiang Mai, 50290, Thailand*

* E-mail: jiratchaya@sut.ac.th

Keywords: Crystallization, Glass-ceramic, Planar Solid Oxide Fuel Cells, Sealant

A $BaO-Al_2O_3-SiO_2-B_2O_3$ (BaBS) glass-ceramic sealant for planar solid oxide fuel cells (SOFCs) with ZnO addition was investigated. Glass transition temperature (T_g), dilatometric softening pointing (T_s) and thermal expansion coefficient (TEC) between 100-500°C of the BaBS glass and ZnO additive glass were determined by dilatometry. The BaBS glass-ceramics, both with and without ZnO additive was formed by isothermal devitrification heat treatment at 800 °C for 30 h, which is the intermediate operating temperature range for planar SOFCs. The crystallization behavior of the sealant glasses was analyzed by XRD and SEM-EDX. The effect of nucleation heat treatment at the temperature of 550 and 590 °C for 5 h on the crystallization behavior of both glasses was also investigated. The result showed the decrease in the glass transition temperature (T_g) and the increase in the thermal expansion coefficient in the glass with 10 wt% ZnO addition. According to the X-ray diffraction, ZnO affected the type of the crystal phases in the BaBS glass-ceramics, in which hexacelsian ($BaAl_2Si_2O_8$), barium silicate ($Ba_2Si_3O_8$), barium borate ($Ba_3B_2O_6$), barium zinc silicate ($BaZn(SiO_4)$) were devitrified. The adhesion interfaces between both glass-ceramics and ceramic electrolytes were observed by SEM-EDX. The effect of ZnO addition and nucleation heat treatment on the interfacial phenomena between the BaBS glass-ceramics and electrolytes are also discussed.

ENR-O-09

Investigation of Electronic Conductivity of Co-Doped $LiFePO_4$ Material for Lithium Ion Batteries by Impedance Spectroscopy Technique

Phongsit Krabao[a] , Sarawut Pongha[a], Nonglak Meethong[a,b,*]

[a] *Department of Physics, Faculty of Science, Khon Kaen University, Khon Kaen, 40002, Thailand.*

[b] *Nanotec-KKU Center of Excellence on Advanced Nanomaterials for Energy Production and Storage, Faculty of Science, Khon Kaen University, Khon Kaen, 40002, Thailand.*

*E-mail address: nonmee@kku.ac.th

Keywords: Impedance spectroscopy; Lithium iron phosphate; Electronic conductivity; Lithium ion batteries.

The increasing concerns about energy and environmental issues have now provoked lithium ion batteries to penetrate into the large scale applications such as electric grid system and electric vehicles. One of the key challenges is obtaining cathode material with high energy density, high safety, low cost, environment friendly and long cycle life. Lithium iron phosphate ($LiFePO_4$, LFP) has proved itself to meet these requirements. However, this material shows inherently low electronic conductivity providing low power density. Cation doping is one of the most promising methods in improving conductivity of this material. Here, we study the electronic conductivity of Co-doped LFP samples synthesized by solid state reaction. The phase composition was characterized by X-ray diffraction confirming the single phase of LFP. The unit cell volume of LFP obtained by Rietveld refinement method shows that it decreases with increasing Co contents. The electronic conductivity of the samples was measured as a function of temperature and doping content by Impedance Spectroscopy Technique. The conductivity of LFP sample is dependent on Co doping level.

Acknowledge: PK acknowledges the financial support from the Thailand Research Fund and Human Resource Development in Science Project (Science Achievement Scholarship of Thailand, SAST)

ENR-O-10

Synthesis, Structure, and Ionic Conductivity of Lithium-Strontium Aluminum/Gallium-Tantalum-Oxides with Perovskite Structure

Thanya Phraewphiphat [a,*], **Muhammad Iqbal**[b], **Kota Suzuki**[b], **Masaaki Hirayama**[b], **Ryoji Kanno**[b]

[a]*National Metal and Materials Technology Center, National Science and Technology Development Agency, 114 Thailand Science Park, Phahonyothin Road, Klong Nueng, Klong Luang Pathum Thani, 12120, Thailand*

[b] *Department of Electronic Chemistry, Interdisciplinary Graduate School of Science and Engineering, Tokyo Institute of Technology, 4259 Nagatsuta, Midori, Yokohama 226-8502, Japan*

*thanya.phr@mtec.or.th

Keywords: Lithium Solid Electrolyte, Perovskite, Lithium Ionic Conductor

Lithium ion conductors have attracted much attention for use as solid electrolytes in all-solid-state batteries. Among the solid electrolyte materials proposed, lithium containing oxides are potential candidates due to their high ionic conductivity and chemical stability over a wide range of operation temperature. The ionic conductivities of new lithium-strontium-aluminum/gallium-tantalum oxides with the perovskite structure were investigated in this study. The lithium containing double oxides, Li-Sr-Ta-*M*-O system (*M* = Al, Ga) with the perovskite structure, were synthesized using solid state synthesis method assisted with the ball-milling method. The partial substitution of smaller Ga^{3+} ions for Ta^{5+} ions produced the new compositions, the structures of which were determined from neutron diffraction measurements using the cubic perovskite structure model with *Pm*-3*m* space group. Vacancies were introduced into the Sr(Li) sites by the formation of solid-solutions with compositions $(Li_xSr_{1-x-y}\square_y)(Ga_{[(1-x)/2]-y}Ta_{[(1+x)/2]+y})O_3$, where the composition range of $0 \leq y \leq 0.20$ was examined for $x = 0.2$, 0.25. The ionic conductivity was improved by the introduction of vacancies and the highest conductivity of 1.85×10^{-3} S cm^{-1} at 250 °C was obtained for $(Li_{0.25}Sr_{0.625}\square_{0.125})(Ga_{0.25}Ta_{0.75})O_3$. The higher ionic conduction was achieved by the introduction of vacancies at the *A*-sites.

ENR-O-11

Multi-walled carbon nanotubes (MWCNTs) on a metal substrate with quantum dots in photovoltaics

Junthorn Udorn[a,*], Hayashi Sachio[a], Shengwen Hou[a], Chaoyang Li[a,b], Akimitsu Hatta[a,b], Hiroshi Furuta[a,b]

[a]*Electronic and Photonic Systems Engineering, Kochi University of Technology, Tosayamada-cho, Kami, Kochi 782-0003, Japan*

[b]*Center for Nanotechnology, Research Institute, Kochi University of Technology, Tosayamada-cho, Kami, Kochi 782-0003, Japan*

Corresponding author: Email addresses:178002a@gs.kochi-tech.ac.jp*
Tel:080-4036-4401(Japan),081-653-1025(Thailand)

Keywords: Multi-walled Carbon Nanotubes (MWCNTs), Quantum dots (QDs), quantum dots sensitized solar cells (QDSSCs), Power conversion efficiency (PCE)

Multi-walled carbon nanotube (MWCNT) forests were utilized as an photoanode for efficiency improvement in CdSe/ZnS (core/shell) quantum dots (QDs) sensitized solar cells (QDSSCs). Multiple electron-hole pairs of QDs are expected to enhance the efficiency in QDSSCs. In this study, QD-treated -MWCNTs as a photoanode for solar cells were investigated. A conductive metal substrate was employed to grow vertically-aligned MWCNTs as compared with a higher sheet resistivity of a semiconducting substrate. It was found that QD-treated MWCNTs on a conductive metal substrate with resistance of 0.0047 Ω/sq showed a higher power conversion efficiency (PCE) of 0.0293 % where QD-treated MWCNTs on the semiconducting substrate with resistance of 259 Ω/sq showed a lower efficiency of 0.0156 % under a measurement of AM 1.5 sunlight intensity. The higher electrical conductance should support to reduce series resistance of solar cells and to be an important factor to increase solar cell efficiency. Also, the other factors of MWCNT density and QD quantity will be further investigated and presented in the conference.

ENR-O-13

Synthesis of Novel Ternary Semiconductor-Silver Bismuth Telluride for Solar Cell application

Patamaporn Termsaithong[a], Phuri Kalnaowakul[a] and Aphichart Rodchanarowan[a, b]*

[a]*Department of Materials Engineering,*
[b]*Center of Advanced Studies in Industrial Technology,*
Faculty of Engineering, Kasetsart University,
50 Ngamwongwan Rd., Ladyao, Chatuchak, Bangkok 10900, Thailand
* Corresponding author: fengacrw@ku.ac.th

Keywords: $AgBiTe_2$, chemical bath deposition, solar cells

In this study, the synthesis of the ternary semiconductor sensitized silver bismuth telluride nanoparticles ($AgBiTe_2$: SBT NPs) was produced in the solution of $AgNO_3$, Bi $(NO_3)_3 \cdot 5H_2O$ and $Na_2S \cdot xH_2O$ using a chemical bath deposition (CBD) method and annealed at 200 ^oC for 3 hr. The amorphous and crystalline of SBT NPs phase have been checked using X-ray Diffraction (XRD) pattern were found in the form amorphous structure and field-emission scanning electron microscopy (FESEM) to investigate the chemical composition and morphology of SBT NPs, respectively. Optical properties of SBT NPs were investigated using both the transmittance (%T) and reflectance (%R) measurement. Optical energy gap (E_g) of STB NPs showed in a range of 1.5-2.4 eV. According to these experimental results, the SBT NPs were successfully synthesized and potentially applied for solar cell application.

ENR-O-14

Silica and activated carbon nanocomposite from rice husks for Lithium ion batteries

Yutthanakon Kanaphan[a], Sarawut Pongha[b], Tuksadon Wutikhun[c], Annop Klamchuen[c], Nonglak Meethong[b,d*]

[a]*Materials Science and Nanotechnology Program, Faculty of Science, Khon Kaen University, Khon Kaen, 40002, Thailand.*

[b]*Integrated Nanotechnology Research Center, Department of Physics, Faculty of Science, Khon Kaen University, Khon Kaen, 40002, Thailand.*

[c]*National Nanotechnology Center (NANOTEC), Klong Luang, Pathumthani 12120, Thailand.*

[d]*Nanotec-KKU Center of Excellence on Advanced Nanomaterials for Energy Production and Storage, Faculty of Science, Khon Kaen University, Khon Kaen, 40002, Thailand.*

*E-mail address: nonmee@kku.ac.th

Keywords: Rice husks; Activated carbon; Silica; Anode; Lithium ion batteries.

Lithium ion batteries have been widely used in numerous portable electronic devices, including laptop computers, mobile phones, and now penetrated into large scale application such as electric vehicles. The battery performance depends on the development of cathode and anode materials. Many research efforts have been done to find next generation anode materials with higher capacities. Silica (SiO_2) is a promising candidate due to its high theoretical capacity of 1,000 $mAhg^{-1}$ about 3 times higher than graphite conventional anode. Activated carbon (AC) has high electrical conductivity due to its high surface areas and morphology. Moreover, SiO_2 and AC can be extracted from biomass waste with simple synthesis methods into nanostructured forms, which can provide excellent electrochemical properties. In this work, SiO_2/AC nanocomposites were prepared by calcination under Argon atmosphere at temperatures between 400 and 1,200 °C. The electrochemical properties including specific capacity, rate capability and cycling stability of these samples were measured by galvanostatic cycling. The reversible capacities of the composites are surprisingly high. The reversible capacities of around 1630-1982 $mAhg^{-1}$ at a current rate of C/10 have been obtained. These are even higher than the theoretical value of SiO_2. This finding will be explained based on the studies of functional groups, crystal, and microstructures obtained by FTIR, XRD, SEM and TEM techniques, respectively. Cycling stability of this composite is also very good, though more improvements are being investigated. The capacity fades less than 75% over 100 cycles. Hence, this rice husks derived SiO_2/AC nanocomposites are considered as a promising anode materials for next generation lithium ion battery.

Acknowledgements: YK acknowledges the financial support from Young Scientist and Technologist Programme, NSTDA (YSTP: SCA-CO-2559-2446-TH)

ENR-O-15

Zeolite Supported Bimetallic Catalyst System: The Effect of Metal Loading For Catalytic Pyrolysis of Jatropha Residue

Vituruch Goodwin[a,*], Phanwatsa Amnaphiang[b], Pimpreeya Thungngern[b], Kong Kah Shin[c], Parncheewa Udomsap[a], and Nuwong Chollacoop[a]

[a]National Metal and Materials Technology Center, National Science and Technology Development Agency, 114 Thailand Science Park, Phahonyothin Road, Klong Nueng, Klong Luang Pathum Thani, 12120, Thailand

[b]College of Nanotechnology, King Mongkut's Institute of Technology Ladkrabang, Chalongkrung Road, Ladkrabang, Bangkok 10520, Thailand

[c]Universiti Teknologi Petronas, Bandar Seri Iskandar, 31750, Tronoh, Perak Darul Ridzuan, Malaysia

*viturucg@mtec.or.th

Keywords: Zeolite, Bimetallic Catalyst, Catalytic Pyrolysis, Jatropha

Two transition metals were loaded on H-ZSM-5 zeolite to produce bimetallic zeolite supported catalysts for catalytic pyrolysis reaction. Ni and Co metal was loaded on H-ZSM-5 via wet impregnation method. The loading sequence was applied using one-step and two-step loading method. The bimetallic catalysts were prepared at Ni+Co metal loading content of 10+10 wt% (Ni:Co=1:1) to 10+20 wt% (Ni:Co=1:2 or 2:1). All bimetallic catalysts supported on H-ZSM-5 were calcined and characterized by X-ray Diffraction (XRD) and Temperature Programmed Desorption of ammonia (NH_3-TPD). The XRD patterns of all bimetallic-ZSM-5 catalysts revealed that there is no structural change in the bimetallic-ZSM-5 samples regardless of different metal loading contents and preparation methods. All XRD patterns illustrated peaks characteristic of ZSM-5, cobalt oxide and nickel oxide. The NH_3-TPD results indicates number of acid sites in bimetallic-ZSM-5. The acid sites of ZSM-5 was weakened with transition metal added. The two-step loading of 10+20 wt% metals on ZSM-5 reduced the peak intensities of NH_3 desorption due to the metal particles aggregate on acid sites of ZSM-5. The two-step 10+20 wt% bimetallic catalysts has the lowest surface acidity, followed by the one-step 10+20 wt%, the two-step 10+10 wt% and the one-step 10+10 wt% bimetallic catalysts, respectively. Jatropha residue was used for catalytic pyrolysis study. The jatropha residue and bimetallic catalyst was pyrolyzed at 500 °C in a pyrolysis-gas chromatography/mass spectrometry (Py-GCMS). The product vapor was analyzed by GCMS for the different groups of organic products such as fatty acid, aldehydes, ketones, aliphatic hydrocarbons, aromatic hydrocarbons and nitrogen compounds. The product from catalytic pyrolysis of jatropha residue with bimetallic zeolite supported catalyst enhance deoxygenation reaction that resulted in high aliphatic and aromatic hydrocarbons product. The one-step loading at ratio Ni:Co = 1:1 (10+10 wt%) given highest hydrocarbons product yield at 57.81%.

ENR-O-16

Two Stage Combustion Burner Using Used Engine Oil as Fuel

Taveesin Lekpradit, Apinunt Namkhat*
Department of Mechanical Engineering, Ubon Ratchathani University,
Warin Chamrap, Ubon Ratchathani, 34190, Thailand
*enapinna@ubu.ac.th

Keywords: Used engine oil, Combustion, Temperature profile, Burner

Nowadays, an increase in numbers of automotive results in the large amount of used-engine oil, which is a waste and has a tremendous effect on the environment. The used-engine oil, however has a relatively high calorific value so that it is interesting to be used this waste as a renewable fuel for heat generation. The present experimental study on used-engine oil combustion in a vertical tube burner therefore had been conducted. The two stage combustion was divided by the air supply to the burner into two levels and the air flow rate of both levels can be adjusted.The fuel in the first stage was heated and vaporized by the incompletes combustion. The exhaust gases and residual fuel vapor from the first stage were then flow to the second combustion stage and the complete combustion was achieved. The combustion temperatures along the length of the burner in both of the single and the two stage combustion had been measured and compared. The amount of exhaust gases at the exit of the burner was also monitored. The experimental results revealed that the temperature profile along the length of the burner in the combustion zone of two stage were higher than those in the single stage as a result of a better mixing of air and fuel. In addition, it also found that an increase in a distance of air supply location between two levels resulted in an increase of the emission.

ENR-O-17

Copper Doped Zinc Oxide: A Promising Material for Biogas Desulfurization

Kannasoot Kanokkanchana[a,*], **Sumittra Charojrochkul**[b], **Waret Veerasai**[a]

[a]*Department of Chemistry, Faculty of Science, Mahidol University, Bangkok, 10400, Thailand*

[b]*National Metal and Materials Technology Center, Pathum Thani, 12120, Thailand*

*kannasoot.kan@mahidol.ac.th

Keywords: Biogas, Desulfurization, Zinc oxide, Hydrogen sulfide

Biogas is a promising renewable energy resource with a high potential to substitute natural gas, which is currently used as CNG/NGV for vehicles. Unfortunately, purification of biogas is challenging by tight restriction of sulfur compounds in fuels and requirement of low temperature desulfurization sorbent. This work has demonstrated a potential of copper doped zinc oxide as a deep desulfurization sorbent material for biogas purification at low temperature (50-200°C). The copper doped zinc oxide with different dopant concentration of 0, 3, 6 and 9 mol.% were synthesized using a facile and cost-effective solution combustion synthesis method. Physico-chemical characterizations revealed successful formation of copper doped zinc oxide solid solution with nano-spherical morphology. The desulfurization performances of the sorbent materials were measured in a fix-bed reactor coupled with a gas chromatograph using 1.005 mol.% H_2S/N_2 at 50, 100, 150 and 200°C. The desulfurization at 50°C indicated a strong correlation between breakthrough capacities and surface areas without any effect of dopant. Contradictorily, the desulfurization at 100-200°C revealed a great role of copper dopant in a breakthrough capacity improvement. The highest breakthrough capacity was achieved using 6 mol.% copper doped zinc oxide sorbent at 200°C, yielding 282.7 mgS/g. It was 3.5 times higher than Alfa Aesar® Hifuel™ A310 desulfurization sorbent based on high surface area zinc oxide tested at the same condition.

ENR-O-18

Porous carbon-doped TiO_2 on TiC nanostructures for co-catalyst free photocatalytic hydrogen production under visible light

Chengwu Yang[a], Xinyu Zhang[a]*, Jiaqian Qin[b]*, and Riping Liu[a]

[a]*State Key Laboratory of Metastable Materials Science and Technology, Yanshan University, Qinhuangdao 066004, P. R. China*

[b]*Metallurgy and Materials Science Research Institute, Chulalongkorn University, Bangkok 10330, Thailand*

E-mail address: jiaqian.q@chula.ac.th, xyzhang@ysu.edu.cn.

Keywords: core-shell nanostructure, TiC@C-TiO_2, photocatalytic hydrogen production, water splitting

Titanium dioxide (TiO_2) as a photocatalyst material has been widely investigated because of its stabilization and hypotoxicity. However, photocatalytic activity of TiO_2 is suppressed by the large band gap and the high recombination rate of charge carrier, which leads to a confined application. Moreover, how to improve the photocatalytic H_2 production without any co-catalyst also remains a big challenge. Here, we report a conceptual strategy in a core-shell nanostructure to simultaneously reduce band gap and charge carrier recombination rate by introducing carbon-doped porous TiO_2 layer on metallic TiC nanostructure using a facile in situ thermal growth method. TiC@C-TiO_2 core-shell nanostructure materials have a higher photocatalytic activity compared with pure P25 and the carbon-doped TiO_2, which result from the enhanced visible light absorption, drastic charge transfer and the large surface area. Notably, the novel core-shell nanostructures still exhibit an excellent photocatalytic H_2 production without Pt co-catalyst. The results demonstrate that TiC is an ideal support for TiO_2 photocatalyst, and this novel core-shell nanostructure can significant shift the position of the band edge of the obtained material. This study presents a design principle for photocatalytic materials towards the highly efficient visible light photocatalysts.

ENR-P-01

The Study of Carbon Nanotubes as Conductive Additive of $Ca_3Co_4O_9$ Anode for Lithium-ion Battery

Natkrita Prasoetsopha[a*], Supree Pinitsoontorn[b,c], Shufen Fan[d], Huey Hoon Hng[d], Santi Maensiri[e]

[a] Department of Materials Engineering, Faculty of Engineering and Architecture, Rajamangala University of Technology Isan, Nakhon Ratchasima, 30000, Thailand
[b] Integrated Nanotechnology Research Center, Department of Physics, Faculty of Science, Khon Kaen University, Khon Kaen, 40002, Thailand
[c] Nanotec-KKU Center of Excellence on Advanced Nanomaterials for Energy Production and Storage, Khon Kaen University, Khon Kaen, 40002, Thailand
[d] School of Materials Science and Engineering, Nanyang Technological University, Singapore, 639798, Singapore
[e] School of Physics, Institute of Science, Suranaree University of Technology, Nakhon Ratchasima, 30000, Thailand

*E-mail address: natkrita.pr@rmuti.ac.th

Keywords: $Ca_3Co_4O_9$, Anode, Lithium-ion battery, Carbon nanotubes

Misfit-layered $Ca_3Co_4O_9$, as anode material for lithium-ion battery, was synthesized by a hydro-decomposition method and investigated the electrochemical properties. $Ca_3Co_4O_9$ sample was characterized using X-ray diffraction, scanning electron microscopy, energy dispersive X-ray spectroscopy and proton-induced X-ray emission techniques. $Ca_3Co_4O_9$ sample does not show any impurity phase. The average particle size of 1-2 μm was observed in the plate-like particle shape. The composition ratio of sample is closed to the nominal composition. To investigate the electrochemical properties, the $Ca_3Co_4O_9$, carbon nanotube (CNT) and polyvinylidene fluoride (PVDF) were used as active mass, conductive material, and binder, respectively. The CNT was used due to its shape and high conductivity. The electrochemical performances were evaluated by galvanostatic cycling and cyclic voltammetry. After charge/discharge, it was found that the specific capacity of $Ca_3Co_4O_9$ sample increases with increasing cycle number. The highest specific capacity of 649 $mAh \cdot g^{-1}$ was obtained in the 50^{th} cycles. The coulombic efficiency was higher 99%, indicating a high ratio of delithiation/lithiation.

ENR-P-02

Microwave-Assisted Preparation of Sodium Silicate Used Rice Husk Ash as Precursor and Applications for Biodiesel Catalyst

Jaturon Kumchompoo[a], **Wasinee Wongwai**[b], **Ratchadaporn Puntharod**[a,b*]
[a]*Department of Chemistry, Faculty of Science, Mae Jo University, Chiang Mai, 50290, Thailand*
[b]*Nanoscience and Nanotechnology Laboratory, Mae Jo University, Chiang Mai, 50290, Thailand*
*ratchadaporn_p@mju.ac.th

Keywords: Microwave-assisted, Sodium silicate, Biodiesel catalyst

Sodium silicate has been reported as heterogeneous catalyst in biodiesel production. Due to it is a solid base material and not combination with reaction medium. In order to save time, energy and cost, rice husk ash is cheap precursor of silica and microwave-assisted method is used for preparation of sodium silicate. In this research, sodium silicate **(**Na_2SiO_3**)** was prepared by rice husk ash reacted with 10 M sodium hydroxide. The mixtures were heated by microwave at 400, 600, and 800 watt for 5 and 10 minutes. The formation of sodium silicate was characterized by Fourier transform infrared spectrophotometer. The vibrations of (Na)O–Si–O(Na) and Si–O–Si were observed at 597-592 and 1350-1000 cm^{-1}, respectively, except at 800 watt disappeared those vibrations. The results of atomic absorption spectrophotometer provided the mole ratio of sodium and silicon was 2:1 as heating the product at 600 watt for 5 and 10 minutes. The phase of sodium silicate was characterized by X-ray diffraction. The X-ray pattern was an agreement with JCPDS No. 00-001-0836. Sodium silicate could be synthesized from rice husk ash by microwave-assisted. It also could be used as catalyst as in biodiesel production from palm oil. The percentage of yield was 81 by volume.

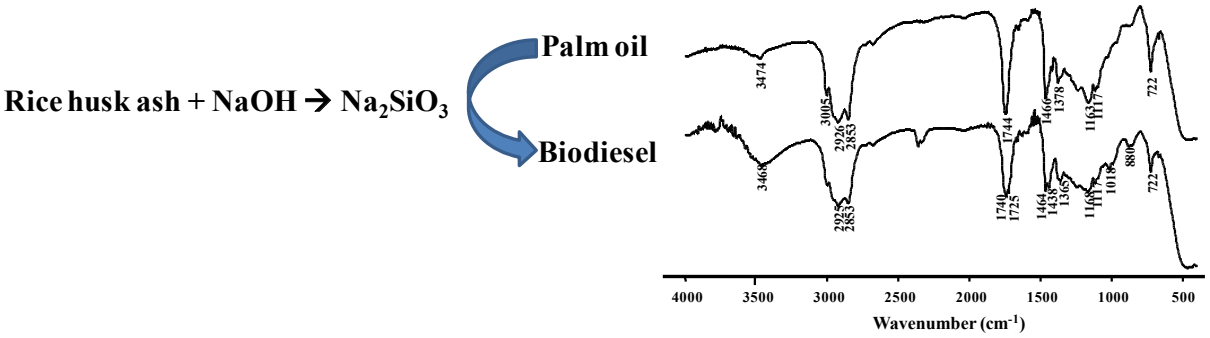

ENR-P-03

Pelletization of Iron Oxide Based Sorbents for Hydrogen Sulfide Removal

Pathompong Janetaisong[a], Viset Lailuck[b], Somsak Supasitmongkol[c,*]
[a,b,c]*National Metal and Materials Technology Center, Pathumthani, 12120, Thailand*
*somsaks@mtec.or.th

Keywords: Iron oxide, Hydrogen Sulfide, Desulfurization, Pelletization

Biogas derived from anaerobic digestion of biological wastes has been extensively used for heating purposes and/or electricity generation. Presence of hydrogen sulfide (H_2S) in biogas has a toxic and corrosive to most equipment such as piping, boilers and power-generating machine. Reducing H_2S content needs to be considered in practical application before utilizing biogas. Among the possible processes to remove H_2S, adsorptive separation is very appealing due to being an economical and effective method involving the use of iron oxide based sorbents. However, these powder sorbents are usually not suitable for use in large-scale gas separation processes due to an increased pressure drop and mass transfer resistance within fixed-bed adsorption columns. In this work, H_2S capture in two iron oxides (ferric oxide (Fe_2O_3) and magnetite (Fe_3O_4)) was experimentally investigated to determine technical feasibility of shaping pellets based on active iron oxide sorbent in removing H_2S from a simulated gas stream (0.35 vol.% H_2S balanced in N_2). Many factors affecting the behavior of gas adsorption such as gas in-flow rate, adsorption temperature, binder loadings and textural characteristics were considered. The pellet strengths were also undertaken using a bulk crushing strength analyzer. The results indicated that higher temperature favors the diffusion of H_2S molecules from the surface into the bulk of iron oxides. At the same temperature, H_2S-sorption capacity of Fe_3O_4 sorbent was higher than that of Fe_2O_3 sorbent, corresponding with the pore volume and surface area of the sorbents. The Fe_3O_4–extruded pellets produced with starch binder (16.67 wt. %) showed better potential in H_2S uptake and material strength when compared to that of other addition of starch levels. Enhancing gas flow rate resulted in reducing mass-transfer resistance of H_2S, leading to an increased gas adsorption in the sorbents. By contrast, an excess of gas flow rate caused a decrease of gas-solid contact time with respect to reduced adsorption performance. The adsorbed H_2S gas can be readily desorbed from the pellets with the desorption temperature below 60^oC and the H_2S-sorption capacity was

ENR-P-04

Multifunctional Magnetic Nanoparticle for Microaglal Biodiesel Production

Kyubock Lee[a,*], Jung Yoon Seo[b], You-Kwan Oh[c]
[a]*Chungnam National University, Daejeon, 34134 Republic of Korea*
[b]*National Nanofab Center, Daejeon, 34141 Republic of Korea*
[c]*Korea Insitute of Energy Research, Daejeon, 34129 Republic of Korea*

*kyubock.lee@cnu.ac.kr

Keywords: magnetic, nanoparticle, microalgae, separation

Separation of microalgae from culture medium is an energy demanding process which covers 20~30% of total cost of microalgal biodiesel production. The dilute dispersion along with their small size of a few micrometers and electronegative surface imposes difficulties during separation. The widely used techniques to separate microalgae include centrifugation, filtration, ultrasound electrolysis-base technologies. However, these methods demand high energy, which is not desirable for low cost production of microalgal biodiesel. Although usage of chemical flocculants was thought to be an efficient separation method, it results in contaminations both in the harvested biomass and in the culture which could not be reused for further cultivation. In this presentation, we introduce magnetic flocculants, namely magnetic particles functionalized with the positively charged compounds, which lead to flocculation of microalgae through an electrostatic interaction and could be separated from the culture medium by using external magnetic field. The separation efficiency is as high as 99% within few minutes without raising contamination issue and furthermore that the culture medium and the magnetic flocculants could be reused for subsequent microalgal culture and separation, respectively. Multi-functionalization of magnetic nanoparticles will be proposed as a way of simplifying multiple downstream processes of microalgae-based biorefinement.

ENR-P-05

One-pot Synthesis of $LiFePO_4$ Nano-particles Entrapped in Mesoporous Melamine-Formaldehyde Matrix as the Promising Cathode Materials for the Next Generation Lithium Ion Batteries

Kantawich Jittmonkong[a], Supacharee Roddecha[a,*], Thanapat Chaipitisiri[a], Nattawat Sritubtim[a], Paisan Kongkachuichay[a], Malinee Sriariyanun[b]

[a]*Department of Chemical Engineering, Faculty of Engineering, Kasetsart University, 50 Ngam Wong Wan Rd. Ladyao, Chatuchak, Bangkok 10900, Thailand*

[b]*Mechanical and Process Engineering, Thai-German Graduate School of Engineering, King Mongkut's University of Technology, North Bangkok, Bangkok 10800, Thailand*

* Corresponding author: fengsrro@ku.ac.th

Keywords: Cathode material, Lithium iron phosphate, Nitrogen-containing carbon material, Melamine-formaldehyde carbon precursor.

Electric vehicles (EVs) draw considerable attention due to the pressure from expensive oil price and environmental issue. Their operation requires high-performance energy storage devices with both high energy and power density. Currently, Lithium Ion Batteries (LIBs) are realized as a state-of-the-art technology providing high energy density, though, they usually exhibit low power density resulting from kinetic problem of electrode materials, especially cathode materials. To develop their power density, the electrode materials must possess high ionic and electronic conductivity. Recently, lithium iron phosphate ($LiFePO_4$), with its olivine structure, has been studied as the potential cathode material for large scale LIBs due to its relatively high theoretical capacity, high stability, environmental benignity, and low cost. However, the main challenge limiting its practical use is the sluggish charge transport. Thus, this work presents a facile approach to enhance charge conductivity of $LiFePO_4$ by coating $LiFePO_4$ nano-particle with a porous carbon matrix material, which contains nitrogen functional groups. The composite of $LiFePO_4$ nano-particles dispersed in a porous N-containing carbon matrix were prepared by a practical one-pot synthesis combining with solvent evaporation. Nitrogen-riched melamine-formaldehyde resin was selected as the nitrogen-containing carbon precursor, while the triblock copolymer Pluronic F127 facilitated as the porous templating agent. As evidenced by X-ray diffraction analysis, the affordable Fe^{3+} starting iron precursor could be reduced to Fe^{2+} to form the targeted $LiFePO_4$ nano-composite product. The 100 nm sized $LiFePO_4$ nano-particles embedded in the porous carbon matrix were investigated by scanned and transmission electron microscopy. Morphology investigation revealed that the amount of Pluronic F127 impact the porosity and specific surface area of the composite product. A thermal stability study demonstrated that the melamine-formaldehyde based carbon coating could tolerate the carbonization temperature up to 600 °C. The preliminary electrochemical performance showed a promising reversible capacity of about 100 $mAh.g^{-1}$.

ENR-P-06

Large Area Fabrication of Stress-induced Lift-off Silicon Foil Using Epoxy

Young Joon Cho[a], Hyo Sik Chang[a,*]
[a]*Chungnam National University, Daejeon, 34134, South Korea*
*E-mail: hschang@cnu.ac.kr

Keywords: Provide a maximum of four keywords. Each keyword should be accompanied by the capital letter denoting the category from which the keyword has been selected.

We investigate a large area (5cm x 5cm) epoxy-induced lift-off of a (100) silicon wafer. This epoxy-induced spalling process has the advantages of reducing metal contamination and lowers the operating temperatures below 100 ℃. The low temperature involved in the proposed process reduce the diffusion of metal species inside the silicon bulk, improving the quality of the silicon foil as compared to the high temperature spalling of silicon. After stress-induced lift-off process, silicon foils have been produced. The thickness of the silicon foil is between 30μm and 100μm. The surface morphology and thickness of Si foil depend on the thickness and hardening of polymer. We fabricated stand-alone Si foil by removing the epoxy layer.

We measured carrier lifetime of Si foil using quasi-steady-state photoconductance (QSSPC) to evaluate a thin Si substrate.

ENR-P-07

Influence of Bi_2O_3 on Crystalline Phase Content and Thermal Properties of Åkermanite and Diopside based Glass-ceramic Sealant for SOFCs

Pornchanok Lawita[a], Apirat Theerapapvisetpong[a,b], Sirithan Jiemsirilers[a,b,*]
[a]*Research Unit of Advanced Ceramics, Department of Materials Science, Faculty of Science, Chulalongkorn University, Bangkok, 10330 Thailand*
[b]*Center of excellence on Petrochemical and Materials Technology, Chulalongkorn University, Bangkok, 10330 Thailand*
*sirithan.j@chula.ac.th

Keywords: SOFC, Sealant, Glass-ceramics, Barium-free

Solid oxide fuel cell (SOFC) is an electrochemical energy conversion device which is considered as clean energy source generator with reliability and relatively inexpensive production cost. One of the most important components for planar design SOFC is the hermetic seal that prevents fuel from leaking out of between the stack of fuel cells. Glass-ceramics are attractive materials as sealing materials for this device. The expected coefficient of thermal expansion (CTE) of the glass-ceramic sealants should be between 9 and 13 x 10^{-6} K^{-1}. Glass – ceramics based on åkermanite ($Ca_2MgSi_2O_7$) crystalline phase were reported their high CTE value from about 10 to 11.3 x 10^{-6} K^{-1}. In this study, glass compositions in the CaO-MgO-B_2O_3-Al_2O_3-SiO_2 system with varying amounts of Bi_2O_3 from 0 to 10 wt.% were prepared by conventional melting and investigated their properties. The selected compositions were derived from ternary åkermanite–forsterite–anorthite phase diagram. Phase composition and quantitative phase analysis of glass–ceramics were examined by X-ray diffractometer. The onset of crystallization (T_x) and crystallization temperature (T_c) were measured by DTA. The thermal properties of bulk glass samples and heat treated samples at 900 ºC for 2 h which were glass transition temperature (T_g), dilatometric softening temperature (T_s), and coefficient of thermal expansion (CTE) were determined by dilatometer. Furthermore, the long-term stability of their CTE was investigated. The samples were continued to soak at 800 ˚C for 100 h and observed their change in CTE value. The results found that the åkermanite phase tended to increase with increasing amount of Bi_2O_3 content.

ENR-P-08

The Study of Crystallization of Polyfluorene and Fullerene Derivatives in Semiconducting Layer of Organic Solar Cells

Wantana Koetniyom[a,b*], Anusit Keawprajak[c], Kanpitcha Jiramitmongkon[c], Udom Asawapirom[c]

[a]Department of Industrial Physics and Medical Instrumentation, Faculty of Applied Science, King Mongkut's University of Technology North Bangkok, Bangkok 10800, Thailand

[b]Lasers and Optics Research Center (LANDOS), King Mongkut's University of Technology North Bangkok, Bangkok 10800, Thailand

[c]National Nanotechnology Center, NSTDA, 111 Thailand Science Park, Phahonyothin Rd, Klong 1 Klong Luang, Pathumthani, 12120, Thailand

*E-mail address corresponding author : nu_ying19@yahoo.com

Keywords: Morphology, Organic solar cells, Semiconducting layer, Additive

This research was focused on the effect of solid additive namely 1,4-dichlorobenzene (PDCB) in the 1:2 (w/w) active layer of benzothiadiazole/thiophene-based copolymers (PFTBzTT) to [6,6]-phenyl-C61 butyric acid methyl ester (PCBM) on the morphology and performance of bulk heterojunction (BHJ) organic solar cells. The active layers were deposited by spin-coating from solutions using chloroform, with different additive concentrations from 0-52 mg/ml. The inclusion of additive into the polymer solution was able to improve the performance of BHJ solar cells. The maximum power conversion efficiency (PCE) of 0.84% achieved for a cell with PDCB concentration of 36 mg/ml after annealing at 180 °C for 20 min. The XRD and TEM techniques used to analyst the crystal structure and morphology of the thin films. From these results were found that PDCB additive presented higher level of PCBM crystal structure by more aggregation of PCBM and a larger extent of phase separation than those of the films without additive.

ENR-P-09

Effect of Clays on Pyrolysis of Jatropha Cake

Chanapha Tankasem[a], Yatika Somrang[b,*]

[a]Department of Chemical Engineering, Faculty of Engineering, King Mongkut's University of Technology Thonburi, Bangkok, 10140, Thailand
[b]National Metal and Materials Technology Center, Pathumthani, 12120, Thailand
*yatikas@mtec.or.th

Keywords: Jatropha cake, Pyrolysis, Clays

Due to the presence of nitrogen element and residual oil in Jatropha cake from extraction process, crude bio-oil derived from pyrolysis inevitably contains nitrogen-containing compounds and fatty acids. The crude bio-oil, in general, has to be further upgraded to remove heteroatoms so that its properties are suitable as a substituent to conventional petroleum-based oils. Catalysts used in refinery processes, such as hydrodeoxygenation or hydrodenitrogenation, have been widely employed to upgrade the crude bio-oil or to co-process the bio-oil with the conventional oils. However, because of the relatively high content of nitrogen and oxygen in the bio-oil, the catalyst performance diminishes by catalyst poisoning or coking. This work, thus, aimed to preliminarily investigate whether naturally-found materials could be employed to reduce these heteroatoms in the bio-oil prior to upgrading or co-processing it with the conventional oils in the existing refinery facilities. Five naturally-found clays have been selected: kaolin, sepiolite, montmorillonite, halloysite and bentonite. Pyrolysis - gas chromatography - mass spectrometry (Py-GC/MS) was used as a tool to pyrolyse the Jatropha cake and characterise the evolving volatiles from pyrolysis. Results showed that in accordance with the reduction of fatty acids, new nitrogen-containing compounds were present instead. These new nitrogen-containing compounds were derived from fatty acids, e.g. oleanitrile from oleic acid. In addition, in terms of hydrocarbon yields, it has been found that hydrocarbons content has improved with the presence of clays, i.e. from 11.70% to 25.31% with montmorillonite at 500 C. Of all clays, montmorillonite exhibits the best activity. In conclusion, in terms of heteroatom removal, it appears these five clays do not lessen nitrogen element significantly; nonetheless, hydrocarbon yield can be improved to some extent.

.

.

ENR-P-10

The effect of calcium-based salt on hydrothermal carbonization of corncob

Promporn Reangchim[a], Kamonwat Nakason[b], Nawin Viriya-empikul[c] and Apiluck Eiad-ua[a,*]

[a] *College of Nanotechnology, King Mongkut's Institute of Technology Ladkrabang, Bangkok, 10520 Thailand*

[b] *Department of sanitary engineering, Faculty of Public Health, Mahidol University, 420/1, Ratchawithi RD., Ratchathewi, Bangkok, 10400, Thailand*

[c] *The Thailand Research Fund (TRF), Phaholyothin Road, Samsan Nai, Phyathai, Bangkok 10400, Thailand*

*E-mail : apiluck.ei@kmitl.ac.th

Keywords: Calcium-based salts; Hydrothermal-carbonization; Corncob; Hydrochar

Corncob represents a great potential as a raw material for the production of high-value added chemicals, fuels and other industrial products. Thus, corncob is suitable residue for study molecular structure through the pretreatment method. In this study, the effect of calcium-based salts on the hydrothermal carbonization (HTC) of corncob were studied at 160, 180, and 200 °C for 2 h. $CaSO_4$ and $Ca_3(PO_4)_2$ were used as a reaction medium. Hydrochar was characterized by Scanning Electron Microscopy (SEM), X-ray Diffraction (XRD) and ATR-Fourier transform infrared spectroscopy (ATR-FTIR). Characteristics of the hydrochar varied with calcium-based salt. Cellulose crystallinity in hydrochar decreased dramatically and carbon content in hydrochar obviously increased when $Ca_3(PO_4)_2$ and $CaSO_4$ were added, respectively. In case of hydrothermal at 180^oC with $Ca_3(PO_4)_2$ and $CaSO_4$, the carbon microsphere was occurred.

ENR-P-11

Process Optimization and Characterization of YSZ Thin Film Electrolyte on Anode Substrate Prepared by Electrophoretic Deposition Technique

Malinee Meepho[a*], Nutthita Chuankrerkkul[a], Sirima Chauoon [b], Rojana Pornprasertsuk[b]

[a]*Metallurgy and Materials Science Research Institute (MMRI), Chulalongkorn University, Bangkok 10330, Thailand.*

[b]*Research Unit of Advanced Ceramics, Department of Materials Science, Faculty of Science, Chulalongkorn University, Bangkok 10330, Thailand.*

*E-mail address : Malinee.M@chula.ac.th

Keywords: Electrophoretic deposition, 8YSZ electrolyte, Anode-supported SOFC.

In this work, the porous NiO-8YSZ substrates were prepared by powder injection molding (PIM) technique. The 8 mol% yttria stabilized zirconia (8YSZ) electrolyte was formed on the anode substrate using electrophoretic deposition technique (EPD). The suspensions containing 8YSZ nanoparticles were dispersed in ethanol by using different contents of PEG as a dispersant (1-19 wt%). The optimization of PEG was obtained at 5wt% which considered from the maximum zeta potential value. Then 8YSZ suspension was deposited on the anode substrate at a constant voltage of 30 V. Effect of co-sintering temperature was investigated in order to obtain dense electrolyte film. Thin and dense electrolyte film was obtained after co-sintering at 1250^{o}C for 1 h with thickness of 6.35 μm. Result from open circuit voltage of the fabricated cell at 800^{o}C was obtained at 1.09 V. It could be confirmed that the sintered film exhibited gas-tight which could be sufficient for technical application.

ENR-P-12

r-GO/MWCNTs nanocomposite film as electrode material for supercapacitor

Suttinart Noothongkaew[a*] and Pattanasuk Chamninok[b]

[a]Department of Physics, Faculty of Science, Ubon Ratchathani University, Ubon Ratchathani 34190, Thailand

[b]Faculty of Science Ubon Ratchathani Rajabhat University 34000, Thailand

*suttinart_n@yahoo.com

Keywords: Graphene Oxide, reduced Graphene Oxide, Thermal annealing, Supercapacitor.

Abstract. We synthesize reduced graphene oxide (r-GO), multiwall carbon, nanotube (MWCNTs), nanocomposite, film via layer by layer (LBL) assembly. This structure is prepared by vacuum filtration and heat-treated at low temperatures of 500°C. The morphology of sample was determined by field emission electron spectroscopy (FE-SEM). The structural detail and the chemical analysis were characterized by using X-ray diffraction (XRD) and X-ray photoelectron spectroscopy (XPS), respectively. The cyclic voltammetry (CV) curve of r-GO/MWCNTs nanocomposite appeared nearly rectangular in shape. The current density (A/g) was gradually increased by increasing the scan rate of the voltage, exceeding a high scan rate of 500 mVs^{-1}. The specific capacitance of the nanocomposite estimated by galvanostatic (GA) charge/discharge measurement is 150 Fg^{-1} at a current density of 10mAg^{-1}. These nanocomposites can be improved for supercapacitor electrodes.

ENR-P-13

Characterisation of NiO-YSZ Porous Anode-Supported for Solid Oxide Fuel Cells Fabricated by Powder Injection Moulding

Nutthita Chuankrerkkul[a,*], Sirima Chauoon[b,c], Malinee Meepho[a], Rojana Pornprasertsuk[b,c]

[a]Metallurgy and Materials Science Research Institute, Chulalongkorn University, Phyathai Road, Pathumwan, Bangkok 10330 Thailand
[b]Research Unit of Advanced Ceramics, Department of Materials Science, Faculty of Science, Chulalongkorn University, Bangkok 10330, Thailand
[c]Center of Excellence on Petrochemical and Materials Technology, Chulalongkorn University, Bangkok 10330, Thailand
*corresponding author: nutthita.c@chula.ac.th

Keywords: ceramic injection moulding, solid oxide fuel cell, porous anode, polyethylene glycol

Powder injection moulding (PIM) has advantages for a cost effective fabrication of large-scale, near-net-shape products. In this work, PIM is carried out to prepare porous anode-supported for solid oxide fuel cells (SOFC) applications. The PIM process started with a preparation of feedstocks by mixing powder with binder. The feedstock is then injected into the mould of desired shapes. The mouldings were subsequently undergo the removal of the binder (debinding) and, finally, sintering. It is shown that porous nickel oxide-yttria stabilized zirconia (NiO-YSZ) anode-supported for SOFC were successfully prepared by PIM technique. In addition, a water-soluble based binder system, consisted mainly of polyethylene glycol (PEG), has been used in this work. This is to avoid the use of organic solvents when wax-based binder was used. Therefore, it can promote more environmentally friendly process. The removal of binder was carried out using water debinding technique. The porous anode for SOFC was subjected to systematic characterisation. The effect of processing parameters, such as powder characteristics and powder/binder ratio has been investigated. Rate of binder removal was also studied. The porous anode specimens were characterised for their properties and microstructure. It was also found that adjusting the sintering temperatures and holding times can controlled the porosity of the specimens.

ENR-P-14

Synthesis of Calcium Titanate by Hydrothermal Method and Modification for Biodiesel Catalyst

Phinnapha Khathippathi[a], Ratchadaporn Puntharod[a,b*]
[a]*Department of Chemistry, Faculty of Science, Mae Jo University, Chiang Mai, 50290, Thailand*
[b]*Nanoscience and Nanotechnology Laboratory, Mae Jo University, Chiang Mai, 50290, Thailand*
*ratchadaporn_p@mju.ac.th

Keywords: Calcium titanate, Hydrothermal method, Biodiesel catalyst

The conventional method to prepare calcium oxide-titanium dioxide is solid state reaction which provides heterogeneous product. While hydrothermal method is homogeneous precipitation. In this work, calcium titanate was synthesized from precursors as calcium carbonate and titanium dioxide by hydrothermal method at 120, 150 and 180 ºC for 24 hours in base conditions. The result was white powder obtained at pH 13 and heated at 180 ºC for 24 hours. The Fourier transform infrared spectrum displayed the bands at 576 and 418 cm^{-1} which assigned to the vibration of Ca–O of calcium titanate and Ti–O of titanate, respectively. X-ray diffractometry results provided the phase of products was calcium titanate (JCPDS files No. 00-042-0423). Scanning electron microscope showed the morphology of calcium titanate was cube-like cage. To improve activity of calcium titanate for application as biodiesel catalyst, it was modified by impregnated in potassium hydroxide in mole ratio of 1:1. The yield of biodiesel over KOH/calcium titanate and calcium titanate was 75 and 70 % by volumn, respectively.

ENR-P-15

Multiwalled Carbon Nanotubes/Cobalt Hydroxide on Polyester Woven Philippine Indigenous Fibers for Supercapacitor Electrode Materials

Stephanie L. Chua[a*] and Christina A. Binag[b,c]
[a]Department of Biochemistry, Faculty of Pharmacy, [b]Department of Chemistry, College of Science, [c]Research Center for the Natural and Applied Sciences, University of Santo Tomas, Manila 1015 Philippines
Corresponding author: stephanie.chua@ust.edu.ph

Keywords: multiwalled carbon nanotube, supercapacitor electrodes, conductive polyester/natural textile, cobalt hydroxides

Supercapacitors are promising energy storage systems particularly due to their low cost, ease of operation, and fast charge/discharge rates. Recent developments of supercapacitor research have delved into incorporating electroactive materials onto fabrics such as cotton, nylon, polyester, etc. to produce flexible, stretchable, and wearable electronics. This study focuses on the preparation of polyester/natural fiber supported multiwalled carbon nanotube/cobalt hydroxide (MWCNT/Co) composites and looks into its application as a supercapacitor electrode material.

MWCNT/Co was prepared by the coprecipitation method and subsequently dispersed in sodium dodecyl sulfate to produce CNT inks. Fabrics composed of polyester woven with Philippine indigenous fibers piña (PPWF) and water hyacinth (WHPWF) were used as base support for the dip coating of the active materials. The MWCNT/Co composites have good conductivities of 0.0333 S/cm and 0.0324 S/cm when deposited on PPWF and WHPWF, respectively. Surface studies reveal the coating of MWCNTs onto the fabrics and the globular aggregated microstructures of cobalt hydroxides, with preferential adhesion to the polyester woven water hyacinth fabric. Further work has been initiated towards the improvement of the areal capacitances of the materials as initial results for MWCNT/Co/PPWF and MWCNT/Co/WHPWF reveal areal capacitances of 0.75 mF/cm^2 and 0.99 mF/cm^2, respectively.

Acknowledgement. This work is supported by the Philippine Council for Industry, Energy, and Emerging Technology Research and Development of the Department of Science and Technology (PCIEERD-DOST).

ENR-P-17

Investigating the impact of double-anodization on the performance of Titania nanotubes in dye-sensitized solar cells

Buagun Samran[a,*], Emmanuel Nyambod Timah[a], Somkuan Photharin[b] and Udom Tipparach[c]

[a]*Division of Physics, Faculty of Science, Nakhon Phanom University, Muang District, Nakhon Phanom, 48000, Thailand*

[b]*Faculty of Science and Engineering, Kasetsart University Chalermphrakiat Sakonnakhon Province Campus, Muang District, Sakon Nakhon, 47000, Thailand*

[c]*Department of Physics, Faculty of Science, Ubon Ratchathani University, Warinchamrab District, Ubon Ratchathani, 34190, Thailand*

* buagun@hotmail.com

Keywords: dye-sensitized solar cell, double-anodization, titania nanotube

In this research we have synthesized titania nanotubes on titanium metal substrate by DC anodization at 50 V. The anodization was done in an ethylene glycol, ammonium fluoride and deionized water electrolyte for 3 hours. Annealing was carried out at 450 ^{o}C for 2 hours. The dye-sensitized solar cells (DSSCs) were assembled by sandwiching an N719-dye coated titania nanotubes in between two transparent conducting oxide glass plates. Each sample was analysed by XRD, SEM and I-V characteristic curve. We investigated the impact of double and single anodization and annealing on the performance of the titania nanotubes in the DSSCs. The results were compared to as anodized. Our findings indicates that anodizing and annealingtwice greatly reduces the performance of the nanotubes by almost 55%. On the other hand, anodizingand annealing onceenhances the performance of the solar cells by about 72 %.

Materials Technology for Environment

ENV-I-01

Design of Metal Oxide Nanostructured Materials for Enhanced Photocatalytic Energy & Environmental Sustainability

Ghim Wei Ho
Engineering Science Programme, National University of Singapore, 9 Engineering Drive 1, 117576, Singapore
Department of Electrical and Computer Engineering, National University of Singapore, 4 Engineering Drive 3, 117576, Singapore
elehgw@nus.edu.sg

Global energy consumption increased dramatically over the years, driven by rising standards of living and a growing worldwide population. The increased demand for energy will require significant growth in energy generation capacity, secure energy sources, and a zero carbon emissions motivations. Among the various alternative energy strategies, the production of chemical fuels by solar energy conversion has been considered as one of the major strategies for solving the global energy issues. In our work, various metal oxide nanostructured materials nanocomposite were synthesized.[1-6] Our findings emphasize on the achievement of tailoring chemical composition, structural design (core-shell, hierarchical structures) and functionalizing to enable improved solar hydrogen production and degradation properties. Notably, the synergistic morphology, interface and crystal lattice engineering aim towards the design of improved catalyst materials and system for photocatalytic solar hydrogen production and pollutant degradation.

ENV-I-02

Modified Soil Compositions for Removals of Acetaminophen

T. Koottatep*, S. Chapagain, N.H. Phong Vo, A. Panuvatvanich and C. Polprasert
Environmental Engineering and Management, Asian Institute of Technology 58 Moo 9 Paholyothin Rd., Klong Laung, Pathumthani 12120, Thailand
Email: thamarat@ait.ac.th

The wide use of Acetaminophen (ACT), which is typically released with human excreta, and the lack of capability of most treatment plants to treat wastewater containing ACT residues have increased the risk of surface and groundwater contamination. Constructed wetlands (CWs) are one of natural wastewater treatment technologies, employing soil-plant interactions in treating pollutants through a number of reactions such as plant uptake, ion adsorption, advanced Fenton reaction. In addition, the wetland plants are well-known to generate H_2O_2 in the surrounding rhizosphere environment for advanced oxidation processes. In this study, the potential of laterite soil in initiating Fenton reactions by its abundant composition of iron (Fe) and its modified structure with activated carbon, cement and crushed shellfish (modified soil) are determined for ACT treatment. The induced H_2O_2 soil environment in the constructed wetland units could remove ACT almost 80% in comparison with the original concentration. About 70% of ACT was reduced at relatively short period i.e. 1 minute, whereas, treatment time of 35 minutes was required to achieve the treatment efficiency of 82%. The results showed the well occurrence of Fenton process on both natural laterite soil and modified media bed (Cement : Laterite soil $_{fine}$: 50% Laterite soil $_{coarse}$: 50% Activated carbon). Likely due to the Fenton reaction is favorable at low pH, the crushed shellfish plays minor contribution in the modified soil in an increasing alkaline environment.

ENV-I-03

Practical Method for Bentonite Recovery from Foundry Sand Dust

Pichaya Rachdawong[a,*] and Areerat Supasirisombat[a]
[a]*Department of Environmental Engineering, Faculty of Engineering, Chulalongkorn University, Bangkok 10330, Thailand*
*pichaya.r@chula.ac.th

Keywords: Bentonite recovery, Foundry sand dust, Active bentonite

Making and utilization of foundry sand molds are always accompanied by generation of foundry sand dusts. In 2010, about 13,000 tons of non hazardous foundry sand waste from iron and steel industries was generated in Thailand. By law, generators must disposed of the waste in industrial landfills although the dust still contain approximately 10-30% of bentonite by weight. Active bentonite is normally acquired and used as a binding agent for making green sand mold. Therefore, instead of paying for the disposal fee, we aimed to recover active bentonite from foundry sand dust. Dust samples were collected from baghouse filters of a large iron foundry factory. Framework for experiments was set up and consists of toxicity test, dust characterization, and determination of optimal values of temperature and duration for heat application. From the toxicity test we found that heavy metal concentrations in the foundry sand dust leachant were within the regulatory limits. Dust characterization revealed that most dusts were still coated by active bentonite at room temperature. Optimal condition of bentonite recovery was at 120 degree celcius and 30 minutes for heat application. The recovery percent of active bentonite mass was at 41.52 at the purity percent of 26.34. Therefore, about half of the original amount of active bentonite present in the waste dust can be recovered for use again. In addition, the diversion of active bentonite mass from waste dust also can result in saving for the disposal cost.

ENV-I-04

Experience in Sustainable Development through Textile Material Developing for the Community Enterprises (OTOPs) in Thailand

Pilan Dhammongkol
Thanapaisal R.O.P., 218 Moo 1, Sukumvit Road, Soi Beethai 80, Bangpoomai, Muang, Samutprakan 10280
pilan_dh@hotmail.com

I am always interested in developing the textile materials for the community enterprises (OTOP). For over ten years, I have worked closely with these community enterprises and found that they had many problems and obstacles with the textile materials, for examples, color bleed, poor fastness to washing, using AZO dyes which are carcinogenic, the material was uncomfortable for wearing because it was too warm and too heavy for comfort, not suitable for daily usage. The color shades were not matched well with each other. So no buyers for their merchandises, the stocks piled up, incurred huge loss. Many of these OTOPs had to close down, and gone with them the native wisdom and know-how.

The government has seen these problems and their effects, has tried to manage, to support and solve these problems for more than ten years. Many aspects of the problems have been dealt with, and finally they have greatly improved.

I started to get a new idea and inspiration to tackle this challenge from a piece of woven cloth I bought from Japan 4 years ago, for 5,000.-Baht. It has small square design just like typical checkered cloth made by local weavers. The cloth is very thin and lightweight. It is made for a scarf. An idea strike me that these local weavers are good and skilled, no need to make any change. What we should do is to develop new colors and weave more lightweight material.

I approached several OTOP clusters, inviting them to develop the materials along this idea by using new materials, but they were not willing to do it out of fear. They were worried about failure, the newly developed material might be pricey, hard to sell. By producing the same old things is safer. I then presented them with a new possibility. I offered to give them yarn dyed with new kind of dyestuff, free of charge, for weaving sample with the conditions that they give me one third of their production, which I would find a market for them. For the rest two third of the material they can keep and sell by themselves. There were 7 clusters agreed to join this project.

After a while, I received the report that the one third material they agreed to give me to find them a market was no need anymore, because those newly developed materials became best sellers. They could sell at a very good price, 3-4 times of the former price. Now they barely kept up with the demand and needed to persuade those giving up weaving to come back by offering 2-3 times more salary. Recently we have seen younger persons becoming weavers.

Now a day, I could see a big growth and progress in community enterprises. They keep on thriving. Their products were selling very well at trade fairs. They are enjoying more income and happy with their crafts. More people are attracted to work in this area. I am confident that these communities will have a happy and peaceful living. Their native wisdom and know-how will also be with them for generations to come.

I am proud that my role and perseverance have brought these OTOPs to come out from their mindset. I am thankful for the 7 brave clusters who dared to step out from former mindset and courageous enough to try new ideas and make them happen. When I present their achievement as an inspiration to other OTOPs, they are very excited and eager to start working on new ideas. They are now ready to come out from the old mindset. From my point of view, this is the sustainable development.

ENV-I-05

Quality Drying of Lumber: From Laboratory to Industry

Nirundorn Matan
Materials Science and Engineering, School of Engineering and Resources, Walailak University, Thasala district, Nakhon Si Thammarat 80160, Thailand
E-mail: mnirundo@wu.ac.th

Keywords: Lumber, Drying, Internal stress, Kiln controller

Without an online tool to control quality of lumber during drying, the kiln operator is forced to employ a conservative drying schedule which could unnecessarily prolong the drying time and consume more energy. An attempt to reduce the drying time and energy by simply accelerating the drying rate might easily lead to a formation of several defects. Such drying defects mainly arise as a result of the internal stress (IS) built up within the lumber during drying. A new restoring force (RF) technique capable of real-time monitoring IS behavior during drying is presented. Analytical and numerical models have been developed to directly relate the measured RF to the magnitude of IS. In parallel, a semi-automatic kiln control system, *Dry*WooD, has been developed for an effective control of drying in the lumber industry. The system, connected using wire-less links, consists of up to 10 kiln control units, a microcontroller and a control software package. The system has been successfully installed and routinely used in two rubberwood sawmills.

In this talk, the effect of several conventional drying strategies on the development of IS will be discussed and the possible application of the measured RF as a controlling parameter in the drying of rubberwood lumber will be demonstrated.

ENV-I-06

Investigation of Ag- GO- TiO_2 Cocatalyst Composites for Photocatalysis Application

Chanchana Thnachayanont[a*], Chabaiporn Junin[a], Attera Worrayingyong[b], Chanapa Kongmak[b], Bralee Chayasombat[a]

[a]*National Metal and Materials Technology Center (MTEC), National Science and Technology Development Agency (NSTDA), Pathumthani, 12120, Thailand*

[b]*Department of Materials Science, Faculty of Science, Kasetsart University, Bangkok, 10900, Thailand*

*E-mail address corresponding author: chanchm@mtec.or.th

Keywords: TiO_2, Graphene oxide (GO), cocatalyst, Photocatalysis

A non- toxic semiconductor catalyst such as titanium dioxide (TiO_2) has been developed and modified as a smart catalyst in terms of electron transfer and self-regeneration. In this work, we modified TiO_2 with graphene oxide (GO) and metal nanoparticles such as silver (Ag) to enhance photocatalytic property of TiO_2 powder. The result showed that Ag- GO- TiO_2 composites exhibited better photocatalytic property in Rhodamine B degradation from 65% to 85% than pure TiO_2 powder. X- ray absorption spectroscopy (XAS) was used to investigate metal species at the surface of the cocatalyst composites. The Ag nanoparticles were formed at the surface and, hence, would enhance electron transfer in the photocatalysis reactions. An improved photocatalytic activity was obtained. During the photocatalysis reaction under illumination, GO can be reduced to reduced graphene oxide being electron acceptors and, hence, reducing electron- hole recombination at the TiO_2 surface in photocatalysis reaction. This cocatalyst composite is very interesting for further study such as in photoelectrochemical (PEC) process. Understanding electrochemical mechanism of the cocatalyst composite is required to improve and modify cocatalyst to use in water purification to reduce cost in catalyst powder separation after water treatment process.

ENV-O-02

On the Application of Electrocoagulation/Flotation (ECF) Technique for Cationic Dye Removal using Aluminium Electrode and Sodium Dodecyl Sulfate (SDS)

Galuh Yuliani*, Rani Nuraini Arifin, Agus Setiabudi
Chemistry Department, Universitas Pendidikan Indonesia, Bandung 40154 West Java, Indonesia
*galuh@upi.edu

Keywords: Electrocoagulation; Flotation; Aluminium electrode; SDS; Cationic dye

The electrocoagulation/flotation (ECF) technique has been regarded as a safe, efficient and environmentally friendly technique for color removal in aqueous solution. In this research, an electrocoagulation cell was constructed using aluminum metal as electrodes. The constructed electrocoagulation cells were then utilized for the removal of cationic dye from model solution. To enhance flotation of the dye particles, sodium dodecyl sulfate (SDS) was added as a surface active agent. Some operational parameters namely electrolysis time, applied voltage, and SDS concentration were investigated. It was found that the optimum conditions were electrolysis time of 10 minute, applied voltage of 5 V, and SDS concentration of 200 ppm. Under these optimum conditions, the cationic dye removal of 87% was achieved. The mechanism of SDS enhanced ECF was also studied. It was concluded that addition of SDS to ECF system may facilitate better and efficient removals of cationic dye from aqueous solution.

ENV-O-03

Preparation, Characterization, and Photocatalytic Properties of rGO-TiO_2-Rubber Composite Sheets for Dye Decomposition in Wastewater

Worapol Tejangkura[a], Chaval Sriwong[a,*], Kittisak Choojun[a,b]

[a] *Department of Chemistry, Faculty of Science, King Mongkut's Institute of Technology Ladkrabang, Chalongkrung Road, Ladkrabang, Bangkok, 10520, Thailand*

[b] *Catalytic Chemistry Research Unit, Department of Chemistry, Faculty of Science, King Mongkut's Institute of Technology Ladkrabang, Chalongkrung Road, Ladkrabang, Bangkok 10520, Thailand*

*E-mail: kschaval@yahoo.com

Keywords: Photocatalysis, Dye decomposition, Rubber composite sheet, Reduced graphene oxide (rGO)

Over the past few decades, the applications of advanced oxidation processes (AOPs) for wastewater treatment, water and air purifications using semiconductor photocatalytic materials have attracted much attention as a facile, low cost, and effective method to remove recalcitrant contaminants. Among photocatalysts, titanium dioxide (TiO_2) is the most extensively used due to its excellent photocatalytic activity. However, the main drawback of TiO_2 powder is its limitation in practical use and in recovery. In order to solve this problem, rubber sheets incorporated with TiO_2 (Rubber-TiO_2) have been prepared and shown to exhibit photocatalytic behavior, and they can also be easily recovered and reused. By comparison, the photocatalytic activity of Rubber-TiO_2 is lower than TiO_2 powder. Recently, reduced graphene oxide (rGO), a two-dimensional sheet of sp^2-hybridization carbon atoms, has attracted a great deal of interest due to its unique large surface area, high mechanical strength, and excellent electron mobility. Thus, in TiO_2-rGO composite, rGO can retard the electron (e^-) - hole (h^+) recombination in photocatalytic process of TiO_2, and can improve the adsorb-ability of pollutant molecules on the surface of TiO_2-rGO catalyst, which enhances the photocatalytic activity. Moreover, it has been reported to strengthen the rubber sheet. Therefore, in this research, we synthesize rubber sheets incorporated with TiO_2 and rGO by fixing TiO_2 suspension and natural rubber latex contents while varying the amounts of rGO loading, using a latex mixing-casting method. This is a very simple, inexpensive, and cost-effective method for fabrication of rGO-TiO_2-rubber (rGOTR) composite sheets. Then, the as-prepared rGOTR sheets were characterized by X-ray diffraction (XRD), attenuated total reflection Fourier-transformed infrared spectroscopy (ATR-FTIR), Raman spectroscopy, scanning electron microscopy (SEM), and energy dispersive X-ray spectrometer (EDS) techniques. The photocatalytic properties of all

composite sheets were evaluated using methylene blue (MB) dye as a model for organic dye pollutants in water under ultra-violet (UV) light irradiation. Compared with the unloaded sample, all the rGO-loaded composite sheets had higher efficiencies for the photodegradation of MB dye solution. This may be due to the combined effect of TiO_2 and rGO, enhancing the photocatalytic performances of rGOTR sheets. Furthermore, the efficiency of the rGOTR sheet upon repeated usage was also studied. The result showed that the composite sheet could be easily used, recovered, and reused many times with no need for cleaning in between successive uses. For the above reasons, rGOTR sheet should be attractive to the water or wastewater treatment industry, as it helps keep the operation cost low.

ENV-O-04

Fabrication Study of Hydrophobic Polyurethane Sponge for Oil-Spills Cleanup

Peeranut Prakulpawong [a], Jinjutha Wiriyanantawong [a], Janista Pornpoonsawat [a], Supan Yodyingyong [b], Darapond Triampo [a,*]

[a]*Department of Chemistry and Center of Excellence for Innovation in Chemistry, Faculty of Science, Mahidol University, Phuttamonthon 4 Road, Salaya, Phuttamonthon District, Nakhon Pathom, 73170, Thailand*

[b]*Institute for Innovative Learning, Mahidol University, Phuttamonthon 4 Road, Salaya, Phuttamonthon District, Nakhon Pathom, 73170, Thailand*

*E-mail address corresponding author: darapond.tri@mahidol.edu

Keywords: hydrophobic silica aerogel, polyurethane sponge, UV-treatment, oil absorption.

Accidental oil-spills and leakage into the environment in both small and large scales can have serious and in some cases catastrophic impact on the environment. In addition to the surrounding water, air and soil, petroleum contamination can spread into the food chain where the effects can be severe and long lasting. There has been continuous work in industrial, academic and government sectors to help resolve this problem. Example methods of oil-spills cleanup are *in situ* burning to burn away the oil, the use of dispersants and microbes to digest the oil into smaller molecules, and the use of booms or blankets to minimize the contamination area. All of the methods mentioned are rather time-consuming, and the spilled oil is not recovered.

In this research, the researchers study the fabrication of oil absorption, hydrophobic polyurethane sponge (PUS) for application in an oil-spill cleanup model. Virgin PUS is initially hydrophilic. PUS is made hydrophobic by incorporating hydrophobic silica aerogel (SA) into PUS 3D porous structure by using UV- treatment. UV- irradiation promotes free radicals on the PUS surface that in turn promotes the attachment of SA onto the PUS surface. Varying time of UV-irradiation and concentration of SA- soaking is done to attain an optimal attachment of SA onto PUS. Fourier-transform infrared spectroscopy (FT-IR) is used to determine the chemical bonding between SA and PUS. Scanning electron microscopy (SEM) is used to confirm the attachment of SA to PUS. Thermal gravimetric analysis (TGA) and wettability testing (WT) are also used to determine the adhesion efficiency of SA to PUS. The loading of SA for with and without UV-treatment is compared. Results show that SA-PUS with UV-treatment has more loading of SA than SA-PUS without treatment. Moreover, the SA-PUS is tested for oil adsorption to simulate oil-spill cleanup. The findings show fast, recoverable oil-spills cleanup with simple method of preparation.

ENV-O-05

A feasibility study of using biofilter media made from biomass ash for nitrogen compound removal in aquaculture

Tahmina Sultana[a,*], Umaporn Sanewirush[b] and Pakamard Saewong[b]

[a]Kasetsart University (KU), Ladyaow Chatuchak, Bangkok -10900, Thailand

[b]National Metal and Materials Technology Center(MTEC), NSTDA, Thailand

*tahminaaust90@gmail.com

Keywords: Waste Water Treatment, Bio-filter media, Coral, Porous pellets.

Abstract: Aquaculture industry needs large volume of clean water supply and because of the regular fish-food leftover and wastes from fish, amount of Nitrogen compounds in the water increases. After a certain period, it is needed to change the water. To handle scarcity of water, sustainable waste water treatment is getting more attention now-a-days worldwide. Coral is still being used illegally as a filter material in water treatment units because of its effectiveness in nitrogen compound removal. In this study, the pellet media made from bagasse ash, rice husk ash and coal bottom ash are introduced as cost effective alternatives of coral. The media are characterized and compared their effectiveness with that of the coral in terms of removal of nitrogen compound wastes. In a given laboratory testing unit, it is found that all the media made from ash give a comparable result to the coral that, the toxic nitrogen wastes are removed within 14

ENV-O-06

Using ZnO Nanorods Coated Porous Ceramic Monolith to Remove Arsenic from Groundwater

Kannika Khwamsawat[a], Jukkrit Mahujchariyawong[a], Supamas Danwittayakul[b] *
[a]*Kasetsart University, Chatuchak, Bangkok, 10900, Thailand*
[b]*National Metal and Materials Technology Center, Klong Luang, Pathumthani, 12120, Thailand*
*supamasd@mtec.or.th

Keywords: Adsorption, Arsenic, Porous ceramic, ZnO nanorod

One-dimensional zinc oxide (ZnO) nanoadsorbents were utilized as an adsorbent for arsenic removal. ZnO nanorods were grown on ZnO nanoparticle seeded porous substrates (2.5 cm x 2.5 cm x 1 cm) by using equimolar concentrations (5, 10, 15, 20, 25 and 30 mM) of zinc nitrate and hexamethylenetetramine at temperatures lower than 100 °C. Morphologies of synthesized nano-adsorbents were investigated using field emission scanning electron microscope (FESEM, Hitachi, SE-8030), while phase compositions and specific surface area were examined by X-ray diffractometer (XRD, PAnalitical, X'Pert PRO) and gas adsorption technique (Quantachrome, Autosorb-1C), respectively. Arsenic adsorption efficiency of each sample upon using a lab scale reactor with 100-mL capacity was studied. In the adsorption process, known concentration of arsenic solution was continuously stirred in the reactor, where a monolith adsorbent was hung at the center of the water container. The arsenic concentrations of the sample solutions before and after adsorption process were measured by using inductively coupled plasma-optical emission spectroscope (ICP-OES) in order to obtain the adsorption efficiencies. SEM micrographs revealed that upon using 20 mM of growth solution concentration, the nanoadsorbent exhibited the most uniform in size and shape of ZnO nanorods (100-nm diameter) covering over the surface of porous substrate. This nanoadsorbent exhibited almost 100% arsenic removal after continuously stirring for 3 hours. In addition, effects of adsorption parameters such as pH, time, and arsenic concentration as well as the comparison adsorptive study between the prepared and the commercial adsorbents will be discussed.

ENV-O-07

Adsorptive and Acid Properties of Zeolite; Effects of synthesize methods

Agus Setiabudi *, **Galuh Yuliani, Nisa Nasrah, Hanifah Permana Putri**
Chemistry Department, Universitas Pendidikan Indonesia, Bandung 40154 West Java, Indonesia
*agus_setiabudi@upi.edu

Keywords: Fly ash; Zeolite Microwave Reflux Adsorption Acidity

Coal utilization as burning fuel has resulted in a mass production of solid wastes, namely fly ash and bottom ash. Due to their huge amount and high heavy metal contents, the disposal of these wastes is highly problematic. Owing to its high silica and alumina contents, fly ash has been utilized as one of raw materials in cement industries. However, the intake of fly ash by the cement industries is still low compare to its soaring production during the coal burning. Therefore, various alternative applications of fly ash have been widely sought. In this research, coal fly ash had been used as starting material for zeolite production using ultrasonic/microwave/reflux methods. The coal fly ash was first washed and dried before the treatment using NaOH 2 M solution followed by ultrasonic, microwave, and reflux methods. The zeolite resulted upon treatment was then characterized by FTIR, XRD, SEM, and acidity. The adsorptive properties of the zeolites and acid washed zeolites were then tested using methylene blue solutions in batch and filter bed modes. The zeolite with the highest adsorption capacity of 100 mg/g was obtained upon acid washing, ultrasonic treatment of 30 minutes and 45 minutes of microwave. The results indicated an alternative application of coal fly ash as starting material for zeolite that can be useful in wastewater treatment processes.

ENV-O-08

Removal of Arsenic from Groundwater using Nano- Metal Oxide Adsorbents

Phitchaya Muensri, Supamas Danwittayakul*

National Metal and Materials Technology Center, 114 Thailand Science Park, Paholyothin Rd., Klong 1, Klong Luang, Pathumthani, 12120, Thailand.

*Email: supamasd@mtec.or.th

Keywords: Arsenic adsorption, Nanoparticles, Nanoadsorbents, Metal oxides

Abstract: Arsenic can be found in groundwater that is harmful to human beings. In this research, we present the potential uses of ZnO microparticles, ZnO and TiO_2 nanoparticles to removal arsenic in groundwater. The experiments of %arsenic removal upon using ZnO microparticles ZnO and TiO_2 nanoparticles were conducted in 25 mL of sample volume with 0.05 g of nano-adorpbents at pH 6. We found that efficiency of arsenic adsorption increased with a reduction of particle size of adsorbents. This can be attributed to the higher specific surface area of TiO_2 (52.41 $m^2.g^{-1}$) exhibited 97%of arsenic removal that was a better efficiency than that the use of ZnO nanoparticles (9.43 $m^2.g^{-1}$) and ZnO microparticles (5.39 $m^2.g^{-1}$), which obtained 96 and 83% of arsenic removal, respectively. Upon using nano-adsorbents to remove arsenic in the solutions with the concentrations of 200-2000 ppb, we found that the %removal of arsenic decreased from 100% to 66% for ZnO and 100% to 73% for TiO_2 nanoparticles. Adsorption capacities upon using ZnO and TiO_2 nanoparticles were 0.47 and 0.72 mg of arsenic/g of sorbents, respectively. We would like to emphasize that TiO_2 nanoparticles exhibited a better adsorption ability to arsenic than that ZnO becauseTiO_2 nanoparticles had smaller particle size and larger surface area allowed the adsorption of hydroxyl groups on the surface that could bond with in coming $HAsO_4^{2-}$ via hydrogen bonding resulting in a better arsenic adsorptive capacity. In this work we will report effects of other adsorption parameters such as pH, time, and process using these adsorbents.

ENV-O-09

Dowel Bearing Strength of Rubberwood

Raphaela Hellmayr[a], Thomas Forte[a], Satjapan Leelatanon[b,*]

[a] Forest Products Technology and Timber Construction, Salzburg University of Applied Sciences, Salzburg, Austria
[b] School of Engineering and Resources , Walailak University, Thasala district, Nakhon Si Thammarat, 80160 , Thailand
*E-mail address: lsatjapa@wu.ac.th

Keywords: Dowel bearing strength, Rubberwood, Finite element method

Dowel bearing tests in parallel and perpendicular to the grain were determined to investigate the dowel bearing strength of rubberwood in structural point of view. Four dowel diameters including 2.4, 3.5, 9.0 and 12.0 mm were tested with the rubberwood samples which were environmentally controlled to reach the moisture content of 6%, 10% and 15%. The tests clearly showed that the larger dowel produced the less bearing strength in perpendicular to the grain. However, the effect of dowel diameter on the bearing strength in parallel to the grain was not explicit because those diameters made almost the same strength. This might be because dowel diameters and width of annual rings had the same size between 2 and 6 mm. The small dowel could compress only on a single layer of the rings, so the strength of the small one was about the same compared to those of the larger one. Moreover, the dowel bearing strength in parallel and perpendicular to the grain was lower when the moisture content was higher, while the bearing strength in both directions slightly increased when the density was greater. However, it was noticed that the density of rubberwood varied in a narrow range from 0.64 to 0.69 g/cm^3. In addition to the dowel bearing strength, failure modes of samples were examined by using the finite element method. The numerical model and the experimental results were in good agreement.

ENV-O-10

Assessment of Hydrophilic Biochar Effect on Sandy Soil Water Retention

Ramida Rattanakam
Kasetsart University, Chatuchak, Bangkok, 10900, Thailand
fscirdr@ku.ac.th

Keywords: Biochar, Water retention, Sandy soil, Soil amendment.

Increasing water holding capacity of sandy soil has been suggested as a significant factor governing an increase in crop production. In sandy soil, due to its course-texture comprising large soil particles without pockets that can hold water and nutrients, water and nutrients retention can be very low. Consequently, many crops have a difficulty in surviving in this kind of soil. Literature has shown that biochar are among the best sandy soil amendments that improves chemical and physical properties of the sandy soil. Pore size distribution characterization revealed that the structure of biochar includes pores with diameters in the range of 0.1-10 μm which can retain plant-available water as well as nutrients. In this study, it is hypothesized that addition of biochar will increase the water-holding capacity of a sandy soil and that the higher the hydrophilicity of biochar, the higher water holding capacity of a sandy soil. For that reason, the effects of hydrophilicity on water uptake by biochars were studied. Biochars were produced from two feedstock at the same production temperature. Then, the hydrophilicity of biochars was modified by treating with hydrophilic salt. Comparison of water uptake capacity between untreated biochars and hydrophilic biochars and the application of these biochars into sandy soil allowed us to assess the effects of hydrophilicity of biochars on water retention of sandy soil.

ENV-O-11

Preparation of Activated Carbon from Sugarcane Bagasse Waste for the Adsorption Equilibrium and Kinetics of Basic Dye

Tawan Chaiwon[a], Panatda Jannoey[b], Auppatham Nakaruk[c], Duangdao Channei[d,e*]

[a]Department of Chemistry and General Science, Faculty of Education, Valaya Alongkorn Rajabhat University under the Royal Patronage, Pathumtani 13180, Thailand

[b]Department of Biochemistry, Faculty of Medical Science, Naresuan University, Phitsanulok, 65000, Thailand

[c]Department of Industrial Engineering, Faculty of Engineering, Naresuan University, Phitsanulok 65000, Thailand

[d]Department of Chemistry, Faculty of Science, Naresuan University Phitsanulok 65000, Thailand

[e]Research Center for Academic Excellence in Petroleum, Petrochemicals and Advanced Materials, Naresuan University, Phitsanulok 65000, Thailand

*E-mail address corresponding author: duangdaoc@nu.ac.th

Keywords: Activated carbon; Sugarcane Bagasse; Adsorption Isotherm; Kinetics

This research aimed to study the preparation of activated carbon from sugarcane bagasse. The adsorbent was prepared by heating sugarcane bagasse waste at 600ºC for 2 hours with the use of sulfuric acid (H_2SO_4) as a chemical activation. The adsorption surface possessed high specific surface area (838.06 m^2/g) with mesoporous diameter. The spherical shape with the size of 120 nm was detected by a transmission electron microscope (TEM). Factors explaining adsorption including adsorption isotherm, adsorption kinetic and adsorption mechanism were constructed from methylene blue adsorption experiments. It was found that the equilibrium data was best represented by Langmuir isotherm model, showing monolayer coverage of dye molecules at the outer surface of sugarcane bagasse carbon. The kinetic of methylene blue adsorption was found to follow the pseudo-second-order model with good correlation (R^2), and that the overall rate of the dye adsorption process appeared to be controlled by the chemisorption process. The mechanisms of the adsorption occurred in two steps. The first linear portion followed the boundary layer diffusion followed by another equilibrium adsorption which represented the intraparticle diffusion. These results indicated that the activated carbon prepared from sugarcane bagasse could be employed as a low-cost alternative to commercial activated carbon in the removal of basic dye pollutant from wastewater.

ENV-O-12

Effect of Cell Wall Constituents On Internal Stress Generation During Drying of Lumber Prepared From Rubber Tree Trunks

Jaipet Tomad[a,*], Sataporn Jantawee[a], Wanchart Preechatiwong[a], Nirundorn Matan[a]

[a] *Materials Science and Engineering, School of Engineering and Resources, Walailak University, Thasala district, Nakhon Si Thammarat 80160, Thailand*

*E-mail: TJaipet@hotmail.com

Keywords: Internal Stress, Drying, Cell Wall Constituents, Rubberwood

The objective of this research is to study effect of extractives and amorphous cell wall constituents on the internal stress profile of lumber prepared from different locations (radius from pith and height from ground) of rubber tree trunks. All specimens prepared from two rubber trees were impregnated with water to attain saturated moisture content prior to testing. Assessment of the internal stress development within the lumber during the drying was monitored in real-time using a restoring force measurement on half-split specimens. The corresponding drying curve was at the same time monitored by periodically weighting two pieces of lumber placed inside the lumber stack in the drying kiln. Drying condition at dry-bulb and wet-bulb temperatures of 90°C and 60°C was used throughout this work. It was shown that the generated internal stress appear to be largely unrelated to the height of the rubber trees. Time required for stress reversal to take place was found to be shorter for the lumber prepared from outer with respect to inner sections of the trunk. However, minimum and maximum forces detected were relatively insensitive to locations of lumber within the trunk. There are two negative force maxima which could attribute to the creep responses during drying of the main amorphous constituents and the extractives within the cell walls, respectively. The second negative maximum gradually disappeared upon water immersion of the specimens. In these specimens, faster stress reversal and higher drying rate in the second drying stage have been observed with respect to the fresh specimens. The force profiles of the water-immersed specimens seem to be insensitive to locations within the tree trunk. The results suggest that the presence of cell wall extractives should retard creep deformation and slow down diffusion of bound water within the cell walls. On the other hand, a large fraction of water molecules suggested to be adsorbed at the interface between the crystalline cellulose and amorphous hemicellulose within the cell wall should accelerate creep deformation and speed up diffusion of the bound water. For a practical point of view, it is suggested that there is no need for rubberwood lumber classification for drying because the minimum force (indicating the risk of surface checking) and the maximum force (indicating the risk of internal checking) were observed to be insensitive to wood locations within the trunk.

ENV-O-13

Improvement of Compressive Strength of Soil by Using Jute Fiber Waste

Md. Bayezid Islam[a*] ,Tahmina Sultana[b], Md. Waliur Rahman[c]

[a]*Asian Institute of Technology (AIT), Pathumthani-12120,Bangkok, Thailand*

[b]*Ahsanullah University of Science and Technology (AUST), Dhaka- 1208, Bangladesh*

[c]*Roads and Highways Department (RHD), Dhaka- 1212, Bangladesh*

*email: bayezid.ait@gmail.com

Abstract: To attain desirable strength of soil, soil reinforcement has been playing a pivotal role since many decades. Although there are many well established methods to reinforce the soil, but now-a-days people are looking for low-cost reinforcing materials. In Bangladesh jute waste is not being used effectively, although jute production is quite good in amount. From this point of view in this study, jute fiber is selected as reinforcing material and focused on improvement of compressive strength of soil. Varying proportions of Jute fiber as 1%, 2%, 3%, 4% and 5% have been mixed with dry soil to make the samples to be tested. The result indicated that the sample prepared with 3% of jute fiber gives the highest value in Unconfined Compressive Strength (UCS) test and adding more than 3% of jute fiber tends to decrease the UCS value. As this study has been done keeping in mind about the embankment construction process in the coastal zones of Bangladesh, where grass turfing is done to protect soil from erosion and inorganic fertilizer is used to grow up the grass which has long term effect on environment. On the other hand jute is 100% biodegradable, when it comes to contact of moist soil, after a certain period it acts as natural fertilizer that helps to grow up the grass and make the root of grass stronger to hold the soil.

Key words: Jute fiber, Waste, Soil reinforcement.

ENV-P-01

The mechanical properties study of Waste Bakelite Aggregate Concrete

Nopagon Usahanunth [a,*], Waranon Kongsong[b], Seree Tuprakay[c] , Sirawan Ruangchuay Tuprakay [d], Suppachai Sinthaworn [e], Sathian Charoenrien [f]

[a] *PhD-Student ,Inspection and Engineering law ,Faculty of Engineering, Ramkhamhaeng University, Bangkok, Thailand*

[b,c] *Assistant Professor ,Inspection and Engineering law ,Faculty of Engineering, Ramkhamhaeng University, Bangkok, Thailand*

[d] *PhD, Lecturer, Faculty of Science and Technology, Suandusit University, Thailand*

[e] *Assistant Professor ,Department of Civil Engineering ,Faculty of Engineering, Srinakarinwirot University, Bangkok, Thailand*

[f] *Director, Engineering Bureau Structural and Systems Engineering Bureau, Public Work Department, Bangkok, Thailand*

Email : [*]konthai98@yahoo.com

Keywords: Conventional Concrete (CC) ,Waste Bakelite Aggregate(WBA) , Waste Bakelite Aggregate Concrete (WBAC)

Abstract

This paper focuses on industrial thermosetting plastic waste reduction by recycling as the material for natural coarse aggregate replacement in concrete. This substitution of aggregate is an integration approach to preserve the natural resources and environment as well as develop the alternative recycled aggregate material to meet 3R principle and sustainable development. One of the thermosetting plastic frequently used as engineering plastic is Bakelite. Bakelite material has been used to produce various components for cars and consumer products industry in Thailand. Bakelite waste is prohibited from disposing of sanitary landfill and direct burning because of unsafe disposal and emission reasons .There are many studies of plastic aggregate to substitute natural coarse aggregate especially PET and PE aggregate. However, there is no study of Waste Bakelite Aggregate (WBA) mixed in concrete in Thailand. This study aim is investigating the mechanical properties of Waste Bakelite Aggregate Concrete (WBAC) compare to conventional concrete (CC).The methodology is based on an experimental program by testing of concrete specimens. The data obtained from sample test according to BS and ASTM standard. These test results present compressive strength, the density of all samples both CC and WBAC. The relationship charts between mechanical properties and the aggregate replacement percentage of natural coarse aggregate replacement will be illustrated including the compressive strength predictable equation model by the correlated parameters. Furthermore, the risk assessment level from chemical extraction of each Waste Bakelite Aggregate replacement fraction in concrete and the durability of WBAC are notified for the utilization. WBAC is an alternative material that can be applied for non-structural concrete product to replace the natural aggregate and helpful in waste plastic pollution mitigation.

ENV-P-02

Performance Photocatalytic Degradation of Methomyl onto Composite Graphene Oxide/Bismuth Vanadate ($GO/BiVO_4$) Nanoparticle

Pusit Pookmanee[a, b*], Pimchanok Longchin[a, b], Jitreephan Phanmalee[a], Viruntachar Kruefu[b], Wiyong Kangwansupamonkon[c] and Sukon Phanichphant[d]

[a]Department of Chemistry, Faculty of Science, Maejo University, Chiang Mai, 50290, Thailand;

[b]Department of Nanoscience and Technology, Faculty of Science, Maejo University, Chiang Mai, 50290, Thailand;

[c]National Nanotechnology Center (NANOTEC), National Science and Technology Development Agency, Pathumthani, 12120, Thailand;

[d]Materials Science Research Center (MSRC), Faculty of Science, Chiang Mai University, Chiang Mai, 50200, Thailand

*E-mail address corresponding author: pusit@mju.ac.th

Keywords: Composite, graphene oxide/bismuth vanadate, photocatalytic, methomyl

Graphene oxide (GO) was synthesized by modified Hummer's method. Bismuth vanadate ($BiVO_4$) nanoparticle was synthesized by solvothermal method at 100 and 200 °C for 3h. Composite graphene oxide/ bismuth vanadate ($GO/BiVO_4$) nanoparticle was fabricated by mixed oxide method with the weight ratio GO and $BiVO_4$ nanoparticle of 0.20:1.00. The physical and chemical properties of GO, $BiVO_4$ and $GO/BiVO_4$ nanoparticle were characterized by X-ray diffractometer (XRD), scanning electron microscope (SEM), energy dispersive X-ray spectrometer (EDS) and surface area analyzer (BET). The performance photocatalytic degradation of methomyl onto $BiVO_4$ and $GO/BiVO_4$ nanoparticle was determined by high performance liquid chromatograph (HPLC). Composite $GO/BiVO_4$ nanoparticle was higher performance photocatalytic degradation of methomyl than $BiVO_4$ nanoparticle.

ENV-P-03

The Photocatalytic Degradation of Methylene Blue using Bismuth Vanadate ($Bi_2VO_{5.5}$) Powder

Jitreephan Phanmalee[a,*], Prakasit Intaphong[a], Wiyong Kangwansupamonkon[b], Sukon Phanichphant[c] and Pusit Pookmanee[a]

[a]Department of Chemistry, Faculty of Science, Maejo University, Chiang Mai, 50290, Thailand;

[b]National Nanotechnology Center (NANOTEC), National Science and Technology Development Agency, Pathumthani, 12120, Thailand;

[c]Materials Science Research Center (MSRC), Faculty of Science, ChiangMai University, Chiang Mai, 50200, Thailand

*E-mail address corresponding author:jitreephan03chemistry@gmail.com

Keywords: Bismuth vanadate, methylene blue, microwave method

Bismuth vanadate ($Bi_2VO_{5.5}$) powder has been successfully prepared by microwave method. Bismuth nitrate and ammonium vanadate were used as the starting precursors with the mole ratio of 2:1 in 2-propanol. The condition of microwave was 500 Watt for 2-6 min. Fine yellow powder was obtained, milled and calcined at 500°C for 2h. The structure of $Bi_2VO_{5.5}$ powder was identified by X-ray diffraction (XRD). The morphology of $Bi_2VO_{5.5}$ powder was investigated by scanning electron microscopy (SEM). The chemical composition of $Bi_2VO_{5.5}$ powder was determined by energy dispersive X-ray spectrometry (EDXS). The functional groups of $Bi_2VO_{5.5}$ powder were investigated by fourier transform infrared spectrometry (FTIR) The photocatalytic degradation of methylene blue (MB) using $Bi_2VO_{5.5}$ powder was studied by ultraviolet-visible spectrophotometry (UV-Vis).

ENV-P-04

Structure and Factors Affecting Mechanical Properties of Bamboo

Suthon Srivaro[1*], Nirundorn Matan[1]
[1]*Materials Science and Engineering, School of Engineering and Resources, Walailak University, Thasala district, Nakhon Si Thammarat 80160, Thailand*
*E-mail address corresponding author: ssuthon@wu.ac.th

Keywords: bamboo, mechanical properties, node effect

Bamboo is now of interest to be utilized as alternative materials for building construction because it is environmentally friendly material and has higher strength than various structural materials. This work gives an overview of structure and important factors affecting mechanical properties of bamboo. The bamboo culm is tubular and separated by nodes. Tissue of bamboo consists of two major cells; vascular bundles and parenchyma cells. Fractions of these two cells along cross section and culm height are not uniform and very dependent on bamboo species. Basically, vascular bundles congest in outer cross section and gradually decrease to the inner culm wall. In view of microscopic and macroscopic structures of bamboo, variation of bamboo's cells and the presence of nodes along the culm height, respectively, could affect mechanical properties of bamboo. It has been clearly proven that most of mechanical properties of bamboo increase with increasing fraction of vascular bundle. However, effect of node on mechanical properties of bamboo is still unclear. According to the literatures, two major findings regarding on node effect have been reported. Firstly, effect of node on some mechanical properties of different bamboo species is qualitatively different. It has been observed that some mechanical properties of some bamboo species have reduced due to the presence of node but the contrast results have also been reported for other bamboo species. Secondly, the quantitative effects of node on the particular mechanical property of different bamboo species are found to be different. No clear description on those obtained different findings among different bamboo species has been provided. This suggests that an investigation to achieve more understanding on the actual role of node on mechanical properties of bamboo both in qualitative and quantitative aspects is still needed.

ENV-P-05

WO_3-doped TiO_2 thin films synthesis by microwave-assisted sol-gel and dip coating technique on glass with highly antibacterial under fluorescent light

Weerachai Sangchay*, Aurasa Namsai and Pichet Chantawee
Faculty of Industrial Technology, Songkla Rajabhat University, Songkhla, 90000 Thailand
*E-mail address corresponding author: weerachai.sang@yahoo.com

Keywords: WO_3-doped TiO_2, Thin films, Antibacterial, Microwave-assisted sol-gel

In the present study, we have prepared WO_3-doped TiO_2 thin films developed on microscope glass slides by microwave-assisted sol-gel and dip coating technique. WO_3-doped TiO_2 thin films were obtained after calcining at a temperature of 500℃. The surface and chemical component were characterized by X-ray diffraction (XRD) and scanning electron microscopy (SEM). The WO_3-doped TiO_2 thin films with WO_3 molar ratio from 0 to 5 mol% were tested for its antibacterial property by using *Escherichia coli* (*E.coli*) under irradiation of fluorescent light. The concentration of *E.coli* was evaluated by plating technique. The result showed that antibacterial ability was significantly improved by increasing WO_3 content comparing with pure TiO_2 thin films, and the best molar ratio of WO_3 was 1 mol%.

ENV-P-06

Exploitation of Ag_3PO_4 Impregnated Alginate Beads for The Photocatalytic Degradation of Dye Solution under Sunlight Irradiation

Katnanipa Wanchai*
Department of Chemistry, Faculty of Science and Technology, Phranakhon Si Ayutthaya Rajabhat University, Phranakhon Si Ayutthaya, 13000, Thailand
*katnanipa@gmail.com

Keywords: Ag_3PO_4-alginate beads, photocatalytic, methylene blue, sunlight irradiation.

Ag_3PO_4-alginate beads (AAB) were synthesized by simple method and their structure was characterized by XRD, FT-IR and SEM/EDS, respectively. The Ag_3PO_4 and AAB were evaluated as the photocatalyst for degradation of methylene blue (MB) under sunlight irradiation. The results showed that AAB exhibited the highest performance for degradation of MB (97.6%) in 60 min. The kinetic studied demonstrated that the photocatalytic reactions followed the pseudo first-order model. Moreover, AAB can maintain full photodegradation activity for at least five cycles. Consequently, the AAB are promising materials for the photocatalytic of dyes or similar organic contaminant in environmental pollution cleanup.

ENV-P-07

Photocatalytic Enhancement of Solar Water Disinfection using ZnO Nanorods Coated Cellulose Paper

Supachai Songngam, Supamas Danwittayakul*

National Metal and Materials Technology Center, 114 Thailand Science Park, Klong 1, Klong Luang, Pathumthani, 12120,Thailand.
*E-mail address: supamasd@mtec.or.th

Keywords: ZnO Nanorods Coated Cellulose Paper, Solar Water Disinfection, SODIS, Water Purification

Nano-structures of ZnO photocatalysts on cellulose support were prepared for the enhancement of solar water disinfection by two-step method where ZnO nanoparticles were first hydrothermally synthesized and deposited on the cellulose substrate followed by the growth of ZnO nanorods onto the ZnO seeded nanoparticles. One dimensional ZnO nanorods grow on preseeded substrates in a liquid bath containing zinc nitrate and hexamethylene tetramine as a source of precursors. Morphologies of synthesized ZnO nanorods grown from different growth conditions were investigated using field emission scanning electron microscope (FESEM, Hitachi, SE-8030), while phase compositions and specific surface area were examined by x-ray diffractometer (XRD, PAnalitical, X'Pert PRO) and gas adsorption technique (Quantachrome, Autosorb-1C) with BET equation, respectively. We found that size of ZnO nanorods increased with an increase of the concentration of the growth solution. XRD patterns revealed that the higher concentration of growth solution having higher intensity of XRD peaks attributed to higher crystallinity. Crystallite sizes of each ZnO photocatalyst was calculated using Scherrer equation and found that the crystallite sizes were in the range of 17-30 nm. Experiments of the enhancement of solar water disinfection of water samples with 10^{-6} CFU *E. Coli.* contaminant were conducted in a lab scale system (200-mL capacity) made from a transparent polyethylene zip lock bag under UV light (a 254 nm UV lamp) where a photocatalyst sample was placed inside at the bottom of the bag facing to the light. In here, we will report the rate of disinfection by recording the reduction of number of bacteria at different light exposure durations and the concentrations of zinc ions released from the photocatalysts after SODIS process determined by inductively coupled plasma-optical emission spectroscope (ICP-OES, Activa, Horiba).

ENV-P-10

Development of Epoxy Composites Reinforcement with Oil Palm Empty Fruit Bunch Fibers for Improvement in Mechanical and Thermal Properties for Bumper Beam in Automobile

Rungsima Chollakup[a,*], Wuttinant Kongtud[a], Jirachaya Boonyarit[a], Wirasak Smitthipong[a,b] and Suteera Witayakran[a]

[a] *Kasetsart Agricultural and Agro-Industrial Product Improvement Institute Kasetsart University, Bangkok, 10900 Thailand*

[b]*Department of Material Science, Faculty of Science, Kasetsart University, Bangkok 10900 Thailand*

*aaprmc@ku.ac.th

Keywords: Epoxy Composites, Oil Palm Empty Fruit Bunch Fiber, Bumper Beam,

Bumper beams are essential in protection of passengers, engine components during frontal collistion. The use of natural fibers have recently become sociable to automotive industry as an reinforcement in epoxy composites for bumper beams due to their mechanical properties, low cost, low density, renewability, recyclability and biodegradability. This research aims to use oil palm empty fruit bunch fibers from palm oil extraction industry to reinforce epoxy resin for bumper beam in cars. Oil palm empty fruit bunch fibers were extracted by two methods; chemical method by treating with 10-30% sodium hydroxide (% by weight of fiber) and mechanical method by steam explosion process at 12-20 kgf/cm^2 for 5 mins. Then, the obtained fibers were bleached by hydrogen peroxide. The important physical properties of the oil palm empty fruit bunch fibers were studied. The results show that the chemical method can eliminate lignin better than the others and provided stronger fibers. Increasing of alkaline concentration yielded to decrease lignin content and increase cellulose content, while no significant difference on fiber size and strength was obtained. In case of steam explosion method, increasing of pressure vapor affected to more dark brown color and disintegrated fibers. It caused less yield, decreasing of fiber size and strength, but no effect on lignin content. Herein, the oil palm empty fruit bunch fibers extracted by chemical method at 30% NaOH and by steam explosion at 12 kgf/cm^2 were used for reinforcing epoxy composite with fiber contents of 0-10% by wt. using non-woven technique compared to glass fiber chopped stand mat. Epoxy composites were formed by adding fiber mates in the mixer of epoxy resin and hardener at ratio of 100:33 and then compressing in compression mold at room temperature under pressure at 125 kgf/cm^2 for 12 hours. The physical, mechanical and thermal properties of all fiber reinforced composites were evaluated. The results show that flexural modulus did not increase with increasing fiber content. However, the fibers extracted by chemical method can support composite from falling apart after testing like glass fiber reinforced composite with fiber contents upper than 7.5% by wt. Impact strength and storage modulus of alkaline treated palm fiber reinforced composites increased when fiber content at more than 7.5%. Thermal properties of composite, analyzed by differential scanning calorimetry (DSC) and dynamic mechanical analysis (DMA) shows that the Tg increased with fiber content. Therefore, oil palm empty fruit bunch fibers used for reinforcement epoxy components for car bumpers should be prepared by NaOH treatment at 30% by weight and then bleaching.

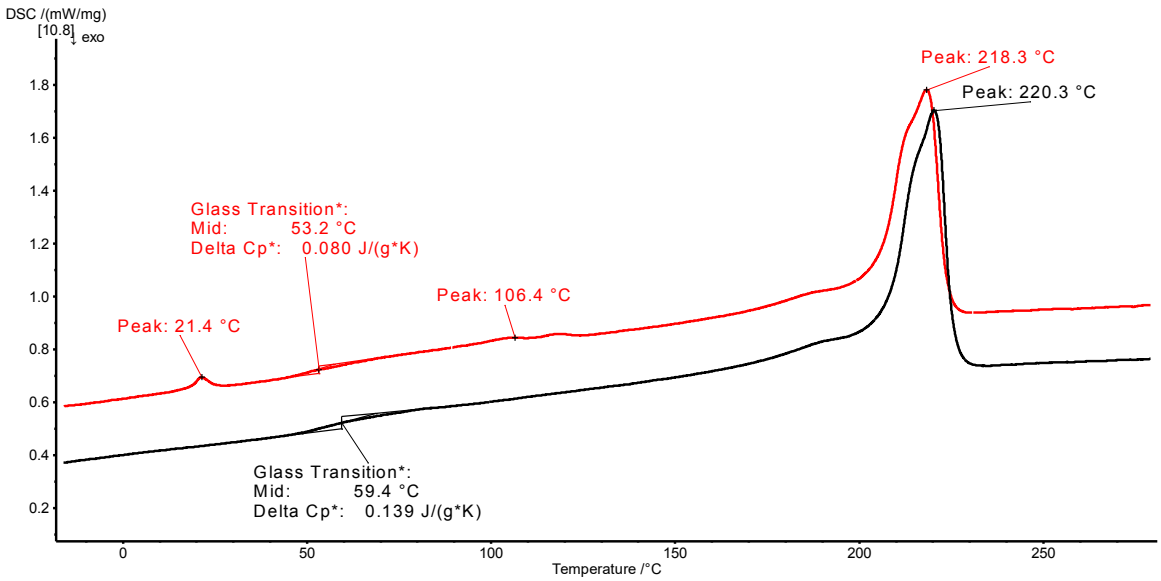

Fig. 1: DSC measurements of PA6 with 30% glass fibers (black curve) and PA6 with 30% glass fibers and impurities (red curve)

ENV-P-13

The Effect of Carboxymethyl Cellulose from Various Agriculture Wastes on the Viscosity and Physical Properties of Low Concentration Solution of Surfactant

Thritima Sritapunya[a,*], Gulisara Sommanas[a], Hathairat Surachaijarin[a]
[a]Division of Polymer Engineering Technology, Department of Mechanical Engineering Technology, College of Industrial Technology, King Mongkut's University of Technology North Bangkok, Bangkok, Thailand
*thritima.s@cit.kmutnb.ac.th

Keywords: Carboxymethyl Cellulose, Agriculture Wastes, Surfactant, Bio-thickener

The goal of this work was the synthesis and the improvement of viscosity of surfactant with carboxymethyl cellulose (CMC) from different types of agriculture wastes to reduce a quantity of waste. Banana peels, bagasse and corn silk as agricultural wastes were selected to synthesis CMC by extraction with NaOH to cellulose. Then cellulose was modified by reacting with monochloroacetic acid to obtain CMC which was investigated the functional group by Fourier Transform Infrared Spectrometer (FTIR). Moreover, a 0.5 wt% of synthesized CMC was added in 14 wt% of sodium lauryl sulfate (SLS) solution to estimate viscosity by rotational viscometer, transparency by visible spectrophotometer and emulsifying by observation, comparing with commercial thickener (PEG400). The results showed that CMCs of all three agriculture wastes can increase the viscosity of the surfactant solution and more increase than solution with PEG400. The SLS solution containing the CMC of corn silk provided the highest viscosity of 22.4 Cp by rotation speed of 250 rpm. However, the values of transparency and emulsifying of surfactant solution with CMCs are slightly lower than that of solution with PEG400, except for the addition of CMC from bagasse, it was precipitated in yellow color in a short time.

ENV-P-14

Determination and Molecular Study of Tannin in Coffee Pulp

Waleepan Rakitikul[a,*]
[a]*Program of Chemistry,Faculty of Science and Technology,*
Chiang Rai Rajabhat University,Chiang Rai, 57100, Thailand
*E-mail: em_waleepan_r@crru.ac.th

Keywords: Tannin, Coffee pulp, DFT, antioxidant.

Currently, Doi Chaang village is the biggest area producing coffee in Thailand. Throughout seedding to cupping, the pulp was removed from coffee cherry after harvesting and left as wast. Tannin was one of many composition in coffee pulp which affects soil nutrition and pH. This study using UV-Visible spectroscopy found 5.68% of condense tannin in coffee pulp. Moreover, the quantum mechanic calculation using Density Functional Theory (DFT) of both condense and hydrolyse tannin results that condense tannin has small HOMO-LUMO gap.

ENV-P-15

Synthesis of carbon nanoparticles from used mobil oil and benzene via solution plasma process

Napatsawan Seangarunthong[a], Parinya Khongthong[a], Gasidit Panomsuwan[b], and Apiluck Eiad-ua[a,*]

[a]College of Nanotechnology, King Mongkut's Institute of Technology Ladkrabang, Ladkrabang, Bangkok, 10520 Thailand
[b]NU-PCC Plasma Chemical Technology Laboratory, Petroleum and Petrochemical College, Pathumwan, 10330 Thailand
*E-mail address: apiluck.ei@kmitl.ac.th

Keywords: Used mobil oil, Carbon nanoparticles, Dye removal, Solution plasma process

Carbon nanoparticles were successfully synthesized from mixing ratio of used mobil oil and benzene via solution plasma process (SPP). In this research, we study the appropriate ratio between used mobil oil and benzene (80:20, 60:40, 40:60 and 20:80) to synthesize carbon nanoparticles. The scanning electron microscope (SEM) and fourier transform infrared spectroscopy (FTIR) were used for characterized morphology, particle size and functional group of carbon nanoparticles. From the results, the maximum yield of carbon nanoparticles is equal to 834 mg., derived from ratio of 20:80 with cluster particles. On the other hand, ratio of 80:20 became to a sheet.

ENV-P-16

Efficiency of Acoustic Noise Reduction Multilayer Wall from Activated Carbon and Rice Straw

Phiphop Narakaew[a,*], Samroeng Narakaew[b]
[a]*Department of Physics, Institute of Science, Lampang Rajabhat University, Muang, Lampang, Thailand, 52100*
[b]*Department of Applied Chemistry, Institute of Science, Lampang Rajabhat University, Muang, Lampang, Thailand, 52100*
*E-mail address corresponding author: aeey2542@yahoo.com

Keywords: Acoustic Noise Reduction Wall, Activated Carbon, Rice Straw

The present work aims with acoustic noise reduction multilayer wall which was built up of rice straw and highly porous rigid material derived from corncob and compared their sound absorption and sound transmission properties with commercial acoustic foam and fiber glass walls. The activated carbon bio-based solid was prepared by chemical activation, NaCl activated reagent, and physical characterized by FT-IR, BET, SEM, and EDX techniques. The results show that a mesopore carbon group with BET surface of 525.26 m^2/g. Four different layers were made of the 3.81 and 1 cm thick rice straw and activated carbon, respectively. The experimental data show that three layers of activated carbon sandwiched rice straw has sound insulation higher than others in the investigated frequency range of 50–10,000 Hz and the sound level at 120 dB.

ENV-P-17

Porous Carbon Material Prepared from Cassava Tuber Char using Chemical Activation Assisted Sonochemical Process

Kamonwan Aup-Ngoen[a,*], Mai Noipitak[a]
[a]*Ratchaburi Learning Park, Office of the President, King Mongkut's University of Technology Thonburi, Thung Khru, Bangkok, 10140, Thailand*
*Kamonwan.aup@kmutt.ac.th

Keywords: Porous carbon, Cassava tuber, Sonochemical process, Carbon support

The preparation of porous carbon material from low cost agricultural residues is presented in this work. The porous carbon was prepared from carbonized cassava tuber (cassava tuber char, CTC) using chemical activation assisted sonochemical process incorporating KOH as activating agent with the CTC:KOH ratio of 1:1 and 1:5. The physical properties such as proximate analysis, ultimate analysis and FT-IR spectra of raw materials were studied using cassava tuber collected from farmland in Kanchanaburi province. The structures of the starting material (precursor) play a significant role in influencing the quality and properties of the as-prepared porous carbon. It was found that the carbonization process created initial porosity in the cassava tuber char, and then the porosity development occurred through the chemical activation assisted sonochemical process at 80 ^{o}C for 4 hours of the experiments. The use of KOH has been found to be effective reagent in the porous carbon preparation. Furthermore, the influence of KOH impregnation ratios on the porosity characteristics of the carbon material product was also investigated in the activation step. Moreover, the properties of cassava tuber-porous carbon were characterized by SEM, FT-IR, XRD, TGA, and multipoint BET analysis. Finally, the application of porous carbon as the carbon support for ZnO photocatalyst has been evaluated and will be discussed by this research.

ENV-P-18

Utilization of rice straw and coconut coir in the fabrication of lightweight precast concretes

Pat Sooksaen [a, b]*, Patcharapon Sathukan [a], Nut Khunchomphu [a], Duangkamon Saetang [a]

[a] *Department of Materials Science and Engineering, Faculty of Engineering and Industrial Technology, Silpakorn University, Nakhon Pathom 73000 Thailand*
[b] *Center of Excellence for Petroleum, Petrochemicals and Advanced Materials, Chulalongkorn University, Bangkok, 10330, Thailand*
* *sooksaen_p@su.ac.th*

This research fabricated lightweight precast concretes using ordinary Portland cement and natural fibers. The fibers were rice straw and coconut coir, which are found in large quantity throughout Thailand as agricultural wastes. The use of natural fibers not only reduces the overall weight but also reduces manufacturing cost due to cement powder saving. Concretes were fabricated with low bulk densities while maintaining high compressive strength values. The amounts of fibers in concrete compositions in this study were: rice straw 30, 40 and 50%vol and rice straw 20%vol mixed with coconut coir 10%vol. The water to cement ratio was kept within the range 0.3-0.4 and the hydration period was carried for 28 days. Coarse rice straw fibers (1-5 mm) and fine rice straw fibers (<1 mm) were treated with 1% sodium hydroxide and found effective for removing hemicellulose, lignin and fatty acids. The treatment improved surface roughness of the cellulose fibers. The adhesion between the fiber surface and cement phase was greatly improved.

The study showed that the lowest density value was obtained from untreated 50%vol coarse rice straw samples (average value = 0.98 g/cm^3) . Lightweight concrete containing 20%vol fine rice straw fiber and 10%vol fine coconut coir in the composition showed high compressive strength value of 138.7 kg/cm^2 with bulk density reduced by 30% compared to cement mortar. The lowest thermal conductivity value was found in specimen with 20%vol fine rice straw mixed with 10%vol coconut coir (0.559 W/m.K) . Low thermal conductivity value of the lightweight concretes could be applied as pre-cast walls possessing energy saving function.

Keywords: Lightweight, Concrete, Rice straw, Coconut coir

***Corresponding Author:**
*Pat Sooksaen, Department of Materials Science and Engineering, Faculty of Engineering and Industrial Technology, Silpakorn University, Nakhon Pathom 73000 Thailand
Email: sooksaen_p@su.ac.th

ENV-P-19

Effect of Firing Conditions on Properties of Porous Hollow Cylindrical Zeolite NaA-Clay Substrates for TiO_2 Coating and Their Photodegradation of Lignin

Nithiwach Nawaukkaratharnant[a,*], Thanakorn Wasanapiarnpong[a,b], Pornapa Sujaridworakul[a,b], Charusporn Mongkolkachit[c]

[a] *Research Unit of Advanced Ceramics, Department of Materials Science, Faculty of Science, Chulalongkorn University, Bangkok, 10330, Thailand*
[b] *Center of Excellence on Petrochemical and Materials Technology, Bangkok, 10330, Thailand*
[c] *National Metal and Materials Technology Center, Pathumthani, 12120, Thailand*
*nithiwach.n@hotmail.com

Keywords: Zeolite NaA, Ball Clay, TiO_2 photocatalyst, Lignin degradation

Palm oil production is one of the major agro-industries in the southern part of Thailand. However, wastewater from the production which is released to a river has brown color due to a remaining of lignin. Photocatalytic technique is interesting to be applied for wastewater treatment. Titanium dioxide (TiO_2) is wildly used to decompose and degrade organic compounds, especially lignin, to be CO_2 and water with assistance of UV/solar light. Nevertheless, removing and recycling of fine TiO_2 powder after treatment process is still a challenge. In this study, hollow cylindrical zeolite-clay substrates were fabricated, following by coating of TiO_2 powder onto their surfaces. Zeolite NaA, ball clay and organic binder were mixed, extruded to be hollow cylindrical tubes and were cut into about 2.5 cm long. The specimens were fired at 650 - 800 °C for 2 hours before characterization. The specimens were tested physical properties, mechanical property and chemical property. After that the specimens were coated by TiO_2 suspension, dried and fired at 300°C for 1 hour. Polyurethane foam was then filled into the hole of the coated tube specimens to make the specimens can be floated on the surface of water. The photodegradation efficiency of lignin was determined under UV irradiation.

ENV-P-20

Adsorption of Reactive Dye (Blue 222) in Solution onto Chitosan-Rice Husk Ash Composite Beads Cross-Linked with Glutaraldehyde

Ratana Sananmuang[1,2]*, Wipharat Chuachuad Chaiyasith[1,2] and Kalayaporn Paroon[1,2]

[1]Research Center for Academic Exellence in Petroluem, Petrochemical, and Advanced Materials
Faculty of Science, Naresuan University, Phitsanulok, 65000, Thailand
[2]Department of Chemistry, Faculty of Science, Naresuan University, Phitsanulok, 65000, Thailand

*E-mail: ratanas@nu.ac.th

Keywords: Adsorption, Reactive dye, Cross-linked chitosan- rice husk ash composite

The dyes using in textile industry have undesirable effects either on human being or the environment. Adsorption is one of the most effective methods used for dye removal. Modified chitosan with some chemicals is recently interesting adsorbent. It would be benefit for dye removal by using modified chitosan with rice husk ash, a low cost material. The aim of this study was to prepare cross-linked chitosan-rice husk ash composite beads and to investigate its adsorption behavior for reactive dye (Blue 222). The BET, SEM and FTIR methods were used for characterization of composite beads. A batch experiment was conducted for adsorption. The adsorption study was carried out by investigating the effect of various parameters including pH (2-12), temperature (20, 30 and 40 °C), contact time (30 minutes and 1-12 hours) and initial concentration (10-850 mg/L). The dye concentrations were measured using UV / VIS Spectrophotometer at the wavelength of 611 nm. The results indicated that the BET of cross-linked chitosan-rice husk ash composite beads was 4.740 m^2/g. The optimum pH for dye adsorption was 2. The adsorption behavior was fitted to Freundlich isotherm.

ENV-P-21

Removal of Reactive Dye Red 195, Blue 222 and Yellow 145 in Solution with Polyaniline-Chitosan Membrane using Batch reactor

Ratana Sananmuang[1,2]*, Wipharat Chuachuad Chaiyasith[1,2] and Kanokwan Wongjan [1,2]

[1]*Research Center for Academic Exellence in Petroluem, Petrochemical, and Advanced Materials*
Faculty of Science, Naresuan University, Phitsanulok, 65000, Thailand
[2]*Department of Chemistry, Faculty of Science, Naresuan University, Phitsanulok, 65000, Thailand*

*E-mail: ratanas@nu.ac.th

Keywords: Reactive dye, Polyaniline- chitosan membrane, Removal

The objectives of this work were to investigate the characteristics of polyaniline-chitosan membrane by SEM, FTIR, tensile strength and percentage elongation. The removal of reactive dyes with polyaniline-chitosan membrane using the adsorption by batch experiment was conducted. Parameters influencing the adsorption were studied at room temperature including pH (2-10), contact time (5,30,60,90,120 and 150 mins) and initial concentration (10,25,50,100,250 and 500 mg/L). The dye concentrations were determined by UV / VIS Spectrophotometer at the wavelength of 423, 540 and 620 nm for Yellow 145, Red 195 and Blue 222, respectively. The results indicated that the tensile strength and percentage elongation of polyaniline-chitosan membrane were 0.032 kN/mm^2 and 15.53 %, respectively. It was found that polyaniline-chitosan membrane could adsorb all types of dye solution at the optimum pH 2. When the adsorption time increased, the adsorption efficiency increased accordingly. Moreover, the isotherm study showed that the polyaniline-chitosan membrane adsorption corresponded to Freundlich model. Besides, it was also found that polyaniline-chitosan membrane gave less adsorption efficiency of reactive dyes than that of chitosan.

Metals, Alloys & Intermetallic Compounds

MET-O-01

Utilization of Binding Ice Flakes with Pulp-Fibers as Fillings on Tube Forming

Takahiro Ohashi[a,*], **Lianpeng Ding**[a]
[a]*Kokushikan University, Setagaya, Tokyo, 154-8515, Japan*
* tohashi@kokushikan.ac.jp

Keywords: tube forming, fillings, hollow product, fiber-reinforced Ice (FRI)

This paper proposes a new filling medium on tube forming process, such as on bending or bulging. Lead or some low temperature melting alloy is conventionally utilized for a lost core in such a process; however, these alloys usually contain lead (e.g., Bi-Pb-Sn-In or Pb-Cd system alloys) or are expensive (e.g, In-Sn system alloys). The authors utilized binding ice flakes with fiber of recycled paper pulp instead of the above alloys for less expensive and more environmentally conscious processes. For the rapid preparation of the filling medium and the uniform mixture of ice and fibers with reducing the influence of the difference of their specific gravity, wet fibers were prepared and mixed with the cooled ice flakes. The moisture included in the fiber acted as an adhesive, and the medium worked as a fiber-reinforced ice. The authors conducted compression tests to find that its crushing strength is almost the same as the tensile strength of lead. In addition, we conducted PoC (Proof of Concept) tests with aluminum alloy tubes for the actual bending and bulging.

Acknowledgement
This research is partially supported by JSPS KAKENHI Grant Number 16K14138, Adaptable and Seamless Technology Transfer Program through target-driven R&D and Matching Planner Program from Japan Science and Technology Agency (JST), and the Amada Foundation Grant Number AF-2015044.

MET-O-02

Bending Limit Curves in Sheet Metal Bending Evaluation

Sansot Panich
King Mongkut´s University of Technology North Bangkok, Bangsue Bangkok, 10800, Thailand.
sansot.p@eng.kmutnb.ac.th

Keywords: Bending Limit Curves, Bendability, Pre-Strain, Material Characterization

For characterising formability of sheet metal materials the so called Forming Limit Curve (FLC) due to the ISO 12004-2 standard to predict material potential, subjected to static multi-axial in-plane load conditions has been developed during recent years. Many experiments have shown that sheet metals can undergo greater bending than predicted by the FLC. The main failure mechanism under bending loads is the intercrystalline fracture. This is due to the fact that the FLC describes first occurrence of membrane instability and no material failure in consequence of an intercrystalline fracture at bending.The FLC is not able to correctly predict the beginning of material failure under bending loads. Hence, a new failure criterion, the so-called Bending Limit Curve (BLC) has been created. However, experiment and simulative approaches concerning the BLC describe the material formability under pure bending conditions, such as flanging and hemming. Thus, the investigation of bendability of sheet metal is of great importance for the evaluation of process robustness for the production of mechanically joined sheet metal assemblies. This new failure criterion for bending processes can be determined with some basic testing and allows a much better prediction of material failure and critical bending strains. In this work, BLCs are determined experimentally for Advanced High Strength Steel grade DP1000, Stainless Steel grade SUS430 and Deep Drawing Steel grade SPCC having a thickness of 1.0 mm. The influence of various punch radii and level of pre-strain on the bending limits are investigated by using the established Three-Point-Bending-Test. Bendability of investigated materials are evaluated by using optical strain measurement system GOM-Aramis to determine maximal achievable bending strain on the specimen.The bending limit curve is a post-processing criterion to asses bending operations in sheet metal forming. To consider the whole strain path of the forming process, from pre-stretching over forming to the bending of the material, three-dimensional failure surfaces can be created precisely in this work. Such surfaces may predict critical bending strains for a given material depending on the bending radius.These surfaces can be implemented in forming simulations to better predict maximum bendability of a sheet metal material.

MET-O-03

Effect of Fold−Forging Techniques on Mechanical Properties of Medium Carbon Steel for Sword Making Process

K. Paveebunvipak*, K. Yu-on, T. Rotpaisarnkit, J. Sakavaratikul, V. Uthaisangsuk

Department of Mechanical Engineering, Faculty of Engineering
King Mongkut's University of Technology Thonburi
126 Pracha Uthit Road, Bang Mod, Thung Khru, Bangkok 10140, Thailand
*Corresponding Author: jing1524@hotmail.com

Keywords: Sword making / Fold-forging / Steel mixing technique / Nam–Phee steel / Mechanical properties

The traditional Samurai sword making procedure principally consists of metal forming at high temperature and quenching. Moreover, two specific techniques are included, namely, fold-forging and steel mixing. During the fold-forging process, steel specimen is heated, halved and forged into a desired semi-finished shape at high temperature. The steel mixing process aims to combine two steel grades with different ductilities in one sword. High carbon steel is basically used for the outer skin, whereas low carbon steel for the inner core of the sword. In this work, the fold-forging and steel mixing processes were applied to the steel grade AISI 1055, a low carbon steel and local Nam-Phee steel, which has been commonly used to produce the known Nam-Phee sword for many years. Afterwards, mechanical properties of produced specimens were investigated and compared. Four conditions of steel specimens were considered, in which the examined steels and both techniques were differently combined. It was found that Nam-Phee steel specimens incorporating the fold-forging technique obviously showed more homogenous and finer microstructure. Their tensile strength, flexural strength and absorbed impact energy were significantly increased. The mechanical properties of the developed Nam-Phee steel were close to those of the Tamahagane steel for Samurai sword. Additionally, AISI 1055 steel specimens with a low carbon ductile steel in the core exhibited much higher flexural strength and impact energy.

MET-O-05

Sintered Dual-phase Steels with Different Alloy Compositions

Monnapas Morakotjinda, Nattaya Tosangthum, Rungtip Krataitong, Pongsak Wila, Thanyaporn Yodkaew and Ruangdaj Tongsri*
Particulate Materials Processing Technology Laboratory (PMPT), National Metal and Materials Technology Center, 114 Paholyothin Road, Khlong Nueng, Khlong Luang, Pathum Thani, 12120, Thailand
*Email: ruangdt@mtec.or.th

Keywords: Sintered dual-phase steels, Pearlite, Bainite, Mechanical properties

Sintered dual-phase steels, consisting of soft and hard structures in their microstructures, were designed on the basis of alloying element effects on continuous cooling transformations (CCT) diagrams and produced via powder metallurgical method. Four different prealloyed powders, e.g., Fe-0.85Mo, Fe-1.5Mo, Fe-1.5Cr-0.2Mo and Fe-3.0Cr-0.5Mo, were added with the same graphite content of 0.3 wt.%. Green parts of the prealloyed powders mixed with such amount of graphite were sintered at 1280 °C for 45 min. After sintering, the sintered parts were allowed to cool in a furnace with a low cooling rate of 0.1 °C/s. All the investigated sintered steels showed dual-phase nature with different types and volume fractions of hard structures. The sintered Fe-1.5Cr-0.2Mo-0.3C steel had pearlite structure as a hard structure whereas the sintered Fe-0.85Mo-0.3C, Fe-1.5Mo-0.3C, and Fe-3.0Cr-0.5Mo-0.3C steels exhibited bainitic grains as hard structures. The hard structure type, volume fraction and morphology seemed to control tensile properties of the sintered dual-phase steels investigated. Denser or finer bainitic structure contributed to tensile strengths higher than its volume fraction. Pearlitic structure contributed the least to tensile strengths. The different types of the hard structures are attributed to the effects of Cr and Mo on the CCT diagrams. Hardenability of the sintered dual-phase steels by bainitic structure was due to high contents of Mo and/or Cr elements. Both alloying elements move both of the ferrite and pearlite transformation curves to the right hand side. The makes steels containing high Mo and Cr be able to harden under slow cooling rates. The sintered Fe-1.5Cr-0.2Mo-0.3C steel showed low hardenability due to low Mo content, by which the pearlite transformation curve is slightly affected.

MET-O-06

Widmanstätten Ferrite in Fast-Cooled Ultralow Carbon Fe-Cr-Mo Steel

Ruangdaj Tongsri [1]*, Wananurat Srijampan [2], Amporn Wiengmoon [2], Namtip Nakeiam[3], Bhanu Vetayanukul [1], Dhritti Tanprayoon [1], Monnapas Morakotjinda [1], Rungtip Krataitong [1], Thanyaporn Yotkaew [1], Nattaya Tosangthum [1] and Ussadawut Patakham[1]

[1] Powder Metallurgy Research and Development Unit (PM_RDU), Thailand National Metal and Materials Technology Center, 114 Paholyothin Road, Khlong Nueng, Khlong Luang, PathumThani 12120, Thailand

[2] Department of Physics, Faculty of Science, Naresuan University, Pitsanulok-Nakhon Sawan Road, Tha Pho, Muang, Pitsanulok 65000 Thailand

[3] Department of Materials Science and Technology, Faculty of Science, Prince of Songkhla University, Karnjanavanit Soi 15 Rd, Hat Yai, Hat Yai District, Songkhla 90110 Thailand

*Email: ruangdt@mtec.or.th

Keywords: Widmanstätten ferrite, Transformation, Autocatalytic nucleation, Diffusional growth

Widmanstätten ferrite (α_W) was observed in sintered Fe-Cr-Mo steels, with ultralow carbon content of 0.0055 wt.% and low carbon content of 0.1 wt.%, which were cooled with cooling rates of ≥ 4.0 °C/s. The α_W sub-unit plate nucleation sites were observed on both the prior austenite (γ) grain boundaries so it was identified as primary α_W and on allotriomorphic ferrite (α_A) so called secondary α_W. Clearly observed that new sub-unit plates of the α_W nucleated on the broad faces of the previously formed α_W. This type of nucleation was defined as autocatalytic or sympathetic nucleation. The sub-unit plate growth, controlled by diffusional mode, was generally agreed by materials researchers. Lengthening of the sub-unit plates was found to depend on the pre-alloyed Fe-Cr-Mo steel powder particle size. The sub-unit plates in the sintered steels produced from < 90 μm and ≥ 90 μm powder particles showed close values of thickness and width but longer plates were observed in the former sintered steel. The presence of α_W caused ferritic grain refinement and tensile strength increase with ductility loss.

MET-O-07

Interaction between Recrystallization and Phase Transformation during Hot Squeezing of Sintered Dual-phase Fe-Cr-Mo-C Steels

Bhanu Vetayanugul[a], Natthawut Suebsing[b], Dhritti Tanprayoon[a], Monnapas Morakotjinda [a], Rungtip Krataitong [a], Thanyaporn Yotkaew [a], Pongsak Wila[a], Amornsak Rengsomboon [a], Ussadawut Patakham [a] and Ruangdaj Tongsri [a*]

[a] Particulate Materials Processing Technology Laboratory ,National Metal and Materials Technology Center, 114 Paholyothin Road, Khlong Nueng, Khlong Luang, PathumThani 12120, Thailand

[b] Department of Physics, Faculty of Science, Ubonratchathani University, 85 Muang Srikhai Subdistrict, Warin Chamrap District, Ubonratchathani 34190 Thailand

* Email: ruangdt@mtec.or.th

Keywords: Hot forming, Dynamic recrystallization, Misorientation, Texture

The sintered Fe-Cr-Mo-0.3C steel showed dual-phase microstructure, consisting of ferrite and bainite grains, after sintering and slow cooling of 0.1 °C/s. To improve density and modify microstructure of the sintered steel, hot squeezing was performed. In the material processing, the as-sintered steel specimens were reheated to 1200 °C for 30 min and then squeezed by a hydraulic press. The hot squeezing took several seconds before the deformed specimens were cooled by air, fan and oil. After hot squeezing, the processed steel showed increased density of up to 7.7 g/cm^3. Grained sizes of the hot-squeezed steel were refined compared to those of the sintered steel. Increase of high misorientation angle (HMA) fraction, as determined by electron backscatter diffraction (EBSD) technique, was observed in the hot-squeezed steel. Texture of the hot-squeezed steel, as determined by pole figure, also changed. The evidences of grain refinement, HMA and texture development in some directions indicated dynamic recrystallization of austenite grains. Microstructures of the hot-squeezed steels showed finer and denser bainite structure, particularly in the samples experienced fast cooling rates. For this reason, the hardness values increased with increasing cooling rates. As the bainitic transformation start temperature was lower than the hot squeezing temperature, the fine-scale recrystallized austenite grains transformed to bainitic structure during cooling. With a high hardness of bainitic structure, together with press and sinter technology, the sintered Fe-Cr-Mo-0.3C steel can be further developed, using a powder forging route, for producing a high strength automotive part.

MET-O-08

Dynamic Recrystallization and Cr_2O_3Pinning Effect during Hot Squeezing of Sintered Ultralow Carbon Fe-Cr-Mo Steels

Amornsak Rengsomboon[a], Bhanu Vetayanukul[b], Jakarin Taorit[c], Dhritti Tanprayoon[b], Monnapas Morakotjinda[b], Rungtip Krataitong[b], Nattaya Tosangthum[b], Thanyaporn Yotkaew[b], Pongsak Wila[b], Ussadawut Patakham[b] and Ruangdaj Tongsri[b*]

[a]Foundry Engineering Laboratory and [b]Particulate Materials Processing Technology Laboratory (PMPT),Thailand National Metal and Materials Technology Center, 114 Paholyothin Road, Khlong Nueng, Khlong Luang, PathumThani, 12120, Thailand

[c]Department of Physics, Faculty of Science, Ubonratchathani University, 85 Muang Srikhai Subdistrict, Warin Chamrap District, Ubonratchathan, 34190, Thailand

* Email: ruangdt@mtec.or.th

Keywords: Hot forming, Dynamic recrystallization, Misorientation, Texture

The sintered Fe-3.0Cr-0.5Mo-0.001C steel showed microstructure consisting of coarse polygonal ferrite (PF) grains and intergranular pores (12% porosity) after sintering and slow cooling of 0.1 °C/s. The specimens of the sintered Fe-3.0Cr-0.5Mo-0.001C steel were hot-squeezed and followed by cooling in different media, e.g., air cooling, fan cooling and oil cooling. The hot-squeezed showed fine grains with reduction of porosity. The hot-squeezed grain sizes, obtained from different cooling media showed slightly different. Electron backscatter diffraction (EBSD) showed changes of materials texture and the increase of high angle misorientation. The finer grain size, texture development and high angle misorientation indicated dynamic recrystallization of the austenite grains during hot squeezing. The insensitivity of the hot-squeezed grains with different cooling media was puzzled. However, the careful characterzation of the hot-squeezed specimens using scanning electron microscopy equipped with energy dispersive spectrocropy showed that the grain boundaries were pinned with chomium oxide particles, which formed during reheating the sintered Fe-3.0Cr-0.5Mo-0.001C steel before hot squeezing. Chomium oxide formation deep down the reheating specimens was due to the interconnected nature of pores in the sintered parts. After hot squeezing with porosity reduction, finer grain size and pinning effect of chromium oxide particles, the hot squeezed Fe-3.0Cr-0.5Mo-0.001C steel showed improved hardness.

MET-O-09

Understanding the Microstructural Features in High-Pressure Die Castings by Analogy with Granular Materials and Suspensions

Somboon Otarawanna[a,*]

[a] *National Metal and Materials Technology Center, Pathumthani 12120, Thailand*
*Corresponding Author: E-mail address: somboono@mtec.or.th

Keywords: Die casting, Defect band, Reynolds' dilatancy, Surface layer

High-pressure die casting (HPDC) is a shape casting process suitable for producing large quantities of complex thin-walled components requiring strict dimensional tolerance and good surface finish. Common alloys for HPDC include aluminum, magnesium and zinc alloys. The HPDC process is relatively complex compared to other shape casting processes, such as sand casting, gravity die casting and low-pressure die casting (LPDC). In the HPDC process, the alloy is injected at high velocity into steel die followed by the application of high pressure to the solidifying alloy, once the die is completely filled. Due to the combination of complex flow/deformation behavior and high cooling rates of the solidifying alloy during HPDC, microstructure formation during the process is not yet fully understood. Developing a better understanding of microstructure formation in HPDC parts is essential for process improvement and better process control that can lead to better part quality and/or higher productivity. The microstructural features in HPDC parts are significantly different to those in other shape casting processes. In this work, the salient microstructural features in HPDC parts are presented and their formation is illustrated by analogy with granular materials and suspensions. The salient microstructural features discussed include defect bands and the surface layer. Defect bands are bands of positive macrosegregation and/or porosity typically follow the surface contour. The formation of defect bands is linked to strain localization and Reynolds' dilatancy in compacted granular materials. The surface layer is a thin layer of material near the casting surface containing a different microstructure compared to the surroundings. The formation of the surface layer is related to the particle migration away from the slip region in suspension flow.

MET-O-10

The Effect of Bottom Ash Additions on the Properties of Sintered Bronze-Graphite Composites

Usanee Pantulap[a*], Ryan C. McCuiston [a], Chiraporn Auechalitanukul[a]

[a]King Mongkut's University of Technology Thonburi, Thung Khru, Bangkok, 10140, Thailand
*usanee@dss.go.th

Keywords: Bottom ash, Bronze, Friction Material, Powder Metallurgy

The aim of this research was to study the effect of bottom ash additions to a bronze-graphite composite, on the sintering behavior as well as on the resultant physical, mechanical and tribological properties. The composites were produced by a powder metallurgy technique from prealloyed Cu-10Sn bronze powder, graphite powder and milled bottom ash powder. The compositions studied were Cu-10Sn bronze with a constant 5 wt. % graphite, and 0-20 wt. % bottom ash. Samples were die compacted under 795 MPa and sintered at 850 ºC for 30 minutes in an open atmosphere furnace. It was found that the sintered density of the composites decreased with increasing amounts of bottom ash. The hardness of the samples increased with bottom ash additions and reached a maximum at 5 wt. % and decreased with further additions. The frictional properties were studied using a ball-on-disc test at ambient temperature. It was found that both the friction coefficient and the wear rate were increased with increasing amounts of bottom ash.

MET-O-11

Properties of Sintered Bronze-Graphite Containing Natural Anhydrite

Chiraporn Auechalitanukul[1] *, Ryan McCuiston[1] , Benjawan Bunlangsup[1], Chanattha Naikorn[1] and Sudachuan Tapanaun[1]
[1]*King Mongkut's University of Technology Thonburi, Thung Khru, Bangkok, Thailand*
*chiraporn.aue@kmutt.ac.th

Keywords: Bronze, Anhydrite, Friction, Microstructure

This study examined the effect of natural anhydrite ($CaSO_4$) additions on the microstructure and frictional properties of a 95bronze-5graphite material prepared by a powder metallurgy process. Natural anhydrite powder ranging from 2 to 8 weight percent was added to a premixed powder composed of copper and tin and mixed before the graphite was added. The powder mixture was compacted into disc shaped samples under a pressure of 500 MPa. The compacted samples were sintered at 750 ºC for 30 minute in a reducing atmosphere. The green and sintered densities of the samples were measured. A microstructural analysis of the sintered samples was also performed. It was found that the green density of the samples decreased with increased anhydrite content. The sintered densities were lower than the green densities due to sample expansion. A finer microstructure was observed in the samples containing anhydrite. The anhydrite additions resulted in the reduction of both the friction coefficient and wear of the bronze-graphite samples. The amount of anhydrite from 2-8 weight percent clearly altered the microstructure of the bronze-graphite samples, however, the level of reduction of the friction coefficient and wear were quite similar among the anhydrite containing samples.

MET-O-12

Mechanical Properties of As-Exposed Al-SiCp Composite Fabricated by Powder Injection Moulding

Tapany Patcharawit[a,*], Arada Nkeekoa[a], Wanphen Tongkerd[a], Sutam Takhampom[a] Supitcha Lapkeaw[a], Nutthita Chuankrerkkul[b]

[a]*School of Metallurgical Engineering, Suranaree University of Technology, 111 University Avenue, Suranaree Subdistrict, Meung, Nakhon Ratchasima, 30000, Thailand*

[b]*The Metallurgy and Materials Science Research Institute, Chulalongkorn University, Phayatai Rd., Pathumwan, Bangkok, 10330, Thailand*

* tapany@sut.ac.th

Keywords: hardness, tensile, composite, powder injection moulding

Aluminium-SiC_p composites are of interest for engineering applications such as microelectronic packaging for aerospace, automotive and microwave applications. This research investigated mechanical properties of powder injection moulded SiC_p-reinforced aluminium composite after exposure at moderate temperatures. Aluminium powder - 20 vol.% silicon carbide particulate feedstock was prepared at 55% solid loading using multicomponent binder. Powder injection moulding was carried out at 170°C prior to sintering at 680°C, followed by solution treatment at 500°C plus artificial aging at 150°C/6hrs. Moderate temperature exposures at 100, 200 and 300°C for 10 and 100 hrs. The as-exposed specimens have been subjected to hardness and tensile tests at room temperature. Microstructure and phase analyses have been evaluated to correlate microstructure-property relations. It was found that as sintered and aged samples provided micro Vickers hardness at 143.0 and 171.6 Hv. Room temperature tensile strength values were however relatively low at 44.6 and 67.8 MPa for as sintered and aged conditions respectively. Increasing exposure temperature and time gave different trends of hardness. Exposure for 10 hours provided increasing hardness with increasing exposure temperature, while exposure for 100 hours led to an opposite result. The maximum micro Vickers hardness was obtained at 182.2 H_v for exposed Al-SiC_p composite at 300°C for 10 hours. Tensile strength was however found deleterious with increasing both exposure temperatures and times. The maximum tensile strength was achieved at 191.2 MPa for exposed Al-SiC_p composite at 100°C for 100 hours. The formation of AlN, Mg_2Si and Al_2Cu was observed in both heat-treated and as-exposed conditions. Furthermore, the highest temperature exposure at 300°C and extended exposure time at 100 hours resulted in the lowest hardness and tensile properties due possibly to the loss of coherency of Al_2Cu precipitates.

MET-O-13

Effect of Aluminum Addition on $Al_xCoFeMnNiZn$ Multi-Component Production

Amnart Suksamran[a], Nawarat Worauaychai[a,*], Nattaya Tosangthum[b], Thanyaporn Yotkaew[b], Rungtip Krataitong[b], Pongsak Wila[b], Ruangdaj Tongsri[b]

[a]Department of Materials Technology, Faculty of Science, Ramkhamhaeng University, Bangkok, 10240, Thailand

[b]Powder Metallurgy Research and Development Unit (PM_RDU), Thailand National Metal and Materials Technology Center, 114 Paholyothin Road, Khlong Nueng, Khlong Luang, Pathum Thani 12120 Thailand

**E-mail: nawaratwor@gmail.com*

Keywords: Multi-component alloys, Mechanical Alloying and Melting Process (MAM), Ni-Based Superalloy, High Entropy Alloys

Five multi-component alloy (MCA) formulations of CoFeMnNiZn (MCA01), $Al_{0.5}CoFeMnNiZn$ (MCA02), $Al_{1.0}CoFeMnNiZn$ (MCA03), $Co_5Fe_5Mn_{30}Ni_{20}Zn_{40}$ (MCA04) and $Al_{8.4}Co_{4.6}Fe_{4.6}Mn_{27}Ni_{18.4}Zn_{37}$ (MCA05) were prepared by mechanical alloying and melting process (MAM). Six-component alloys of MCA01-MCA05 were designed using empirical formulae for high entropy alloys. Phase formation and microstructure of MCA were evaluated by X-ray diffraction (XRD) and scanning electron microscopy (SEM). The results showed that MCA01 was partially melted by MAM process. However, MCA02-MCA04 could be melted and casted by MAM process. The microstructures of as-casted MCA02 and MCA03 showed dendritic solidification. Nevertheless, the as-casted MCA04 showed microstructure similar to that of Ni-based superalloy, i.e., the as-casted MCA04 consisted of dendritic γ matrix and interdendritic γ′ phase. Moreover, egg type core shell structure was found in the interdendritic regions of the MCA05 alloy. In addition, the Al-added MCA02 and MCA03 alloys showed crystal structures of FCC1, FCC2 and BCC. MCA4 alloy demonstrated crystal structure of FCC whereas MCA05 alloy had crystal structures of FCC and Primitive Cubic.

MET-O-14

Effect of Si Content on Mechanical Properties of Ti-Si-N Ternary Alloys Prepared by Spark Plasma Sintering

P. Khemglad[a], J. Kajornchaiyakul[b], K. Kondoh[c] and A. Khantachawana[d,*]
[a]*Department of Mechanical Engineering, Faculty of Engineering, King Mongkut's University of Technology Thonburi, 126 Pracha Uthit Rd., Bang Mod, Thung Khru, Bangkok 10140, Thailand*
[b]*National Metal and Materials Technology Center, Pathumthani 12120,Thailand*
[c]*Joining and Welding Research Institute, Osaka University, 11-1, Mihogaoka, Ibaraki, Osaka 567-0047, Japan*
[d]*Department of Mechanical Engineering and Biological Engineering Program, Faculty of Engineering, King Mongkut's University of Technology Thonburi, 126 Pracha Uthit Rd., Bang Mod, Thung Khru, Bangkok 10140, Thailand*
*anak.kha@kmutt.ac.th

Keywords: Ti-Si-N Ternary Alloys, Spark Plasma Sintering, Substrate Powders

In the present work, the strengthen mechanism of Ti-Si-N ternary alloys prepared by Spark Plasma Sintering (SPS) was investigated. Ti, Si and TiN substrate powders were prepared in order to obtain nominal composition of Ti-0.35Si-1TiN and Ti-0.7Si-1TiN (wt %). Homogenization was performed before extrusion. Microstructure and phase identification were analyzed by Optical Microscope (OM) and X-ray diffraction (XRD). In order to evaluate the mechanical properties of extruded specimens, micro hardness test and tensile test were carried out. The XRD results show that no Si and TiN particles are remained after SPS and no any reaction caused of intermetallic compound during heat treatment and extrusion processes. It is found that the abnormal phase with high N-content was observed in matrix phase. It is also obvious that increasing Si from 0.35Si to 0.7Si (wt %) can increase yield stress and ultimate tensile stress from 1006±15 to 1092±5 MPa and 1089±10 to 1170±10 MPa, respectively. Hence, the strengthening mechanism by addition Si content into Ti-1TiN (wt %) is only solid solution mechanism.

MET-O-15

Role of SiC in Sintered Fe-Mo-Si-C Steels

Thanyaporn Yotkaew[a], Monapas Morakotjinda[a], Kridsana Poolnak[b], Amonrat Duangpeth[b], Piyanuch Nakpong[b], Rungtip Krataitong[a], Nattaya Tosangthum[a] and Ruangdaj Tongsri[a]*

[a]Particulate Materials Processing Technology Laboratory (PMPT), Thailand National Metal and Materials Technology Center, 114 Paholyothin Road, Khlong Nueng, Khlong Luang, Pathum Thani 12120, Thailand

[b] Department of Chemistry, Faculty of Science and Technology, Rajamangala University of Technology Krungthep, Bangkok 10120, Thailand

*Email: ruangdt@mtec.or.th

Keywords: Fe-Mo steel, Bainite, Pearlite, Retained austenite

Silicon additions with proper content range can suppress the cementite (Fe_3C) formation in carbide-free bainitic steels, classified as advanced high-strength steels. Since silicon carbide (SiC) mixed with Fe-based powder decomposed at sintering temperatures and produced alloying Si and C elements it was used for alloying with pre-alloyed Fe-0.85Mo and Fe-1.5Mo powders to make sintered Fe-Mo-Si-C steels with microstructural variety depending on SiC content and cooling rates after sintering. Varied contents of SiC powder, e.g., 1, 2, 3, 4 and 5 wt.%, were mixed with the pre-alloyed powders. The powder mixtures were cold-compacted and sintered at 1280 °C for 45 min. After sintering, specimens were cooled with different cooling rates of 0.1 and 5.4 °C/s. The added SiC powder contents of 1 and 2 wt.% decomposed completely into elemental Si and C atoms, which dissolved in austenite Fe-Mo grains during sintering. The austenite Fe-Mo-Si-C transformed to ferrite, bainite, martensite and retrained austenite, depending on carbon content and cooling rate. Carbide-free bainitic steel, characterized by lower bainite structure and filmy retained austenite, could be produced by sintering the Fe-1.5Mo + 2 wt.% SiC powder compact and by fast cooling of 5.4 °C/s. The added SiC powder contents of 3 and 4 wt.% decomposed partially and/or completely into elemental Si and C atoms, which dissolved in austenite Fe-Mo grains during sintering. In addition to the dissolution of Si and C atoms in austenite Fe-Mo grains, the high contents of dissolved Si and C caused local melting at SiC peripheries. During slow cooling of 0.1 °C/s, graphite solidification from the melt consumed carbon from surrounding austenite Fe-Mo grains and resulted in the formation ferrite rings around the prior SiC sites. The Fe-Mo matrix next to the ferrite rings were pearlite and mixed pearlite and bainite. This type of microstructure resembled to that of ductile cast iron. With fast cooling rate of 5.4 °C/s, the microstructure consisting of bainitic/martensitic Fe-Mo matrix surrounding the prior SiC sites without ferrite ring formation was observed. Sintering of the Fe-Mo + 5 wt.% SiC powder compacts resulted in compact melting. The sintered Fe-Mo-Si-C steels with ductile iron-like microstructure showed promising tensile properties.

MET-O-16

Effect of SiC Particle Size on Sintered Fe-Mo-Si-C Steels

Pongsak Wila[a], Pimpichaya Thamwaro[b], Bhanu Vetayanukul[a], Dhritti Tanprayoon[a], Monnapas Morakotjinda[a], Rungtip Krataitong[a], Thanyaporn Yotkaew[a], Nattaya Tosangthum[a], Ussadawut Patakham[a] and Ruangdaj Tongsri[a]*

[a] *Particulate Materials Processing Technology Laboratory (PMPT), Thailand National Metal and Materials Technology Center, 114 Paholyothin Road, Khlong Nueng, Khlong Luang, PathumThani, 12120, Thailand*

[b] *Department of Materials Engineering and Production Technology, Faculty of Engineering, King Mongkut University of Technology North Bangkok, Thailand*

* Email: ruangdt@mtec.or.th

Keywords: Fe-Mo-Si-C steel, Sintering, SiC decomposition, Diffusion

Generally, particulate materials have surface areas inversely proportional to their particle sizes. The surface area is one of the prime factors controlling interaction between two or more particulate material types. In the preparation of sintered Fe-Mo-Si-C steels, the interaction between pre-alloyed Fe-Mo and SiC powders is the key phenomenon. Difference in SiC particle size or surface area that will differentiate the final material microstructure and property is the motivation for this research. The sintered Fe-Mo-Si-C steels having microstructure similar to that of a ductile cast iron, were designed based on thermodynamic background regarding SiC decomposition, Si diffusion into Fe-Mo matrix and C precipitation. This type of material is expected to replace typical ductile cast irons in some applications, which require delicate and small parts with better tolerance. The sintered steels were produced by sintering the powder mixture compacts (Fe-Mo + 4 wt. SiC) and slow cooling after sintering. Added SiC powder particle sizes were varied as < 20 μm, 20-45 μm and > 45 μm. The common microstructural feature of the sintered steels was that black particles were enveloped with ferrite grains, which were further surrounded by pearlite. The ceramic particle size showed effects on microstructure, physical and mechanical property of the sintered steels. Sintered density, tensile strength, elongation and hardness of the sintered steels decreased with increasing SiC powder particle size. The decreases of such properties with increasing SiC particle size could be related to black particle distribution and the ratio of pearlite : ferrite : black particle. The nature of interaction between SiC and Fe-Mo matrix was also dependent on the SiC particle size. During sintering the interaction between a SiC particle and Fe-Mo matrix resulted in formation of Fe-Mo-Si-C alloy and local melting within the prior SiC particle periphery. During cooling, graphite precipitated by nucleation on the surface of non-melted Fe-Mo-Si-C alloy and growth radially. The ratio between solidified graphite and the non-melted Fe-Mo-Si-C alloy depended on SiC particle size. Small SiC particles showed large proportion of solidified graphite and vice versa.

MET-O-17

Retained Austenite in Sintered Bainitic Fe-Mo-Si-C Steels

Dhritti Tanprayoon[a], Monapas Morakotjinda[a], Suphakan Kijamnajsuk[a], Kridsana Poolnak[b], Amonrat Duangpeth[b], Rungtip Krataitong[a], Thanyaporn Yotkaew[a], Nattaya Tosangthum[a] and Ruangdaj Tongsri[a]*

[a]Particulate Materials Processing Technology Laboratory (PMPT), Thailand National Metal and Materials Technology Center, 114 Paholyothin Road, KhlongNueng, KhlongLuang, PathumThani, 12120, Thailand

[b]Department of Chemistry, Faculty of Science and Technology, Rajamangala University of Technology Krungthep, Bangkok 10120, Thailand

* Email: ruangdt@mtec.or.th

Keywords: Characterization, Retained austenite, Bainite, Martensite

In the development of the advanced steels, high amount of the retained austenite is utilized to obtain the TRIP mechanism. Silicon is one of the alloying elements that help stabilizing the retained austenite. Combined with its price competitiveness, this element is proved to be attractive for the industries.

In this study, the microstructure and the mechanical properties of Fe-C-Mo-Si materials were investigated. Silicon carbide (SiC) up to 4 wt.% was introduced to the pre-alloyed Fe-0.85Mo powder as the silicon and carbon sources. The samples were sintered at 1280°C in vacuum. After that, they were quenched in 5 bar N2. Retained austenite was found in the sintered parts with bainitic and martensitic structures. The presence of bulk retained austenite indicated an incomplete bainitic transformation which was the result from silicon, a carbide suppressing element. Moreover, the porosities of the sample with 0.4% SiC were greatly decreased by the formation of the liquid phase during the sintering process.

MET-O-18

Modification of Microstructure and Tensile Property of Sintered Fe-Cr-Mo-C Steel by Nickel Addition

Nattaya Tosangthum, Monnapas Morakotjinda, Rungtip Krataitong, Pongsak Wila, Thanyaporn Yodkaew and Ruangdaj Tongsri*
Particulate Materials Processing Technology Laboratory (PMPT), National Metal and Materials Technology Center, 114 Paholyothin Road, Khlong Nueng, Khlong Luang, Pathum Thani 12120, Thailand
*Email: ruangdt@mtec.or.th

Keywords: Fe-Cr-Mo-Ni-C steel, Phase transformation, Ferrite, Bainite

Nickel (Ni) is one of the alloying elements promoting the formation of acicular ferrite at the expense of proeutectoid ferrite. The Ni addition reduces the steady-state nucleation rates, J_s^*, of grain boundary ferrite allotriomorph in Fe-C-Ni alloys. Due to such reasons, Ni was added to modify the microstructure of the sintered steel, investigated in this study, with the aim of improved mechanical properties. The sintered steel, produced from pre-alloyed Fe-Cr-Mo powder mixed with 0.3 wt.% C, was modified by Ni addition and cooling rate. The alloy compositional change was performed additions of varied nickel contents of 1.0, 1.5, 2.0, 2.5 and 3.0 wt.%. The material processing variables were investigated by using two different cooling rates of 0.1 and 5.4 °C/s. Under the cooling rate of 0.1 °C/s, the sintered Fe-Cr-Mo-3C steel without Ni addition showed dual-phase microstructure consisting of ferrite (soft phase) and bainite (hard structure). With Ni additions, the dual-phase microstructure was replaced by bainitic structure. Microstructural heterogeneity was observed due to the presence of Ni-rich areas, which increased with increasing added Ni contents. Under the cooling rate of 5.4 °C/s, the sintered Fe-Cr-Mo-3C steels with and without Ni additions showed bainitic structure. Microstructural heterogeneity was similar to that of slowly cooled steel. Ni additions not only modified the sintered steel microstructure but increased tensile strength and elongation. In general, Ni pushes the C-curve of pearlite transformation to the right hand side and lowers the martensite start temperature. The absence of ferrite from the sintered steel with only 1 wt.% Ni addition and slowly cooled at 0.1 °C/s suggests that Ni strongly suppresses the austenite → ferrite transformation. In another word, Ni promotes bainite formation in the sintered Fe-Cr-Mo-Ni-C steels.

MET-O-19

Combination Effects of Nickel and Graphite on Sintered Fe-Mo + SiC Alloy

Rungtip Krataitong[a], Kornrawee Munpakdee[b], Dhritti Tanprayoon[a], Monnapas Morakotjinda[a], Bhanu Vetayanukul[a], Thanyaporn Yotkaew[a], Nattaya Tosangthum[a], Pongsak Wila[a], Ussadawut Patakham[a] and Ruangdaj Tongsri [a]*

[a]Particulate Materials Processing Technology Laboratory (PMPT), Thailand National Metal and Materials Technology Center, 114 Paholyothin Road, Khlong Nueng, Khlong Luang, PathumThani, 12120, Thailand

[b]Department of Materials Engineering and Production Technology, Faculty of Engineering, King Mongkut University of Technology North Bangkok, Thailand

* Email : ruangdt@mtec.or.th

Keywords: Sintered Fe-Mo steel, Spherical particle, Vermicular particle, Bainite

The sintered Fe-Mo + 4 wt.% SiC steels show microstructure similar to that of ductile cast iron, i.e., black spheroidal particle surrounded with a ring of ferritic grains, which are further enveloped with mixed dominant pearlite and bainite structure. In this work, such microstructures were modified by addition of 2 and 4 wt.% nickel and 0.1, 0.2, 0.3 and 0.4 wt.% graphite. It was found that the combinations of fixed 2 wt.% nickel with varied graphite contents caused changes, i.e., change of black spheroidal particles to black vermicular particles, the decrease of ferritic grain volume fraction and the change from mixed dominant pearlite and bainite structure to upper bainite structure. By fixing nickel content at 4 wt.% but varying graphite contents, the change of black spheroidal particles to black vermicular particles still persisted whereas the rings of ferritic grains disappeared. In another word, both black spheroidal and vermicular particles were surrounded by upper bainite structure. This type of structure was similar to that of an austempered ductile iron (ADI). Despite the upper bainite was present, the additions of nickel within the investigated contents showed no significant effect on tensile strength increase but elongation value reduction.

MET-O-20

Wear Properties of Sintered Fe-Mo-Si-C Steels with Spheroidal Graphite Iron/Compacted Graphite Iron-like Microstructures

Kittikhun Ruangchai[a], Amporn Wiengmoon[a], Monnapas Morakotjinda[b], Rungtip Krataitong[b], Dhritti Tanprayoon[b], Thanyaporn Yotkaew[b], Nattaya Tosangthum[b], Ussadawut Patakham[b] and Ruangdaj Tongsri[b]*

[a]Department of Physics, Faculty of Science, Naresuan University, Pitsanulok-Nakhon Sawan Road, Tha Pho, Muang, Pitsanulok, 65000, Thailand

[b]Particulate Materials Processing Technology Laboratory (PMPT), Thailand National Metal and Materials Technology Center, 114 Paholyothin Road, Khlong Nueng, Khlong Luang, Pathum Thani, 12120, Thailand

* Email: ruangdt@mtec.or.th

Keywords: Fe-Mo-Si-C alloy, Nodular ductile iron, Compacted graphite iron, Wear

Some of our previous works indicate that the contact between Fe and Fe-based materials with SiC ceramic at elevated temperatures can result in SiC decomposition, which produces alloying Si and C elemental atoms. Similarly graphite powder can decompose to produce alloying C atoms. Due to the aforementioned facts, both SiC and graphite powders were added to the pre-alloyed Fe-Mo powders to investigate their effects on alloying behaviors during sintering. Sintered Fe-Mo-Si-C steels, having microstructural features similar to that of a spheroidal graphite iron and/or compacted graphite iron, i.e., black nodular and/or vermicular particles were enveloped by ferrite grains, which were surrounded by pearlitic structure, were prepared from pre-alloyed Fe-0.85Mo powder added with fixed 4 wt.% silicon carbide powder and varied graphite powder contents. The graphite powder addition caused morphological change from black nodular to black vermicular particles and resulted in decrease of black nodular/vermicular particle fraction, increase of pearlite fraction and slight change of ferrite fraction. The black nodular particles were either graphite or Fe-Mo-Si-C/graphite core-shell particles whereas vermicular particles were totally composed of carbon. The microstructural features showed influence on mechanical property of the sintered Fe-Mo-Si-C alloys. Wear properties of the sintered steels were strongly affected by their microstructural components. The sintered Fe-0.85Mo + 4 wt.% SiC steels showed highest friction coefficient and volume loss. Addition of graphite to the sintered Fe-0.85Mo + 4 wt.% SiC steels, not only changed morphology and chemistry of black particles but also reduced friction coefficient and volume loss. The reduction of both determined wear properties were attributed to the presence of vermicular graphite particles.

MET-O-21

Characterization of Sintered Fe-Mo + SiC + H-BN Alloy

Ussadawut Patakham[a], Pattraporn Rojanasakulpisuit[b], Dhritti Tanprayoon[a], Bhanu Vetayanukul[a], Monnapas Morakotjinda[a], Rungtip Krataitong[a], Thanyaporn Yotkaew[a], Nattaya Tosangthum[a], Pongsak Wila[a] and Ruangdaj Tongsri[a]*

[a]Particulate Materials Processing Technology Laboratory (PMPT), Thailand National Metal and Materials Technology Center, 114 Paholyothin Road, Khlong Nueng, Khlong Luang, PathumThani, 12120, Thailand

[b]Department of Materials Engineering and Production Technology, Faculty of Engineering, King Mongkut University of Technology North Bangkok, Thailand

* Email : ruangdt@mtec.or.th

Keywords: Sintered Fe-Mo steel, Boron, SiC decomposition, Mechanical property

In general, boron (B) is a very powerful hardenability element that is added to steel in minute amount. The effectiveness of B to give hardenability depends on its segregation to the austenite grain boundary where the formation of grain boundary ferrite at transformation temperature is suppressed. This work aims to explore the interaction between B and constituent elements in pre-alloyed Fe-Mo + 4 wt.% SiC powder mixture. B was added in the form of H-BN, which decomposed into B and N when contacted with Fe-based powders at high temperatures. B acted as an alloying element while N could act as an alloying element or escaped from the sintered part in the form of N_2 through the interconnected pores. In order to test the hypothesis that the interaction between Fe-Mo and SiC powders depends on SiC powder particle size, the added SiC powder particle sizes were varied as < 20 µm and > 45 µm. Addition of finer SiC powder particles (< 20 µm) provided better mechanical properties of the sintered steels due to improved nodularity and even distribution of black spheroidal particles. Regarding the effect of B addition, B was found to decrease physical and mechanical properties, compared to those of the B-free sintered Fe-Mo + 4 wt.% SiC steels. B formed complex boride along grain boundaries between pearlite grains. At the prior SiC sites, B also formed spheroidal boron carbide particles by the interaction with carbon. Therefore the in-situ composite material produced from Fe-Mo + 4 wt.% SiC + 0.25 H-BN powder mixture showed microstructural feature consisting of black spheroidal boron carbide particles enveloped with ferrite grains, which were further surrounded by pearlite grains, whose boundaries were thickened by complex boride.

MET-O-22

Improvement of Semi-Solid Sate Joining of SSM Aluminum Alloys.

Patsapon Binrohim[a], Prapas Muangjunburee[a,*]
[a] *Department of Mining and Material Engineering, Faculty of Engineering, Prince of Songkla University, Hatyai 90112 Thailand*
*mprapas@eng.psu.ac.th

Keywords: semisolid joining, SSM A356 joining

Abstract: Improvement of semisolid state joining of SSM aluminum alloys was studied for macrostructure, microstructure and mechanical properties of SSM A356. The butt-joint of SSM A356 was weld using portable drill-tip stirrer with diameter 4 mm drill clockwise rotation. The samples were heated by induction heating coil. The controlling temperature during joining was measured. The joining process studied 3 conditions were 1100 rpm, 1750 rpm, 2200 rpm of stirring rate, speed of welding was 75 mm/min. The best condition for semisolid state joining of SSM aluminum alloys was 1750 rpm of stirring rate and speed of welding 75 mm/min. The result of best condition was obtained from analysis macrostructure, microstructure and mechanical properties compare with other condition of joinings.

MET-O-23

Fastenerless-Riveting Utilizing Friction Stir Forming for Dissimilar Materials Joining

Takahiro Ohashi[a,*], **Hamed Mofiidi Tabatabei**[a], **Tadashi Nishihara**[a]
[a]*Kokushikan University, Setagaya, Tokyo, 154-8515, Japan*
* tohashi@kokushikan.ac.jp

Keywords: Friction stir forming (FSF), Dissimilar materials joint

This paper proposes a new joining approach for dissimilar materials, called 'the fastenerless-riveting,' employing the friction stir forming (FSF). The FSF is a friction stir process invented by Nishihara[1] in 2002. In FSF, a substrate material was put on a die firstly. Next, friction stirring was conducted on the back surface of the material. The material then deformed and precisely filled the cavity of the die due to high pressure and heat caused by the friction stirring. The authors utilized the FSF approach to generate rivet like joints as followings. First, a substrate which is capable for friction stirring, i.e. an aluminum alloy plate, was put on a dissimilar material plate having holes, i.e. a steel plate. The authors call the former 'the host member,' the latter 'a joined member.' These members were put on a die having the cavity to fabricate the head of the rivet-like structure. Then FSF was conducted to form the stems and heads of the structure. Joint members are able to be stacked within the forming limit. In this study, a 3mm-thick A5083P-O aluminum alloy plates was utilized as the host member and a 0.7mm-thick SPCE steel plate as the joined member. The authors investigated the forming conditions, i.e. tool spindle speed, tool feed rate, tool pass and the corresponding results, including the volume of the generated stem and head of the individual rivet-like structure.

References

[1] T.Nishihara, Japanese Patent, 4,646,421.(2002).

MET-O-24

Quantitative Evaluation of Hot Cracking Susceptibility of MGS6 GZ-60 Hardfacing Weld Metal Based on High Temperature Ductility Curve

Rittichai Phaoniam*, Teerayu Kanchanasangtong ,Paisan Inprachong,

Rajamangala University of Technology Krungthep, Bangkok, 10120, Thailand

Keywords: Hardfacing weld metal, Hot cracking, Trans-varestraint test, High temperature ductility curve

In a recycle-rubber shredding machinery, hardfacing welding is more beneficial of repairing damaged cutting edge blades. However, undesired situation as cracking etc. probably occurs during welding because of inappropriate procedure. Therefore, this research is aimed to study the hot cracking susceptibility based on high temperature ductility curve in a hardfacing weld metal. The weld metal of MGS6 GZ-60 according to DIN 8555 standard was studied, which is widely welded to build up on broken tools. Comparative Experiment including specimens were divided into 3 kinds of different weld metals as; high strength-ER70-6, austenitic-ER308L, and hardfacing-MGS6 GZ-60, specimen size of 200x75x6 mm. Trans-varestraint test was used to investigate for hot cracking based on strain analysis of weld metals. This test was implemented with varying different strains during a GTA-welding. Strains were applied through 5 levels of bending block radius, namely R70, R120, R200, R300, and R300 mm. Welding parameters were set of 150 A, DCEN polarity, welding speed of 0.7 mm/s, and argon shielding gas of 10 L/min. In order to achieve the high temperature ductility curve, it is necessary to obtain the temperature at where the critical strain occurs. Temperature history at the trailing edge of the molten pool was measured using immediately inserting a thermocouple type R in a diameter of 0.5 mm due to its ability of data acquisition during the rapidly cooling rate. Consequently, high temperature ductility curves in each weld metals were established by the relationship between the critical strain obtained by Trans-varestraint test and the cooling curve (temperature-time). High temperature ductility curves were used in order to predict critical strain to cracking as a function of temperature in solidification range. After then, characteristics of the different cracked weld metals were comparatively observed with optical microscopic and scanning microscopic electron (SEM). The hot cracking susceptibility of weld metals was quantitatively evaluated through the maximum crack length, the number of crack length and high temperature ductility curves. As the results revealed that all weld metals increasing hot cracking with increasing the amount of strains during welding, especially in the hardfacing weld metal of MGS6 GZ-60 has a tendency of more high temperature cracking than austenitic and high strength weld metal respectively. In additional to, the results of the maximum crack length and the number of crack length exhibited in the hardfacing weld metal of MGS6 GZ-60. This indicates that high temperature cracking need to consider substantially when repairing damaged parts by hardfacing welding. Computational welding simulated to estimate the critical strain for appropriate welding procedure should be additionally investigated to alleviate these situations in the future.

MET-O-25

Phase equilibria and thermodynamic properties of the Ag-Bi-Cu-Sn Pb-free solder calculated by CALPHAD approach.

Wojciech Gierlotka
National Dong-Hwa University, Hualien, 97401, Taiwan
wojtek@mail.ndhu.edu.tw

Keywords: Pb-free soldering, Intermetallics, Thermodynamics, Phase equilibria.

The knowledge about phase equilibria and phase transformations is essential for engineers and allows them to prepare and manage technological processes. The phase equilibria in binary, or even in simple ternary systems, are quite easy to determine by experiment; however, in cases of complicated ternaries and higher-ordered systems, experimental procedures can be difficult as well as time consuming. The CALPHAD method permits to predict phases relationship based on Gibbs energies of binary and higher-ordered systems. In this work, the calculation of phase equilibria, phase transformations and phase relationships of the quaternary Ag-Bi-Cu-Sn alloys is presented and discussed.

MET-O-26

The Investigation of Attenuation in AISI 316 Stainless Steel Weld for Ultrasonic Testing

Mai Noipitak[a,*], Boonhlua Khwansri[a]
[a]*Ratchaburi Learning Park, Office of the President, King Mongkut's University of Technology Thonburi, Thung Khru, Bangkok, 10140, Thailand*
*mai.noi@kmutt.ac.th

Keywords: Distance amplitude correction curve, Microstructure, Stainless steel, Ultrasonic testing

Ultrasonic testing is the one of Non-Destructive Testing methods that used to detect the internal discontinuities in the stainless steel weld. Codes and standards for stainless steel construction provided the procedure and acceptance criteria for ultrasonic testing. This research aimed to study and describe the effect of microstructure on shape of distance amplitude correction (DAC) curve and ultrasonic inspectability in stainless steel weld. Two calibration blocks (side drilled hole block) were prepared from AISI 316 stainless steel plate according with ASME section V version 2013. One calibration block was varied the grain size by annealing process. The annealing temperature and holding time were 1,200 ºC and 4 hours, respectively and then cooled down in air. Butt joint welding specimens AISI 316 were prepared to establish the artificial discontinuities. Lack of fusion and drill hole, diameter 1 and 2 mm, were selected to establish as discontinuities. Specimen was welded by gas tungsten arc welding and shielded metal arc welding process. Then, the gain size and microstructure of two calibration blocks were analyzed by microscope. The macrostructure, gain size and microstructure were determined by microscope and scanning electron microscopy (SEM), respectively. Longitudinal and transverse wave with probe frequency 2.25 and 5 MHz and angle probe 45, 60 and 70 degree were used to describe the effect of microstructure on shape of DAC curve and to investigate the ultrasonic inspectability in stainless steel weld. The experiment results found that the ultrasonic energy of longitudinal and transverse wave in calibration blocks decreased as the gain size increased. The attenuation due to gain size affected to the shape of DAC curve. The grain size in heat effected zone (HAZ) of weld specimen is larger than base material and the ultrasonic transverse wave can be detected lack of fusion and drill hole diameter 2 mm but cannot detected drill hole diameter 1 mm. The usefulness of this research can be applied for searching the discontinuities in the weld zone of stainless steel by ultrasonic. The attenuation of ultrasonic energy in the weld zone of AISI 316 is high and the amplitude showed at the screen is very low. This is reason can be made the operator wrong result interpretation, if they did not consider about the attenuation from microstructure.

MET-O-27

Effect of Cooling Rate on the Microstructural and Mechanical Properties of Sn-0.3Ag-0.7Cu-0.05Ni Solder Alloy

Kokaew Inkong, Phairote Sungkhaphaitoon*
Department of Materials Science and Technology, Faculty of Science, Prince of Songkla University, Hat Yai, 90112, Thailand
*E-mail phairote.s@psu.ac.th

Keywords: Lead-free solder, Cooling rate, Intermetallic compound, Microstructure

The effect of cooling rate on the microstructural and mechanical properties of Sn-0.3Ag-0.7Cu-0.05Ni lead-free solder alloy was studied. The microstructure of specimens was characterized by using a scanning electron microscopy (SEM) and an energy dispersive X-ray (EDX) spectroscopy. The mechanical properties was performed by a universal testing machine (UTM). The results showed that the cooling rate of water-cooled specimens was about 1.72 ^{o}C/s and the cooling rate of mold-cooled specimens was about 0.05 ^{o}C/s. To compare the different cooling rates, it was found that the grain size of water-cooled specimens was finer than that of the mould-cooled specimens. This resulted in an increment of mechanical properties of solder alloy. A higher tensile strength (33.10 MPa) and a higher elongation (34%) were observed when water-cooled and mold-cooled systems were used, respectively. The microstructure of Sn-0.3Ag-0.7Cu-0.05Ni lead-free solder alloy solidified by both cooling systems exhibited three phases of β-Sn, Ag_3Sn and $(Cu,Ni)_6Sn_5$ IMCs.

MET-O-28

The Thermal-Aging Effect on the Microstructure Evolution and Shear Strength of the Sn-Rich Au-Sn Soldering between AlTiC and Si Substrate in Microelectronics

Panaaek Athichalinthorn[a], Jidsucha Darayen[b], Wachira Puttichaem[c], RatchateeTechapiesancharoenkij [a], and Boonrat Lohwongwatana[b,*]

[a]Department of Materials Engineering, Faculty of Engineering, Kasetsart University, 50 Ngamwongwan Rd,Chatuchak, Bangkok, 10900 Thailand

[b]Innovative Metals Research Unit, Department of Metallurgical Engineering, Faculty of Engineering, Chulalongkorn University, 254 Phayathai Road, Pathumwan Bangkok, 10330 Thailand

[c]Western Digital (Thailand) Co., Ltd. 140 Moo 2 Klongjig, Bangpa-in, Ayutthaya 13160 Thailand.

* Corresponding author's email address: boonrat@gmail.com

Keywords: Micro soldering, Lead-free soldering, Conductive bonding, Au-Sn Intermetallic Alloy

Abstract

The Au-Sn soldering alloys are commonly used in microsoldering process for microelectronic industry due to fluxless process and relatively low melting temperature with good eutectic microstructures. This study investigated the microstructures of Au-Sn soldering between AlTiC and Si substrates with Ti/Pt/Au under bump metallization (UBM). The microstructures of the solder samples under three conditions: before bonding, after bonding and after thermal-cycle aging, were investigated. The shear strength values of pre-aging and post-aging soldering were compared. The thermal-cycling temperatures were from -40 to 125 ^{o}C for 300 cycles. The intermetallic compounds (IMCs) of the AuSn solders consist of AuSn, $AuSn_2$, and $AuSn_4$. After thermal-cycle aging, the bonding strength was increased due to the improved IMC bonding between solders and UBM; the shear surfaces were rougher due to the growth of AuSn and $AuSn_2$.

MET-P-01

Improvement of structural, morphological and mechanical properties of CrN_x sputtered thin films by vacuum annealing process

Aparporn Sakulkalavek[a,*], Intira Nualkham[a], Rachsak Sakdanuphab[b]

[a]*Department of Physics, Faculty of Science, King Mongkut's Institute of Technology Ladkrabang, Ladkrabang, Bangkok 1052*
[b]*College of Advance Manufacturing Innovation, King Mongkut's Institute of Technology Ladkrabang, Ladkrabang, Bangkok 10520*

*E-mail aparporn.sa@kmitl.ac.th

Keywords: CrN_x, Annealing process, Reactive magnetron sputtering

In this study, CrN_x thin films were prepared on 304 stainless steel substrate by DC reactive magnetron sputtering technique. Different N_2 gas partial pressure from 10 to 30% was employed in the sputtering process while sputtering power, sputtering pressure and total film thickness were kept constant. In order to improve structural, morphological, and mechanical properties, vacuum annealing process was adopted on the CrN_x thin films at the temperature of 400 ºC. The standard characterization techniques such as X-ray diffraction, scanning electron microscope, atomic force microscope and hardness (load force of HV0.1) were used to reveal the properties of as-deposited and annealing films. The as-deposited films show two-phase crystal structure of Cr_2N and CrN depending on N_2 gas partial pressure. After the annealing process, the films effectively enhance the crystal structure and found the phases change from Cr_2N to CrN for the film deposited at low N_2 partial pressure. The surface roughness of the films was between 5 - 20 nm, and as expected the annealing films shows smoother surface than the as-deposited films. Hardness of the CrN_x films is in the range of 7 to 10 GPa. The mechanism of improvement in structural and mechanical properties of annealing films is introduced based on strain relaxation.

MET-P-02

Effects of Processing Parameters on Microstructure and Properties of ADC12 Aluminium-Silicon Alloys Produced by Die Casting

Kasem Charoenrut[a], **Chaiyasit Banjongprasert**[a*]
[a]*Department of Physics and Materials Science, Faculty of Science, Chiang Mai University, Chiang Mai 50200, Thailand*

*E-mail address chaiyasit.b@cmu.ac.th

Keywords: Aluminium-Silicon alloys, Pressure Casting, ADC12, EBSD

This work investigates the effects of processing parameters on the microstructure and properties of ADC12 alloys. ADC12 is an Al-Si alloy with 10-11wt%Si. The alloys were produced by pressure die casting with different chemical compositions and processing parameters. The ADC12 samples were selected in this work with different iron contents and casting pressures. Then, a microstructure was observed by using scanning electron microscope with electron backscatter diffraction including energy dispersive x-rays. The microstructure consists of an α-Al, eutectic structure and intermetallic phases of AlFeMnSi. The intermetallic phases found in the microstructure was the key factors leading to failure including the defects from the casting process such as shrinkage porosity and gas porosity. The failure parts of ADC12 was reduced from 10% to less than 2% by developing the new chemical composition and processing parameters. More details on the new alloy compositions and processing parameters will be discussed.

MET-P-03

Effect of Compaction pressure and Sintering time on the Properties of Cu-10Sn Bronze

Narut Nakrod[a*], Ryan McCuiston[a], Chiraporn Auechalitanukul[a]

[a]King Mongkut's University of Technology Thonburi, Thung Khru, Bangkok, 10140, Thailand
*narutnakrod@gmail.com

Keywords: Bronze, Powder Metallurgy, Porosity, Sintering

Bronze-based composite materials are well known for use as friction materials. They are produced by powder metallurgy techniques from bronze powder, which acts as a matrix, and various friction modifying additives. The objective of this work was to study the effect of compaction pressure and sintering time on the properties of the unmodified bronze matrix material. The bronze powder used was prealloyed with a composition of Cu-10Sn. The specimens were pressed by uniaxial die compaction under pressures of 282 to 339 MPa. The sintering experiments were conducted in a vacuum tube furnace at 800 ^{o}C with sintering times of 30, 45, and 60 min. From the results, it was found that the density of the samples increased with increasing compaction pressure. A microstructural examination of the samples for the different sintering times showed them to look very similar. Finally, the highest sintered density of 7.24 g/cm^3 was obtained at 800 ^{o}C for 60 min.

MET-P-04

Properties of Sintered Bronze-Graphite Containing Calcium Sulfate Derived from Waste Plaster Molds

Chiraporn Auechalitanukul[1] *, Ryan McCuiston[1] , Benjawan Bunlangsup[1], Chanattha Naikorn[1] and Sudachuan Tapanaun[1]
[1]King Mongkut's University of Technology Thonburi, Thung Khru, Bangkok, Thailand
*chiraporn.aue@kmutt.ac.th

Keywords: Bronze, Calcium Sulfate, Friction, Microstructure

This study examined the effect of calcium sulfate additions on the microstructure and frictional properties of a 95bronze-5graphite material, commonly used for frictional applications. The samples were prepared using a powder metallurgy process. The calcium sulfate powder was obtained from recycled plaster molds previously used for ceramic slip casting. The plaster molds were cleaned, crushed and ball milled to obtain powder, which was calcined at 400 ºC for 4 hours and screened. 2 to 8 weight percent calcium sulfate powder was added to a premixed powder composed of copper and tin and mixed before the graphite was added. The powder mixture was compacted into a disc shape under a pressure of 500 MPa. The compacted samples were sintered at 750 ºC for 30 minutes in a reducing atmosphere. It was found that the green density of the samples decreased with increased amounts of calcium sulfate. After sintering, the densities were found to have decreased due to sample expansion. A finer microstructure was observed in the samples containing calcium sulfate powder, possibly due to a grain boundary pinning effect. The addition of calcium sulfate resulted in the reduction of both the measured friction coefficient and wear of the bronze-graphite samples. However, the addition of calcium sulfate powder above 6 weight percent appeared to show decreasing effects.

MET-P-05
Investigation of burst rupture disc

Warunee Borwornkiatkaew, Niphon Chumchery, Kosit Wongpinkaew*
National Metal and Materials Technology Center, Phahonyothin Road, Pathumthani, 12120, Thailand
*Corresponding author, E-mail: kositw@mtec.or.th

Keywords: rupture disc, shear dimple, austenaite, pressure vessel.

Nowadays a rupture disc has widely been used throughout industry to protect a pressure vessel, equipment or system from over pressurization. Rupture discs are constructed from carbon steel, stainless steel, hastelloy, graphite, and other materials, as required by the specific use environment. It has a single-use membrane that fails at a different predetermined pressure. Rupture discs provide instant response to an increase or decrease in system pressure, but once the disc has ruptured it will not reseal.
In this case, the rupture disc was burst during operation however, the pressure guage did not produce any alarm (over pressurization was not found). Therefore, the fracture pattern, metallography and mechanical property were investigated in order to explore the root cause of the failure. According to the metallogical and mechanical analysis, it could be concluded that the pressure guage was malfunction.

Figure 1: A photograph of a busted-rupture disc.

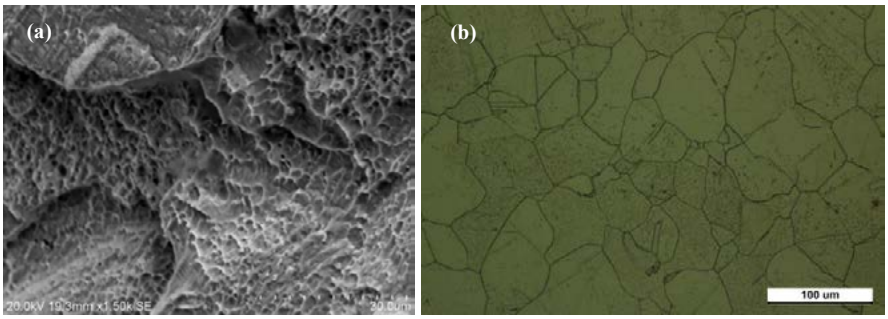

Figure 2: (a) a SEM micrograph at fracture surface and (b) an optical micrograph of microstructure of rupture disc.

References

1. Michael Z., Rupture Disk Troubleshooting: Canadian process equipment & control news, April 2009.
2. Charles Y., Numerical modeling of the Disk Pressure Test up to failure under gaseous hydrogen: Journal of Materials Processing Technology 212, 2012: 1761– 1770.
3. Benbella Sh., Experimental and theoretical investigation of gas–liquid flow pressure drop across rupture discs: Nuclear Engineering and Design 240, 2010: 1458–1467.

MET-P-07

Sheet Metal Formability Characterization

Nopparat Seemuang[a,*], Sansot Panich[a], Taratip Chaimongkon[b]

[a]Deparment of Production Engineering, Faculty of Engineering
[b]Division of Tools and Die Engineering Technology, Department of Mechanical Engineering Technology, College of Industrial Technology
King Mongkut´s University of Technology North Bangkok, Bangsue
Bangkok, 10800, Thailand.
*nopparat.s@eng.kmutnb.ac.th

Keywords: Formability Characterization, Fukui test, Cup drawing test, Erichsen test

The main goal of this study is to characterize sheet metal formability by simulative experimental test setup. The experimental tests were precisely performed for four different materials, namely, stainless steel SUS304, structure steel SS400, deep drawing steel SPCC, and aluminium Al1000, with a thickness of 1.0 mm. The formability characterization of all materials were carried out on a 60 kN hydraulic press machine. Stretch-drawing of materials was conducted by using Fukui cup test with conical and flat punches. The stretchability was precisely examined through the Erichsen test and the cup drawing test was finally performed to obtain material drawability. The universal tensile testing machine was used to determine the strain hardening index, n, and normal anisotropy coefficient, r, in three loading directions i.e. 0^0, 45^0, and 90^0, from the rolling direction (RD). The experimental results show that deep drawing steel SPCC shows better formability than SUS304, SS400, Al1000, respectively regarding their stretching-drawing, stretching and drawability. This can be attributed to the instrinsictive properties of the materials such as strain hardening level and r-value which well correlate to simulative experimental formability tests.

MET-P-08

Study of Microstructure and Corrosion Resistance of Zinc Electrodeposits Before and After Black Chromating

Kanokwan Saengkiettiyut[a,*], Pranee Rattanawaleedirojn[a], Adisak Thueploy[a], Jumpot Wanichsampan[a], Yuttanant Boonyongmaneerat[a]

[a]*Metallurgy and Materials Science Research Institute, Chulalongkorn University, Bangkok, 10330, Thailand*

* kanokwan.s@chula.ac.th

Keywords: Zinc, Electrodeposition, Corrosion resistance, Chromating

In this work, microstructure and corrosion properties of zinc electroplated steel before and after black chromating was investigated. The test samples are prepared by electrodeposition process, using a commercially-available alkaline electrolyte. Subsequently, the galvanized samples are applied with a black chromate-based passivation layer and a clear top-coat layer. Their microstructure is examined using X-ray diffractometry and scanning electron microscopy. The corrosion resistance of the samples is assessed with the salt spray test, following the ASTM B117, electrochemical impedance spectroscopy, and potentiodynamic polarization in 5 wt.% NaCl solutions. The study shows that the zinc electroplated steels exhibits (110) crystallographic orientation. The passivation and top-coat layers do not affect the microstructure of the zinc layer, and cover uniformly on the zinc layer for all sets of samples. The corrosion resistant results obtained from salt spray testing and electrochemical testing revealed that the microstructure of zinc coatings prepared by using different applied current do not influence obviously on their corrosion resistance. While black passivation followed by top coating provide a significant improvement on corrosion resistance of the coatings, respectively.

MET-P-09

Factors Affecting on the Corrosion Resistance of Electroless Ni-Zn-P Coated Steel

Pranee Rattanawaleedirojn[a,*], Kanokwan Saengkiettiyut[a], Yuttanant Boonyongmaneerat[a], Jumpot Wanichsampan[a]
[a]*Metallurgy and Materials Science Research Institute, Chulalongkorn University, Bangkok, 10330, Thailand*
*pranee.r@chula.ac.th

Keywords: Ni-Zn-P, Electroless deposition, Corrosion resistance

Electroless Ni-Zn-P coating with the optimal content of Ni and Zn in the alloy can provide high corrosion resistance for steel. The Ni-rich phase of this high hardness Ni-Zn-P alloy offers barrier protection property while the sacrificial protection property is obtained from the alloy with proper content of Zn. In this work, the Ni-Zn-P coating was prepared on steel substrate by using the alkaline electroless deposition. The parameters of deposition process including, complexing agent concentration, bath pH, zinc ion and nickel ion concentration were systematically studied. The microstructural morphology and elemental composition of the coatings were characterized by scanning electron microscopy. It was found that complexing agent, zinc ion and nickel ion concentration play an important role on Zn content of the Ni-Zn-P alloy whereas alkalinity of the solution bath directly affects the deposition rate. The results of corrosion resistance study investigated by linear polarization technique illustrated that the corrosion potential (E_{corr}) of Ni-Zn-P coatings was negatively shifted by an increase of Zn content in the alloys. From this work, the E_{corr} of 83%Ni-11%Zn-6%P coating prepared in this system was slightly lower than steel. To achieve a higher effect of sacrificial protection for corrosion protection of steel, the Ni-Zn-P with higher content of Zn should be further studied.

MET-P-10

Extension of Creep Lifetime of Iron-Nickel-Base Superalloy at high temperature by adjusting Ti/C ratio

Chien-Lin Lai[1], Ming-Yen Li[1], Shih-Ming Kuo[1], Yeong-Tsuen Pan[1]

[1] *New Materials Research & Development Department, China Steel Corporation, 1 Chung Kang Road, Hsiao Kang, Kaohsiung 81233, Taiwan, R.O.C.*

***Email: 185124@mail.csc.com.tw**

Keywords: Nickel-Based Superalloy, Creep, High temperature

ABSTRACT

Improvement of creep characteristic of iron-nickel-based superalloy at high temperature by specific production processes was carried out in this study. By adjusting the Ti/C ratio, the creep lifetime of the alloy developed in this study was increased to 1.8 times of magnitude relative to the same grade commercial creep-resistant product. The extension of time to rupture could be attributed to the precipitation of both nanometer-scale TiC and submicron coherent $M_{23}C_6$ which act as pinning points for individual dislocations and grain boundaries resulting in strengthening and suppression of grain boundary sliding. Since the strengthening effect of TiC and $M_{23}C_6$ occurred before the common γ' strengthening, the newly developed iron-nickel-based alloy can be used in a relatively harsh environment where the alloy might rupture during the incubation period of γ'.

MET-P-11

Residual and Tensile Stress Measurement in Carbon Steel by Magnetic Barkhausen Noise Technique

Mai Noipitak[a,*]
[a]*Ratchaburi Learning Park, Office of the President, King Mongkut's University of Technology Thonburi, Thung Khru, Bangkok, 10140, Thailand*
*mai.noi@kmutt.ac.th

Keywords: Stress measurement, Carbon steel, Microstructure, Barkhausen noise technique

The Magnetic Barkhausen Noise (MBN) technique can evaluate the residual stresses in carbon steel and provide information about the relationship between residual stress level and MBN signal. This research work is based on the analysis of MBN signals obtained from carbon steel samples. ASTM A36 and A516 carbon steel were used to vary the residual stress by heat treatment process with 5 conditions: annealing, normalizing, quenching in oil, quenching in water and quenching in salt water. The microstructure and hardness of samples also were varied by these heat treatment processes. Twelve samples (including base materials) were cut to analyze the microstructure and hardness by the microscope and hardness testing machine. Reference materials from each condition were established to refer the MBN signals. The MBN technique was used to evaluate the residual stresses from heat treatment process on each reference materials. Then each sample was prepared to tensile specimen. All specimens were applied static tension load below yield point. The load was increased at 25 N/mm^2 (MPa) in increment. Each tensile stresses level were measurement by MBN technique at 0 and 90 degree of direction of tension axis. The experimental results found that the MBN signal amplitude changed as the condition of heat treatment changed and the relationship between tensile stress and MBN signal showed linear correlation. This research is useful to understand and guide for establishing the reference materials for residual stress measurement by MBN technique.

Polymers

POL-I-01

Polymer Research in Thailand: Past, Present and Future

Krisda Suchiva
Rubber Technology Research Centre
Faculty of Science, Mahidol University, Nakhon Pathom, Thailand
krisda.suc@mahidol.ac.th

Keywords: Polymer research, Thailand, Petrochemical industry, Polymer industry

Before 1980 there was little polymer research in Thailand. The development of the petroleum and petrochemical industries in Thailand, beginning in 1980, may be regarded as the "catalyst" for development of polymer research in Thailand. This was supported and strengthened by 1) the Thai Government initiative to send more than 1,000 scholarship students to study abroad as part of human resource development programme in the fields of materials science and technology 2) The establishment of the National Metal and Materials Technology Center (MTEC) in 1986 to provide funding for polymer research and research facilities in universities and research institutes.

Polymer research and development in Thailand has been conducted to support the petrochemical and related downstream industries including the plastics, textiles, coatings and adhesive industries. The other industry which also drove polymer research in Thailand is the natural rubber industry. Therefore, polymer research in the past, and even presently, was not advanced but rather involved established technologies such as polymer blends and composites, chemical modifications of polymers, biopolymers, biodegradable plastics, polymer compounding, polymer recycling, utilization of agricultural and industrial wastes and textile finishing. The objective of the research is mainly utilization of the country's natural resources such as chitin, chitosan, natural fibres, starch and, in particular, natural rubber.

Recently, more advanced polymer research begins to take place as the advanced materials industries are beginning to be established in Thailand such as the biomedical, the pharmaceutical and the electronic industries. Global interests in nano-materials and nanotechnology also initiated widespread research in these fields in Thailand but the work are rather academic in nature as there are lacks of modern equipment necessary for serious research in this field and also the nanotechnology-based industry in the country.

Polymer research in Thailand so far has been rather scattered and most are not connected with industrial applications or social benefits. The research subjects are not focused especially on the ones which are competitive for Thailand. This is the area which will have to be improved in the future. Natural rubber (NR) is an example of natural resource which Thailand has real competitive advantage. Sustainability of NR is extremely important not only for Thailand but for the whole world. Therefore, research into NR all along its value chain should be increased. The other industries which should be competitive for Thailand are the food and agricultural industries. Therefore, research into food additives developed from local resources, food rheology, polymers in agriculture should be the other focused research areas. Polymers in health and medicine should also be focused on for future polymer research in Thailand. Although the competitiveness of Thailand in these fields are not very strong but the problem of health and well-being of the Thai people have to be attended to and selected successes can be built upon if properly managed. Thailand cannot afford to rely totally on imported medical technology.

POL-I-02

Hierarchic Structures and Propeties of Natural Rubber

Seiichi Kawahara [a,*]
[a]*Department of Materials Science and Technology, Faculty of Engineering Nagaoka University of Technology, Nagaoka, Niigata 940-2188, Japan*
*kawahara@mst.nagaokaut.ac.jp

Natural rubber is well-known to be superior in mechanical properties such as tensile strength, tear strength, green strength and so forth. In the last century, therefore, attempts to analyse a primary structure of natural rubber were made to elucidate a relationship between the structure and properties. For instance, a fundamental structure of natural rubber is known to consist of -terminal, 2 *trans*-1,4-isoprene units, about 5,000 *cis*-1,4-isoprene units and - terminal, aligned in this order. Furthermore, the -terminal is composed of phospholipids linking to fatty acids and the -terminal is a modified dimethylallyl group linking to a functional group, which is associated with the proteins. Thus, the branching structure is inherently formed in natural rubber. The outstanding properties of natural rubber is partly associated to the branching structure. However, in order to understand an origin of the outstanding properties of the rubber, we are required to analyse hierarchal structure of natural rubber, since the proteins and the phospholipids are immiscible with natural rubber. In the present study, the relationship between the structure and mechanical properties was investigated in relation to the nanomatrix structure, which was discovered in this century.

Natural rubber particles in latex are covered with the proteins and phospholipids. Therefore, the proteins and phospholipids of the particles may merge into each other to form a dispersion medium, when the latex is coagulated. Natural rubber may, thus, possess the nanomatrix structure[1], which consists of natural rubber particles of about 1 m in diameter as a dispersoid and the nanomatrix of the proteins and phospholipids as a medium. Figure 1 shows TEM images for fresh natural rubber, natural rubber and DPNR, which were stained with phosphotungstic acid. In the TEM images, phase separated structure was found for fresh natural rubber and natural rubber, in which bright domains represent natural rubber and gloomy domains represent non-rubber components. The rubber particles of various sizes were well dispersed in the nanomatrix of the proteins and phospholipids. The thickness of the matrix was dependent upon the protein contents. For example, total nitrogen contents were 0.777 w/w% for fresh natural rubber (Figure 1a) and 0.251 w/w% for natural rubber (Figure 1b). This implies that the natural rubber particles are covered by a membrane layer, i.e. protein-lipid complex; hence, the proteins and phospholipids may essentially form the nanomatrix after coagulation of the latex. On the contrary, no phase separated structure was found for DPNR (Figure 1c). This may be explained to be due to the removal of the proteins from natural rubber: The nanomatrix structure was associated to the outstanding properties of natural rubber.

[1] S. Kawahara, *et. al. Macromolecules*, **41** (2008) 4510-4513.

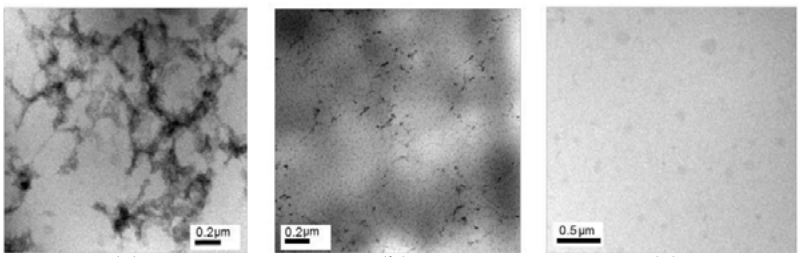

(a) (b) (c)

Figure 4 TEM images for fresh natural rubber, natural rubber and DPNR.

POL-O-01

Effect of Calcium Carbonate on Crystallization Behavior and Morphology of Poly(3-hydroxybutyrate-*co*-3-valerate)

Sitthi Duangphet[a,b,*], Damian Szegda[c], Karnik Tarverdi[d], Jim Song[d]
[a]*School of Science, Mae Fah Luang University, Muang, Chiang Rai, 57100, Thailand*
[b]*Materials for Engineering and Environment Research Group (MEE), Mae Fah Luang University, Muang, Chiang Rai, 57100, Thailand*
[c]*Impression Technologies Ltd, Coventry, CV5 9PF, United Kingdom*
[d]*Institute of materials and manufacturing, College of engineering and physical sciences, Brunel University, London, UB8 3PH, United Kingdom*
*E-mail: sitthi.dua@mfu.ac.th

Keywords: PHBV, Calcium carbonate, Crystallization, Morphology

The effects of calcium carbonate ($CaCO_3$) concentration on crystallization behaviors and morphology of poly(3-hydroxybutyrate-*co*-3-hydroxyvalerate) (PHBV) were investigated. Two $CaCO_3$ loadings consisted of low concentration (5%wt) and high concentration (20%wt) were compared with unloaded PHBV in this study. The morphologies of PHBV composites were considered on the freeze fractured specimens and investigated by scanning electron microscopy (SEM). The SEM images revealed that increasing number of $CaCO_3$ resulted in agglomeration. Moreover, the molecular weight determination via gel permeation chromatography (GPC) indicated the slightly improvement on molecular weight of PHBV with an occurrence of $CaCO_3$ accredited to surface treatment reagent on $CaCO_3$ particle. Both agglomeration and molecular weight development might effect on crystal growth rate and mechanism. The crystal growth behavior of melt-crystallized PHBV with difference amount of $CaCO_3$ was studied by polarized optical microscopy (POM) while the crystal structure was examined by X-ray diffraction (XRD). The rate of crystal growth determined from POM at selected crystallization temperatures revealed that the addition of small amount of $CaCO_3$ accelerated the crystal growth rate whereas excess amount of $CaCO_3$ dropped the crystal growth rate. The POM images also illustrated the change of crystal growth process as a presence of $CaCO_3$. The unloaded PHBV clearly showed nucleation and growth mechanism while PHBV composites displayed the nucleation and then combination of crystals during the growth process. However, the crystal structure on all PHBV composites was not affected by $CaCO_3$ as observed by XRD.

POL-O-02

Low Haze and Antifog Performance of 2-layer Poly(lactic acid) Based Films

Pitcha Liewchirakorn[a], Wannee Chinsirikul[b], Duangdao Aht-Ong[a,c,*]

[a]*Department of Materials Science, Faculty of Science, Chulalongkorn University, Bangkok, 10330, Thailand*

[b]*Polymer Research Unit, National Metal and Materials Technology Center, National Science and Technology Development Agency, Pathum Thani, 12120, Thailand*

[c]*Center of Excellence on Petrochemical and Materials Technology, Bangkok, 10330, Thailand*

*duangdao.a@chula.ac.th

Keywords: Poly(lactic acid), Poly(butylene adipate-co-terephthalate), Antifog, Haze.

For fresh-cut and ready-to-eat packaging films, antifogging agents (AFs) are commonly used to adjust surface tension of the films and help spread water vapor condensation over films' surface and suppress the formation of discrete droplets of water. AFs are available in the form of solutions, creams, and gels. In general, coating may be considered a costly process, thus, another practical blending method to incorporate AF into film was selected in this study. Obviously, there is limited information about antifogging study for poly(lactic acid) (PLA) lidding film, both type and dosage of suitable AFs. In terms of PLA lidding films, they can be fabricated by blending PLA with flexible polymer such as poly(butylene adipate-co-terephthalate) (PBAT) to increase toughness and flexibility. However, such PLA/PBAT blends have higher haze as compared to the neat PLA. From our previous work, the content of 20 wt% of PBAT in PLA (20PBAT/80PLA) can change peel mechanism (peel from PLA sheet) from tearing of PLA film to peeling of 20PBAT/80PLA film (with low haze of 4%). In this research, films were fabricated by cast extrusion technique. The migration behavior of commercial polyglycerol ester as selected AF, was investigated by varying the amount of this agent from 2, 3.5, to 5 wt% in single layer films of 20PBAT/80PLA. Antifog properties were examined by cold fog test. Haze of films were analyzed by haze meter. Films' hydrophobicity were measured by contact angle technique. ATR-FTIR technique was used to analyze the presence of functional group of polyglycerol ester of each film. The results showed that 3.5 and 5 wt% of AF in 20PBAT/80PLA single layer film can provide clear films without droplet of water within 7 days and 3 hours, respectively, by cold fog test, whereas the lower amount of AF (2 wt%) film was mainly covered with discrete droplets of water throughout the test of 30 days. The suitable amount of AF was selected to incorporate into seal layer of 2-layer films which consisted of the seal layer of 95(20PBAT/80PLA)/5 polyglycerol ester and core layer of PLA. The thickness of seal layer/core layer were 20/15 and 10/15 μm. Selected proper 3.5 and 5 wt% of AF was incorporated into inner layer of 2-layer lidding film. Considering films with AF of 3.5 and 5 wt%, it was clearly seen that 5% of AF could reduce haze and also decreased films' hydrophobicity as presented in a reduction of contact angle compared with film without AF. Meanwhile, 3.5 wt% of AF could not reduce contact angle and discrete droplets of water within 30 days. It should be noted that the migration rate of AF in thin 2-layer film (10/15 μm) appeared to be higher than 20/15 μm film. Films' surface by cold fog test could become clear without water droplet within 4 days for 10/15 μm and 7 days for 20/15 μm film. Haze of 10/15 μm film decreased from 5.7 to 3.6, while 20/15 μm film decreased from 10.7 to 7.6 for each film without and with AF on its surface.

POL-O-03

Effect of Poly(hexamethylene succinamide) on Crystallization of Poly(L-lactic acid)

Panadda Yueagyen[a], **Amornrat Lertworasirikul**[a,*]
[a]*Department of Materials Engineering, Faculty of Engineering, Kasetsart University, Bangkok 10900, Thailand*
*Corresponding author: E-mail: fengarl@ku.ac.th

Keywords: Poly(L-lactic acid), Poly(hexamethylene succinamide), Nucleating agent,Crystallization

Poly(L-lactic acid) (PLLA) has good mechanical properties and it is a biodegradable polymer. However, its crystallization rate is slow and crystallization period is long. Moreover, its crystallization temperature is high, which is 116 ^{o}C. Consequently, long processing cycle is required for production of high crystallinity PLLA. Addition of nucleating agent is an efficient way to solve this problem. Aliphatic amide, i.e., *N,N*-ethylenebis(12-hydroxystearamide) and ethylenebis-stearamide were reported as nucleating agent for PLLA [1-2]. In this study, the effect of aliphatic polyamide which is poly(hexamethylene succinamide) (PHSu) on crystallization behavior of PLLA was investigated. PHSu was synthesized by melt polymerization. Its chemical structure was characterized by Fourier transform infrared spectrometer (FT-IR), carbon-13 nuclear magnetic resonance (^{13}C-NMR) and thermal properties were characterized by differential scanning calorimeter (DSC) and thermal gravimetric analysis (TGA). 1-10 %wt of PHSu was blended with PLLA by melt extrusion. The crystallization behavior of blends were investigated by polarize optical microscope (POM) and DSC. It was found that the crystallization temperature, crystallization period and degree of crystallinity were affected by PHSu. The crystallization temperature and crystallization period tended to decrease whereas degree of crystallinity tended to increase when PHSu content increased. At PHSu content of 10%wt, the crystallization temperature was lower than that of neat PLLA 23 ^{o}C while the crystallization time was shorter than that of neat PLLA 34 minutes and the degree of crystallinity of the blend was 20%.

References

[1] J.Y. Nam, M. Okamoto, H. Okamoto, M. Nakano, A. Usuki, "Morphology and crystallization kinetics in a mixture of low-molecular weight aliphatic amide and polylactide", Polymer 47 (2006) 1340-1347.

[2] A.M. Harris, E.C. Lee, "Improving mechanical performance of injection molded PLA by controlling crystallinity", Journal of Applied Polymer Science 107 (2008) 2246-2255.

POL-O-04

Effect of Poly (D-lactic acid)-*co*-Polyethylene glycol on Crystallization of Poly (L-lactic acid)

Ploypawee Kaewlamyai[a], Amornrat Lertworasirikul[a,*]
[a]*Department of Materials Engineering, Faculty of Engineering, Kasetsart University, Bangkok 10900, Thailand*
*Corresponding author: *E-mail:* fengarl@ku.ac.th

Keywords: Crystallization, Nucleating agent, Poly (lactic acid), Stereocomplex

Poly (lactic acid) is a biopolymer derived from renewable resources and it can be disposed without creating harm to environment. Poly (lactic acid) can be formed by thermoplastic processes and has good mechanical properties. However, its disadvantages are high crystallization temperature, slow crystallization rate, poor heat stability and low ductility. In the past, it was found that poly (D-lactic acid) (PDLA) can form complexes with poly (L-lactic acid) (PLLA) and the complexes could accelerate crystallization of the poly (lactic acid) and increases the degree of crystallinity and consequently the heat stability is improved. Nonetheless, the ductility is further decreased. It is known that polyethylene glycol (PEG) can improve ductility of PLLA. In this research, PDLA was copolymerized with PEG with attempt to improve both crystallization behavior and ductility. Poly (D-lactic acid)-*co*-polyethylene glycol (PDLA-*co*-PEG) was synthesized by ring opening polymerization using D-lactide and PEG at D-lactide: PEG ratio of 10:3 wt%. The PDLA-*co*-PEG was blended with PLLA with PDLA-*co*-PEG content of 0 to 50 wt% by melt blending process. Results from Fourier transform infrared spectrometer (FT-IR) and X-Ray diffractometer (XRD) confirmed the stereocomplex formation between PDLA-*co*-PEG and PLLA. Characterization by differential scanning calorimetry (DSC) revealed that glass transition temperatures and crystallization temperatures of the blends were decreased in the presence of PDLA-*co*-PEG. Storage moduli of PLLA/PDLA-*co*-PEG specimens obtained from dynamic mechanical analysis (DMA) decreased as PDLA-*co*-PEG content increased. POM micrographs of blends with PDLA-*co*-PEG content of 1-5 wt% obviously showed that crystallization rate was increased. PDLA-*co*-PEG has potential to be an effective nucleating agent and efficient plasticizer for PLLA.

POL-O-05

Morphology and Properties of Polyoxymethylene/Polypropylene/ Microcrystalline Cellulose Composites

Nipawan Yasumlee, Sirirat Wacharawichanant*
Department of Chemical Engineering, Faculty of Engineering and Industrial Technology, Silpakorn University, NakhonPathom 73000, Thailand
*sirirat.che@gmail.com

Keywords: Polyoxymethylene, Polypropylene, Microcrystalline Cellulose, Polymer Composites

The effects of microcrystalline cellulose (MCC) on mechanical, thermal and morphological properties of polyoxymethylene (POM)/polypropylene (PP) blends at various MCC and PP contents were investigated. The contents of PP were used at 10, 20, 30, 40 and 50% by weight and MCC were added at 3 and 5 phr by melt mixing using an internal mixer at 200°C. The morphology of the blends without and with MCC were observed by scanning electron microscopy (SEM). From SEM analysis, the morphology of POM/PP blends clearly demonstrated a two phase separation of dispersed PP phase and matrix phase of PLA due to the difference in polarity of POM and PP. When adding the MCC in the blends the morphology slightly changed due to the interaction poor adhesion between MCC and polymer phases. The tensile properties found that the incorporation of MCC at 5 phr could improve Young's modulus of POM/PP blends in a range of 10-30 wt% of PP. While the tensile strength, stress at break and strain at break of the blends slightly changed with addition of MCC. The thermomechanical properties showed the storage modulus of POM/PP blends decreased increasing PP content due to the storage modulus of PP was lower than that of POM. The storage modulus of the blends was improved after adding MCC due to the reinforcing effect of the MCC. The thermal properties found that the addition of MCC had no effect on the melting temperature of the blends. The blends exhibited was higher decomposition temperature than pure POM. The degradation temperature of POM and PP are 350.4°C and 431.2°C, respectively. The all blends showed that the degradation temperature increased when increasing of PP content when compare with POM due to PP was more thermal stability than POM. Therefore, it may be inferred that the addition of PP could enhance the thermal stability of the POM/PP blends. While the incorporation of MCC did not improve the thermal stability of POM/PP blends due to the degradation of MCC was lower than that of POM and PP.

POL-O-06

Poly(lactic acid)-Polybutylene Succinate-Activated Carbon Composite Foams

Kittimasak Ketkul[a], Poonsub Threepobnatkul[a,*], DaruneeAussawasathien[b], Kittipong Hrimchum[b]

[a]*Department of Materials Science and Engineering, Faculty of Engineering and Industrial Technology,SilpakornUniversity,NakhonPathom, 73000, Thailand*

[b]*National Metal and Materials Technology Center (MTEC), KhlongNueng, KhlongLuang, PathumThani 12120, Thailand*

*E-mail address corresponding author: poonsubt@yahoo.com

Keywords: Poly(lactic acid), Polybutylene succinate, Activated carbon, Foam.

Polymer blends of poly(lactic acid) (PLA) and polybutylene succinate (PBS) containing activated carbon (AC) were formed to be foam by using azodicarbonamide (ADC) through an extrusion process. The composite foams containing 5 phr of AC had lower density than those without AC loading for PLA:PBS ratios of 90:10, 80:20, 70:30, and 60:40. The incident of higher void fraction was the consequences of more foaming nucleation centers which were induced by adding AC in the composite foam. Maximum reduction of density by 50% with the void fraction of 50% was achieved when AC were applied at 5 phr with the PLA:PBS ratio of 80:20. The addition of AC in composite foams enhanced the crystallization in PBS phase but had no effects on PLA crystallinity. The thermal stability of composite foams with and without AC dosages for each PLA:PBS proportion was slightly changed. The mechanical properties of composite foams such as tensile strength and elongation at break would be investigated as well.

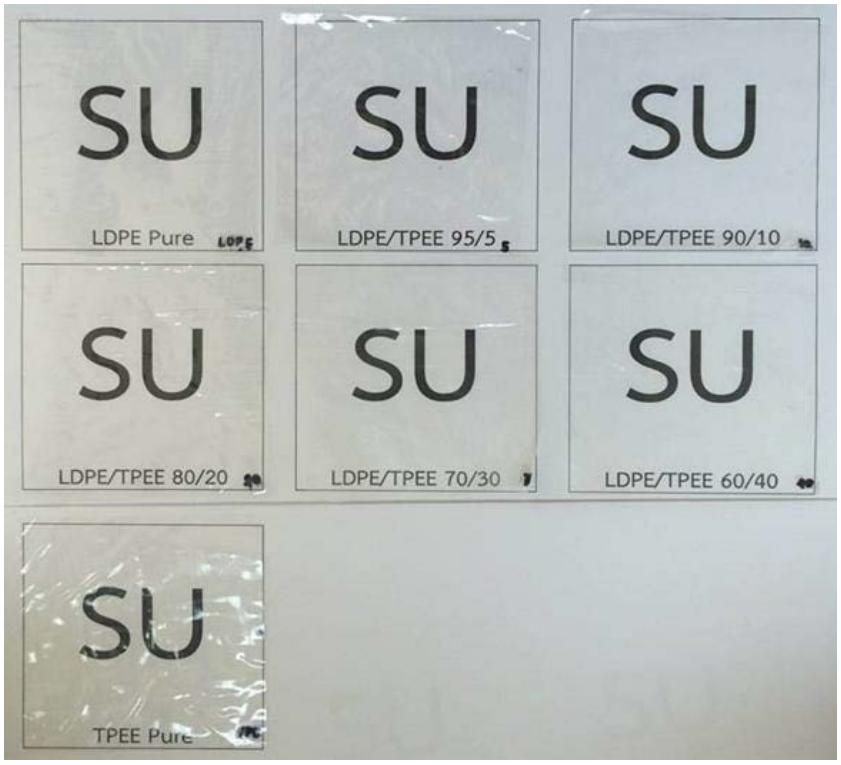

Figure 1. Physical appearance of blend films using the various blend ratio (in wt%) between LDPE and TPEE.

POL-O-08

Numerical Simulations of Geometric Extrudate Swelling in Polymer Melt Extrusion Using Arbitrary Lagrangian Eulerian (ALE) Based Finite Element Method on Free Surface

Mongkol Kaewbumrung[a,*], Tatiya Trongsatitkul[b]
[a]*Department of Mechanical Engineering , Faculty of Engineering and Technology , Pathumthani University, Pathum Thani, 12000, Thailand*
[b]*The School of Polymer Engineering, Institute of Engineering, Suranaree University of Technology, Nakhon Ratchasima 30000, Thailand*
*Mongkol.kaewbumrung@gmail.com

Keywords: Arbitrary Lagrangian Eulerian, Free Surface, Geometric swelling

Extrudate swell prediction in plastic extrusion process remains one of the most challenging issues in the field of numerical simulations. The challenge arises from two important elements involving the simulation process. Firstly, a suitable representation of the constitutive behavior of the polymer melt must be used. To be specific, the representation includes viscosity model, boundary condition, and viscoelastic behavior. Secondly, special treatment of free surface simulation for the melt exiting from the die lip. This causes a necessity to employ special techniques for improving accuracy of the extrudate swell prediction. The objective of this work was to apply Arbitrary Lagrangian Eulerian (ALE) technique based finite element method on free surface for extrudate swell simulation. The parameters including geometry, nonlinear viscosity, volume flow rate, and wall boundary were investigated. The High Performance Computing (HPC) was applied to optimize the numerical error regarding mesh independence. The results illustrated the advantage of the use of ALE technique which allowed large element distortions fitting for extrudate sell situation. An improvement in the accuracy of the extrudate swell prediction can be beneficial for die design which should ultimately yield an increase in extrudate product quality.

POL-O-09

Preparation of TO_2/WO_3 Composite Nanofiber by Electrospinning

Patthamapa Chakornpradit[a,*], Manisara Phiriyawirut[a,b], Vissanu Meeyoo[b,c]
[a] *Department of Tool and Materials Engineering, Faculty of Engineering, King Mongkut's University of Technology Thonburi, Bangkok, 10140, Thailand*
[b] *Nanotech-KMUTT Center of Excellence on Hybrid Nanomaterials for Alternative Energy, King Mongkut's University of Technology Thonburi, Bangkok 10140, Thailand*
[c] *Department of Chemical Engineering, Mahanakorn University of Technology, Thailand*
*newneenew@gmail.com

Keywords: Cellulose acetate, Titanium dioxide, Tungsten trioxide, Electrospinning

TiO_2 has been utilized in many applications such as air-water purification, anti-fogging, and anti-corrosion. The limitation of using TiO_2 for these applications is such it requires a UV light to activate. Many researchers have been trying to improve the activity by doping with other metals such as Fe, Ag, Au, etc. to allow TiO_2 to harvest the broader spectrum of light. However, TiO_2 was unable work in the absence of light. To overcome this, energy storage substances such as WO_3 and V_2O_5 are introduced. It was found that the efficiency of the system is relied on the contact between TiO_2 and energy storage substances. In this work, the preparation of cellulose acetate/TiO_2/WO_3 composite nanofiber via sol-gel by electrospinning process for improving the photocatalytic efficiency was investigated. The polymer was removed from fibers by a heat treatment. Microstructure and elemental composition of TiO_2-WO_3 nanofiber were evaluated by scanning electron microscope (SEM) and energy dispersive microscopy (EDX), respectively. The results showed that the nanofiber of TiO_2 and WO_3 were achieved with the average diameter range of ca. 310-701 nm and both TiO_2 and WO_3 are well dispersed along fiber length, confirmed by an EDX analysis. The results also showed that the smoothness of fiber surface was decreased with WO_3 contents. The photocatalytic activity of the materials were also tested for methylene blue degradation. TiO_2/WO_3 exhibited the highest activity comparing to pure TiO_2 and WO_3. Moreover, it was found that a TiO_2/WO_3 specimen possessed the energy storage ability as a result, it showed the photocatalytic activity in the absence of light. Details of the development and how the material work the absence of light will be discussed in the presentation.

POL-O-10

Silane Modified-WO_3 for Improving Photochromic Properties of PC/WO_3 Composite Films

Tanes Sangpraserdsuk[a,*], Manisara Phiriyawirut[a,c], Jatuphorn Wootthikanokkhan[b,c]

[a] *Department of Tool and Materials Engineering, Faculty of Engineering, King Mongkut's University of Technology Thonburi, Bangkok, 10140, Thailand*

[b] *Division of Materials Technology, School of Energy Environment and Materials, King Mongkut's University of Technology Thonburi, Bangkok 10140, Thailand*

[c] *Nanotech-KMUTT Center of Excellence on Hybrid Nanomaterials for Alternative Energy, King Mongkut's University of Technology Thonburi, Bangkok 10140, Thailand*

*sangpraserdsuk@hotmail.com

Keywords: Photochromic, Tungsten oxide, Polycarbonate, Silane coupling agent

Tungsten oxide (WO_3) is interesting to work on the research and development of building applications that can be used for preparing Polycarbonate (PC) exhibiting the photochromism phenomena. Photochromic WO_3 powder, prepared by the sol-gel technique [1], was used for mixing with PC via a solution blending. Furthermore, in order to improve a compatibility between WO_3 and the polymer, chemical structure on the surface of the metal oxide was modified by treating it with 9 wt% of the γ-Glycidoxypropyltrimethoxysilane (γ-GPMS). The aim of this work was to investigate morphological and optical properties of the composites. Comparisons of structure-properties of the PC composites containing two different types of WO_3 were also of interest. Changes in chemical structure of the silane treated WO_3 was verified by the presence of the FTIR peaks at 2935, 2863 (C-H, stretching) and 1110 cm^{-1} (C-O, stretching). The presence of Si element on the surface of modified WO_3 was also confirmed by the results from XRF technique. SEM images of the composites showed that the modified WO_3 particles were agglomerated whereas the normal WO_3 particles were distributed uniformly within PC matrix. In our opinion, this could be attributed to the poorer solubility of the silane treated metal oxide. From the color index test, it was found that color differences, upon the exposure to sunlight, of the modified WO_3/PC was 6.82. This was greater than that of the normal WO_3/PC (4.44). The decoloration (bleaching) time of PC composite films was also decreased from 72 to 24 hour after using the modified WO_3 as a replacement. Last but not least, we found that optical properties of the modified WO_3/PC films, described in term of IR absorption, were inferior to those of the normal WO_3/PC analogue. After exposure to sunlight, percentage absorbance in the IR region of the modified WO_3/PC specimens increased from 22% to 35%. This implies that, the PC should be compounded with some stabilizers to enhance a durability of the composite film. In overall, this study suggested that a greater color change, a faster response, and a better reversibility of PC/WO_3 composite under the sunlight can be improved by modifying the metal oxides with the silane coupling agent. The above effect could be ascribed to the enhanced UV light photochromism of WO_3 by supporting of water molecules existed in the silane [2].

References

[1] A. Tasasoa, P. Ngaotrakanwiwat, Synthesis of nano-WO_3 particles with PEG for chromic film, Energy Procedia 79 (2015) 704-709.

[2] Z. Luo, J. Yang, H. Cai, H. Li, X. Ren, J. Liu, X. Liang, Preparation of silane-WO_3 film through sol–gel method and characterization of photochromism, Thin Solid Films 516 (2008) 5541–5544.

POL-O-11

Effect of Silicon Carbide on Thermal and Mechanical Properties of Polypropylene Composites

Watthanaphon Cheewawuttipong [*], **Worapong Boonchouytan, Romdorn Burapa**
[a]*Material Processing Technology Research Unit, Department of Industrial Engineering, Faculty of Engineering, Rajamangala University of Technology Srivijaya*
*E-mail address Watthanaphon.c@rmutsv.ac.th

Keywords: Polypropylene, Silicon carbide, Melt compounding, Combination size

The purpose of this research was to enhance the thermal and mechanical properties of polypropylene composites filled with silicon carbide by melt compounding. In this study was investigated the effect of filler content and particle size, the combination of different sizes of silicon carbide in term of thermal and mechanical properties. The result showed that the content of filler had an influence on improving thermal and mechanical properties of polypropylene composites. Which the large size of silicon carbide was higher thermal and mechanical properties of polypropylene composites than the small size of silicon carbide. Moreover, the combination of two different sizes of silicon carbide had significantly enhanced the thermal and mechanical properties at the same total content of silicon carbide. The SEM photograph indicated that the combine size silicon carbide were more uniformly dispersed than a single size of silicon carbide. In addition, several models for predicting the thermal conductivity of the composites were studied.

POL-O-12

Enhancement of Dielectric β-phase PVDF Piezoelectric Composite by Base Modified Surface Activated Carbon Nanofiller

Saiwan Nawalertpanya[a,*], Thorin Teeradechwanichkul[b], Prapapan Noisupap[a]
[a]*Chemical Engineering department, Engineering Faculty, King Mongkut's University of Technology Thonburi, Bangkok, Thailand, 10140, Thailand*
[b]*Electronic and telecommunication Engineering, Engineering Faculty, King Mongkut's University of Technology Thonburi, Bangkok, Thailand, 10140, Thailand*
*saiwan.bua@kmutt.ac.th

Keywords: Polyvinylidene fluoride, Piezoelectric, Composite, Nanofiller

The piezoelectric polyvinylidene fluoride (PVDF) composite doped with Activated carbon nanofiller (AC) were prepared by solution casting and hot press technique. PVDF becomes recently interesting because of its piezoelectric property which is unfortunately not high enough compared with piezoelectric ceramic such as PZT. The use of polymeric piezoelectric material has although a lot of advantage such as high mechanical properties. This low electric property of polymer could be improved by several methods such as poling process or the addition of some solid filler such as carbon black. In this research, the uncharged surface of activated carbon nanofiller was initially modified by strong base such as NaOH which could effectively increase electric charge on the surface of the nanofiller. The interaction between slightly charged solid particle filler and positive charged PVDF polymer chain induced the more orientated PVDF phase to be more electroactive β-phase. The effect of different mass fractions of such modified nanofiller on the electroactive formation and dielectric properties of the composite were thoroughly studied. Poling process was also applied to all sample in order to enhance piezoelectric properties of the composite. Many spectroscopy techniques such as Fourier transformation infrared spectroscopy (FT-IR) were used to confirm the enhancement of β-phase content in PVDF matrix. This result correlated with the increasing dielectric properties of PVDF/AC composite. The experimental results showed furthermore that their piezoelectric properties then improved by poling technique. Their FT-IR spectrums showed that poling process and addition of 0.3% activated carbon surface pretreated by NaOH increased the most electroactive β-phase to 0.9682 which is effectively high compared with pure PVDF. Piezoelectric and dielectric properties was also studied and correlated perfectly with the enhancement of β-phase content of PVDF matrix.

POL-O-15

Medicated Pressure Sensitive Adhesive Patches from STR-5L Block Rubber: Effect of Preparation Process

Rungtiwa Waiprib[1,a], Ekwipoo Kalkornsurapranee[2,b], Wiwat Pichayakorn[1,c,*]
[1]*Department of Pharmaceutical Technology, Faculty of Pharmaceutical Sciences, Prince of Songkla University, Songkhla, 90112, Thailand*
[2]*Department of Materials Science and Technology, Faculty of Science, Prince of Songkla University, Songkhla, 90112, Thailand*
[a]wairungtiwa@gmail.com, [b]ekwipoo.k@psu.ac.th, [c]wiwat.p@psu.ac.th
[*]Corresponding author

Keywords: Pressure sensitive adhesives, Patch, Rubber, Hydroxyethyl cellulose

STR-5L is a high quality block rubber in Thailand that is interesting to apply in medical and pharmaceutical products because it has very low impurity but high uniformity. In this study, medicated pressure sensitive adhesive (PSA) patches were developed by melt blending technique using hydroxyethyl cellulose (HEC) as tackifier and paraffin oil as softener. Two roll mill was used to blend all ingredients and the thin patches were rolled out. Various preparation parameters were studied such as initial viscosity of rubber (60 or 80 Mooney viscosity; MV), mastication time (5-20 minutes), step of mixing, mixing time (35-80 minutes) and gap between rollers (0.1-0.4 mm). The suitable processing conditions were optimized. It was found that the rubber having initial viscosity of 80 MV provided better physical properties, for example, higher force T-peel, lap shear strength and shear holding time. Longer mastication time increased the shear holding time of patches. At 70 minutes of mixing time, the patches showed the highest shear holding time and did not leave any residue on the testing equipment surface. Moreover, the shear holding time decreased when the gap between rollers was expanded. Mixing method with the sequential addition of STR-5L, HEC and then paraffin oil, provided good PSA patches. In addition, the plasticity retention index of PSA patches increased when HEC was added in the formulation. Next, lidocaine or its hydrochloride salt in powder form could be blended into this PSA to be the homogeneous patches. This lidocaine PSA patches for local anesthetics application on the skin would be evaluated in further study.

POL-P-01

Effect of Preparation Techniques of Pineapple Leaf Fiber/PHBV Composites on Final Properties

Pongsathorn Chaletera[1], Rapheephun Dangtungee[1,2], Suchart Siengchin [1,2,3*]
[1]Department of Mechanical and Process Engineering, The Sirindhorn International Thai-German Graduate School of Engineering (TGGS), King Mongkut's University of Technology North Bangkok, 1518 Pracharaj 1,Wongsawang Road, Bangsue, Bangkok 10800, Thailand
[2]Center of Innovation in Design and Engineering for Manufacturing (CoI-DEM), King Mongkut's University of Technology North Bangkok, 1518 Pracharaj 1, Wongsawang Road, Bangsue, Bangkok 10800, Thailand
[3]Natural Composite Research Group, King Mongkut's University of Technology North Bangkok, 1518 Pracharaj 1, Wongsawang Road, Bangsue, Bangkok 10800, Thailand
* Corresponding author, e-mail: suchart.s.pe@tggs-bangkok.org

Keywords: Poly(hydroxybutyrate-co-hydroxyvalerate)(PHBV), Pineapple leaf fibers(PALF), Solution casting, Compression moulding

Great effects are undertaken to improve the mechanical, thermal, and selected other properties of bio-polymers using natural fibers such as sisal and flax [1-2]. It was recognized earlier that the preparation technique has a strong impact on the final properties of resulting composites. The topic of this research is to study on comparing the effect of different preparing techniques and volume fraction of natural fiber reinforced on bio-polymer, and how they affect selected mechanical, thermomechanical and water absorption properties. Natural fiber biocomposites composed of Poly(hydroxybutyrate-co-hydroxyvalerate) (PHBV) as a matrix and Pineapple leaf fibers (PALF) as an reinforcement were produced by solution casting and compression molding technique. The PALF were prepared by immersing in NaOH (5%) solution for 1 hour at room temperature. The treated PALFs were wash by tap water until pH 7 then air dried at 80°C for 24 hours and cut into the length of approximately 0.5 mm. In the solution casting techniques, PHBV/PALF were mixed in chloroform that was used as solvent. The mixture was stirred constantly at 60°C, stirring for 30 minute then casted on glass plate and dried in the oven at 70°C for 1 hour. In the compression molding technique, after melt mixing in the kneader (at 180°C for 25 minute and rotor speed of 60 rpm), the compounds were compression molded by a hot press. The mechanical properties of the PALF/PHBV composite films were evaluated by tensile and dynamic mechanical analysis (DMA). The morphology was observed by optical microscope. Moreover the water uptake and the diffusion coefficient of the composites were calculated. The preliminary results are in line with the expectation of increasing tensile modulus (cf. figure 1). This was considered to be as the result of improvement of PALF dispersion in PHBV matrix for solution casting and compression molding technique.

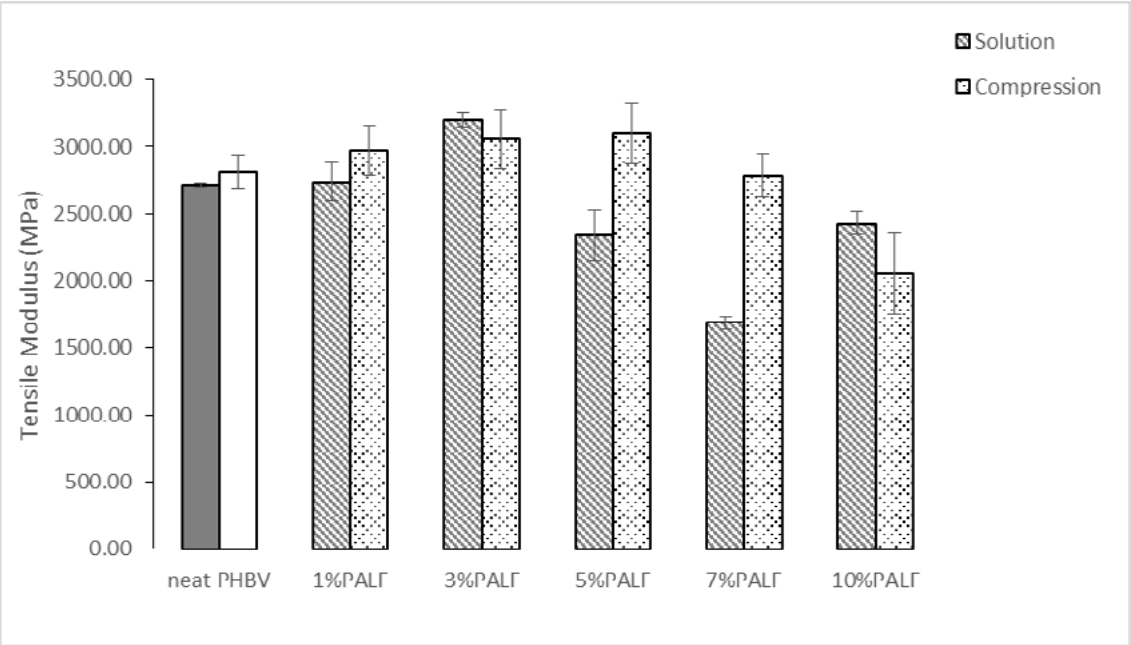

Figure 1: Tensile modulus of PALF/PHBV composites prepared from solution casting and compression technique.

REFERENCE:

[1] SIENGCHIN S.: REINFORCED FLAX MAT/MODIFIED POLYLACTIDE (PLA) COMPOSITES: IMPACT, THERMAL AND MECHANICAL PROPERTIES, MECHANICS OF COMPOSITE MATERIALS 50 (2014), 257-266.

[2] DANTUNGEE R., TENGSUTHIWAT J., BOONYASOPON P., SIENGCHIN S.: SISAL NATURAL FIBER / CLAY REINFORCED POLY(HYDROXYBUTYRATE-CO-HYDROXYVALERATE) HYBRID COMPOSITES, JOURNAL OF THERMOPLASTIC COMPOSITE MATERIALS 28 (2015), 879-895.

POL-P-02

Effect of Octenyl Succinate Starch on Properties of Thermoplastic Tapioca Starch Blend

Manisara Phiriyawirut*, Thanagorn Duangsuwan, Nutthaphong Uenghuab, Chatchai Meena

Department of Tool and Materials Engineering, Faculty of Engineering
King Mongkut's University of Technology Thonburi, Bangkok, 10140, Thailand
* Manisara.pee@kmutt.ac.th

Keywords: Thermoplastic Starch / Tapioca Starch / Octenyl Succinate Starch

Water resistant of thermoplastic starch was drawback property, in order to solve this property modified starch with hydrophobic group was chosen. Octenyl succinate starch are produced by reaction of octenyl succinic anhydride, to form a substituted starch with hydrophilic and hydrophobic groups. This research study on properties of the thermoplastic starch from tapioca starch/octenyl succinate starch blend on the weight ratio of 0/100, 25/75, 50/50, 75/25, 100/0. The compounds were mixed by internal mixer and shaped by compression molding. Temperature of mold was 135-140^{o}C with 1000-1500 MPa for 9 minutes. From the results, it was found that as mixed octenyl succinate starch was decreased the density thermoplastic starch of dued to low density of octenyl succinate starch as compared to tapioca starch. The water resistance of thermoplastic starch blend was increased as increasing octenyl succinate starch content for short time interval (10 min.) but no significantly different for long time interval (1 hrs.). The mechanical properties of thermoplastic starch, in terms of tensile strength, Young's modulus and elongation at break, was increased by adding 25% of octenyl succinate starch due to synergy effect of octenyl succinate phase. Thermal degradation was also investigated by TGA technique. It was found that as increasing octenyl succinate starch content, thermal degradation of thermoplastic starch blend was quite retarded.

POL-P-03

The Smart Blending for Multilayer Structure of PLA/EVOH

Pornlada Pongmuksuwan [a], Wanlop Harnnarongchai [a,*]
[a]Department of Materials and Production Technology Engineering, Faculty of Engineering, King Mongkut's University of Technology North Bangkok, Bangkok, 10800, THAILAND
*wanlop.h@eng.kmutnb.ac.th

Keywords: Multilayer structure, Extrusion, PLA, EVOH.

The concept of smart blender to form a multilayer structure of PLA/EVOH has been proposed. Unlike conventional mixing, smart blending provides a formation of multilayer structure by dictating the motion of stir rod to agitate melts. The PLA and EVOH are supplied separately by a single-screw extruder. An experimental rig is assembled at the end of a co-extruder and melt from an extruder entered an experimental rig via a cylindrical port. The molten EVOH is recursively stretched and folded in an experimental rig of PLA major phase to give an alternating layer structure. The rod is rotated by variable speed motor that is independently controllable. The rod rotational speed and volumetric flow rates of EVOH and PLA are of our interest in this study. The experimental results suggest that the injected stream of EVOH are converted to multiple and distributed sheets ranging thickness from 50 to 300 μm. The characteristic folding of EVOH melt very depends on the volumetric flow rate of the screw extruder and rod rotational speed. However, the coalescence of EVOH layer is observed for high rod rotational speed.

POL-P-04

Effect of Synthesized Ag Nanoparticles with the Different Amounts of Polyvinylpyrrolidone on the Antibacterial Properties of Ag-Natural Rubber Hybrid Sheets

Warot Prasanseang[a], Chaval Sriwong[a,*], Kittisak Choojun[a,b]
[a] *Department of Chemistry, Faculty of Science, King Mongkut's Institute of Technology Ladkrabang, Chalongkrung Road, Ladkrabang, Bangkok, 10520, Thailand*
[b] *Catalytic Chemistry Research Unit, Department of Chemistry, Faculty of Science, King Mongkut's Institute of Technology Ladkrabang, Chalongkrung Road, Ladkrabang, Bangkok 10520, Thailand*
*E-mail: kschaval@yahoo.com

Keywords: Microwave-assisted method, Silver nanoparticles, Natural rubber hybrid sheet, Antibacterial properties

Ag-natural rubber (AgNR) hybrid sheets were successfully prepared with a green, simple, and low cost method. In this method, the colloidal silver (Ag) nanoparticles were firstly synthesized by using a microwave-assisted method under studying the effect of polyvinylpyrrolidone (PVP) concentrations without reducing agents. Then, the AgNR hybrid sheets were prepared by latex mixing-casting method of natural rubber latex (60% HA) with the colloidal Ag nanoparticles. The characteristic absorption, particles sizes, and shapes of the obtained colloidal silver nanoparticles were examined through UV-visible spectroscopy (UV-vis) and transmission electron microscopy (TEM) techniques. While the as-prepared AgNR hybrid sheet samples were also characterized by using X-ray diffraction (XRD), attenuated total reflection Fourier-transformed infrared spectroscopy (ATR-FTIR), Raman spectroscopy, scanning electron microscopy (SEM), and energy dispersive X-ray spectrometer (EDS) techniques. The antibacterial properties of AgNR hybrid sheets were investigated by inhibition zone method with Gram-positive and Gram-negative bacteria, i.e., *Staphylococcus aureus (S. aureus)* and *Escherichia coli (E. coli)*, respectively. The results showed that the prepared AgNR sheets exhibited excellent antibacterial properties against these bacteria. Besides, the antibacterial activities of AgNR sheets were also strongly dependent on the synthesized Ag nanoparticles by utilizing the different amounts of PVP.

POL-P-05

Mechanical and Thermal Properties of PS-g-NR Blended with Natural Rubber: Effect of Grafting Percentage of PS in PS-g-NR

Tarakol Hongkeab[a] and Peerapan Dittanet[a,*]
[a]*Department of Chemical Engineering, Faculty of Engineering/Kasetsart University, Bangkok, 10900, Thailand*
[*]E-mail address corresponding author: fengppd@ku.ac.th

Keyword: Natural rubber, Latex, Graft copolymer, Polystyrene

Polystyrene grafted natural rubber (PS-g-NR) was synthesized by emulsion copolymerization and used as reinforcing agent for improved mechanical and thermal properties of natural rubber. The copolymerization reaction was carried out at 60°C at different reaction time (15 min, 30min, 60min, 120min and 360 min) to control the grafting percentage of PS in PS-g-NR copolymer. The effect of PS grafting percentage in PS-g-NR on mechanical and thermal properties of NR compound was investigated. Those properties include tensile properties, tear strength, hardness, swelling in oil and accelerated thermal ageing test. The functionality and morphology of PS-g-NR were characterized by Fourier transform infrared spectroscopy (FTIR) and transmission electron microscopy (TEM). It was revealed that a core-shell structure contained a core particle of NR and a shell of PS. The polystyrene grafting percentage was calculated to be 12.16%, 16.27%, 17.08%, 22.16% and 23.16% for 15 min, 30min, 60min, 120min and 360 min, respectively.

POL-P-08

Charged Iridium(III) Complexes with Varied Side Chain Length in OLEDs

Natsiri Wongsang[a], Kittiya Wongkhan[a], Somboon Sahasithiwat[b], Laongdao Kangkaew[b], Rukkiat Jitchati[a,*]

[a]*Organometallic and Catalytic Center (OCC), Department of Chemistry, Faculty of Science, Ubon Ratchathani University, Warinchamrap, Ubon Ratchathani Province, 34190, Thailand*

[b]*National Metal and Materials Technology Center (MTEC), Thailand Science Park (TSP), Paholyothin Road, Khlong Nueng, Klong Luang, Pathumthani 12120, Thailand*

*E-mail: rukkiat_j@hotmail.com

Keywords: Iridium, Charged complex, OLEDs

Organic light emitting diodes (OLEDs) have been intensive studied in recent years which will be replaced LED technology in the future. OLEDs can be fabricated by a simple technique such as spin-coating, dip-coating or inkjet printing. Especially, the iridium(III) complexes have been used because of their high quantum yields, short exited state lifetime and easily tunable emission wavelength . Herein, the varied side chains of the four charged iridium(III) complexes were synthesized and characterized. The core materials were designed with 9,9-bis(4-methoxyphenyl)-4,5-diazafluorene as the bulky N^N ligand which prevent the π-π stacking interaction in the solid state e.g. methyl, hexyl, iso-hexyl and *n*-octyl. Their photophysical and electrochemical properties were investigated. OLEDs were fabricated with the structure ITO/PEDOT:PSS/PVK:complex (10:7 by weight)/TPBi/LiF/Al. The similar colors were obtained with varied OLED performances. We concluded that the long alkyl chain can increase the solubility to affect the excellent film-forming property of emitting layer. Therefore, the device based on the *n*-octyl chain namely [(9,9-bis(4-octyloxyphenyl)-9H-cyclopentadipyridine-N-N′)-bis-(2-phenylpyridine-$C^{2'}$,N)-iridium(III)] haxafluorophosphate (**C8ppy**) showed the maximum current efficiency and brightness of 11.37 cd/A and 1,766 cd/m^2, respectively.

POL-P-09

Strength Properties Improvement for Preparation Wood Plastic Composite by Polyester Resin and Rice Straw

Panot Kosentor[a], Don Kaewdook[a*] and Akito Takasaki[b]
[a]*Advanced Manufacturing Technology Research Laboratory, Faculty of Engineering, Thai Nichi Institute of Technology, Suanluang, Bangkok, 10250, Thailand*
[b]*Department of Engineering Science and Mechanics, Shibaura Institute of Technology, Tokyo, 135-8548, Japan*
*don@tni.ac.th

Keywords: Rice straw, Renewable fibers, Wood plastic composite, Mechanical strength.

Rice is the main product of Thai farmer and rice-straw is by-product which was generated. Rice straw is biomass waste which have potential to use as renewable fiber for preparing eco-material. Objective of this study aims to reduce waste from agriculture and increase value to make wood plastic composite. Also, this study aims to determine and optimize parameter to improve mechanical strength of wood plastic composite made from rice-straw and polyester resin matrix. In order to improve the existing properties of wood to be replaced by wood plastic composite. This study have two parts. The first part focus on ratio of rice straw and polyester resin are mixed with various ratios (10:90, 20:80, 30:70, 40:60, 50:50 and 40:60) and second part has focus on temperature of baking after compression molding at various temperatures (120°C, 140°C, 160°C, 180°C, 200°C, 220°C, 240°C, 260°C and 280°C). The result show that, height bending strength and compressive strength occurred at low rice-straw ratio. Also, bending strength and compressive strength were increasing after baking. Wood plastic composite can use to produce the part of high environmental resistivity and increase lifetime of produce at environment uncontrollable. And preventing to aggression from termites and insects which is a problem that is often found in the using of wood materials.

POL-P-11

Gelatin Films and Its Pregelatinized Starch Blends: Effect of Plasticizers

Suchipha Wannaphatchaiyong[1,a], Prapaporn Boonme[1,b], Wiwat Pichayakorn[1,c,*]
[1]*Department of Pharmaceutical Technology, Faculty of Pharmaceutical Sciences, Prince of Songkla University, Songkhla, 90112, Thailand*
[a]suchipha@gmail.com, [b]prapaporn.b@psu.ac.th, [c]wiwat.p@psu.ac.th
[*]Corresponding author

Keywords: Gelatin, Pregelatinized starch, Plasticizer, Film

Green biofilms are attractive materials to use in many applications including packaging, agriculture, food, pharmaceuticals and medicals. In this study, the erodible gelatin biofilms and gelatin/commercially pregelatinized tapioca starch blended biofilms were developed which pregelatinized starch might reduce the hygroscopic property of gelatin and then could decrease the degradation rate of films. However, these films were brittle and lack of elasticity. Therefore, several plasticizer blends were investigated to prove this problem. The aim of this study was to investigate the effect of types and amounts of well-known safety plasticizers on the properties of both gelatin and pregelatinized starch blended biofilms. Films were prepared by casting method. Each of glycerol, propylene glycol (PG), or polyethylene glycol 400 (PEG400) was added into gelatin solution in different amounts (5-30 part per hundred of gelatin; phg) and the mixtures were then dried in 50˚C. It was found that all types and amounts of plasticizer could be blended into gelatin solution and the transparent films were formed, except the PEG400 blended film gave opaque character. However, 30 phg glycerol blended film could not be peeled off because it was too softy. When the amount of plasticizer blends increased, the tensile strength decreased and the elongation at break increased. These gelatin films dissolved and eroded very quickly. Pregelatinized starch was also blended, and the amounts of starch (5-30 phg) and types of plasticizer (25 phg) were studied. Pregelatinized starch dispersions mixed well in the gelatin solution and gave the homogenous films. These blended films swelled and eroded in water completely in 2 hours. Increase the amount of starch gave longer swelling time and decreased the degradation rate of blended films. The tensile strength of glycerol blended films slightly increased when increasing the amount of starch but those of PEG400 and PG blended films were not different. The elongation at break of all plasticizers blended films decreased when the amount of starch increased. The morphology, Fourier transform infrared spectroscopy and differential scanning calorimeter confirmed their compatibilities in these films. In application, either lidocaine or its hydrochloride salt was mixed in these gelatin films to use as local anesthetic on the pain skin, and their physicochemical properties were evaluated.

POL-P-12

Self-reinforced Composites from Pineapple Leaf Fibers

Supachok Tanpichai[a,*], **Suteera Witayakran**[b]
[a]*Learning Institute, King Mongkut's University of Technology Thonburi, Bangkok, 10140, Thailand.*
[b]*Kasetsart Agricultural and Agro-Industrial Product Improvement Institute, Kasetsart University, Bangkok, 10900, Thailand.*
*Supachok.tan@kmutt.ac.th

Keywords: Agricultural waste, Cellulose, Mechanical properties

Cellulose has been recently attracted more interest as promising reinforcement used in composites due to light weight, biodegradability, renewability, low-cost and non-toxicity. Pineapple leaf fibers with diameters of 43 ± 0.1 μm were treated by steam explosion and sodium hydroxyl treatments to obtain microfibers with diameters of 3.4 ± 1.4 μm. Networks of pineapple leaf fibers and microfibers were then prepared using handsheet forming machine. Meanwhile, microcrystalline cellulose was totally dissolved in a mixed solvent of lithium chloride and *N*,*N*-dimethylacetamide to prepare a cellulose solution. After that, the networks were soaked with the cellulose solution, and the cellulose composites were finally prepared. Mechanical properties of the composites were investigated to study effect of cellulose networks with different diameters. The higher tensile strength and modulus were obtained from the composites with microfiber networks in comparison with the composites with network of untreated pineapple leaf fibers. This is due to a larger surface area of microfibers interacted with the cellulose matrix. The composites prepared in this work could be potentially used for packaging and biomaterial applications.

POL-P-13

Physical and Mechanical Properties of Wood Plastic Composites from Teak Wood Sawdust and High Density Polyethylene (HDPE)

Duangkhae Bootkul[a,*], Thammanun Bootkul[b] and Saweat Intarasiri[c]

[a]*Department of General Science (Gems and Jewelry), Faculty of Science, Srinakharinwirot University, Bangkok 10110, Thailand*

[b]*T. Bauer Construction Company, Tambol Tapong, Rayong 21000, Thailand* [c]*Science and Technology Research Institute, Chiang Mai University, Chiang Mai 50200, Thailand*

*saweat@gmail.com

Keywords: Wood plastic composite (WPC), Teak wood sawdust, High density polyethylene (HDPE), Physical and mechanical properties.

Teak sawdust is a by-product from furniture industry that has been produced in huge quantities every year. It is mostly left out in the garbage or burn as waste. Efforts to find utilization of this material have resulted mostly in low value. However, teak wood sawdust waste can be considered as an alternative to fabricate fiber reinforced polymer composites for furniture function. This study was undertaken to determine the physical and mechanical properties of wood plastic composites, which were made under laboratory conditions by hot pressing of high-density polyethylene (HDPE) with teakwood sawdust as filler. Seven levels of mixed flour, 10, 20, 30, 40, 50, 60 and 70%, based on the composition by weight was added to the HDPE powder with palm oil as coupling agent. A flat-press was used to manufacture testing specimens in dimensions 5.8 x 7.3 cm^2. As expected, by increasing mixed flour content, water resistance of the panels was negatively influenced. Investigation of the mechanical property of the composites material, according to the American society for testing and materials (ASTM) method, was done by impact strength tester. The measurement results were found that impact strength was decreased upon the increasing of the sawdust up to 30 % mixing then gradually increased. The best appearance of composites material in comparison to natural woods was 30% sawdust powder. The present study reveals that the flat pressing technology can be considered an alternative to produce large dimension wood plastic panels. The materials were applied for construction of a Thai spirit house as an outdoor decoration.

POL-P-14

Degradation of Silica-reinforced Natural Rubber by UV Radiation and Humidity in Soil

Manuchet Reowdecha[a], Chalermchat Sukthaworn[a], Peerapan Dittanet[a], Nantina Moonprasith[c], Thipjak Na Lampang[c], Surapich Loykulnant[c], Paweena Prapainainar[a,b*]

[a] *National Center of Excellence for Petroleum, Petrochemicals and Advance Material, Department of Chemical Engineering, Faculty of Engineering, Kasetsart University, Bangkok 10900, Thailand*

[b] *NANOTEC Center for Nanoscale Materials Design for Green Nanotechnology and Center for Advanced Studies in Nanotechnology for Chemical, Food and Agricultural Industries, Kasetsart University, Bangkok 10900, Thailand*

[c] *National Metal and Materials Technology Center, PathumThani 12120, Thailand*

*E-mail fengpwn@ku.ac.th

Keywords: Natural rubber, High ammonia concentrate latex (HACL), Fresh latex (FL)

Nowaday natural rubber trees in Thailand have been grown in many areas while its prices is depressed. Researches have been carried out widely in order to help increasing the value of natural rubber. In this research study, the degradation of natural rubber to be applied to the application in agriculture products such as rubber mulch may help maximize the value and minimize the cost to agriculturist. This work included the synthesis of rubber composites from high ammonia concentrate latex (HACL), fresh latex (FL), their blends with 10, 20 wt% loading of silica particles. They were molded by film casting. The experimental study of rubber degradation of rubber samples with and without silica particles was done by putting the sample underground and at the surface under state accelerated degradation test box which include solar simulator lamp for a period of 45 days. Samples were characterized by scanning electron microscopy (SEM) to view the dispersion on cross-section area between natural rubber and silica filler, thermogravimetric analysis (TGA) was used to analyze the thermal stability of the natural rubbers composites. Mechanical property of the sample after irradiation was tested by focusing on tensile strength (MPa), modulus at 100% elongation (MPa), and elongation at break (%) to compare their appearances with and without the filler. It was found that thermal degradation of natural rubber compounds consisted of one main loss step between 341 °C and 420.0 °C. The result showed good dispersion of Si in the rubber samples. Moreover, it was found that before degradation, HACL/Si had higher tensile strength than that of HACL. FL/Si also had higher tensile strength than of FL. After degradation, HACL/Si had lower tensile strength than that of HACL. FL/Si also had lower tensile strength than that of FL. Elongation @ break value of HACL/Si and FL/Si after degraded had decreased obviously.

POL-P-15

Degradation Test of Natural Rubber/Chitosan Composite

Chalermchat Sukthaworn[a], Manuchet Reowdecha[a], Peerapan Dittanet[a], Nantina Moonprasith[c], Thipjak Na Lampang[c], Surapich Loykulnant[c], Paweena Prapainainar[a,b*]

[a]National Center of Excellence for Petroleum, Petrochemicals and Advance Material, Department of Chemical Engineering, Faculty of Engineering, Kasetsart University, Bangkok 10900, Thailand

[b]NANOTEC Center for Nanoscale Materials Design for Green Nanotechnology and Center for Advanced Studies in Nanotechnology for Chemical, Food and Agricultural Industries, Kasetsart University, Bangkok 10900, Thailand

[c]National Metal and Materials Technology Center, PathumThani 12120, Thailand

*E-mail fengpwn@ku.ac.th

Keywords: Natural Rubber, Chitosan, Degradation

Degradable material from chitosan and natural rubber latex was prepared by solution casting without surface treatment of 20wt% and 10wt% chitosan loading to study thermal and mechanical properties of this material after degradation test in aging condition. The test was done in an acrylic degradation box with 600 Watt light and high humidity for accelerate degradation condition in rubber composite. Sample included high ammonia concentrated latex (HA) with no filler, fresh latex (FL) with no filler, HA with chitosan filler, FL with chitosan filler and natural rubber with natural filler like shrimp shell for compare the result with chitosan filler. These materials were characterized by scanning electron microscopy (SEM) for morphological study, TGA for thermal properties study, and tensile testing for mechanical properties study. After degradation test, weight of sample was compared with that before degradation. Weight loss confirmed the degradation of natural rubber/chitosan composite. Thermal properties from TGA both before and after degradation showed that the fillers had effect on these composite material. TGA result in natural rubber/chitosan composite with aging at temperature 100 ℃ for 10 hrs and 20 hrs. SEM and pictures were compared before and after degradation of HA and FL with no filler, chitosan filler and shrimp shell. It was clearly seen that the samples were degraded by changing in shape and size. Tensile testing values of HA with no filler were 1.4 0.5, 1.1 MPa, those of HA with chitosan filler were 2.6, 1.3, 0.7 MPa, those of FL with no filler were 0.9, 0.9, 1.1 Mpa, those of FL with chitosan filler has 0.8, 0.9, 1 MPa in normal condition, aging condition at 10 and 20 hrs, respectively. It showed that longer aging time increased could lead to the degradation in chitosan/HA. Therefore, chitosan had effect on degradation of natural rubber.

POL-P-16

Mechanical, Thermal and Hydrolytic Degradation of Stereocomplexed PLL/PDL–PEG–PDL Blends

Aphinan Saengsrichan[a], Wootichai Khotasen[a], Puttinan Meepowpan[a], Patnarin Worajittiphon[a], Robert Molloy[a,b], Chaiyapruk Katepetch[c], Narin Kaabbuathong[c], Winita Punyodom[a,*]

[a]*Polymer Research Laboratory, Department of Chemistry, Faculty of Science, Chiang Mai University, Chiang Mai 50200, Thailand*

[b]*Materials Science Research Center, Faculty of Science, Chiang Mai University, Chiang Mai 50200, Thailand*

[c]*PTT Research and Technology Institute, Wang Noi, Ayutthaya 13170, Thailand*

*E-mail: winitacmu@gmail.com

Keywords: Stereocomplexed PLL/PDL–PEG–PDL blends, mechanical and thermal properties, hydrolytic degradation

In this research, stereocomplexed polylactide (Sc-PL) was prepared by the solvent blending of poly(L-lactide) (PLL) with poly(D-lactide) (PDL) and some synthesized poly(D-lactide)-*b*-poly(ethylene glycol)-*b*-poly(D-lactide) (PDL-PEG-PDL) triblock copolymers with different PDL segment lengths, PDL_{357}-PEG_{182}-PDL_{357}, PDL_{188}-PEG_{182}-PDL_{188} and PDL_{87}-PEG_{182}-PDL_{87}. PEG is an attractive biopolymer not only as biocompatible to polylactide but also gives a large increase in elongation with the small decrease in tensile strength. The effects of the PDL sequence length on the mechanical and thermal properties of solution-cast films were studied. PLL, PLL/PDL (60:40 wt %), and PLL/PDL-PEG-PDL (60:40 wt %) films that achieve full stereocomplexation were characterized by a combination of differential scanning calorimetry (DSC), thermogravimetry (TG) and tensile testing. The results showed that Sc-PL had a high melting temperature of around 200-220 °C, which is approximately 40-50 °C higher than that of homochiral crystals of PLL or PDL, while the addition of 40 wt % PDL-PEG-PDL to PLL could significantly increase the elongation at break of the PLL/PDL-PEG-PDL blended films. Synergistic effects of stereocomplexation between the PLL and PDL together with plasticization by the PEG are considered to be the dominant factors. In addition, the PLL/PDL-PEG-PDL blended films showed a higher thermal stability than PLL alone at temperatures above 375 ºC. Finally, the hydrolytic degradation of the Sc-PL films was studied both in water and in phosphate buffer saline (PBS) at room temperature. The degradation was followed in terms of mass loss, surface changes and thermal properties. Tuning the hydrolytic degradation by stereocomplexation is of critical importance for utilizing PLL in different commercial applications.

POL-P-17

Study and Development of Irradiation-based Processing System for Natural Rubber Vulcanization

K. Kosaentor[a,*], E. Kongmon[a], C. Thongbai[a], J. Saisut[a], N. Kangrang[a], S. Rimjaem[a]

[a]*Plasma and Beam Physics Research Facility, Department of Physics and Materials Science, Faculty of Science, Chiang Mai University, Chiang Mai 50202, Thailand*

*kittiya_k@cmu.ac.th

Keywords: Vulcanization, Linear accelerator, Geant4

Natural rubber is an important export product of Thailand, which presently contributes about 40% of global production and export. In normal vulcanization processes, chemical substances were added to improve the rubber properties. This may cause allergic for the user due to the additive substances. Vulcanization using an accelerated electron beam does not need to add possibly toxic chemical compounds, e.g. sulfur. Thus, it was proved to be a non-allergic method for high quality natural rubber vulcanization. This research develops an electron linear accelerator system for rubber vulcanization with variable electron energy and current of 0.5-4 MeV and 10-100 mA, respectively. This range of the electron beam energy and current will give different absorb dose, which is the most important parameter for electron beam processing. The absorb dose depth and distribution in natural rubber latex are simulated by using a Monte Carlo Method program, GEometry ANd Tracking (GEANT4). Study results on the dose distribution of electron beam penetration in the natural rubber latex will be presented in this paper with the aim to find the optimum condition of electron beam properties for sufficient natural rubber vulcanization.

POL-P-18

Mechanical and Thermal Properties of PLA Melt Blended with High Molecular weight PEG Modified with Peroxide and Organo-Clay

Chanchai Thongpin[a,*], Chaiwat Tippuwanan[a], Kwanchai Buaksuntear[a] and Teerani Chuawittayawut

[a]*Department of Materials Science and Engineering, Faculty of Engineering and Industrial Technology, Silpakorn University, Sanamchandra Palace Campus, Nakornpathom, 73000, Thailand.*

*E-mail: THONGPIN_C@su.ac.th, cmaterials@hotmail.com

Keywords: Effect of molecular weight of PEG, organo clay, Thermal properties, Mechanical properties

The thermal and mechanical properties of poly (lactic acid) melt blended with high molecular weight PEGs, which were PEG1000 and PEG6000, were prepared and compared. The contents of PEG added were varied: 10, 12.5 and 15 % by weight. The blends were also modified with organic peroxide in order to induce crosslinking in both PLA and PEG and also to avoid transesterification of PLA by PEG. The transesterification could cause PLA to be degraded during mixing and storage. Mechanical performance of PLA/PEG blend was also modified by the addition of organic modified clay, Cloisite30B, C30B, using master batch clay (concentrated C30B in PLA). The content of C30B in the blends was kept at 3 phr with respect to PLA/PEG blend. The results reveal that PLA was toughening by addition of PEG. As PEG1000 and PEG6000 are wax at room temperature, the migration of PEG was less compare to low molecular weight PEG which is generally being in liquid form. The presence of PEG induced PLA to perform cold crystallization. T_m in PLA was slightly changed whereas degree of crystallinity of PLA was decreased. Peroxide modification of the blends resulted in lowering in crystallization of PLA. The mechanical properties of PLA/PEG were enhanced by addition of peroxide. The mechanical and thermal properties were found to be improved. The whitening of specimens during tensioning was noticeable. XRD could indicate intercalation and exfoliation of clay in the blends. SEM confirmed the plastic deformation of PLA during tensioning. The optimum properties in term of toughening and thermal stability were found at PEG content at 15% for both PEGs.

POL-P-19

Investigation of Radical Polymerization of Furfuryl Methacrylate Using ESR

KyoungHo Kim,[1] Taeheon Lee,[1] Atsushi Kajiwara[*2] and Hyun-jong Paik[*1]
*[1]Department of Polymer Science & Engineering, Pusan National University, Busan, 609-735, Korea, *hpaik@pusan.ac.kr*
*[2]Department of Materials Science, Nara University of Education, Takabatake-cho, Nara 630-8528, Japan, *kajiwara@nara-edu.ac.jp*

Keywords: electron spin resonance, furfuryl emthacrylate, radical polymerization

The research on biomass material has been huge attracted interesting in recent. Among them, furfural widely developed furan-derived monomer can be respectively prepared from C5 and C6 carbohydrate resources. Furfural has been industrial commodity for many decades because it can be prepared quite readily and economically from a vast array of agricultural or forestry wastes.

Furan-derived materials have been researched as biomass materials to replace petroleum chemicals for various areas. Additionally, one of major motivations to study furan-derived monomers is their function for Diels-Alder (DA) reaction with dienophiles. The DA reaction using furan-derived compound has been investigated in the several years for new polymeric materials. Furthermore, thermally reversible DA cycloaddition is a convenient route for the formation of carbon-carbon bonding under mild conditions and this feature has been exploited in the preparation of self-healing polymers carrying functionalities, either as the polymer chain-end or in the repeating units.

Although furan-derived monomer have been considered as promising materials for smart material, the monomers, such as furfuryl methacrylate (FMA), have problem to overcome. Due to their two kinds of reactive double bond which could be participate in polymerization, furan-derived monomers make gel formation by crosslinking. Therefore to control the gel formation, furan-derive monomers have been polymerized with comonomer or in diluted condition. R. Sastre et al proposed a kinetic model for the simulation of the polymerization of FMA to estimate the possible variation and determine the concentration of radicals and degree of cross-linking.

Electron spin resonance (ESR) spectroscopy is a powerful tool to understanding both the kinetics and mechanism of radical polymerizations. Therefore in this study, propagating radical of FMA was estimated by steady-state ESR during radical polymerization. Kinetic constants for the addition reaction of the diphenylphosphonyl radical to FMA and other monomers with similar sturucture were determined by time resolved ESR.

In steady-state ESR spectrum, polymerization of furfuryl methacrylate methylacrylate radicals were observed. This spectrum was similar when compared with polymerization of butyl methacrylate. And time-profile time-resolved ESR show diphenylphosphonyl radical prefer to attack methacrylate double bonds than furan ring double bonds almost 40 times.

POL-P-20

Photo-oxidative Degradation Polyethylene Containing Titanium Dioxide and Poly(ethylene oxide)

Tawat Soitong[a], Nichapa Yodkeeree
[a] *Program in Materials Science, Faculty of Science, Maejo University, Chiang Mai, Thailand*
*E-mail: stawat@gmail.com

Keywords: Polyethylene, Poly(ethyleneoxide), Titanium dioxide, Photo-degradation

Biodegradable Polyethylene (PE) may be used in the fabrication of plastic films which can replace common films prepared from nondegradable polymers. A photodegradable polyethylene composite film was prepared by mixing titanium dioxide/poly(ethylene oxide) into the PE matrix (PE/TiO_2/PEO). The composites films were prepared using 0-3 wt.% of TiO_2 and 0-10 wt.% of PEO by melt mixing. It was then compression molded in to films at 180 ˚C. The photo-degradation test was performed under 400 W UV lamp in the ambient air. The resulting composite materials were investigated by the Fourier transform infrared spectra (FTIR), Scanning electron microscope (SEM), weight loss monitoring, and X-ray diffraction spectra (XRD). The results show that the PE/TiO_2/PEO composites film has a high photocatalytic activity, the weight loss rate of it is about two times higher than that of PE/TiO_2 film and ten times higher than that of neat PE film. The FTIR spectra of the neat PE and PE composite films after UV irradiation showed that the carbonyl peak intensity for neat PE film is very low, while in composite films the intensity is greater. The degraded PEO produced an acid and an aldehyde, which were able to facilitate PE degradation and the addition of PEO/TiO_2 brought about the facilitative effect of the PE degradation.

POL-P-21

Influence of Molecular Weight on the Non-isothermal Melt Crystallization of Biodegradable Poly(D-lactide)

Wanich Limwanich[a,*] **Sawarot Phetsuk**[b], **Puttinan Meepowpan**[b], **Nawee Kungwan**[b], **Winita Punyodom**[b]

[a]*Faculty of Sciences and Agricultural Technology, Rajamangala University of Technology Lanna, Chiang Mai 50300, Thailand*

[b]*Polymer Research Laboratory, Department of Chemistry, Faculty of Science, Chiang Mai University, Chiang Mai 50200, Thailand*

*E-mail address wanich.lim@gmail.com

Keywords: Crystallization, Kinetics, Differential Scanning Calorimetry (DSC), Poly(D-lactide)

The influence of molecular weight of poly(D-lactide) (PDL) on the melt crystallization was successfully investigated by non-isothermal differential scanning calorimetry (DSC) technique. The synthesized PDLs with three different number average molecular weights ($\bar{M}_n$) of 2.39×10^5 (PDL1), 1.09×10^5 (PDL2) and 0.61×10^5 (PDL3) were utilized in this study. From DSC kinetics analysis, it was found that the rate of PDLs crystallization increased with increasing cooling rate. Furthermore, the crystallization rate of PDLs was dependent on molecular weight and determined to be in the following order: PDL3 > PDL2 > PDL1. The crystallization mechanism was analyzed by the Avrami, Ozawa and Liu models. The mechanism of all PDLs crystallization was nucleation with three dimensional growths. Furthermore, the molecular weight of PDLs affected not only the crystallization rate but also the thermal property. The melting temperature (T_m) of PDLs increased with increasing of molecular weight but the heat of melting (ΔH_m) decreased.

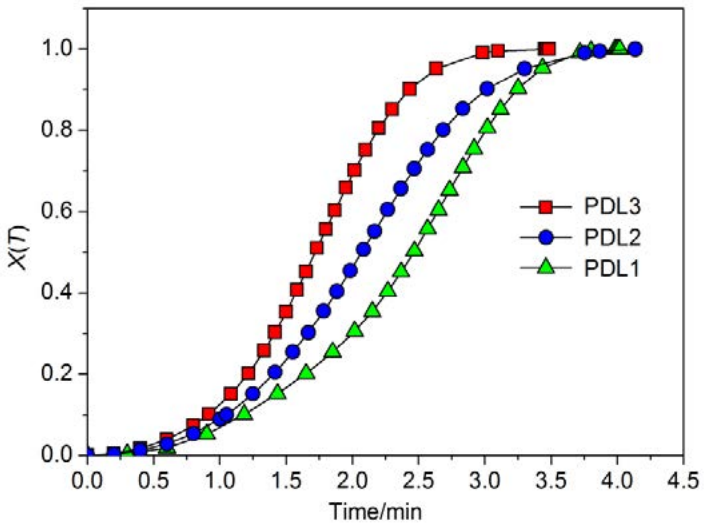

POL-P-22

Toughening of Poly(buthylene succinate) with Epoxidized Natural Rubber: Mechanical, Thermal and Morphological Properties

Sudsiri Hemsri[a,*], Nudchanart Tanusorn[a], Rungrapee Santi[a], Anisara Runthod[a]
[a] *Department of Materials Science and Engineering, Faculty of Engineering and Industrial Technology, Silpakorn University, Mueng, Nakhon Pathom, 73000, Thailand*
*sudsirihemsri@yahoo.com

Keywords: Poly(buthylene succinate), Epoxidized natural rubber, Toughening, Morphology

Poly(butylene succinate) copolymer (PBS) is one of attractive biodegradable polyesters with excellent biodegradability, good tensile strength, processability and thermal stability. However, PBS possesses low impact and toughness properties which have prevented it from being used in many applications. To overcome these drawbacks, blending PBS with another flexible polymer seems to be an attractive approach for improving toughness of PBS bioplastics. Thus, in this study, epoxidized natural rubber (ENR) with 50 mol% epoxide content was blended with PBS to improve toughness of the resulting PBS-based plastics. The PBS/ENR blends were melt-processed in an internal mixer. Dicumyl peroxide (DCP) was used as vulcanizing agent for crosslinking the ENR phase in the PBS/ENR blends. The compositions by weight of the PBS/ENR blends ranged from 100/0, 95/5, 90/10, 80/20 and 70/30 and all blends were compression-molded. Mechanical properties including tensile properties as well as impact properties, thermal properties determined by thermal gravimetry analysis (TGA) and morphologies the polymer blends were investigated.

The morphology results investigated by a scanning electron microscope (SEM) revealed that the PBS/ENR blends were immiscible and dispersed rubber particles in the blends became larger when the ENR content increased. However, the addition of DCP into polymer blends reduced agglomeration and size of the dispersed rubber particles. Incorporation of ENR into PBS remarkably enhanced ductility and impact strength of the blends. Moreover the PBS/ENR blends with DCP provided superior mechanical and impact properties compared to those without DCP.

POL-P-24

Fabrication and Characterization Mixed Matrix Membrane of Polysulfone/polyimide–carbon Nanotubes

Tawat Soitong[a], Nichapa Yodkeeree
[a] *Program in Materials Science, Faculty of Science, Maejo University, Chiang Mai, Thailand*
*E-mail: stawat@gmail.com

Keywords: Polyimide, Polysulfone, Carbon nanotube, Mixed matrix membranes

In this work, Copolyimides were prepared from one-step polymerization of 6FDA (4,4'-(Hexafluoroisopropylidene)diphthalic anhydride) and ODA (4-Aminophenyl ether). The typical procedure is as follow: firstly, ODA and NMP (N-Methyl-2-pyrrolidone) were added in a three-necked round-bottomed flask equipped with a nitrogen balloon. After the ODA had been fully dissolved, 6FDA was added to the mixture. The reaction lasted 24 hours under a nitrogen atmosphere at room temperature and formed a viscous transparent poly(amic acid) intermediate. Mix matrix membrane were prepared form polyimide/poysulfone (80:20 by weight) solution filled with 0.1-1.0 weight percent of carbon nanotube (CNTs). Then, the solutions using a 0.45 um filter and casted onto a clean glass plate. Finally, the film was heated through various stages in oven to remove the solvent and the water formed. The heating procedure was 85 ^{o}C for 0.5 h, 115 ^{o}C for 0.5 h, 150 ^{o}C for 0.5 h, 180 ^{o}C for 1 h, 210 ^{o}C for 1 h, and 270 ^{o}C for 1 h. The membranes were characterized by using Fourier transform infrared spectroscopy (FTIR), Scanning electron microscopy (SEM), Differential scanning calorimetry (DSC), Thermal gravimetric analysis (TGA), gas permeation measurements CO_2 and CH_4 and tensile properties. The FTIR spectra of the polyimide films showed the absorption bands at about 1783 cm^{-1} (C=O asymmetric stretching), 1726 cm^{-1} (C=O symmetric stretching), 1370 cm^{-1} (C-N stretching) and 721 cm^{-1} (C=O bending), which are characteristic for imide rings. The structure of the polysulfone/polyimide showed the bands at 1000–1100 cm^{-1} is related to O=S=O bound of polysulfone. The SEM showed the carbon nanotube dispersed at lower loading but some agglomerations at higher loading. The glass transitions temperature and degradation temperature was increased by increasing the polyimide to polysulfone because of high thermal stability of polyimide. CH_4 permeability decreased from 0.613 Barrer for membrane without polyimide to 0.542 Barrer for membranes polyiminde/polysulfone 80:20 by weight. However the CH_4 permeability of membranes polyiminde/polysulfone increased by increasing the carbon nanotube with low selectivity. Addition of carbon nanotube into polymers matrices affects the diffusion of gases. Gases with larger molecular diameter diffuse slower through porous structure of nanotube thus the nanotube acts as molecular sieve. However, in some circumstances, due to nano scale interfacial voids formation which cannot be observed in SEM images, selectivity will decline.

POL-P-25

Study of Polymer type on Microstructure of Polymer Nanofiber by Electrospinning Technique

Pojanart Rattanavoraviset[a,*], Supattra Wongsaenmai[a]
[a]*Program in Materials Science,Faculty of Science, Maejo University, Sansai, Chiang Mai, 50290, Thailand*
*E-mail address: ploy_trumpet.za@hotmail.com

Keywords: barium orthotitanate, conventional mixed oxide method, polymethylmethacrylate

In this work, polyvinyl pyrrolidone (PVP) and polyvinylalcohol (PVA) nanofiber was prepared by electrospinning technique. A homogeneous solution of PVP/ethanol and PVA/DI water were prepared by varying PVP/PVA concentration in the range of 6–12 wt.%. The solutions were electrospun at 10-20 kV DC by maintaining tip to collector distance (TCD) of 8-20 cm. Those parameters were studied into two parts such as solution parameters (polymer concentration) and process parameters (voltage, collection distance). The functional groups were characterized by Fourier transform infrared spectroscopy (FTIR). The microstructure was characterized by a scanning electron microscope (SEM). The correlation of working parameters can affect the fibers morphologies morphologies and diameters.

POL-P-27

Effect of Loofah Fiber on Mechanical Properties of Epoxy Resin

Apaipan Rattanapan[a,*], Pornsri Sapsrithong[a]
[a]Division of Polymer Engineering Technology, Department of Mechanical Engineering Technology, College of Industrial Technology,
King Mongkut's University of Technology North Bangkok, Bangkok, 10800, Thailand
*apaipan.r@cit.kmutnb.ac.th

Keywords: Epoxy resin, Loofah fiber, Polymer composites, Mechanical properties

In this research, epoxy resin composites reinforced with loofah fiber was successfully prepared by using hand lay up technique. The effect of alkaline treatment, fiber volume and fiber orientation, including machine and transverse direction on the mechanical properties were evaluated by tensile, impact and hardness tests. From the experimental, it was found that the flexural modulus and hardness of loofah fiber reinforced epoxy resin were higher than the unreinforced composites. The addition of loofah fiber decreased the flexural strength and impact strength of the composites when compared with composites with no additional loofah fiber. However, it was observed that the mechanical properties of loofah fiber reinforced epoxy resin increased with an increase in fiber volume and alkaline treated fiber reinforced epoxy resin exhibits improvement in mechanical properties as well. Additionally, the mechanical properties of composites reinforced with two plies of loofah fiber by same orientation (2 plies with only machine direction) exhibited better values than cross-ply orientation (2 plies with both machine and transverse direction).

POL-P-29

Influence of Pyrolytic Carbon Black Prepared from Waste Tires on Mechanical Properties of Natural Rubber Vulcanizates

Sarawut Prasertsri* **and Sansanee Srichan**
Laboratory of Advanced Polymer and Rubber Materials (APRM), Department of Chemistry, Faculty of Science, Ubon Ratchathani University, Sathonmark Rd., Warinchamrab, Ubon Ratchathani 34190, Thailand
*sarawut.pra@gmail.com, sarawut.p@ubu.ac.th

Keywords: Waste Tires, Pyrolytic carbon black, Natural rubber, Mechanical Properties

Waste tires have become an important issue worldwide and represent a major environmental problem. At present, there are three methods for reclaiming waste tires including retreading, recycling and pyrolysis techniques. The pyrolysis is a process of the thermal decomposition of waste tires in the absence of air, which transform used tires into gas, oil, steel and carbon black waste. This research aimed to investigate the possibility of pyrolytic carbon black (PCB) used as filler in natural rubber (NR) and its effect on Mooney viscosity, cure characteristics and mechanical properties compared with commercial carbon black (N774). The results revealed that Mooney viscosity, hardness, 100% modulus and heat build-up tended to increase with increasing both PCB and N774 loading, whereas elongation at break and rebound resilience decreased. However, the maximum tensile and tear strengths appeared at the optimum filler loading for both PCB and N774. At similar filler content, PCB-filled NR compounds have higher cure time, heat build-up and thermal resistance. Nevertheless, they exhibited lower Mooney viscosity and mechanical properties compared to N774-filled NR. Finally, it can be concluded that PCB could be utilized as filler in NR compound to act as semi-reinforcing filler and was classified as a filler to reduce costs.

POL-P-30

Study on Latex-state ^{13}C-NMR Spectroscopy

Yusuke Iizuka, Seiichi Kawahara*
Department of Materials Science and Technology, Nagaoka University of Technology, Nagaoka, Niigata, 940-2188, Japan
*kawahara@mst.nagaokaut.ac.jp

Keywords: Latex-state ^{13}C-NMR, Molecular motion

Introduction

Latex-state NMR spectroscopy is a unique technique to characterize a hydrophobic rubbery polymer as a soft material dispersed in water. It may enable to investigate mobility of the polymers in dispersoid and movement of dispersoid in water in terms of resolution of the NMR spectroscopy and relaxation time. In the previous work, the mobility of PBA was classified into 3 categories: that is, the motion of main chain carbons (α-relaxation), the motion of carbon linking to main chain (β-relaxation) and the motion of butyl carbon of ester group (γ- relaxation) [1],[2]. In the present study, the relationship between the relaxation time and the mobility of PBA was precisely investigated by latex state ^{13}C-NMR spectroscopy. Characteristic temperatures of all carbon atoms of butylacrylate (BA) units were determined in relation to the reported values of the reference temperatures of PBA, i.e. $T\alpha$(240K), $T\beta$(157K), $T\gamma$(140K).

Experimental

Emulsion polymerization of BA of 0.56 mol/L was performed with ammonium persulfate of 1.5×10^{-3} mol/L in 200 ml deionized water in the presence of sodium dodecyl sulfate at 80 ºC for 2 hours. Unreacted monomer was removed with a rotary evaporator under reduced pressure. Volume mean particle diameter of the resulting dispersoid in the latex was measured by Coulter LS230. Latex state NMR measurements were carried out at 323-353K with a JEOL JNM AL400 FT-NMR spectrometer, operating at 399.7 and 100.4 MHz for ^{1}H and ^{13}C, respectively.

Result and Discussion

Figure1 shows latex-state ^{13}C-NMR spectra for PBA, which were obtained at 323, 338 and 353 K. Seven signals at 35, 41, 174, 64, 30, 19 and 14 ppm were assigned to C1, C2, C3, C4, C5, C6 and C7 of the BA units.Half width of the signals was dependent upon temperature. Figure2 shows a master curve of the half width superposed with T-T_x, where T_x is characteristic temperature for each carbon of the BA units. Values of T_x were determined, as follows; T_α for C1 and C2, 240 K; $T\beta$ for C3, 155 K; $T\gamma$ for C4, 140 K; $T\delta$ for C5, 63K; $T\varepsilon$ for C6, 21; $T\zeta$ for C7, 4K. This demonstrates that local motions of PBA are more active than those of main chain.

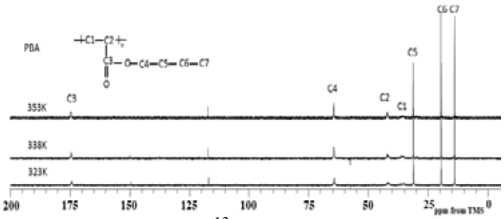

Figure1 Latex-state ^{13}C-NMR spectra for PBA at 323, 338 and 353K

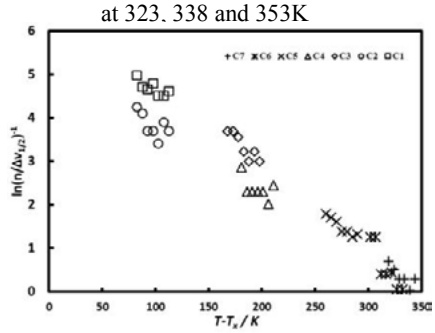

Figure2 The master curve of the half width superposed with T-T_x

Reference

[1] H.Kikuchi, et.al., Macro moleculels.,26, 7326 (1993).
[2] J.G.Ribelles, et.al., J. Appl. Polym. Sci., 38, 1145 (1989).

Surface Engineering and Heat Treatment

SUR-O-01

Effects of Heat Treatment on Microstructure and Properties of Thermal Sprayed Ni-based alloy Coatings

Phuangphaga Daram[a], Suphitcha Moonngam[a], Chaiyasit Banjongprasert[a,b,*]
[a]*Department of Physics and Materials Science, Faculty of Science, Chiang Mai University/ Chiang Mai, 50200, Thailand*
[b]*Materials Science Reseach Center, Faculty of Science, Chiang Mai University/ Chiang Mai, 50200, Thailand*
*E-mail chaiyasit.b@cmu.ac.th

Keywords: Ni-based alloys, Thermal sprayed coating, Heat treatment, Corrosion

Arc sprayed NiCrMoX based coating, both as-sprayed and as heat-treated at 1100^{o}C for 1 hr, have been studied. The microstructural characteristics of the as-sprayed and heat-treated coatings were characterized by scanning electron microscopy (SEM) and X-ray diffraction (XRD). Immersion test was performed in 20%H_2SO_4 solution at 40±5^{o}C for 200 hr. The vickers hardness tester was used to estimate the mechanical properties. The results showed that as-sprayed and heat-treated coatings were dense with a low porosity of ~ 2-3 vol%. The both coatings consisted of Ni(Cr,Mo) matrix phase and oxide layers. The XRD analysis revealed the presence of γ-Ni phase, but heat-treated coating consisted of small peaks of Ni_3Al, Ni_3Mo, NiO, Cr_2O_3 and $NiCr_2O_4$. The heat treatment improved the corrosion resistance of the NiCrMoX based alloy coating. In addition, hardness of heat-treated coating was found to be higher than that of as-sprayed coating. These researches thus demonstrated that heat treatment could improve the corrosion resistance and mechanical properties.

SUR-O-02

Tribological of thermal sprayed coating under slurry erosion.

Chalermchai Sukhonkhet*, Panadda Niranatlumpong,
Hathaipat Koiprasert and Kittichai Nin-on
National Metal and Materials Technology Center, Pathumthani, 12120, Thailand.
*chalers@mtec.or.th

Keywords: slurry erosion, erosion testing, thermal sprayed coating

Erosion damage may occur from impingement of solid particles suspended in fluid. Erosive wear is commonly found in slurry or liquid transportation such as in pipe, propeller, pump and equipment used in slurry transport. Improvement of surface hardness is essential in the protection of component from erosion. This research concerns the slurry erosion resistant property of Al_2O_3, Cr_2O_3 and WC-17%Co thermal sprayed coatings. The work employed a slurry jet erosion test at an impingement angle of 90 degree. The result shows that WC-17%Co is superior under slurry erosion condition when compare with Al_2O_3, Cr_2O_3 ceramic coatings and a 304 stainless steel reference specimen. Ceramic Coated sample displays similar slurry erosion rate to the reference specimen due to the loss of the brittle ceramic coating in an early state of the experiment. After the initial period of the experiment, the ceramic coated sample effectively becomes a stainless steel substrate. Al_2O_3, Cr_2O_3 ceramic coatings are supposed to improve the erosion resistance of the stainless steel due to their relatively high hardness. However, the findings reveal the ineffectiveness of the coating. This is likely to be due to their low fracture toughness in comparison to the WC-17%Co coating, together with the severely of the slurry erosion.

SUR-O-03

FLAME SPRAY COATING FOR EROSION PROTECTION ON WATER WALL PIPE IN BIO-MASS FIRED POWER PLANT BOILER

Vasin Lertvijitpun[a], Pisak Lertvijitpun[a,*]
[a]*Department of Welding Engineering Technology, Faculty of College of Industrial Technology, King Mongkut's University of Technology North Bangkok, Bangsue, Bangkok, 10800, Thailand*
*pisak.l@cit.kmutnb.ac.th

Keywords: SOLID PARTICLE EROSION, FLAME SPRAY COATING, P91, P11

Erosion on surface of high-temperature service material effects on life time of them such as the economizer that is the sub-system in power plant boiler. In water tube boiler system, eroded surfaces were occurred by the various shape of particle on its outer surface at the service temperature in the range of 600-700 ˚C. Thermal spray is one of various technique which used for the repairing or building up new surface. The objective of this experiment is to study the influence of thermal spray coating parameters on the erosion resistance of SA335 grade P91 (Fe-9Cr-1Mo-1V) coated by Ni-Cr-B-Si-Fe (10680 produced by eutectic company) with oxy-acetylene thermal spraying process. The coating parameters were distance between nozzle to substrate at 10, 15mm and travel speed of 1.0, 1.5mm/s, leading to difference heat inputs and cooling rates. The hardness of coating surfaces were measured by Vickers hardness test method at 5kgf. The microstructure of coating surfaces were examined by optical microscope (OM) and scanning electron microscope (SEM). Moreover, solid particle erosion resistance of coating surfaces were investigated on the erosion test rig room temperature. Erosion rate of samples were assessed by weight loss measuring with the electronic balance (0.0001g resolution) comparative with the traditional material such as SA335 grade P91, P11 (these materials usually used for economizer component). Finally, the relationship between erosion resistance and hardness was studied, coincide with the microstructure examination. According to the erosion resistance assessment, it was found that the erosion rate of coating surface was higher than the traditional material except P11. However, the coating parameters played an important role on the erosion resistance. The heat input and cooling rate concerned with coating parameters was further discussed with the erosion behavior in this research.

SUR-O-04

Thermal Sprayed Technique for Preparing HEA-Reinforced Oxide Matrix Composite

Hathaipat Koiprasert*, Ruangdaj Tongsri, Thanyaporn Yotkaew, Pongsak Wila, Suphakan Kijamnajsuk, Chalermchai Sukhonkhet
National Metal and Materials Technology Center, Pathumtani, 12120, Thailand
*hathaik@mtec.or.th

Keywords: High Entropy Alloy, Thermal Sprayed Coating, CoCuFeMnNi

The aim of this experimental work was for comparison between two different raw material preparation methods on air plasma spraying, e.g., (i) blended elemental and (ii) mechanically alloyed high entropy alloy (HEA) powders. In general, HEA consists of five or more than five principal elements. Proportion of each principal elements in equimolar or near-equimolar ratios. The HEA is designed for improving some properties of materials such as hardness, high strength, wear resistance, corrosion resistance and oxidation resistance. This research using air plasma spraying technique for preparing coating from multi-component powder mixtures of Co, Cu, Fe, Mn, Ni with equiatomic ratio. The first coating produced from the blended elemental powders showed Fe, Ni, Cu splats and oxide particles and/or splats including CoO, NiO distributed randomly in the coating, which had high hardness. The second coating produced from mechanically alloyed powders showed oxides particles and/or splats including CoO, M_3O_4 (M=Fe, Mn, NiMn), and CoCuNiFeMn high-entropy alloy (HEA) splats within the coating, which had hardness values twice of that of the first coating. Microstructure of the second coating showed character of HEA reinforced ceramic matrix composite, i.e., the HEA splats were embedded within complex oxide matrix. Moreover, the porosity of the second coating was 4.6%, which was lower than that of the first coating (5.3%porosity). From the experimental results, it was indicated that the mechanical alloying was an important step for raw material preparation for thermal spraying of CoCuFeMnNi coating. From thermal spraying experiment, it suggests that the cause of alloy oxidation is due to high oxygen potential in air hence the ratio between HEA/oxide can be improved by using a controlled-atmosphere thermal spraying technique, which is recommended for further investigation.

SUR-O-05

Effect of Impingement Angle on Erosion Resistance of HVOF Sprayed WC-10Co-4Cr Coating on CA6NM Steel

Anurag Hamilton[a,*], Ashok Sharma[a], Upender Pandel[a]

[a]*Department of Metallurgical and Materials Engineering,*

Malaviya National Institute of Technology Jaipur, Jaipur-302017, India

*E-mail address corresponding author: ahamilton.2107@gmail.com (Anurag Hamilton)

Keywords: CA6NM steel, HVOF, Microstructure, Erosion resistance

Abstract

In the present investigation, WC–10Co–4Cr coating was deposited by high velocity oxy-fuel (HVOF) process on CA6NM hydro turbine steel to improve its erosion resistance. The coating was characterized in term of crossectional microstructure, phase, microhardness and fracture toughness using a field emission scanning electron microscope (FESEM), X-ray diffractometer and microhardness tester respectively. Solid particle erosion resistance of the substrate and coating were evaluated by air jet erosion tester at two different impingement angles (30° and 90°). Coating microstructure has shown a homogeneous and well-bonded structure with less porosity and interlaminar oxidation. The microhardness of the coating was observed more than three times higher than CA6NM substrate. This resulted in significant improvement in erosion resistance of coated CA6NM steel at both impingement angles. Coating showed mixed mode(ductile and brittle) of erosion behavior, while the uncoated substrate exhibits mainly ductile behavior. Eroded surfaces of coated and uncoated substrate were also analyzed by FESEM to correlate with findings.

SUR-O-06

Sintered Metal Microstructure Influenced by Deep Rolling and Carburizing Processes

Sai-yan Primee [a,*], Nutthapol Saingam [a], Sirawut Ruangsart [a]
[a]*Department of Production Engineering, Faculty of Engineering, King Mongkut's University of Technology North Bangkok, Bangsue, Bangkok, 10800, Thailand*

* stein2074@yahoo.de

Keywords: Sintering metal, Deep rolling, Carburizing, Hardness

In general, mechanical parts produced by metallic powder can be used right after sintering process. However, the mechanical properties of sintered parts need to be improved in order to increase strength and service lifetime. This research aims to improve the mechanical properties of sintered metal parts by deep rolling and carburizing processes. For steel, mechanical surface treatment such as deep rolling is normally applied to increase the hardness to the near surface of material. Additionally, carburizing process is normally used to increase hardness, case depth and to improve microstructure. This study used metal powder NC100.24 mixed by Zinc-stearate at the ratio of 100:0.8. Then, bars with dimension 20 x 20 x 186mm were made from the mixed powder, and heated at the sintering temperature of 1100°C for 75 minutes. The sintered bars were then machined to be a cylindrical shape with a diameter of 14 mm and 180 mm in length. All specimens were separated into three groups by the treatment processes, including the deep rolling, carburizing, and deep rolling-carburizing processes. The force used for deep rolling process were 0.25, 0.5, 0.75, and 1 kN. The carburizing condition was at 950°C and 120 minutes. Microstructure analysis and micro hardness testing were then performed to evaluate the specimens after the strength improvement. The results show that the greater applied force in deep rolling, the deeper hardened depth observed. However, applying the greater force in deep rolling followed by carburizing results in the smaller case depth. In contrast, the use of lower rolling force and carburizing increases the depth of hardened layer. Also, the combination of mechanical surface and heat treatment shows the better improvement in hardness of sintered metal compared to the use of a single treatment process.

SUR-O-10

Structural Characterization of Reactive DC Magnetron Co-Sputtered Nanocrystalline CrAlN Thin Film

Amonrat Khambun, Adisorn Buranawong, Nirun Witit-Anun*
Plasma for Sciences Research Laboratory, Department of Physics, Faculty of Science, Burapha University, Chonburi 20131, Thailand
*E-mail address: nirun@buu.ac.th

Keywords: Magnetron co-sputtering, Deposition time, CrAlN thin films, Hard coating.

Nanocrystalline CrAlN thin films were deposited on silicon substrates by reactive DC magnetron co-sputtering technique. The effect of deposition time on crystal structure, elemental composition, thickness, microstructure and hardness of the thin films were characterized by XRD, EDS, AFM and FE-SEM and nanoindentation, respectively. The as-deposited films were formed as a (Cr,Al)N solid solution with (111), (200) and (220) plane. The lattice constants were in range of 3.992 - 4.046 Å. The as-deposited films exhibited a nanostructure with a crystallite size in range of 15 - 35 nm. The thickness and roughness increased from 197 nm to 998 nm and 1.6 nm to 8.1 nm, respectively, with increasing the deposition time. The elemental composition of the films varied with the deposition time. The cross section analysis by FE-SEM showed columnar structure and dense morphology. The film hardness decreased from 39 GPa to 25 GPa with increasing the deposition time and crystallite size of (200) plane.

SUR-O-11

Hardfacing of 3.5% Chromium cast steel by Flux Cored Wire Arc Welding Process

Teerachod Treeparee[a], Prapas Muangjunburee[a,*]
[a]*Department of Mining and Materials Engineering, Faculty of Engineering, Prince of Songkhla University, Hatyai, Songkhla, 90112*
* mprapas@eng.psu.ac.th

Keywords: 3.5% chromium cast steel, Buffer, Hardfacing, Abrasive wear

Abstract: Hardfacing weld is a technique which mainly improve and extend the useful life of engineering components. The purpose of this research is to develop welding procedure for one layer and three layers hardfacing of 3.5% Chromium cast steel and to study wear behavior of hardfacing layers. Flux Cored Wire Arc Welding (FCAW) process has been used as a welding process of this research by choosing austenitic stainless steel and martensitic hardfacing wire to weld the buffer and hardfacing layer, respectively. Preheating was also used in this study. Abrasive wear test of hardfacing deposit were conducted in accordance of procedure "A" standard of ASTM G65. In addition, macrostructure, microstructure and worn surface deposits were analyzed by using optical microscope. The result found that there are no crack and defect in the Heat Affected Zone (HAZ) and other regions. The hardness of preheating sample in HAZ regions were lower than the ones without preheating. Therefore, preheating samples should be done before welding. The abrasive wear resistance of three layers hardfacing deposits was better than one layer hardfacing deposit because one layer hardfacing deposits were diluted from buffer layer more than three layers hardfacing deposit. Moreover, the hardness of one layer hardfacing deposit was lower which cause high loss of weld deposit.

SUR-O-12

Study on friction characteristics of nano filler for friction material

R. Chamnipan[a], S. Chutima[a], V. Uthaisangsuk[a,*]
[b] *King Mongkut's University of Technology Thonburi, 126 Pracha Uthit Road, Bang Mod, Thung Khru, Bangkok 10140, Thailand*
**Corresponding Author: vitoon.uth@kmutt.ac.th*

Keywords: Friction material; Nano filler; Friction stability; Contact area

Nanomaterial has increasingly applied in several engineering components. Due to its extremely small size, high surface area to volume ratio and large interfacial surface area are provided. In this study, tribological properties of a commercial friction material including $BaSO_4$ particle with three different sizes from nano to micro scale were investigated. First, specimens of the friction materials with phenolic resin matrix were produced by hot pressing technique. A pin−on−disc tribometer was used to investigate effects of the $BaSO_4$ fillers on coefficient of friction as a function of applied pressure, friction stability and wear. For surface analysis, scanning electron microscope (SEM) and atomic force microscopy (AFM) were used to examine wear characteristics such as worn surface, contact area and 3−D surface topography. The results obviously showed that the nano filler not only improved friction stability, but also increased wear resistance of the friction material specimens. These determined tribological properties were also correlated with the size of the nano fillers.

SUR-O-13

Surface Modified Sterling Silver using Nitrogen Ion Implantation Technique

Benya Cherdhirunkorn[a]*, Ratirot Srisakul[a], Amarinee Learknok[a], Daungkae Bootkul[b], Saisamorn Niyomsoan[c], Kittisan Mongkolsuttirat[d] and Saweat Indarasiri[e]

[a]Department of Physics, Materials Science Program, Faculty of Science and Technology, Thammasat University, Patumthanee 12020, Thailand
[b]Gemology and Jewelry Division, Faculty of Science, Srinakharinwirot University, Bangkok 10110, Thailand
[c]Faculty of Gems, Burapha University, Chanthaburi 22170 Thailand
[d]Department of Mechanical Metrology, National Institue of Metrology, Patumthanee 12120, Thailand
[e]Institute for Science and Technology Research and Development, Chiang Mai University, Chiang Mai 50202, Thailand

***E-mail**: benya@tu.ac.th

Keywords: Nitrogen ions implantation, Sterling silver, Surface hardness

Surface modified sterling silver (925 silver) was prepared using nitrogen ion implantation technique with the nitrogen ions energy of 70 keV. Nitrogen ions with the fluence of $1x10^{16}$, $5x10^{16}$, $1x10^{17}$ and $5x10^{17}$ ions/cm^2 were implanted on the surface of polished samples. The effects of implanted nitrogen ions on the surface hardness, corrosion resistance and microstructure of surface modified sterling silver were studied. The hardness of samples was measured using a micro vickers hardness tester and a nanoindenter. The corrosion resistance of the samples under 3 conditions; normal air, Sulphur and Sodium chloride atmospheres, was obtained by measuring the change in color of the corrosive samples using a spectrophotometer. It was found that the higher ion fluence could markedly improve both surface hardness and corrosion resistance of the samples. In addition, the microstructures and chemical compositions of the samples were investigated using SEM and EDX techniques.

Conference Secretariat
National Metal and Materials Technology Center
114 Thailand Science Park, Pahonyothin Rd., Khlong Neung,
Khlong Luang, Pathum Thani 12120, Thailand
Tel. +66-2564-6500 ext. 4680
E-mail: conferences@mtec.or.th

www.mtec.or.th/msat-9